Effect of Wall-Soil Interface Parameters on Seismic Response of Retaining Walls

Mohammadhashem Arabzadeh

A thesis

in

The Department

of

Building, Civil and Environmental Engineering

Presented in Partial Fulfillment of the Requirements

for the Degree of Master of Applied Science (Civil Engineering) at

Concordia University

Montreal, Quebec, Canada

February 2018

CONCORDIA UNIVERSITY

School of Graduate Studies

This is to certify that the thesis prepared

By: Mohammadhashem Arabzadeh

Entitled: Effect of Wall-Soil Interface Parameters on Seismic Response of Retaining Walls

and submitted in partial fulfillment of the requirements for the degree of

Master of Applied Science (Civil Engineering)

complies with the regulations of the University and meets the accepted standards with respect to originality and quality.

Signed by the final Examining Committee:

Dr. A. M. Hanna, BCEE Chair

Dr. S. Narayanswamy, MIE Examiner

Dr. A. Bhowmick, BCEE Examiner

Dr. A. Bagchi, BCEE Supervisor

Approved by _____

Chair of Department or Graduate Program Director

_____ 2017 _____

Dean of Faculty

Abstract

Effect of Wall-Soil Interface Parameters on Seismic Response of Retaining Walls

Mohammadhashem Arabzadeh

Reinforced soil retaining walls are important public structures. Typically there are two kinds of reinforced soil retaining walls: cantilever retaining walls and Geosynthetic reinforced soil retaining walls. While seismic performance of retaining walls is very important for public safety in the event of an earthquake, there are very limited studies on that. The main objectives of the present thesis are to (i) examine the behavior of the interface between structure and soil under various loading and boundary conditions for RC cantilever retaining walls; (ii) conduct sensitivity study on the seismic response of such walls considering the key parameters such as the cohesion (C), friction angle (φ), shear stiffness (K_s), normal stiffness (K_n) and dilation (ψ); and (iii) study the size (height) effect of the relating walls on the seismic performance of such walls.

In order to achieve the above objectives, a baseline model of an RC cantilever retaining wall has been constructed for static and dynamic analysis using the Finite Difference Method (FDM). The data for the baseline model are obtained from a published work on seismic response such a wall subjected to an earthquake in India (1991 Uttarkashi earthquake, 20th October), which used the Finite Element Method (FEM) for analysis. The validated baseline model is then used for an extensive parametric study on the static and dynamic behavior of the system which is not available in the literature.

Based on the results of numerical modeling, in the static condition, wall deformation was decreased by increasing the cohesion (C), friction angle (φ), shear stiffness (K_s), normal stiffness (K_n) and dilation (ψ) values. The dynamic behavior of the wall was quite different from the static behavior. With increasing the values of shear strength parameters (Cohesion and friction angle) and also shear stiffness (K_s), the wall displacements increased whereas with increasing normal stiffness (K_n) value, the wall deformation decreased.

A sensitivity analysis of wall-soil interface parameters on seismic response of the retaining wall was carried out using the ground motion records from Canada earthquake motion database (6th March, Quebec, 2005) and the results were compared to the Uttarkashi earthquake in India. The results of this comparison showed that the response parameters in terms of the retaining wall deformation are similar for both earthquakes.

Moreover, parametric studies on the behavior of the soil retaining walls under Montreal earthquake with three different heights (3 m, 6 m and 9 m), and two different types of soil (clay and sand) and eight input earthquakes motions were performed. Results show that the behavior of wall facing in terms of displacement in both horizontal and vertical direction is different, and the type of soil has a main role in the wall deformation.

Finally, a statistical estimation of parameters between soil and retaining wall structure was done. According to this statistical study, cumulative percentage distribution of cohesion (C) and stiffness parameters (shear and normal) against wall deformation were calculated. Then, lower and upper boundary ranges of wall-soil parameters were established for both static and dynamic condition.

Acknowledgements

Firstly, I would like to express my sincere gratitude to my thesis supervisor Prof. Bagchi for the continuous support of my thesis, for his patience, motivation, and immense knowledge. His guidance helped me in all the time of research and writing of this thesis. I would also like to thank Prof. Attila Zaski for his supervision in the initial phase of my graduate study at Concordia University.

Also, I express my warm thanks to Dr. Ali Mortazavi, Amir Kabir University, and Dr. Miad Saberi, Laval University, for technical support and guidance during the course of this research.

My sincere thanks also goes to my best friend, Sina Amoushahi, GHD Company, for providing me with technical support and continuous encouragement throughout my years of study and through the process of researching.

Last but not the least, I would like to thank my family: my parents and to my brothers and sisters for supporting me emotionally throughout writing this thesis and my life in general.

Table of Contents

List of Figures

List of Tables

List of Abbreviations

FEM	Finite Element Method
FDM	Finite Difference Method
FOS	Factor of Safety
PGA	Peak Ground Acceleration
SSR	Shear Strength Reduction

Chapter 1. Introduction

1.1. Background

Reinforced earth structures, developed in 1970's in USA, are composite structures that are constructed by artificial reinforcing strips within soil (Kishan, 2010). They have similar function as traditional retaining walls, but could be higher. Furthermore, the reinforcement enhances the earth by increasing soil-bearing capacity and diminishing the settlement (Government of India, 2005).

Principally there are two main methods for the design of reinforced-soil retaining walls: pseudo static and pseudo dynamic approaches. They are based on an iterative equivalent linear classic and incremental elastic analysis approaches, respectively (Muthucumarasamy, 1992). For both reinforced and unreinforced walls, the shortcoming of calculating pseudo dynamic pressure on a rigid vertical retaining wall is eliminated by some analytical methods such as the horizontal slices method (Ghanbari, 2008).

In addition, the seismic behavior of retaining structures under earthquake loading is one of the most important aspects in the study of retaining wall structures. Generally, the seismic design of retaining walls is carried out by both pseudo static and dynamic analyses. Mononobe and Okabe (1924), developed the pseudo static approach for design of retaining walls (Mononobe, 1929. Nouri, 2008. Okabe, 1926).

Moreover, the interaction between retaining structure and soil is an important aspect for both static and seismic analyses. In recent years, investigation of Soil Structure Interaction (SSI) has been extensively developed for dynamic analysis of retaining walls structure, and Enrique Luco (1973) was one of the pioneers who developed the theories for SSI in this context (JE, 1973).

Typically, a soil structure interaction (SSI) method is based on added motion formulation theory and use of three dimensional structural system (RClough, 1993). Typically, there are two common numerical methods to investigate the seismic response of reinforced-soil retaining walls according to pseudo static and dynamic time-history analysis; Finite Element Method (FEM) and Finite Difference Method (FDM) (Richardson and Lee, 1975. Bathurst and Hatami, 1988).

The finite element method has been developed to simulate the behavior of geotechnical earth structure under static and dynamic loading conditions. The FEM is a numerical modeling approach in which continuous media is replaced by finite number of elements interconnected at finite number of grid points. This method can be used to calculate the displacement field at grid points and stresses within elements. A number of researchers have used the FE approach to investigate the behavior of reinforced-soil retaining wall under earthquake loading (Collin, 1986. Rowe, and Ho, 1997). In most of the studies, the simulation of dynamic soil structure response is conducted by considering nonlinear soil behavior (Segrestin and Bastick, 1988. Helwany et al. 2001).

On the other hand, the finite difference method is one of the oldest numerical techniques used for the solution of sets of differential equations. In the finite difference method, every derivative in the relative equations is replaced by an algebraic expression written in terms of the field variables such as stress or displacement at separate point within elements.

A number of dynamic analysis studies used the finite difference method to simulate reinforced-soil retaining wall and also investigated wall-soil interaction behavior under seismic loading (Hatami, and Bathurst, 2001. Callisto and Soccodato, 2007. El-Emam, M., Bathurst and Hatami, 2004. Krishna, 2010. Green and Ebeling, 2003).

Most of the FDM studies used the commercially available software, FLAC for the simulation of earth retaining wall structure. FLAC is a two-dimensional, explicit, finite difference program based on the Lagrangian calculation scheme. This program simulates the behavior of structures built of soil that can come across with plastic flow when their yield limits are reached.

1.2. Problem statement

Reinforced earth walls are one of the most important permanent public structures. During last two decades, the use of various soil retaining structures have increased in infrastructural civil projects such as cantilever walls, gravity walls and steepened slopes. Also, one of the most important issues in earth retaining structure is the earthquake resistant design.

Most of earth retaining structures are built in urban areas and their failure poses great hazards to the local habitants such as Montreal earthquake on September 16, 1732, with considerable damage, including cracked walls and 300 damaged houses. The 1988 Saguenay earthquake (25^{th} November) also caused damage to buildings and urban infrastructure around Quebec City.

Furthermore, the destructive effects of earthquakes in the earthquake prone areas highlights even more the significant role of reinforced earth walls. Thus, design and construction of the earth retaining structures under earthquake condition is as an essential issue in civil engineering projects. Considering the above, the proposed research is very important.

1.3. Research objectives

While there are some recent numerical studies reported on reinforced-soil retaining walls, most of them considered the behavior of interface between structure and soil under dynamic conditions without any rigorous treatment to the effect of the variation in key parameters and ground motions. In order to address these shortcomings, the present thesis focuses on the following objectives.

(i) To examine the behavior of the interface between structure and soil under various loading and boundary conditions for RC cantilever retaining walls;

(ii) To conduct sensitivity study on the seismic response of such walls considering the key parameters such as the cohesion (C), friction angle (φ), shear stiffness (K_s), normal stiffness (K_n) and dilation (ψ); and

(iii) To study the size (height) effect of the relating walls on the seismic performance of such walls.

In order to achieve the above objectives, the followings tasks have been undertaken.

(a) The behavior of interface between structure and surrounding soil material of retaining walls is investigated considering the continuously yielding joint model.

(b) Because the behavior of interface has a critical role in separation and slip of the soil and structure, in accordance with that, displacement and stress response change. A sensitivity analysis of the parameters associated with this model is carried out determine the influence of the key parameters in the seismic response of retaining wall structure.

(c) The effects of the shear strength and stiffness parameters of interface between wall and soil under earthquake loading is investigated numerically and results is compared with an earthquake in Canada (Quebec).

(d) A parametric study is conducted on the behavior of the reinforced soil retaining walls with three different wall height, two different kind of soil for a set of earthquakes relevant to Montreal.

(e) A statistical study is conducted to estimate the lower and upper bound ranges of wall-soil interface parameters.

1.4. Layout of thesis

This thesis is composed of seven chapters. Chapters 1 and 2 consist of introduction and literature review, respectively. In order to investigate the seismic response of cantilever reinforced-soil retaining wall, the finite difference method considered to design of retaining wall as presented in chapter 3. Then in chapter 4, the effect of shear strength and stiffness parameters of interface on seismic response of retaining wall is investigated. Furthermore, in chapter 5, based on acceleration time-history of an earthquake in eastern of Canada (Quebec), a sensitivity analysis of wall-soil interface parameters on seismic response of retaining wall is investigated and compared with a similar earthquake in India and a range of wall-soil interface parameter value is performed. Moreover, in chapter 6, a parametric study on the behavior of the reinforced soil retaining walls with different condition of wall height and soil properties under Montreal earthquake loading is performed. Finally, summary and conclusions of this study is presented in chapter 7.

Chapter 2. Literature Review

2.1. Introduction

Most of cases investigated in literature review section are divided into two main parts: geosynthetic reinforced soil retaining walls or cantilever earth-retaining walls. All of the studies conducted in this section consist of a dynamic model of retaining walls (reinforced earth walls or cantilever retaining walls), that is constructed based on the Finite Element Method (FEM) and Finite Difference Method (FDM). In fact, most researchers used two-dimensional plane strain numerical models (FEM or FDM) to investigate the behavior of retaining walls in both reinforced earth walls and cantilever retaining walls under earthquake loading. Also, in most case studies, the numerical results were compared to physical modelling.

Most of the numerical studies covered in the literature review section considered the behavior of interface between structure and soil under dynamic conditions. Also, some studies considered the wall-soil interaction as a continuum or with an interface that effects the earthquake response. Most numerical analyses results focused on the effect of seismic loading on wall displacement, displacement between facing units and acceleration response throughout the height of the wall.

A number of researchers have considered the behavior of soil and the effects of soil properties on the behavior of reinforced-soil retaining walls under earthquake loading. Furthermore, the constitutive model to represent geomechanical material behavior was the Mohr-Coulomb shear failure criterion.

In addition, in order to apply acceleration time-history in dynamic analyses, several earthquake motions with different dominant frequency range were used in most cases. Some of studies used a series of shaking table tests for simulation of behavior of a wall.

2.2. Type of retaining walls

Reinforced soil retaining walls can be broadly categorized into following two types; Cantilever retaining walls and Geosynthetic reinforced soil retaining walls. The two main types of retaining walls are explained below in further detail.

2.2.1. Cantilever retaining wall

Cantilever earth-retaining walls are made of cast-in-place and steel-reinforced concrete. Also, cantilever retaining walls is able to retain soil behind it according to internal strength characteristics and rigidity. Figure 2.1 shows a typical cantilever earth retaining wall.

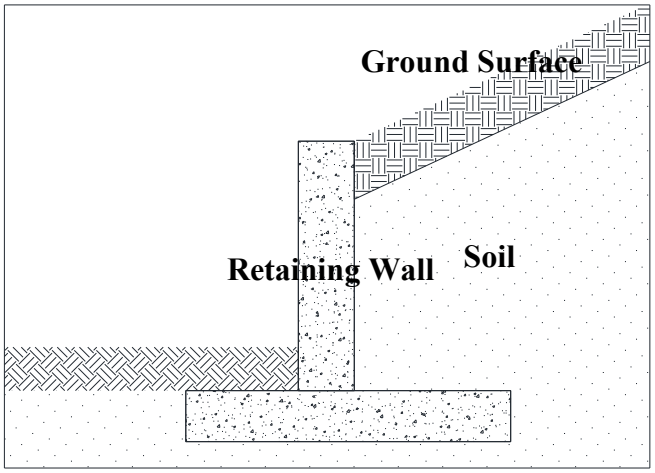

Figure 2.1. Cantilever earth-retaining wall

2.2.2. Geosynthetic reinforced soil retaining wall

Geosynthetic reinforced-soil retaining walls consist of several horizontal layers of geosynthetic or steel reinforcements extended into a soil backfill and are generally pinned to a hard facing (Figure 2.2).

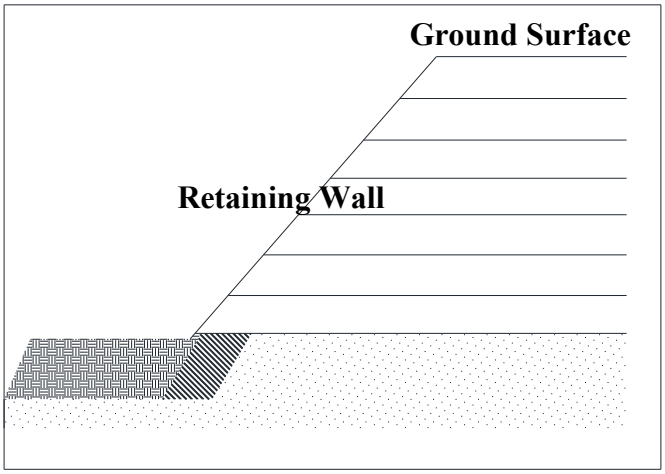

Figure 2.2. Geosynthetic reinforced soil retaining wall

2.3. Seismic analysis of reinforced soil retaining walls using numerical modeling

A number of studies have approached the seismic analysis of reinforced soil retaining walls using numerical modeling such as Finite Element or Finite Difference methods (Siddharth and Siddharth, 2015. Cai and Bathurst, 1995). Some of these works are further explained as follows.

Cai and Bathurst (1995), used a FEM numerical approach to study the load-deformation response under simulated earthquake on geosynthetic reinforced segmental retaining walls. In that study, the reinforcement material was simulated using a similar hysteretic model and wall-soil interface shear was investigated (Cai and Bathurst, 1995). The initial configuration of geogrid reinforced retaining wall in Cai and Bathurst research is illustrated in Figure 2.3.

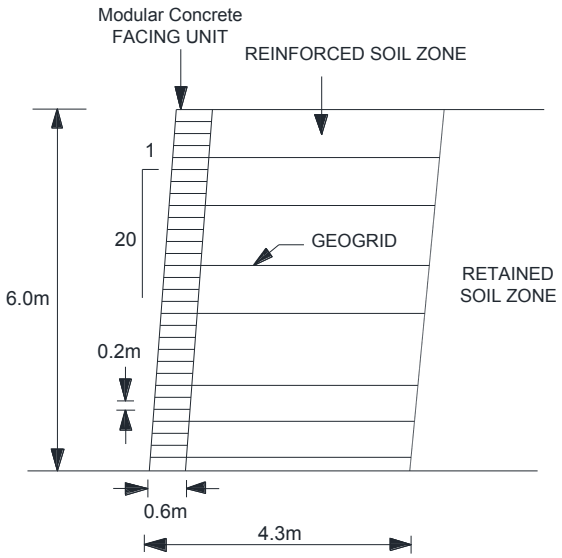

Figure 2.3. Geometrical parameters of geogrid reinforced soil wall in Cai and Bathurst study (1995)

In the above study, the wall designed according to static loading considered the "tie-back wedge" method based on Coulomb's earth pressure theory. And also, in the numerical analyses, the factors of safety (FOS) used was recommended by the NCMA (The National Concrete Masonry Association).

The initial configuration of the finite element mesh of a soil reinforced retaining wall model in Cai and Bathurst study (1995) is shown in Figure 2.4.

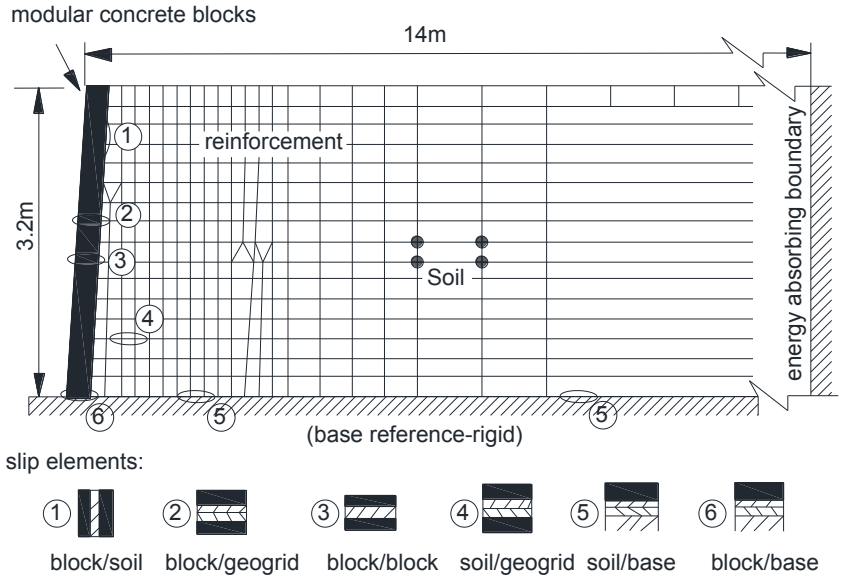

Figure 2.4. Finite element mesh for simulation of retaining wall in Cai and Bathurst study (1995)

With regard to Figure 2.4, the bottom and top portion of the numerical model in the study considered fix and free, respectively. The energy absorbing boundary were applied to the right side of the model as the boundary condition.

The failure criterion for simulation of the soil behavior in the above study was the Mohr-Coulomb shear failure criterion. According to Figure 2.5, the shear behavior of granular soils under cyclic loading was simulated by a non-linear and hysteretic constitutive relation that follows the Masing rule during unloading and reloading (Finn, W.D.L., Yogendrakimar and Yoshida, 1986).

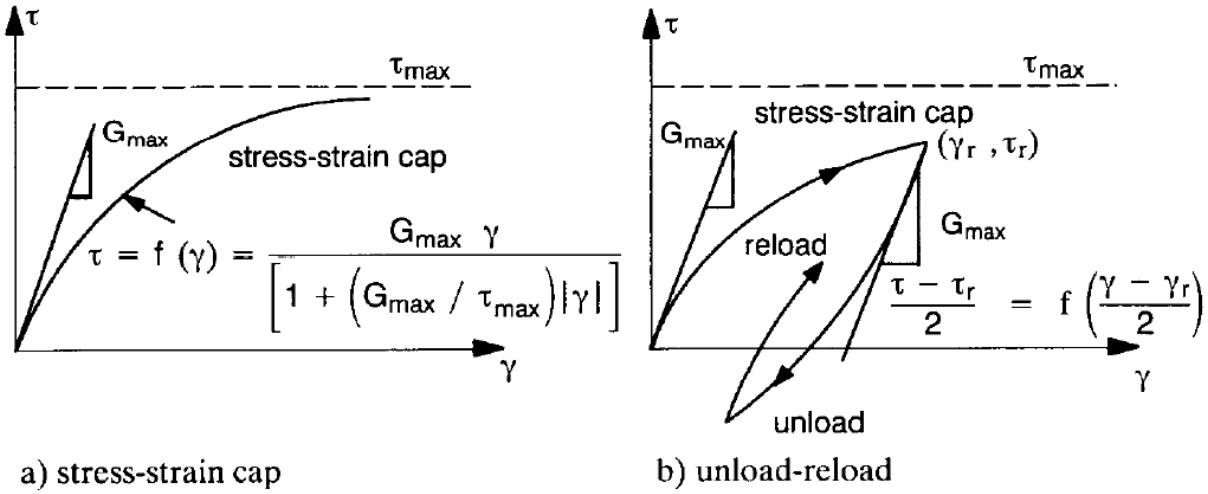

Figure 2.5. The failure criterion used in Cai and Bathurst study (1995)

Equation 1 shows the relation between shear stress τ and shear strain ɣ for the initial loading phase.

$$\tau = f(\gamma) = \frac{G_{max}\gamma}{[1+(G_{max}/\tau_{max})|\gamma|]} \quad (2\text{-}1)$$

Where,

G: Initial shear modulus

τ_{max}: Maximum shear stress

The Masing stress-strain relation for the unloading or reloading condition was obtained by follow equation (Cai and Bathurst, 1995):

$$\frac{\tau-\tau_r}{2} = \frac{G_{max}(\gamma-\gamma_r)/2}{[1+(G_{max}/2\tau_{max})|\gamma-\gamma_r|]} \quad (2\text{-}2)$$

Where, γ_r and τ_r, are the stress state at which the shear stress reverses direction.

According to Figure 2.6, in Cai and Bathurst study, the base reference acceleration time-history used in the dynamic analysis was a scaled El-Centro 1940 earthquake record. Based on spectrum analysis of the input acceleration record, the dominant frequency range obtained was between 0.5 Hz and 2 Hz. Figure 2.7 shows the displacement-time histories at selected locations along the retaining wall face due to the ground excitation with a peak acceleration of 0.25g (Cai and Bathurst, 1995).

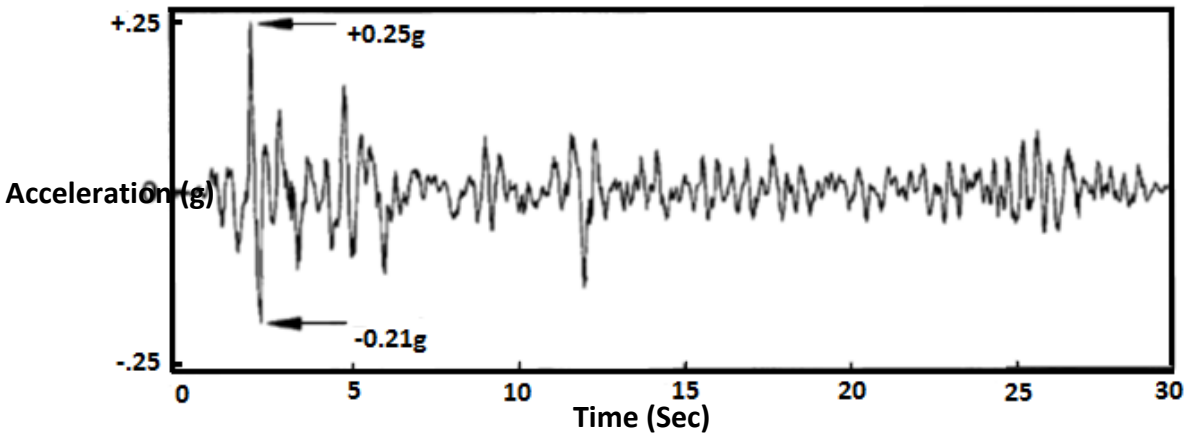

Figure 2.6. Acceleration time-history of base reference input acceleration in Cai and Bathurst study (1995)

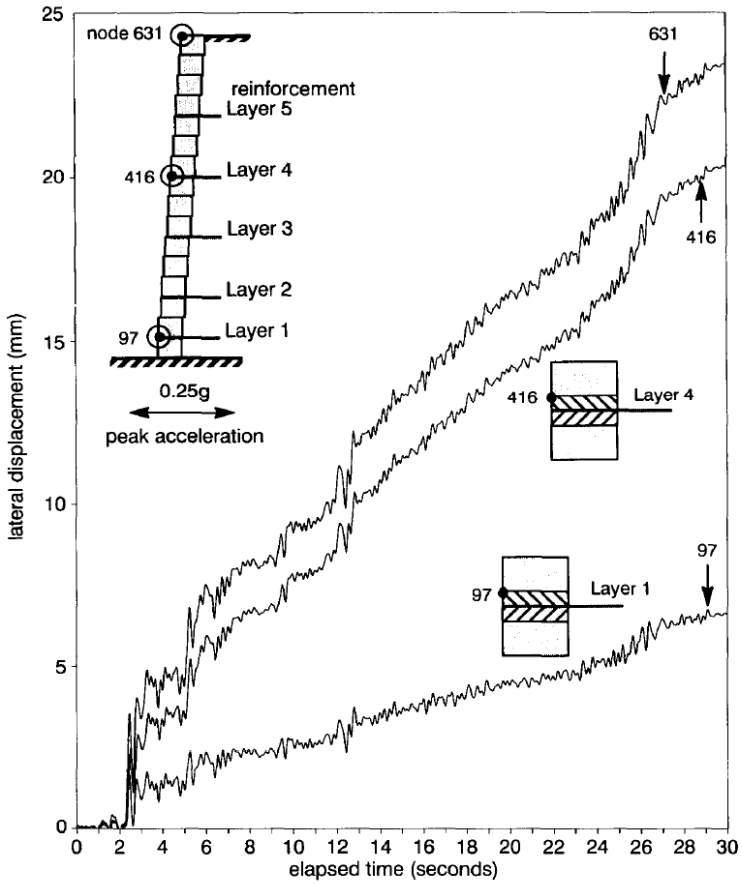

Figure 2.7. Displacement time-history at selected locations in Cai and Bathurst study (1995)

Karpurapu and Bathurst (1995), developed a Finite Element model to investigate the behavior of geosynthetic reinforced-soil retaining walls and also the FEM result was compared to the physical modelling (Karpurapu and Bathurst, 1995). A schematic diagram of the retaining wall modeled in (Karpurapu and Bathurst, 1995) and the instruments installed for monitoring the structure is shown in Figure 2.8.

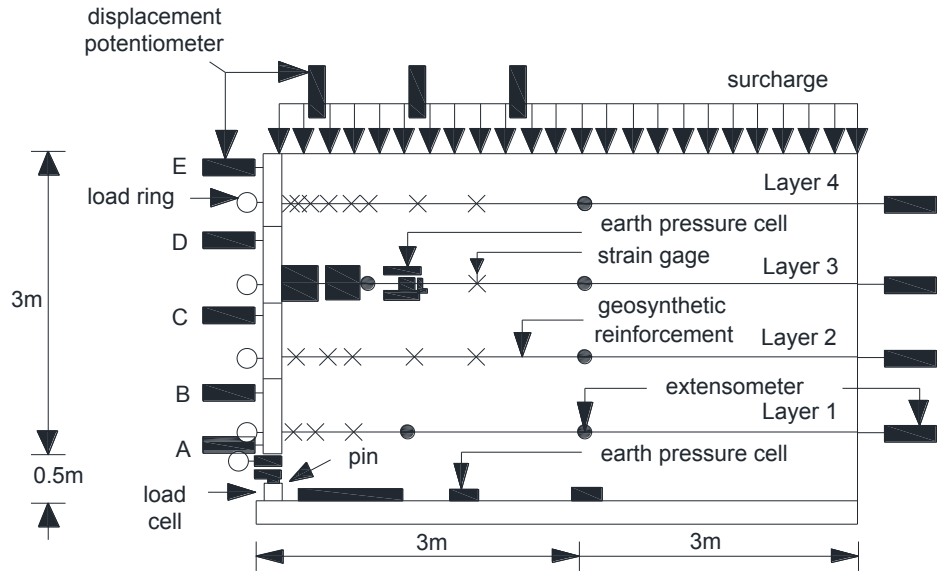

Figure 2.8. Initial configuration of the retaining wall and the instruments that was installed for monitoring in Karpurapu and Bathurst work (1995)

Figure 2.9 shows the initial configuration of Finite Element analysis in Karpurapu and Bathurst research.

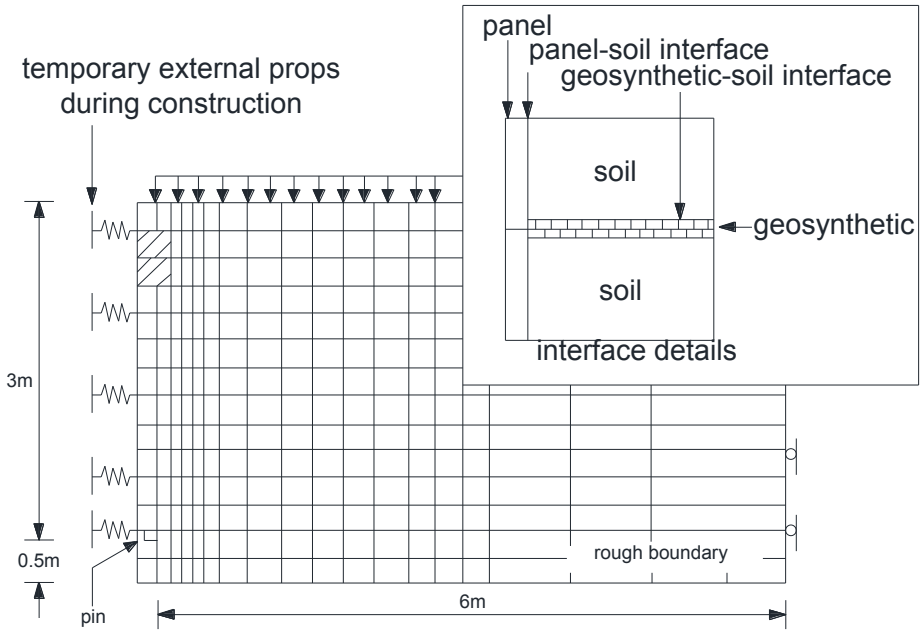

Figure 2.9. Finite element mesh for simulation retaining wall in Karpurapu and Bathurst work (1995)

According to Figure 2.9, the bottom of Finite Element model was fixed in both X and Y directions. The right side was fixed in X direction. The surcharge pressure was applied on the top of the model in increments of 0.25 KPa per load step.

In the above study, a modified form of hyperbolic constitutive model was used for simulation of the soil behavior with a minimum number of parameters. Furthermore, the related parameters were obtained by routine laboratory testing. Also, for simulation of reinforced soil structures, the stick-slip type models and hyperbolic models were used. In addition, the interface parameters between the wall panels and backfill soil were determined by direct shear test and pull out test.

For considering time history in dynamic analysis, the l00 hour isochronous curve used in the models since the surcharge pressure increments applied in roughly 100 hour time steps in the physical experiments.

Also, some of the numerical models were performed with a soil dilation value of 0 (ψ=0) and 15 degree (ψ=15). Figures 2.10 shows a comparison of the wall displacements, which were obtained from the numerical modeling and laboratory measurement.

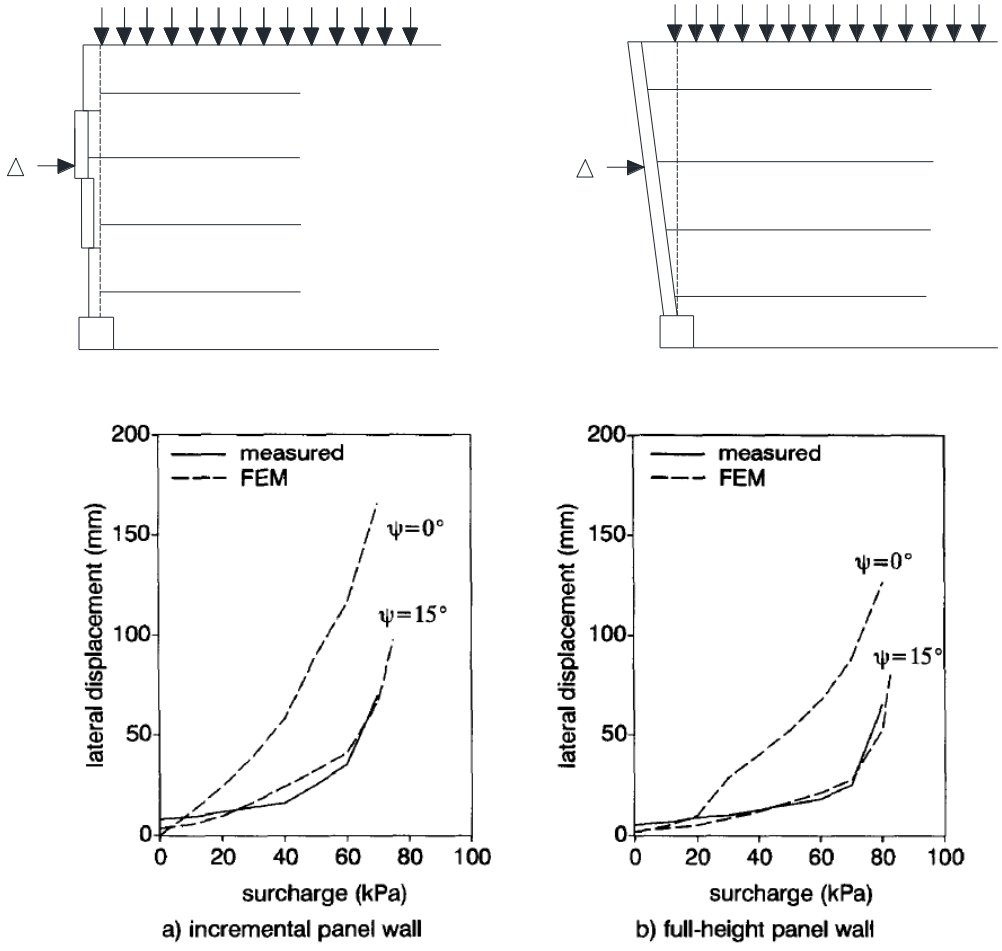

Figure 2.10. Lateral panel displacements at the end of surcharge increments in Karpurapu and Bathurst work (1995)

Ling et al, (1995), developed a generalized plasticity soil model and also bounding surface geosynthetic model using finite element method to investigate the behavior of geosynthetic-reinforced soil retaining walls (Ling et al. 1995). The configuration of the Public Works Research Institute Wall (PWRI) as used in Ling et al, (1995) is shown in Figure 2.11.

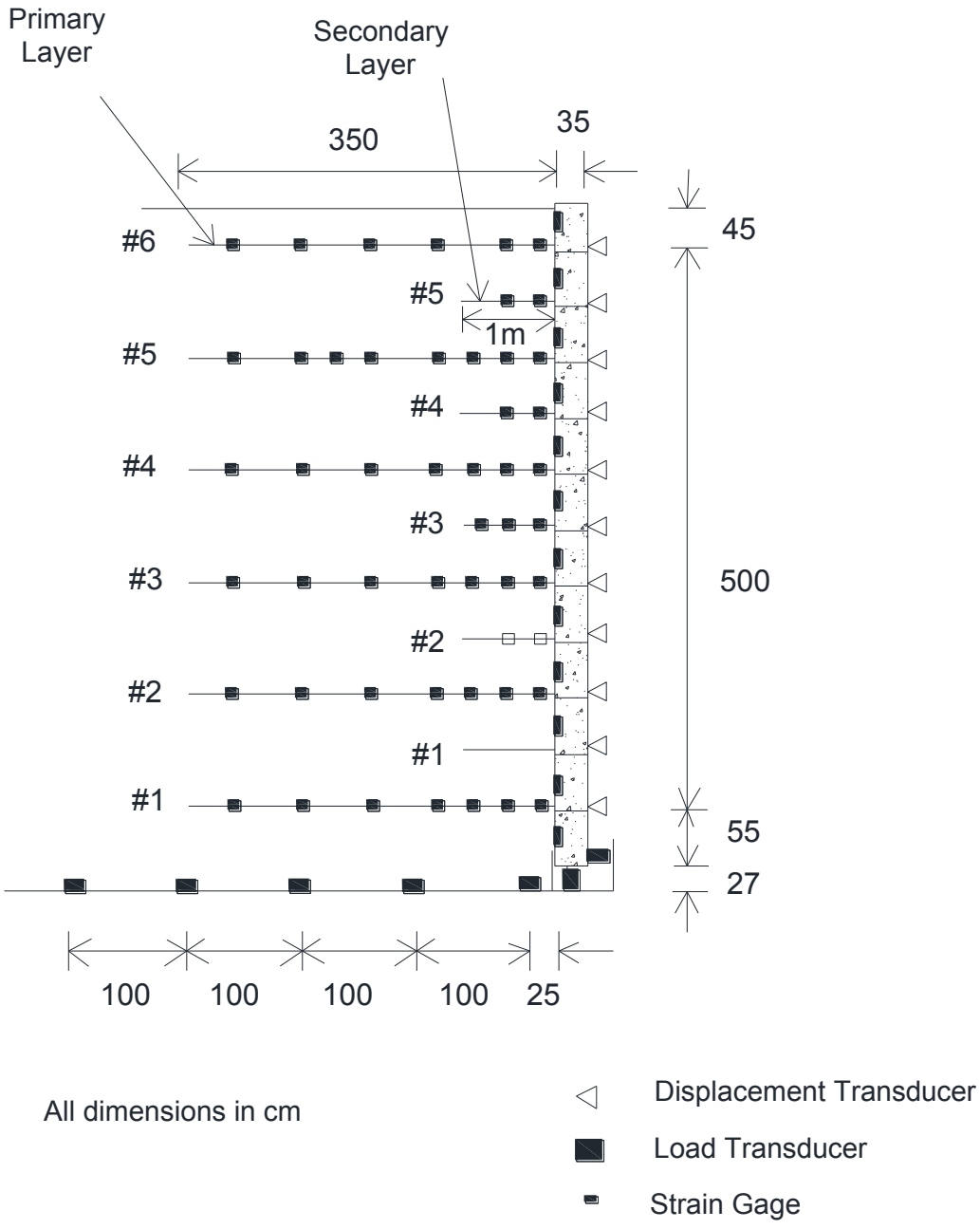

Figure 2.11. Public works research institute wall in Ling et al, study (1995)

In Ling et al. study, the finite element analysis for both PWRI (Public Works Research Institute) and centrifuge retaining walls were done under two-dimensional plane strain condition by a modified version of Diana–Swandyne-II (Zienkiewicz et al. 1998). The typical finite element mesh for the retaining wall model is shown in Figure 2.12.

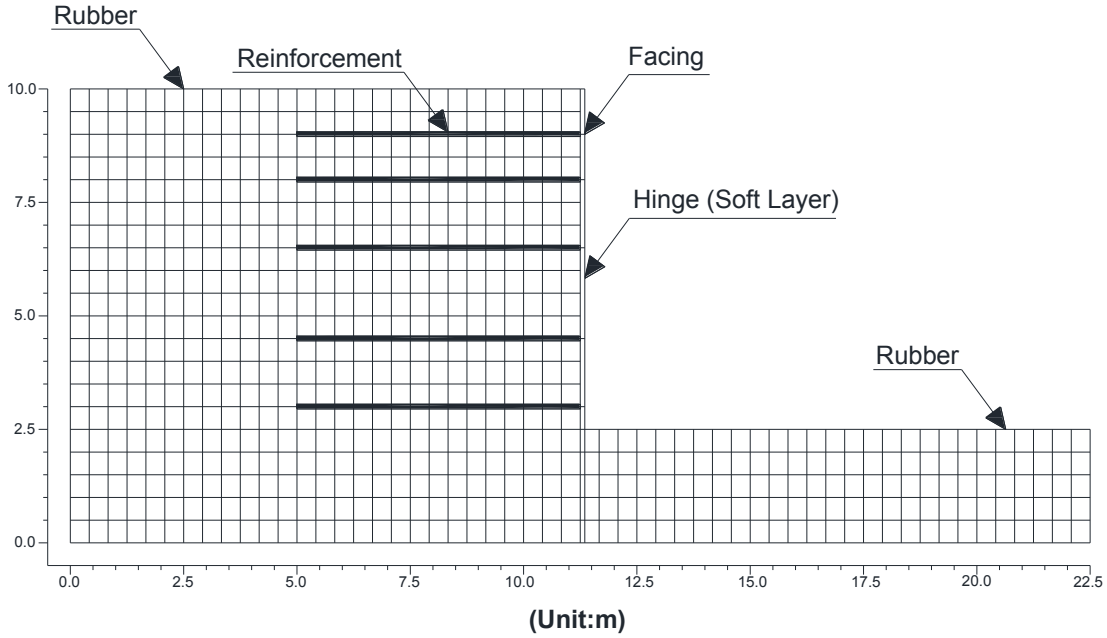

Figure 2.12. Initial configuration of finite element mesh in Ling et al, study (1995)

According to Figure 2.12, in Ling et al, (1995) for both right and left sides of the numerical model, rubber forms used as a boundary wave absorbers. The bottom of the model is fixed in both directions X and Y, and the top of the model was free.

The above model used the Mohr-Coulomb failure criteria with tension cutoff for modelling the soil behavior. A generalized plasticity soil model (Ling and Liu, 2003) was used to simulate the soil behavior. This behavior of soil, was an improvement over the Pastor–Zienkiewicz–Chan model (Pastor and Chan, 1990), which was developed specifically for simulating the behavior of sands under dynamic loading. The generalized plasticity soil model needed 15 parameters for simulating cyclic loading, in which Ling et al. study of these parameters were obtained from static tests. In addition, for simulation of the behavior of a wall, Ling et al, (1995) used a series of five shaking table tests. In the centrifugal shaking table tests, 20 cycle sinusoidal wave with 2 Hz frequency and of acceleration amplitude of 0.2g were used and the results were compared with the results of analysis. According to Figure 2.13, the horizontal displacements of the facing wall, the

lateral stress distributions behind the wall and the vertical stress distributions at the foundation, were compared to the measured values for the different fill heights during the course of construction.

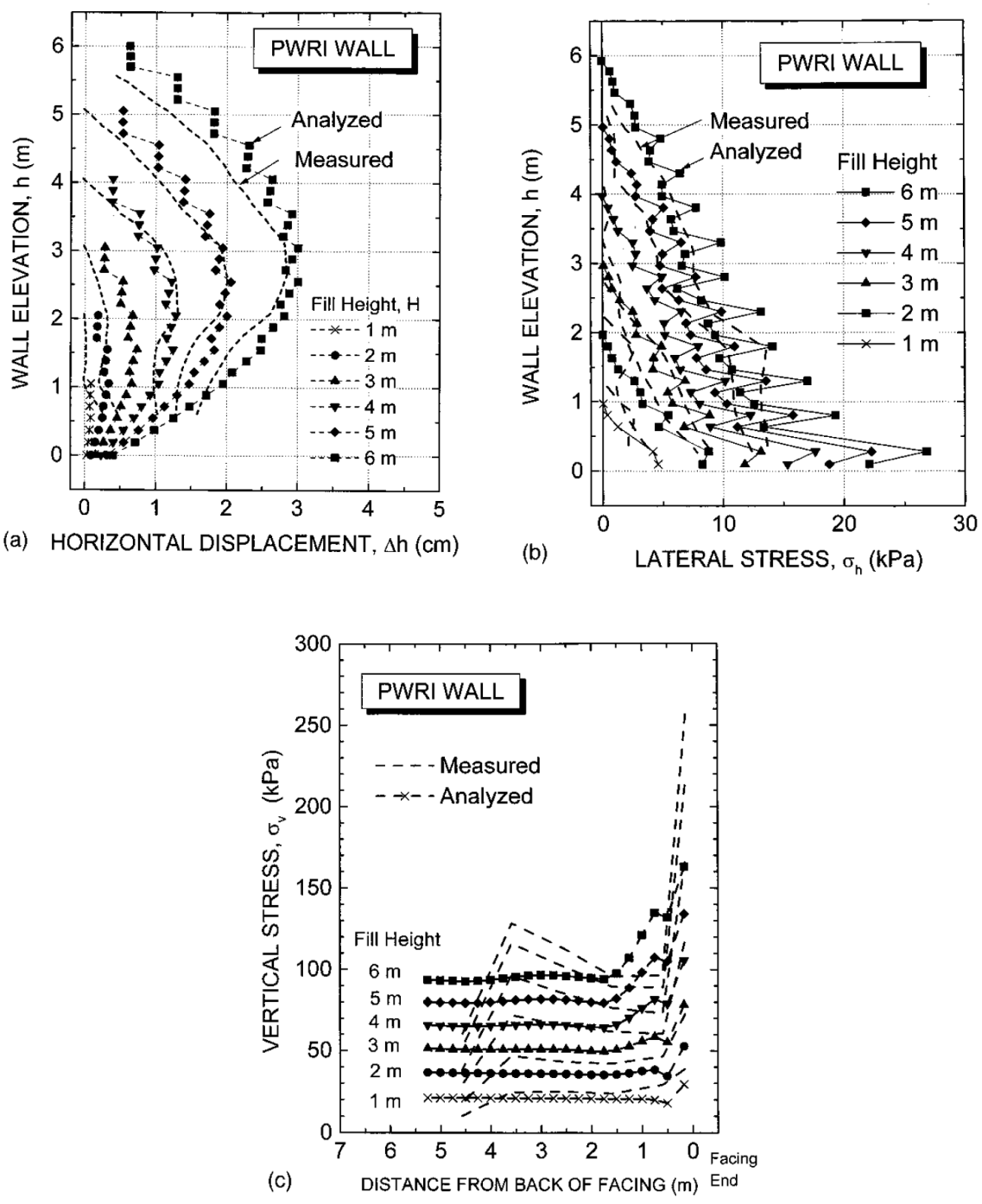

Figure 2.13. Public Works Research Institute Wall results; a) Facing horizontal displacement, b) Lateral earth pressure, c) Vertical stress (Ling et al. 2004)

Ling et al. (2005), in another study, carried out a parametric study on the behavior of reinforced-soil wall under earthquake loading by finite element method. In that study, the effects of soil properties, earthquake motions, and reinforcement layouts were considered.

In the above study, a series of two-dimensional plane strain finite element models were analyzed using a modified version of Diana-Swandyne-II program (Zienkiewicz et al. 1998). The base case of the Finite Element mesh is illustrated in Figure 2.14.

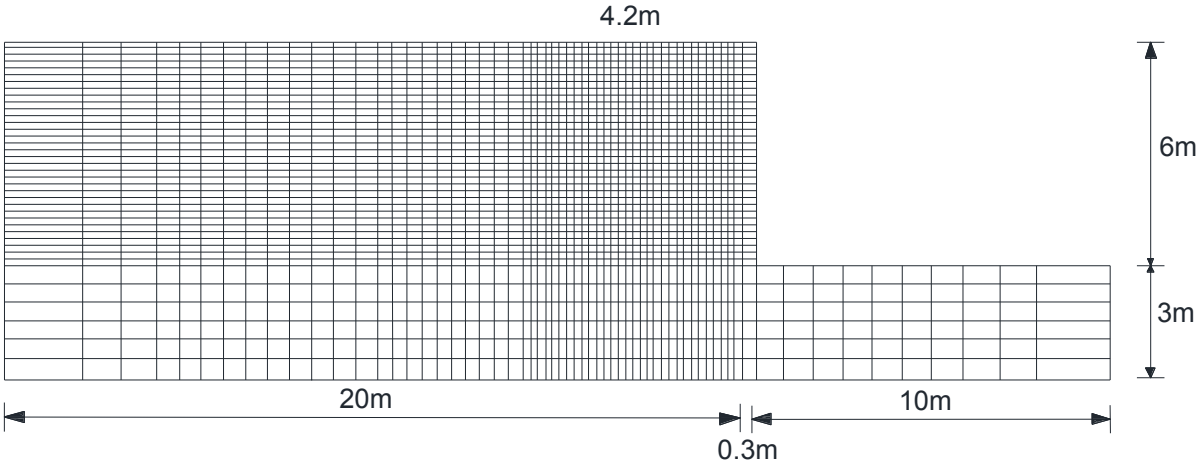

Figure 2.14. Initial configuration of finite element mesh in Ling et al, study (2005)

To eliminate the effect of artificial boundary on the structure, the right side of the model extended to a distance of 10 m. Furthermore, the side boundaries (left and right) of model were rollers as boundary wave absorbers whereas velocities fixed in the bottom. In the dynamic analysis, to prevent the reflection of the boundary waves, the columns of elements close to the side boundaries assigned softer elastic properties and larger width.

Soil failure criteria used in the Ling et al study (Ling et al. 2005) was Mohr-Coulomb failure criteria to simulate block–block and soil–block interactions.

In order to apply seismic analysis, which, several earthquake motions used in dynamic models as shown in Figure 2.15.

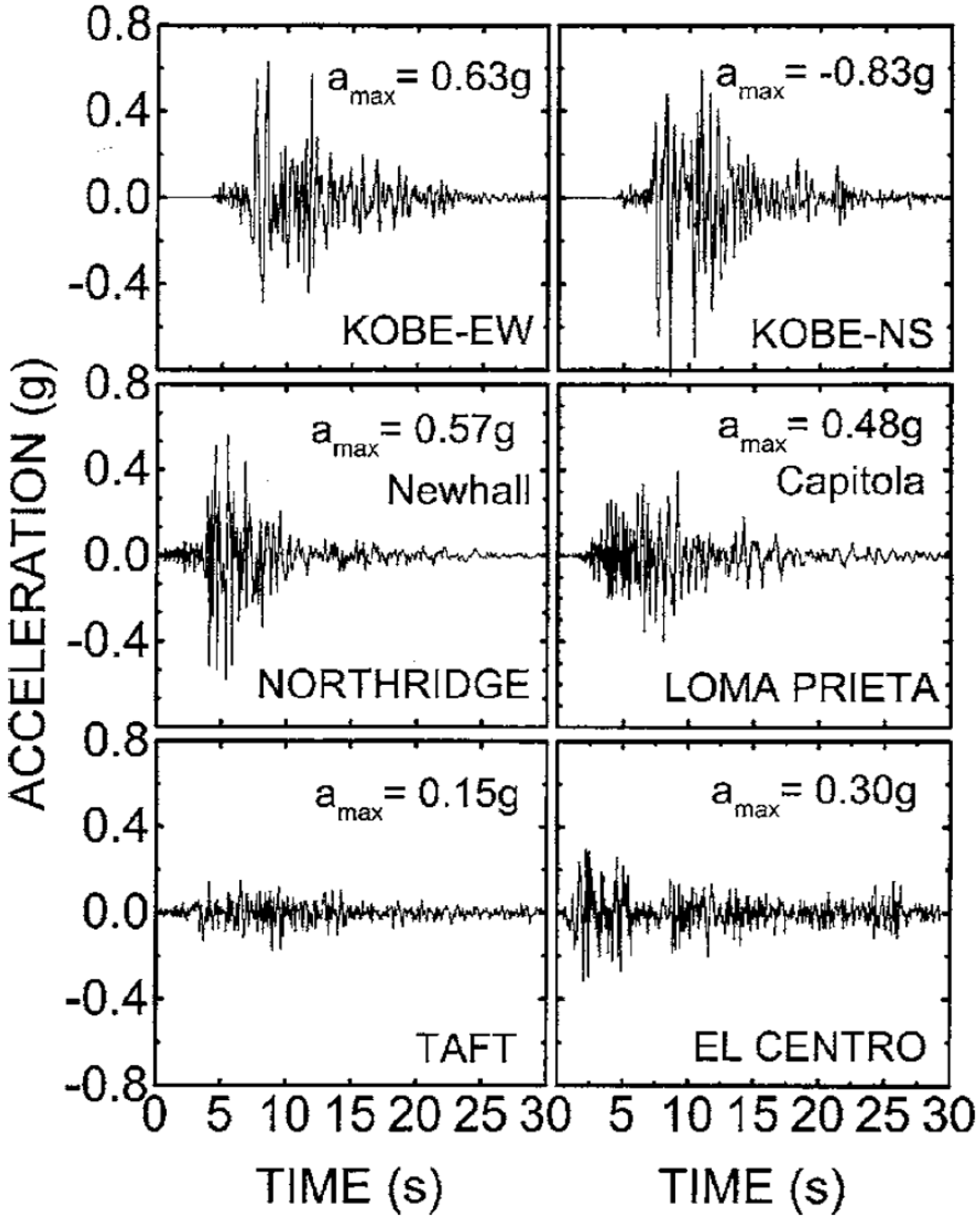

Figure 2.15. Earthquake motions used in Ling et al, study (2005)

Figure 2.16 illustrates the effect of earthquake motions on the wall performance in Ling et al. study (2005) for three different parameters; facing lateral displacement, maximum reinforcement (Geosynthetic) and lateral earth pressure behind facing.

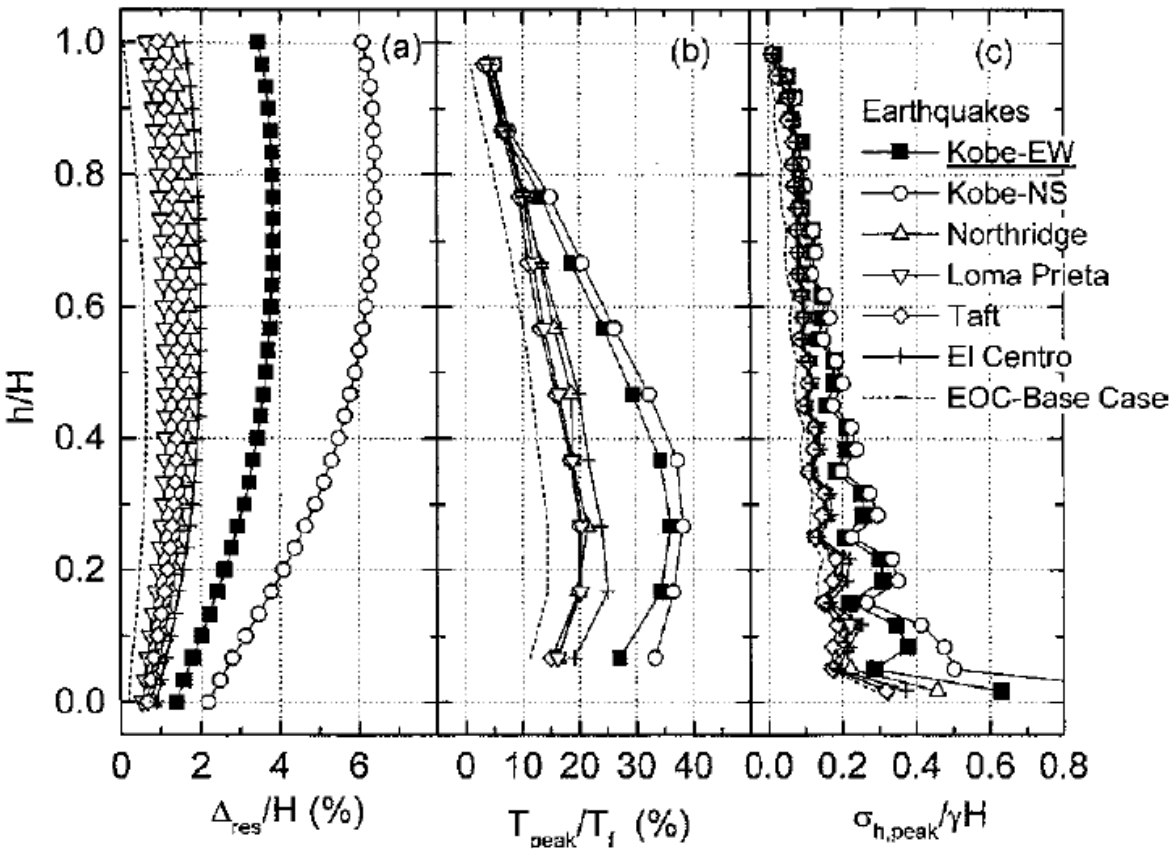

Figure 2.16. Effect of earthquake motions on seismic wall performance; a) facing lateral displacement; b) Maximum reinforcement; c) lateral earth pressure behind facing in Ling et al. study (2005)

Bathurst and Hatami (2001), investigated the effect of different design parameters on dynamic response of a geosynthetic reinforced-soil retaining wall by using numerical analysis. The FDM was used to simulate the dynamic models in that study (Hatami and Bathurst, 2001).

Initial configuration of the retaining wall and the zoning of finite difference model is demonstrated in Figure 2.17.

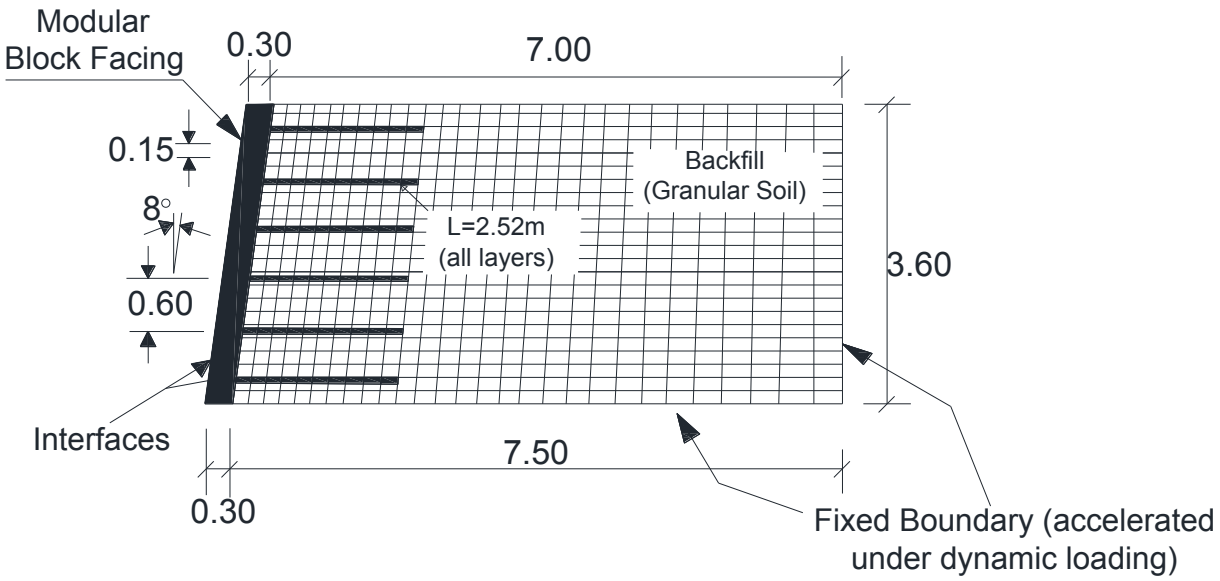

Figure 2.17. Finite difference mesh of retaining wall in Bathurst and Hatami study (2001)

In the finite difference model in Bathurst and Hatami study (2001), the right side and the bottom boundary were fixed and the top of model was free in both X and Y direction. The backfill soil was simulated base on the Mohr-Coulomb failure criterion.

In order to conduct dynamic analysis in the above study, a series of 8 ground motions as shown in Figure 2.18 were selected and used as input accelerograms to the retaining wall model (Naumoski et al. 1993). Furthermore, Figure 2.19 shows the time histories of lateral displacement at the top of the wall for 8 ground motion recorded as input acceleration.

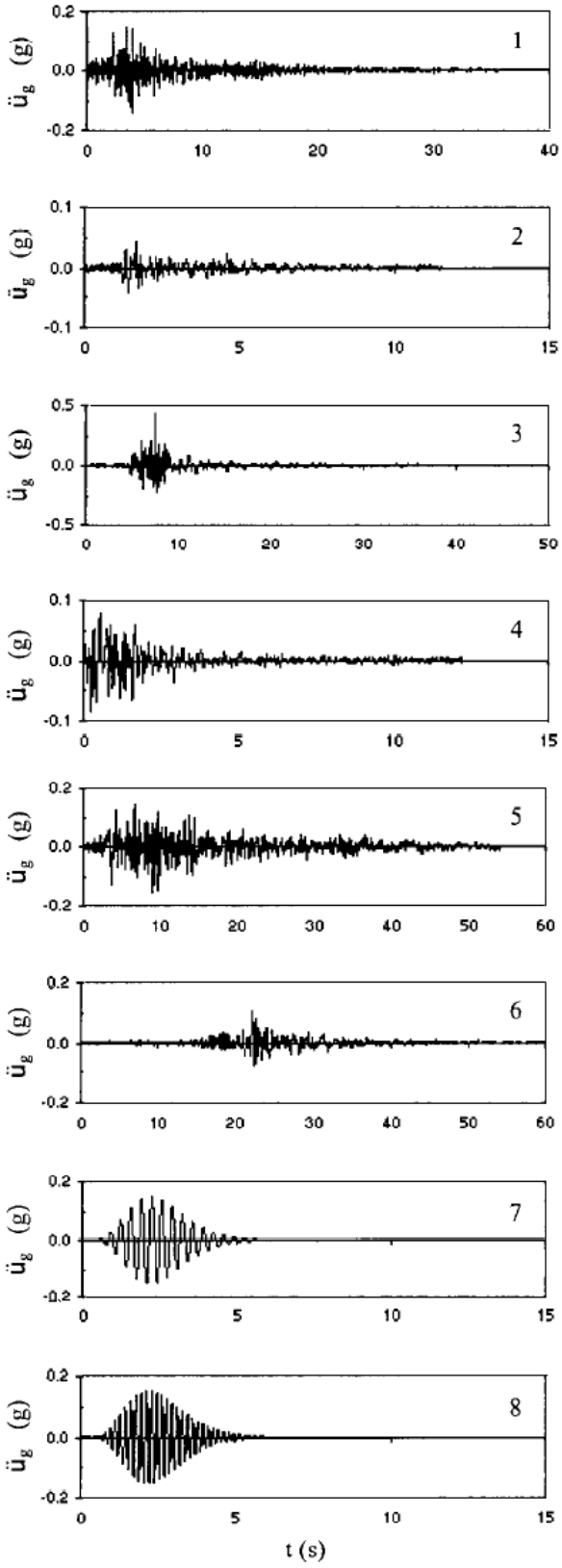

Figure 2.18. Input acceleration histories applied to dynamic models in Bathurst and Hatami study (2001)

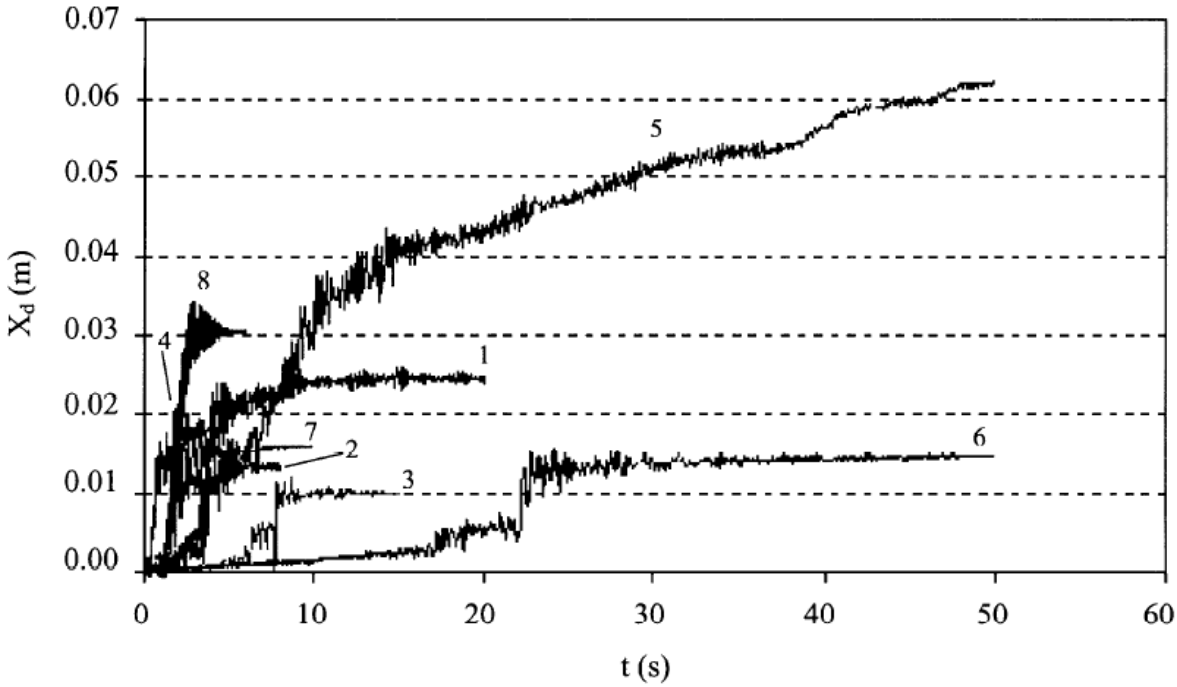

Figure 2.19. Time history of facing lateral displacement at the top of wall for 8 ground motion recorded in Bathurst and Hatami study (2001)

The response of reinforced soil retaining walls to base acceleration using a series of reduced-scale shaking table tests and numerical modeling (Finite Difference method) was investigated in El-Emam et al., study (2004). In that study, the numerical modelling results obtained from the FLAC code (1998) were verified by physical test results.

Figure 2.20 shows the initial configuration of a plain-strain Finite Difference analysis in the research reported in (El-Emam et al. 2004).

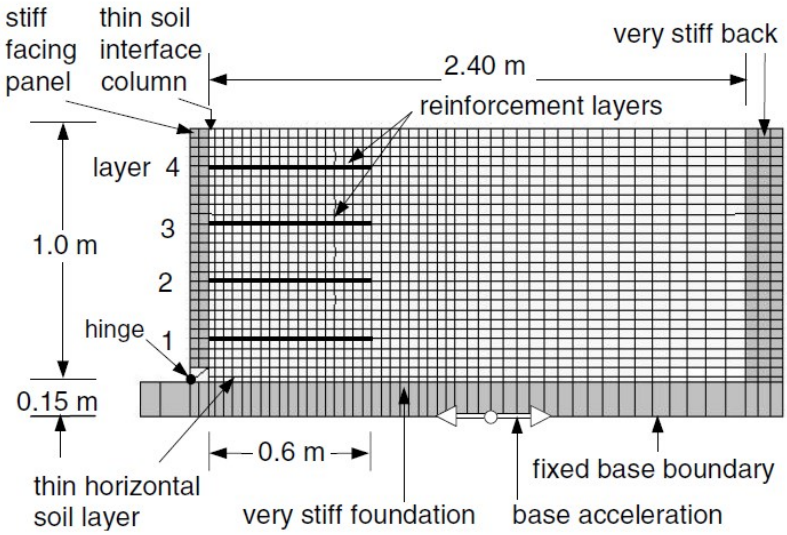

Figure 2.20. Initial configuration of Finite difference mesh for soil model retaining wall in El-Emam et al. research (2004)

According to Figure 2.20, the bottom of the numerical model has a fixed base. For right side of the model used very stiff material as well as a facing panel. Also, the top of the numerical model was free in both X and Y directions. Moreover, the material properties used in (El-Emam et al. 2004) followed Mohr-Coulomb failure criterion. As the input earthquake motion, a stepped-amplitude sinusoidal velocity function with a frequency of 5 Hz and zero vertical velocity was applied horizontally to all nodes on the boundary at the foundation level. According to the Figure 2.21, the input velocity amplitude was increased every 5 seconds in steps of 0.05g base acceleration increments until excessive deformation occurred.

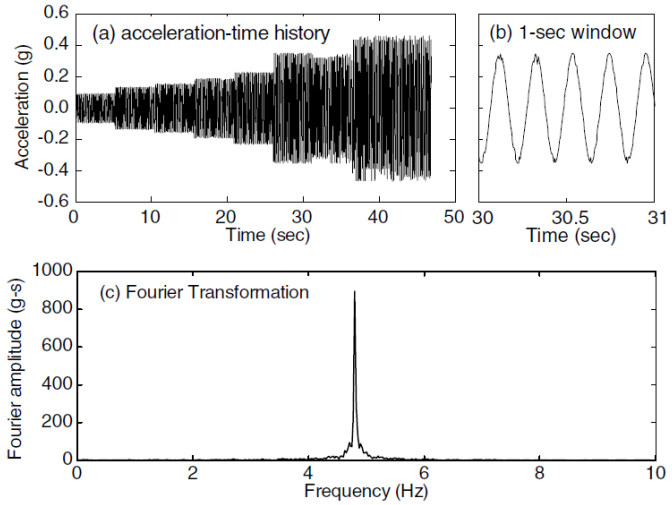

Figure 2.21. Input base acceleration used in dynamic models in El-Emam et al. research (2004)

Typical deformation shapes for both numerical and physical models are shown in Figure 2.22.

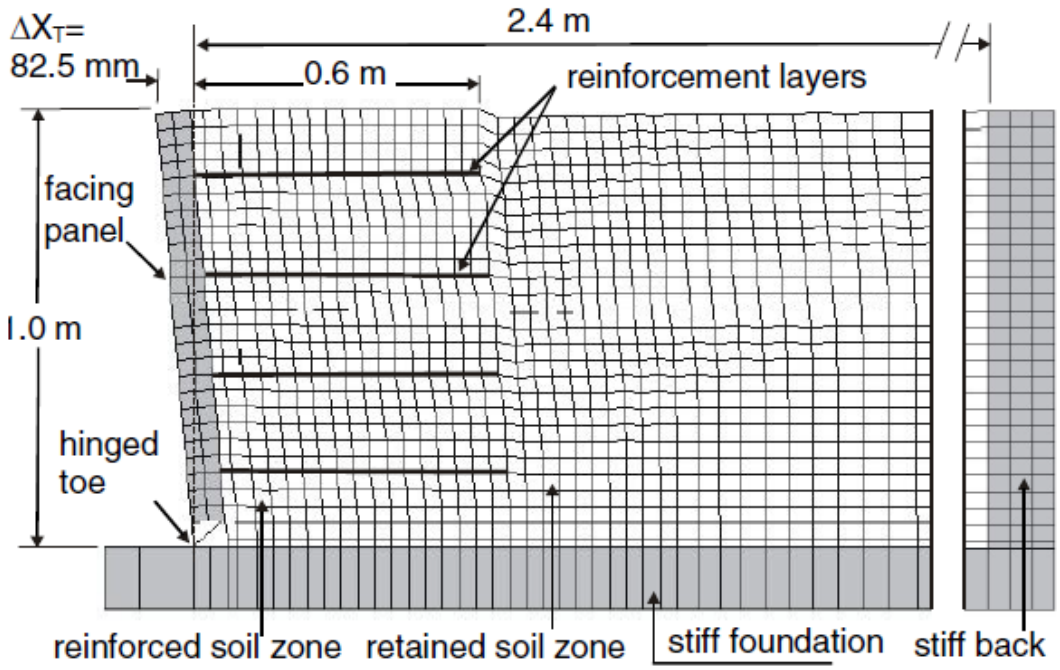

a) numerical model deformation

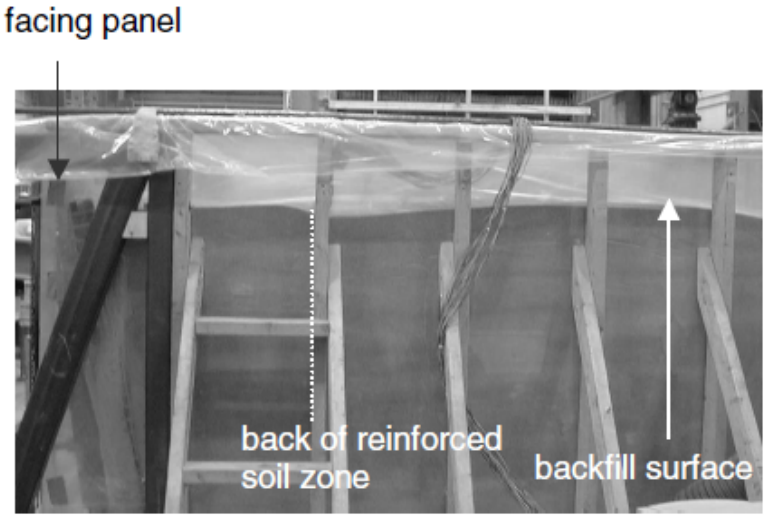

b) reduced-scale shaking table model

Figure 2.22. Numerical and physical model deformation in El-Emam et al. research (2004)

Callisto and Soccodato (2007) presented the result of the dynamic numerical analysis of a cantilever retaining wall confined in a coarse-grained soil. In that study, the retaining wall was designed using the pseudo static method and a small seismic coefficient and a recorded acceleration time-history was considered, which was applied to the bedrock level. The numerical simulation was based on a hysteretic soil model following a plastic yield criterion.

The initial configuration of the finite difference grid of retaining wall with an excavation in Callisto and Soccodato study is illustrated in Figure 2.23.

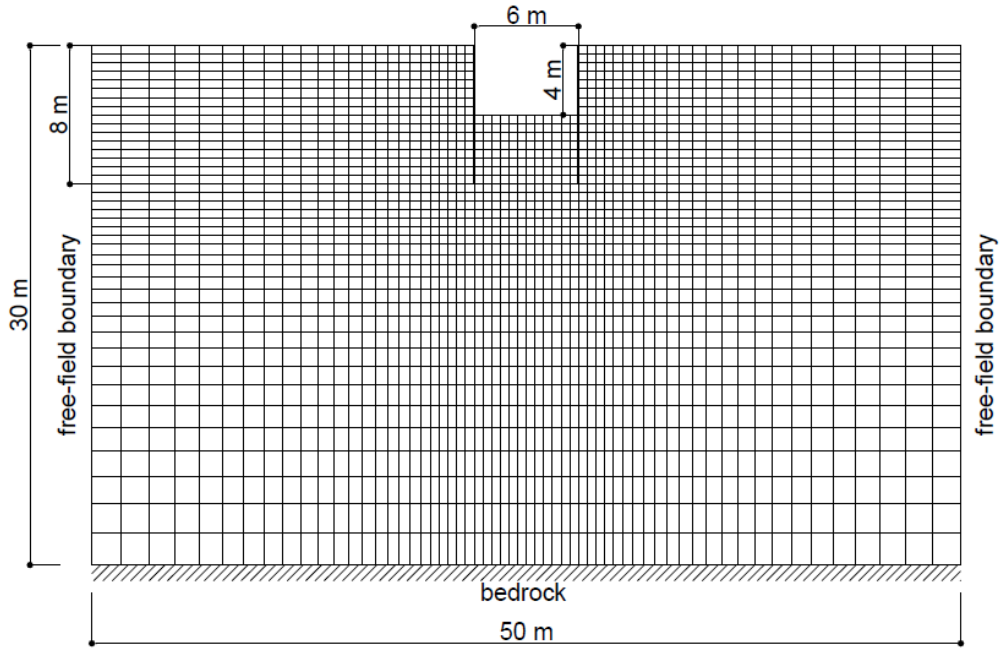

Figure 2.23. Initial configuration of finite difference of retaining structure in Callisto and Soccodato study (2007)

According to Figure 2.23, the bottom of the model in (Callisto and Soccodato, 2007) consists of bed rock and the acceleration time-history was applied to that level. On the right and left side of model, the dynamic boundary applied as quiet boundaries (Lysmer and Kuhlemeyer, 1969) that in turn were connected to free-field boundaries. In that study an elastic-perfectly plastic soil model with a Mohr-Coulomb failure criterion was used to simulate the soil behavior.

Also, in that study, dynamic models conducted in one-dimensional conditions by applying the vertical propagation of shear waves. In the first step, single frequency acceleration pulses (Ricker wavelets) applied as input data. Then, according to a database of the Italian acceleration time histories recorded on rock a real seismic recording data was used. Actually, in dynamic model, the

Tolmezzo NS time-history was applied which was characterized by the highest Arias Intensity Ia = 0.79 m/s and by a peak acceleration a_{max} = 0.357g. Also, the accelerations were chosen to be 0.35 g according to the Italian code and the maximum acceleration on rock associated to a return period of 475 years.

The deformation of the wall and the ground surface in Callisto and Soccodato model is shown in Figure 2.24.

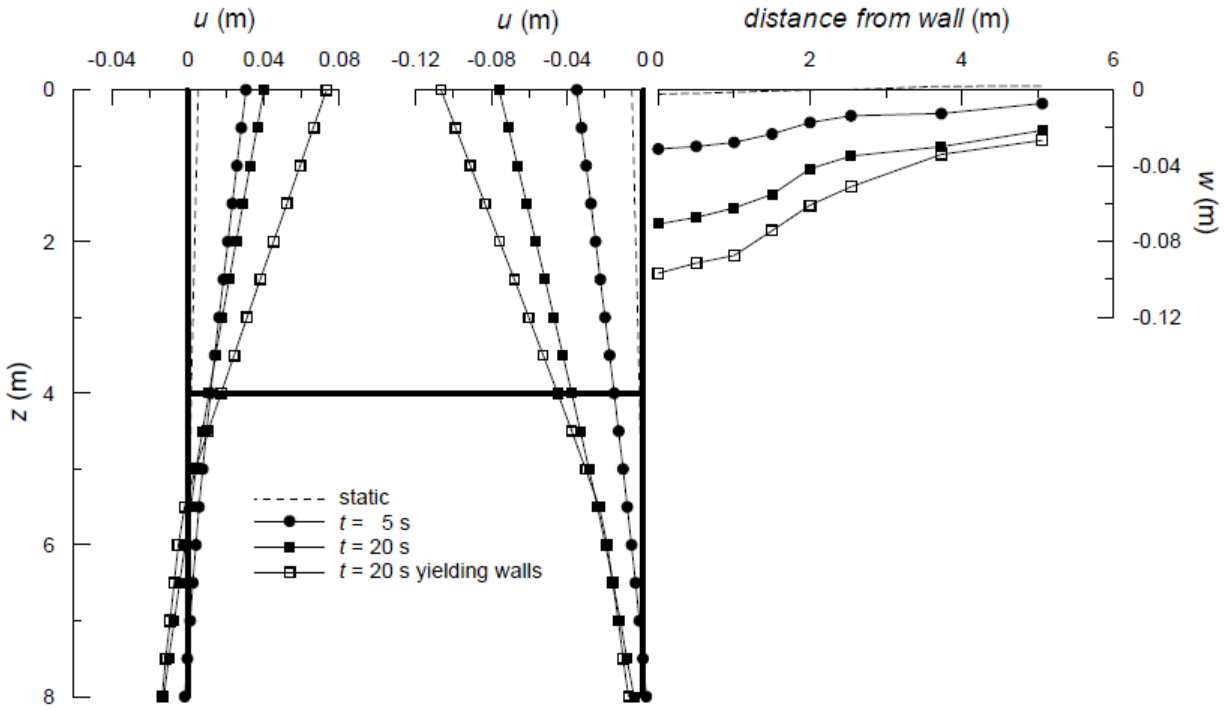

Figure 2.24. Walls deformation and ground surface in Callisto and Soccodato model (2007)

Green and Ebeling (2003), presented the dynamic response of cantilever earth-retaining walls using finite difference method and FLAC software. Green and Ebeling determined the wall and soil model parameters and simulated the wall-soil interface. The numerical results were compared with the results of a simplified techniques for computing dynamic earth pressures and permanent wall displacements (Green and Ebeling, 2003). The initial configuration of cantilever earth-retaining walls in Green and Ebeling study is illustrated in Figure 2.25.

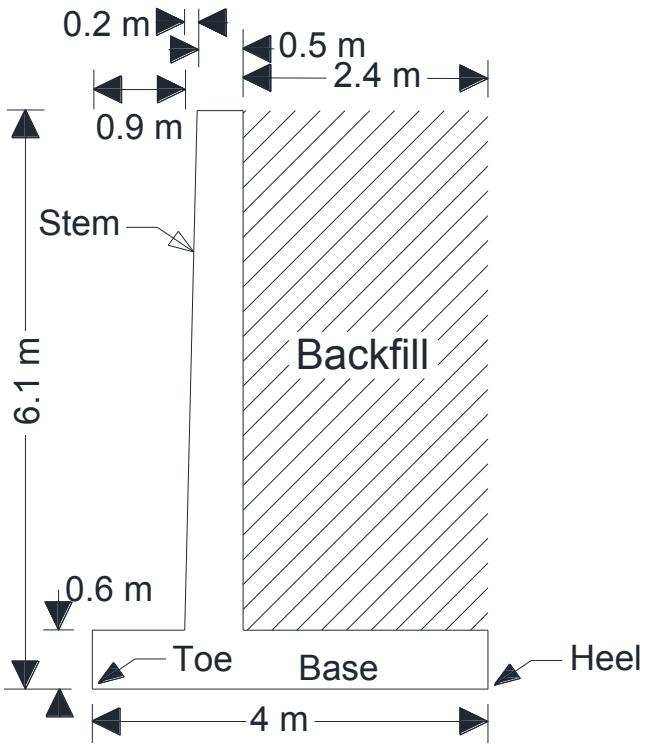

Figure 2.25. Initial configuration of finite element model of cantilever earth-retaining wall in Green and Ebeling study (2003)

The FLAC model base on finite difference method in Green and Ebeling study is shown in Figure 2.26.

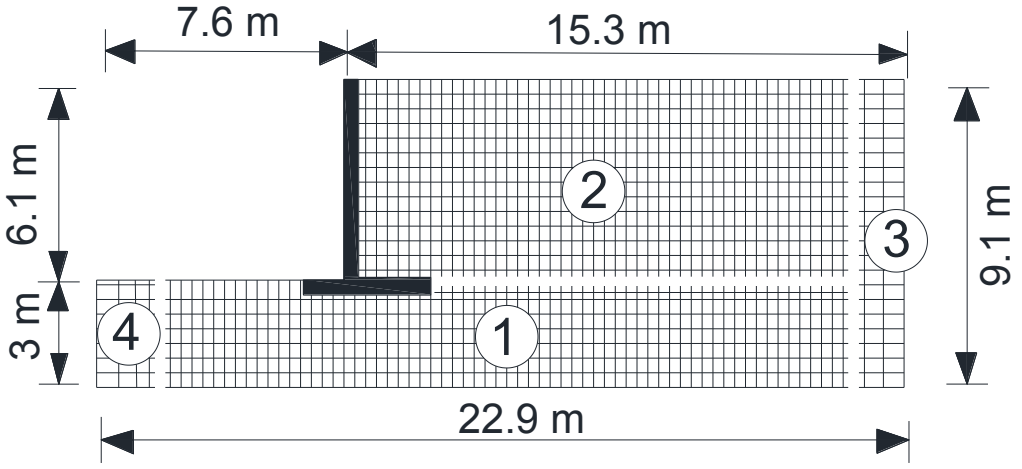

Figure 2.26. Finite difference mesh using FLAC software in Green and Ebeling study (2003)

In the FLAC models in (Green and Ebeling, 2003), the boundaries condition was applied according to time-history recorded of Loma Prieta earthquake (1989). Also, an elasto-plastic constitutive model based on Mohr-Coulomb failure criterion was used to model the soil behavior.

In the above study, a free-field acceleration time-history recorded at the surface of a USGS site class B profile during the 1989 Loma Prieta earthquake was used in dynamic analysis. Also, a 1-D site response analysis performed using a modified version of SHAKE91 (Idriss & Sun 1992). Also, Figure 2.27 shown the comparisons of the wall displacement which is obtained by numerical modeling (FLAC software) and Newmark sliding block analyses (Newmark 1965).

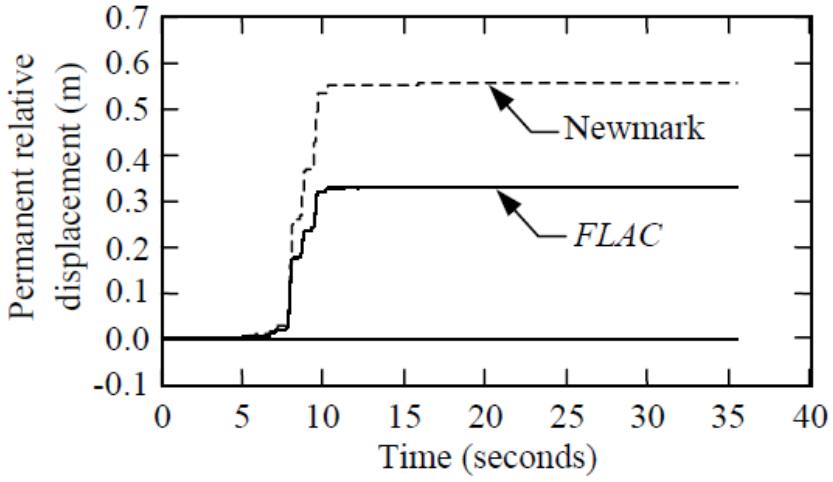

Figure 2.27. Comparison of the wall displacement from FLAC results and Newmark sliding block analysis in Green and Ebeling study (2003)

Parihar and Saxena (2010) investigated the effects of wall-soil-structure interaction on seismic response of retaining walls. They used a FE numerical approach to examine wall-soil interaction as a continuum or with interface and its effect on earthquake conditions. The deformation process was modeled based on a plane strain condition and used input acceleration in the form of a typical earthquake motion. The cantilever retaining wall used in (Parihar and Saxena, 2010) is shown in Figure 2.28.

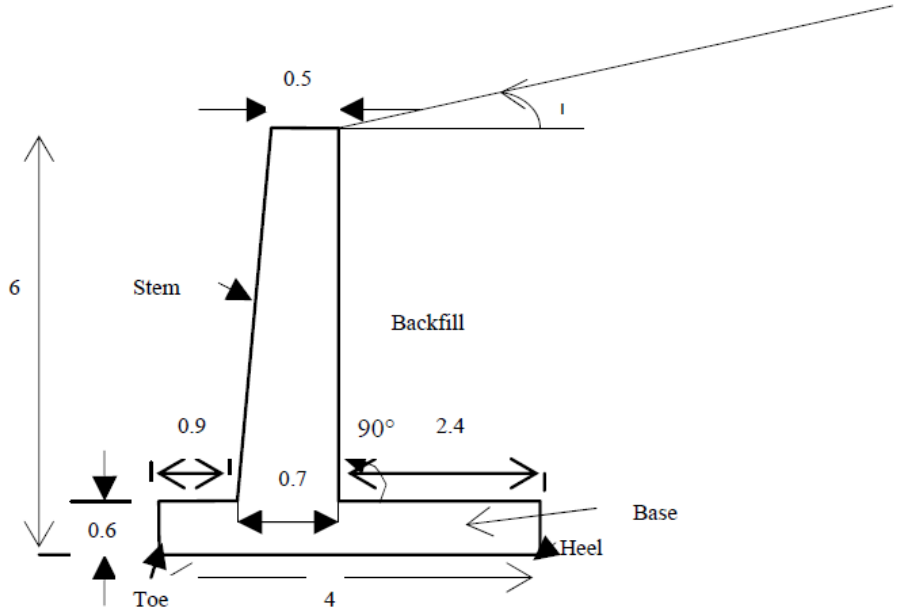

- *All dimensions are in meter (m).*

Figure 2.28. Geometrical parameters of cantilever retaining wall in Parihar and Saxena study (2010)

The plane-strain two-dimensional finite element model used in Parihar and Saxena study is shown in Figure 2.29.

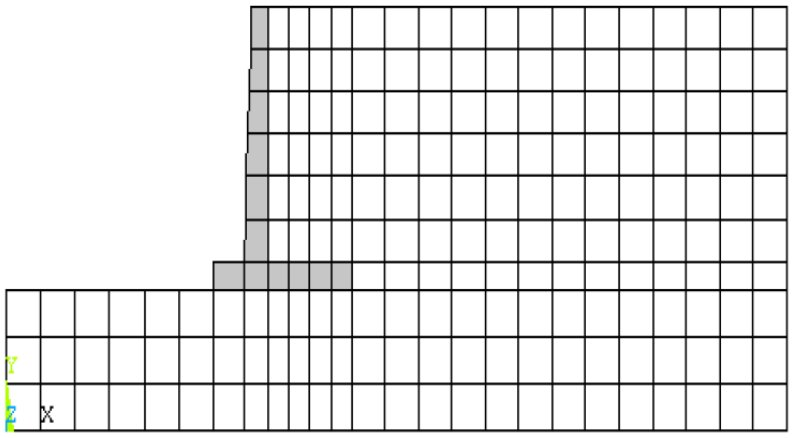

Figure 2.29. Zoning of finite element model in Parihar and Saxena study (2010)

In Parihar and Saxena study, in the backfill section, the artificial boundary was put at 2.5 times the height of wall towards the heel side and equal to the height of the wall towards toe side. And also, the right and left side were fixed in both X and Y direction. In the foundation part, the soil

were modelled to a depth of 0.5 times the height of wall and the velocity were fixed in both horizontal and vertical direction.

For dynamic analysis, the 1991 Uttarkashi earthquake with a PGA of 0.242g or 2.372 m/sec^2 were used as input motion data applied to the retaining wall model. Duration of the recorded time-history of the motion was 40 seconds. According to Figure 2.30, most of the peaks occurred within 20 seconds of the motion.

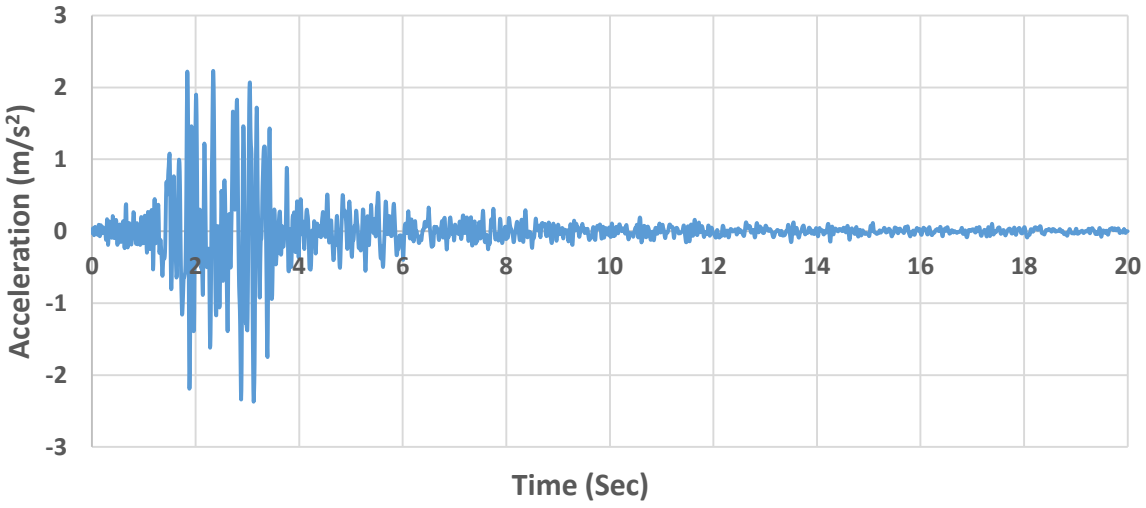

Figure 2.30. Input time-history in Parihar and Saxena study (2010)

Krishna (2010) investigated seismic lateral earth pressure on retaining wall structure using the Finite Difference method. In that study, the behavior of cantilever retaining walls under dynamic loading was simulated using the FLAC software (Itasca, 2008).

Two-dimensional numerical model using Finite Difference method and FLAC software in that research is illustrated in Figure 2.31.

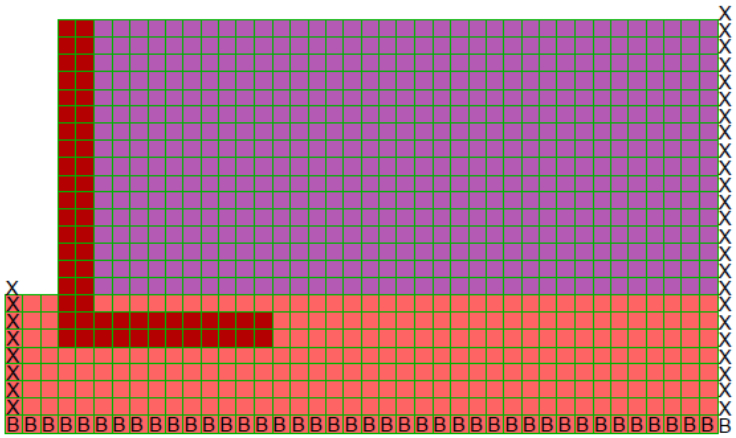

Figure 2.31. Finite difference mesh of cantilever retaining wall in Krishna research (2010)

According to Figure 2.31, the right and left side of the numerical model in (Krishna, 2010) was fixed in X direction and the bottom was fixed in both X and Y directions. The back fill material was simulated as Mohr-Coulomb material with typical properties corresponding to uniform-coarse sand.

The dynamic load applied as a velocity in the form of an excitation of targeted acceleration and frequency. Also, each Finite Element model was set up by 10 cycles of sinusoidal excitation of different acceleration between range of 0.1 to 0.5g and frequency levels of 2Hz to 10 Hz. The variation of seismic earth pressures determined in that study at different acceleration levels is presented in Figure 2.32.

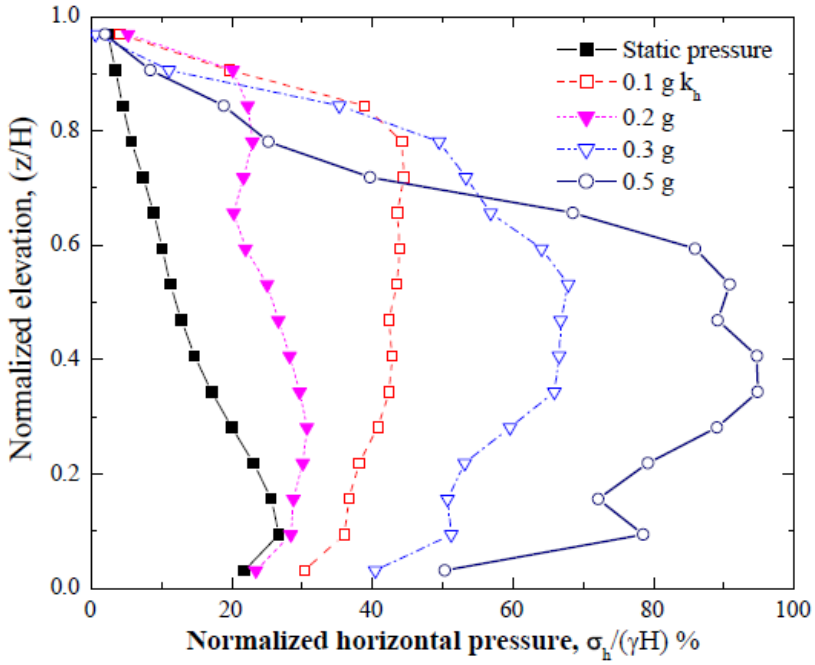

Figure 2.32. Seismic earth pressure at different acceleration levels in Krishna research (2010)

2.4. Summary

All of the studies in literature review have focused on geosynthetic reinforced soil retaining walls and also cantilever earth-retaining walls. Case studies conducted in this chapter were analyzed under earthquake loading condition numerically by either FEM or FDM. Furthermore, a number of research works were conducted on the behavior of wall-soil interface of retaining walls under earthquake loading. Also, they considered the behavior of soil properties and its effects on the behavior of interface between structure and soil under dynamic condition.

The main issues identified in literature review are the lack of adequate studies on wall-soil interface behavior on the dynamic response of earth retaining walls and influence of key parameters. In the current thesis, the validation of the numerical models is carried out based on the work by Parihar and Saxena (2010). In that study, only the effect of wall-soil interface on the retaining wall deformation was investigated, no parametric study or the effect of different earthquakes motions on wall-soil system was reported

Chapter 3. Numerical Modeling of Cantilever Earth-Retaining Wall using Finite Difference Method

3.1. Introduction

Considering the restrictions of the pseudo static limit equilibrium method to simulate both static and dynamic analyses, numerical methods have been developed accordingly. In recent years, numerical methods have become quite powerful in analyzing the static and dynamic behavior of earth retaining structures.

Most of studies conducted with numerical analysis are generally based on the Finite Element Method (FEM) and Finite Difference Method (FDM). In order to investigate the seismic response of reinforced-soil cantilever retaining wall, the Finite Difference Method (FDM) is considered here. At the first step, a static model of cantilever retaining wall is developed in FDM. Then, dynamic analysis is conducted with earthquake ground motion.

Finally, for the purpose of validation, the numerical results are compared with the available published results.

3.2. Retaining wall geometry

The initial configuration of cantilever retaining wall in this study is shown in Figure 3.1. The retaining wall design is conducted according to “basic retaining wall design guideline” as given in (Brooks, 2010).

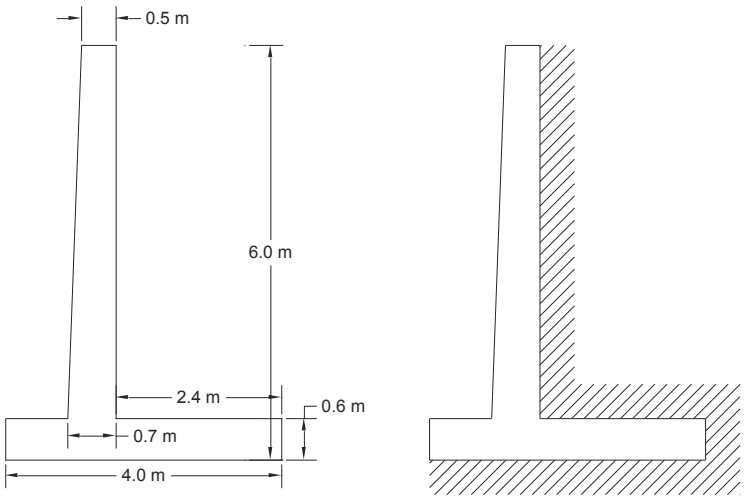

Figure 3.1. Cantilever retaining wall geometry (Brooks, 2010)

3.3. Finite difference method

Finite Difference Method (FDM) is one of the oldest numerical technique used for the solution of sets of differential equations. In the FDM, every derivative in the relative equations is replaced by an algebraic expression written in terms of the field variables such as stress or displacement at separate point within elements. But Finite Element Method (FEM) is a numerical modeling approach in which continuous media is replaced by finite number of elements interconnected at finite number of nodes. This method can be used to calculate the displacement at the nodes and stresses within elements.

3.4. FLAC Model

Most of FDM studies used FLAC software for the simulation of earth retaining wall structure. FLAC is a well-known, commercially available, two-dimensional explicit Finite Difference program based on the Lagrangian formulation. This program simulates the behavior of structures built of soil that can come across with plastic flow when their yield limits are reached. FLAC is widely used in soil and dynamics of soil. In addition, various constitutive models are available in the FLAC and can be modified by the user with minimal effort. FLAC also provides some built-in structural elements, which can be used as reinforcement or structural supports, and interface elements as well (Itasca, 2015). The dynamic option expands FLAC's analysis capability to a wide range of dynamic problems in disciplines such as earthquake engineering, seismology and retaining walls.

In this research, the behavior of interface between the retaining wall structure and the surrounding soil material is investigated using FLAC 8.0 (Itasca, 2015) which uses Finite Difference method.

For fitting the grid to a problem region, it is important to experiment with the model to assess boundary effects. In this study, for the purpose of definition of model boundary, the first step starts with a coarse grid and bracket the boundary effect using fixed and free boundary conditions while changing the distance to the boundary. Then, the resulting effect of changing the boundary is evaluated in terms of differences in displacement calculated in the region of interest. Finally, according to the Figure 3.2, the best fit for model boundary selected.

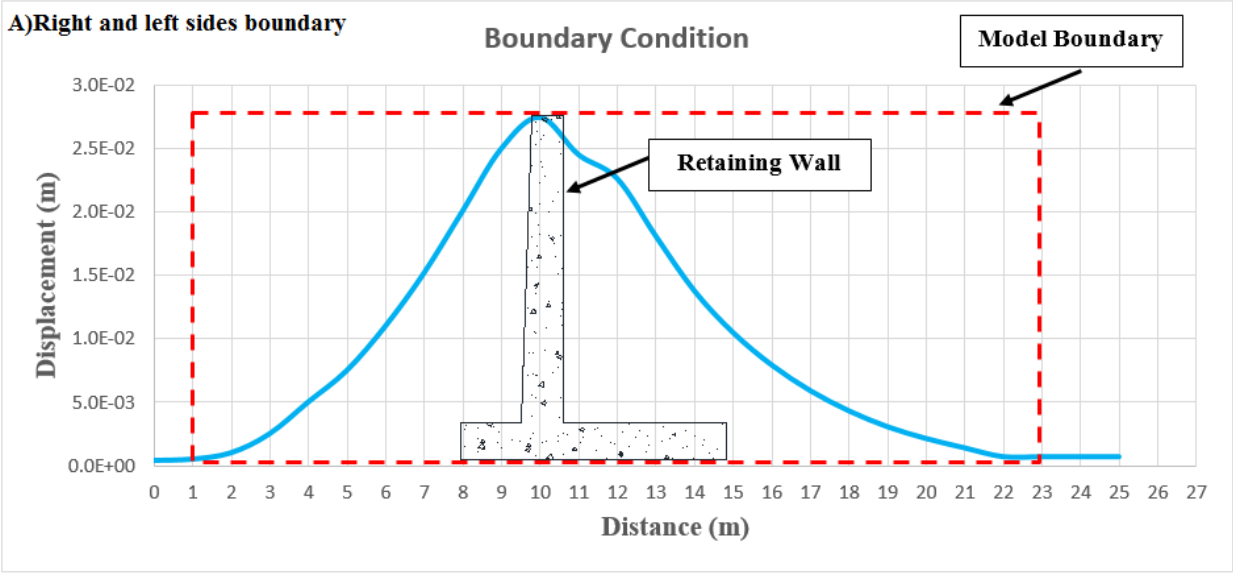

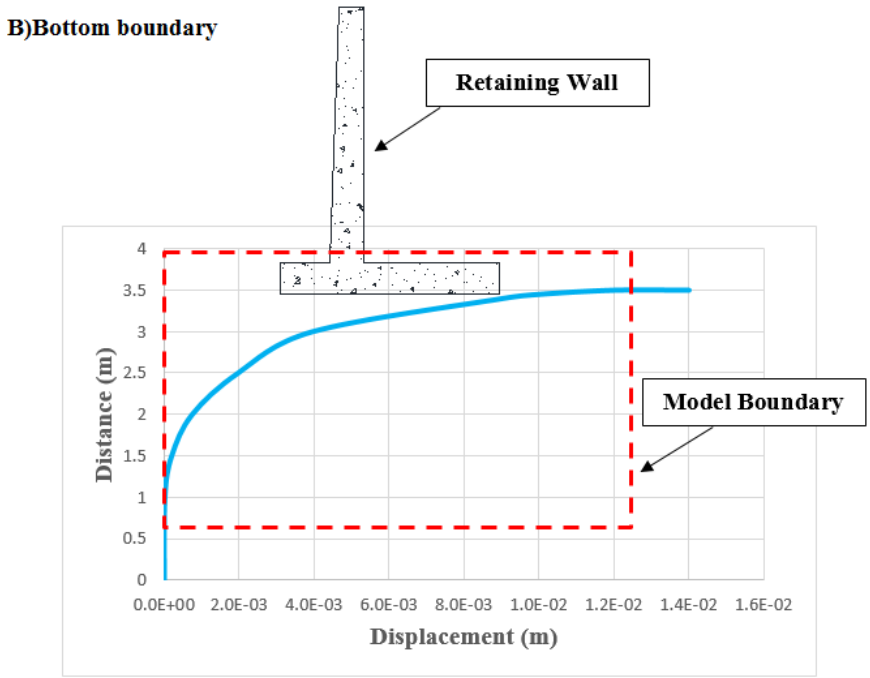

Figure 3.2. Model boundary definition for A) right and left sides B) bottom boundary

The initial configuration of numerical modeling by FLAC is illustrated in Figure 3.3.

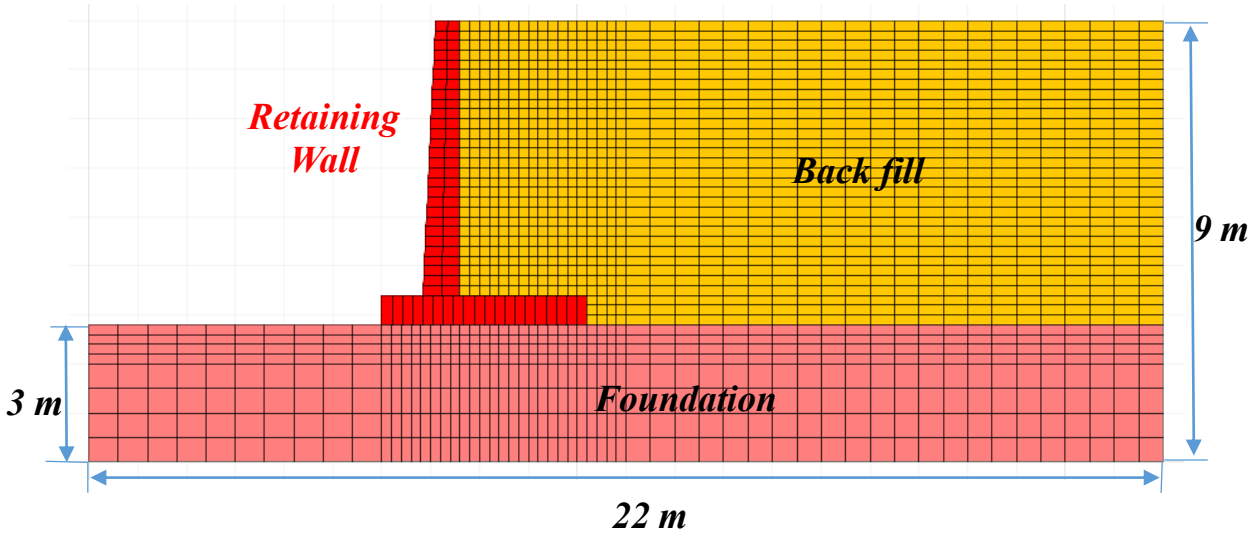

Figure 3.3. Initial configuration of cantilever retaining wall modeled by FLAC

3.4.1. Mesh generation

Unlike many numerical software based on the finite element method, FLAC organizes its zones in a row-and-column fashion, like a crossword puzzle. FLAC program, a pair of numbers (its row and column numbers) is used as a particular zone rather than by an arbitrary ID number, as in finite element programs (Itasca, 2015).

For optimizing the mesh size of retaining wall numerical model by FLAC program, a number of different numerical model with different mesh generation examined. According to Figure 3.4, displacement values are changing with increasing node numbers. But after a number of nodes (2320 nodes), displacement trend is almost constant. For this purpose, retaining wall numerical model built based on 2320 nodes.

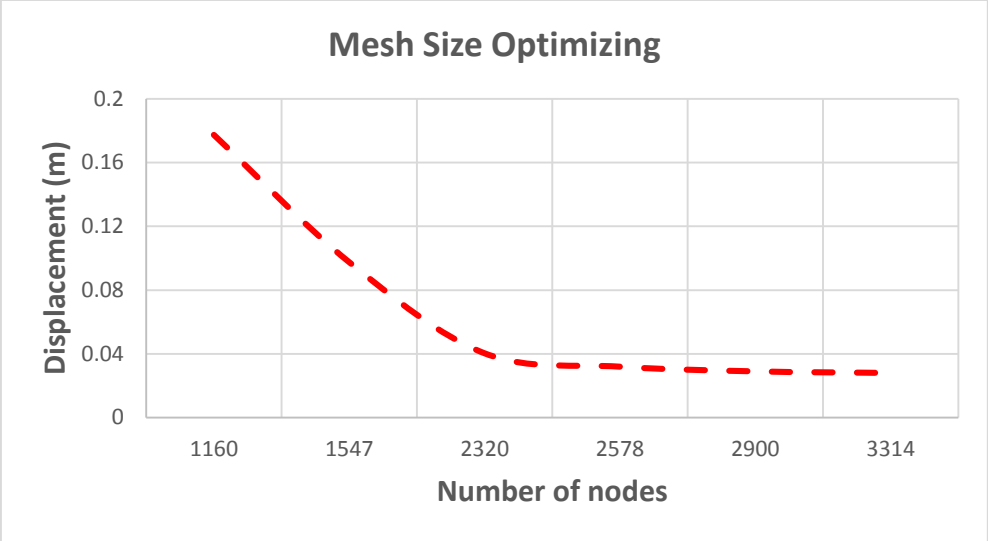

Figure 3.4. Mesh size optimizing for FLAC model of retaining wall

3.5. Static analysis

The objective of this section is to look into a retaining wall behavior from a numerical point of view in static condition when considering boundary condition and soil behavior of material. Also with considering active soil pressure.

3.5.1. Static boundary condition

The boundary conditions in a numerical model consist of the values of the field variables, including stress and displacement, which are prescribed at the boundary of the numerical grid.

According to Figure 3.5, the boundary conditions in this model consist of roller boundaries on the left and right sides of the model, as well as a fixed base while, the top boundary in this model is a free surface.

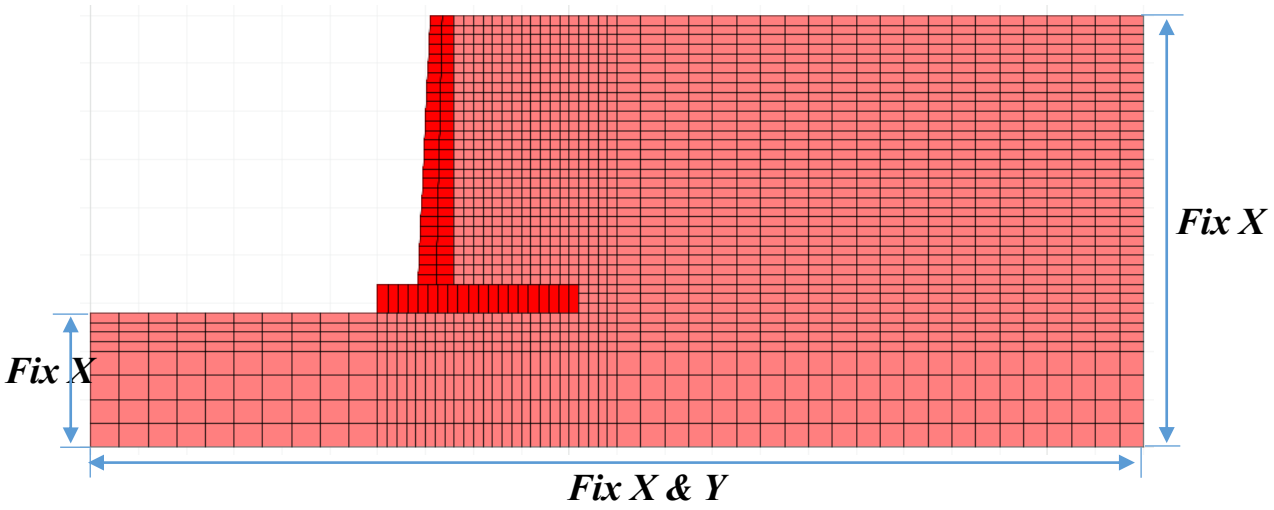

Figure 3.5. Static boundary condition in FLAC model

3.5.2. Soil constitutive model

The Mohr-Coulomb model is applicable for most general engineering studies involving soil. Also, Mohr-Coulomb parameters for cohesion and friction angle are usually more readily available than other properties for geo-engineering materials. For this purpose, in this study the Mohr-Coulomb failure criteria is used for simulating soil behavior model. The basic criterion for the material failure in FLAC is the Mohr-Coulomb relation, which is a linear failure surface corresponding to shear failure according to Equations 3-1 and 3-2 (Itasca, 2015).

$$f^s = \sigma_1 - \sigma_3 N_\varphi + 2c\sqrt{N_\varphi} \quad (3\text{-}1)$$

Where;

$$N_\varphi = (1 + \sin\varphi)/(1 - \sin\varphi) \quad (3\text{-}2)$$

σ_1 = Major principal stress (compressive stress is negative)

σ_3 = Minor principal stress

φ = Friction angle

c = Cohesion

Mohr-Coulomb failure criterion is in Figure 3.6.

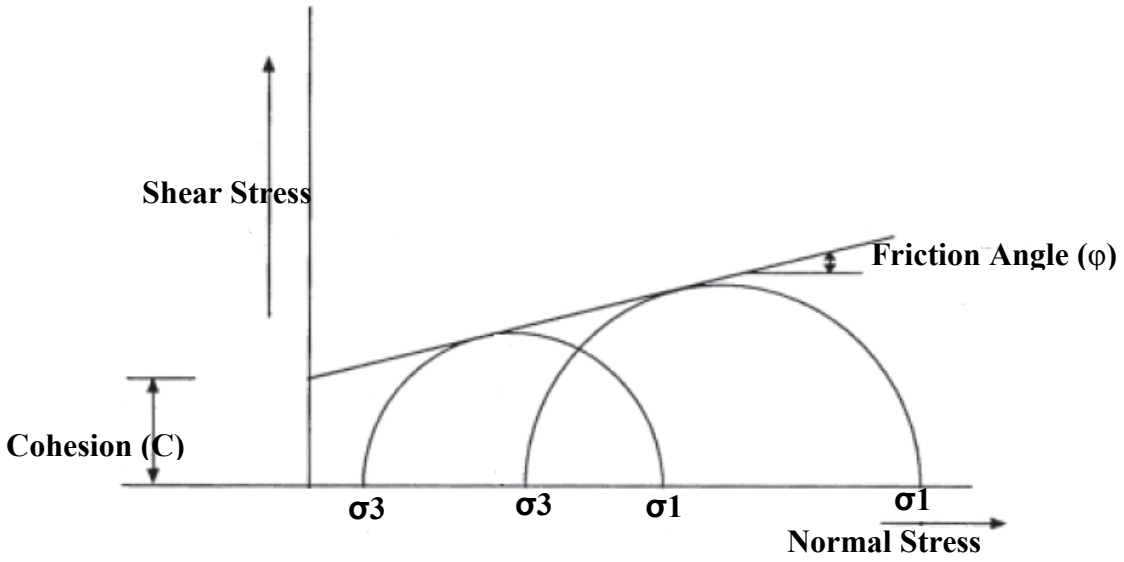

Figure 3.6. Mohr-Coulomb failure criterion (Portland Cement Association, 1992)

According to Figure 3.6, friction angle (φ) is the internal friction of a given soil mass which is related to the sliding friction between individual soil grains and the interlocking of soil particles. Cohesion (C) is analogous to two sheets of flypaper with their sticky sides in contact.

In addition, the angle of friction is the angle between the normal force (N) and the resultant force (R) of normal force and friction. But, the angle of repose is the angle of maximum slope, where an object is placed on the slope just begins to slide. The major difference between them is that the angle of friction is defined for rigid bodies while angle of repose is defined for granular particles. Furthermore, the angle of shearing resistance (internal angle of friction, angle of frictional resistance; φ) is approximate angle of repose for clean sand; it reduces with moisture content and is zero for a sheared, saturated clay (Portland Cement Association, 1992) .

Furthermore, the principal stresses (σ_1, σ_2, σ_3) and principal directions are evaluated from the stress tensor components, and ordered so that according to following equation (Itasca, 2015):

$$\sigma_1 \leq \sigma_2 \leq \sigma_3 \quad (3\text{-}3)$$

According to Equation 3-3, the failure criterion may be represented in the plane (σ_1, σ_3) as shown in Figure 3.7.

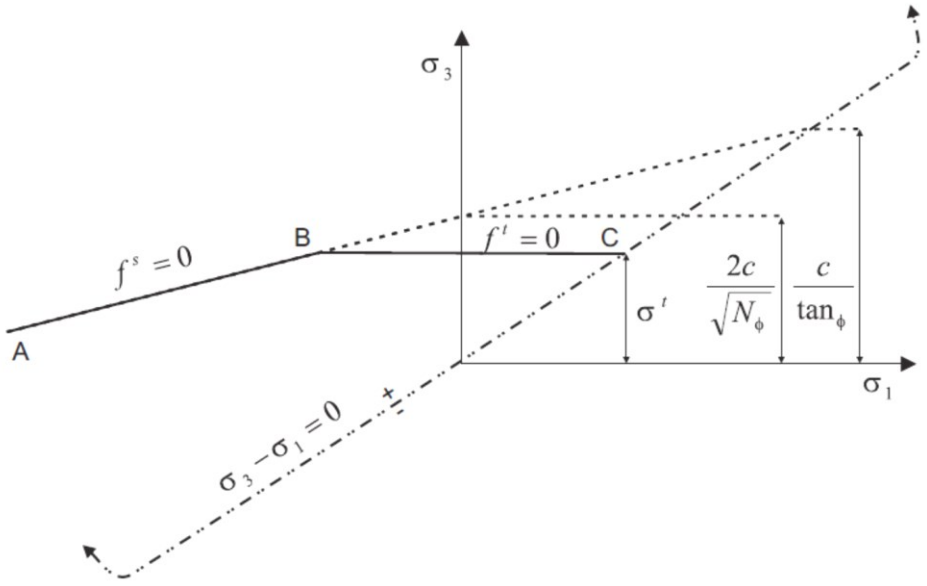

Figure 3.7. Mohr-Coulomb failure criterion in FLAC (Itasca, 2015)

As stated in Figure 3.7, the failure envelope is defined from point A to point B by the Mohr-Coulomb yield function according to Equation 3-1 and from B to C by a tension yield function according to follow equation:

$$f^t = \sigma^t - \sigma_3 \quad (3\text{-}4)$$

3.5.3. Material properties

According to Figure 3.3, the numerical model consists of two kind of soil as a backfill and foundation. The material properties of backfill and foundation and also concrete as retaining wall are shown in Table 3.1.

Table 3.1. Material Properties in FLAC model (Parihar and Saxena, 2010)

	Density (Kg/m^3)	Bulk Modules (Pa)	Shear Modules (Pa)	Cohesion (Pa)	Friction Angle (Degree)	Dilation Angle (Degree)	Tension (Pa)
Back fill	1960	1.67e7	1e7	0.0	35	0.0	0.0
Foundation	2700	3.33e9	1.53e6	3e4	40	0.0	0.0
Concrete	2360	1.19e10	1.08e10	----------	----------	----------	----------

3.5.4. Model parameters for wall-soil interface

Interface elements are used to model the interaction between the reinforced concrete retaining wall and the soil. However, FLAC does not allow interface elements to be used at the intersection of branching structures (e.g. the intersection of the stem and base of the cantilever wall). Interface elements are used along the contact surfaces between the soil and wall, as depicted by the hatched areas in Figure 3.8.

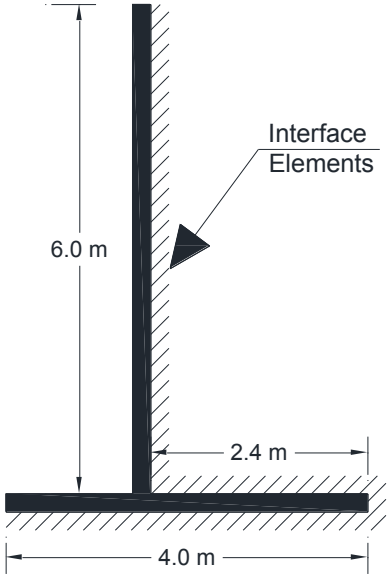

Figure 3.8. Location of interface elements in the FLAC model

The interface properties between soil and wall is presented in Table 3.2.

Table 3.2. Soil-wall interface properties in FLAC model (Parihar and Saxena, 2010)

Normal Stiffness (Kn) (Pa)	Shear Stiffness (Ks) (Pa)	Cohesion (C) (Pa)	Friction Angle (ϕ) (Degree)	Dilation Angle (ψ) (Degree)
9.93e8	3.3e8	0.0	26.6	0.0

3.5.5. Safety factor

Factor-of-safety calculation can be performed for stability analyses. Factor of safety calculation is performed here based on shear strength reduction (SSR) method. The shear strength reduction method is an increasingly popular numerical method for evaluating factor of safety in geotechnics problems and relevant for the Mohr-Coulomb materials. The factor of safety calculated in this

study for retaining wall is 1.54 (Figure 3.9) which is greater than the minimum safety factor value (1.5) for retaining walls according to "basic retaining wall design guideline" (Brooks, 2010).

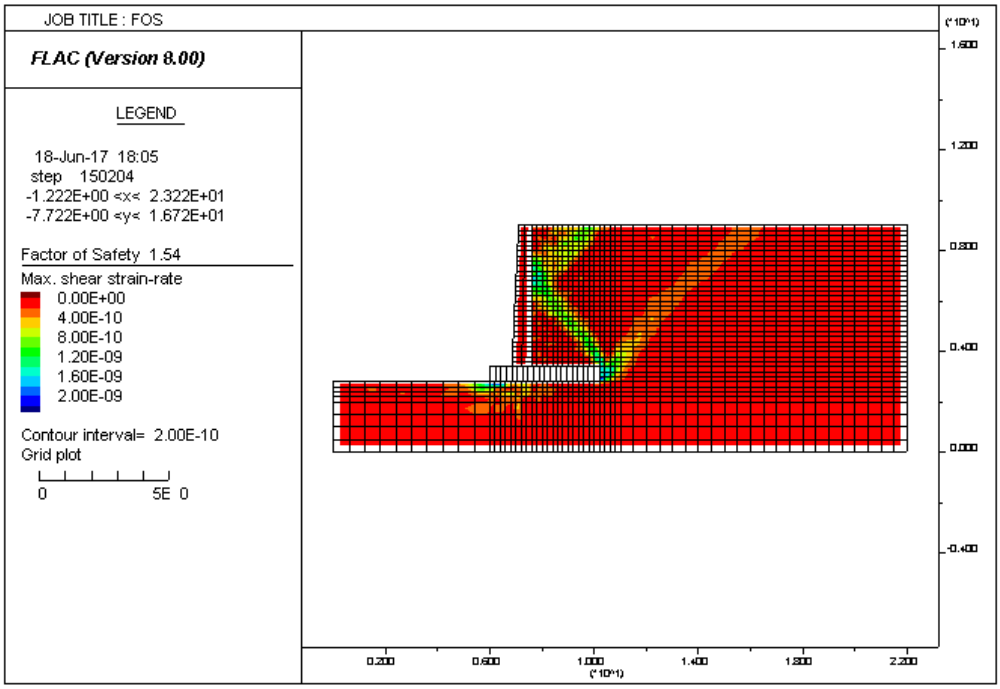

Figure 3.9. Safety factor in FLAC model

3.5.6. Static results

Figures 3.10 and 3.11 show displacement contours in X and Y directions respectively in the static condition. According to displacement contours, maximum displacement occurs in the top of the retaining wall.

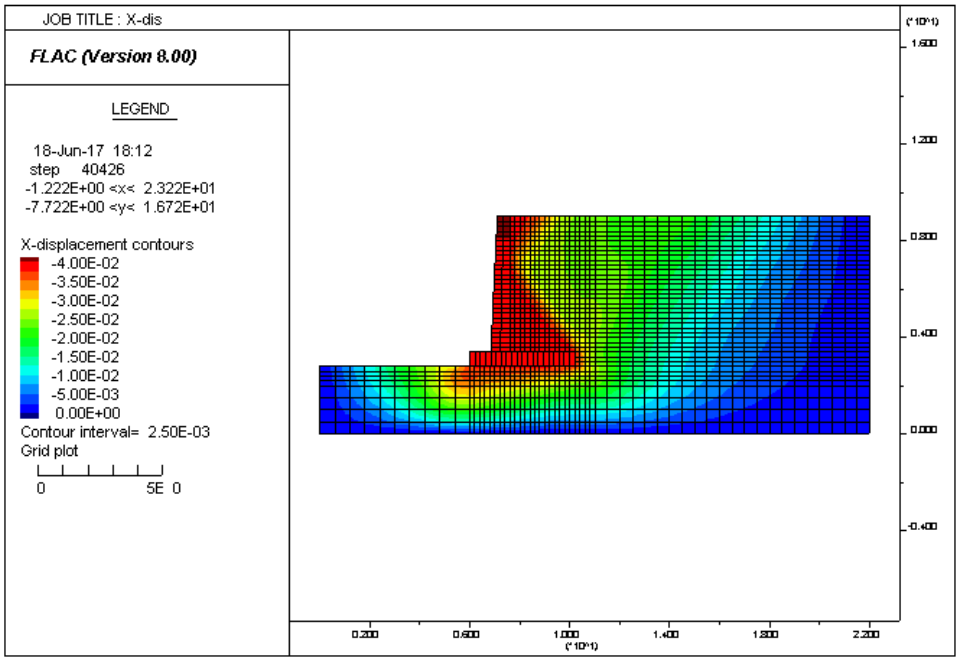

Figure 3.10. Displacement contour in X direction in static condition

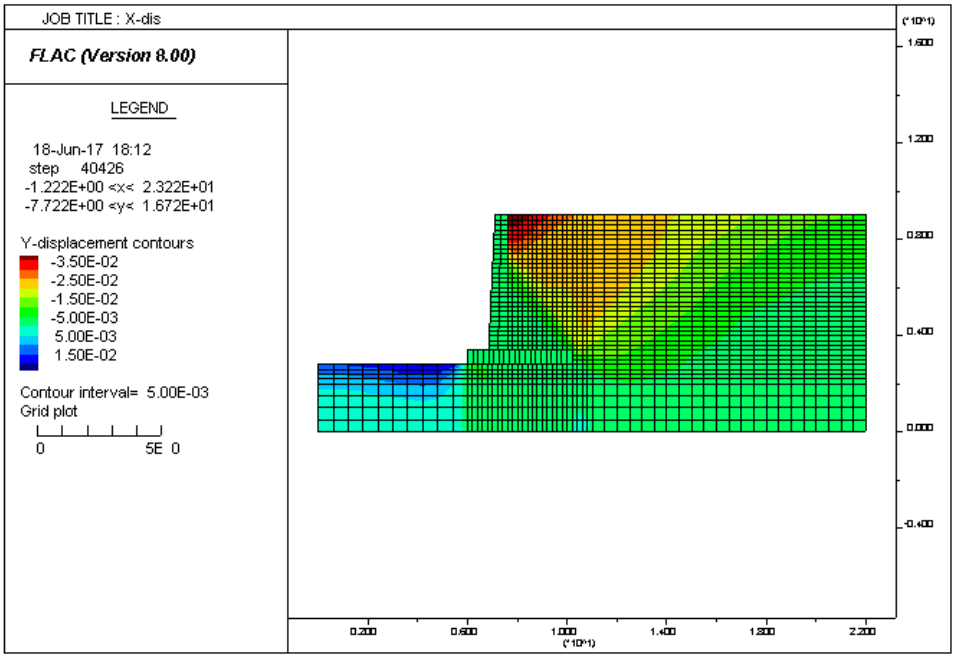

Figure 3.11. Displacement contour in Y direction in static condition

Also stress contours in X and Y direction respectively are presented in Figures 3.9 and 3.10 in static condition. According to Figures 3.12 and 3.13, maximum stress happens in the toe of retaining wall.

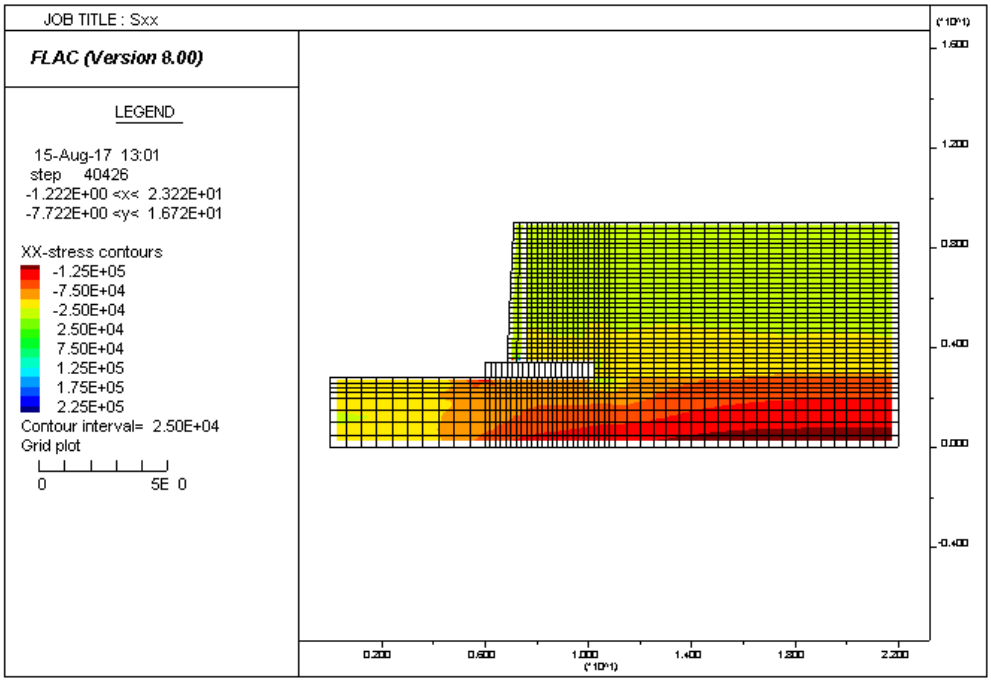

Figure 3.12. XX-Stress contour in static condition

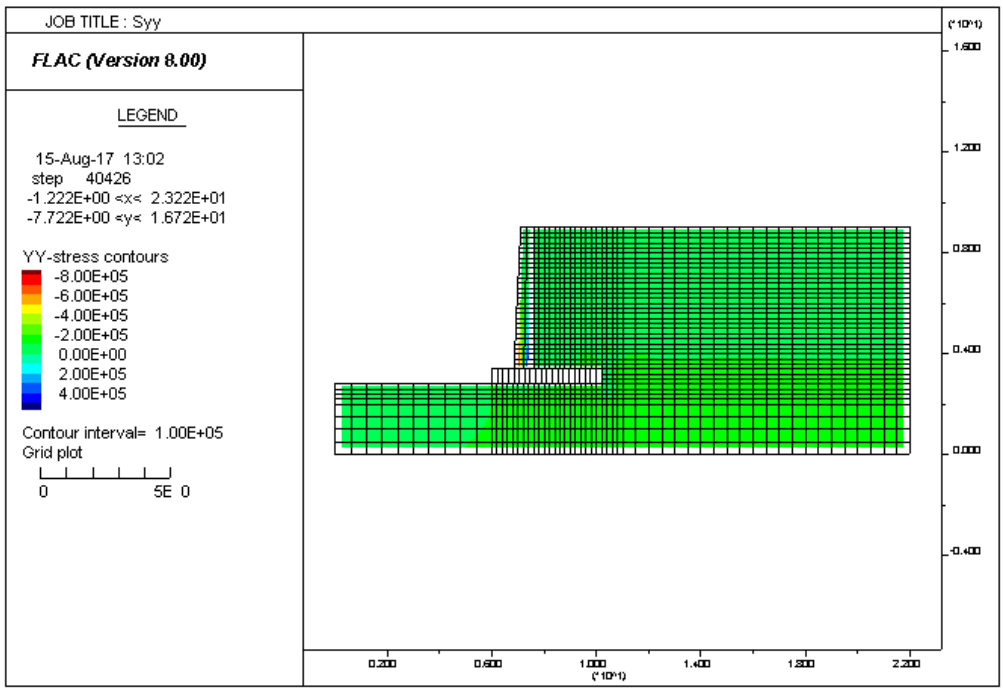

Figure 3.13. YY-Stress contour in static condition

3.6. Dynamic analysis

Dynamic analysis of cantilever retaining wall is conducted using an earthquake ground motion considering a dynamic boundary conditions. In FLAC, the dynamic analysis is based on the explicit finite difference scheme to solve the full equations of motion, using lumped grid point masses derived from the density of the materials in the surrounding zones.

3.6.1. Dynamic boundary condition

In static analyses, fixed or elastic boundaries can be realistically located at some distance from the region of the wall. While in dynamic problems, such boundary conditions cause the reflection of outward propagating waves back into the model and do not allow the necessary energy radiation. For this purpose, using of larger model can reduce the boundaries effect on the problem, because material damping will absorb most of energy in the waves reflected from distant boundaries. Although this solution results in a large computational burden, the alternative is using quiet or absorbing boundaries. The relation between velocity and stress wave with the speed of wave propagation is according to follow Equations:

$$\sigma_n = 2(\rho C_p)v_n \quad (3\text{-}5)$$

$$\sigma_s = 2(\rho C_s)v_s \quad (3\text{-}6)$$

Where;

σ_n: Applied normal stress

σ_s: Applied shear stress

ρ: Mass density

Cp: Speed of p-wave propagation through medium

Cs: Speed of s-wave propagation through medium

v_n: Input normal particle velocity

v_s: Input shear particle velocity

And Cp and Cs are given by:

$$C_p = \sqrt{\frac{K+4G/3}{\rho}} \quad (3\text{-}7)$$

$$C_s = \sqrt{G/\rho} \quad (3\text{-}8)$$

Where K and G are bulk and shear moduli respectively.

On the other hand, the seismic input is normally illustrated by plane waves propagating upward through the underlying material. For this purpose, at the side of the model the boundary conditions should account for the free-field motion that would exist in the absence of the structure.

The dynamic boundary conditions are applied in the FLAC model shown in Figure 3.14. Quiet boundary conditions are assigned in both the X and Y directions of model and after that free-field boundary is set for the side boundaries. Then, the dynamic input is assigned to the bottom boundary as a velocity record is converted into a shear-stress boundary condition.

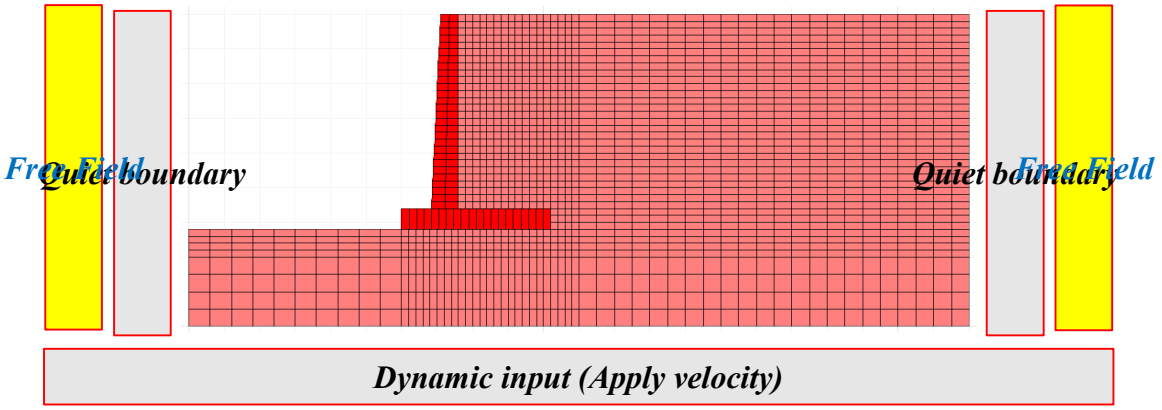

Figure 3.14. Dynamic boundary condition in FLAC model

3.6.2. Input earthquake motion

In this study, for dynamic analysis, the 1991, Uttarkashi earthquake in India, which recorded a PGA of 2.372 m/sec^2 as the input motion data applied to the retaining wall model (Figure 2.30). Duration of recorded acceleration time-history of the motion was 40 seconds. According to Figure 3.30, as most of the peaks occurred within 20 seconds of the motion.

3.6.3. Dynamic results

In order to investigate the behavior of retaining wall deformation in seismic condition, according to Figure 3.15 a history point is considered at the top of the wall.

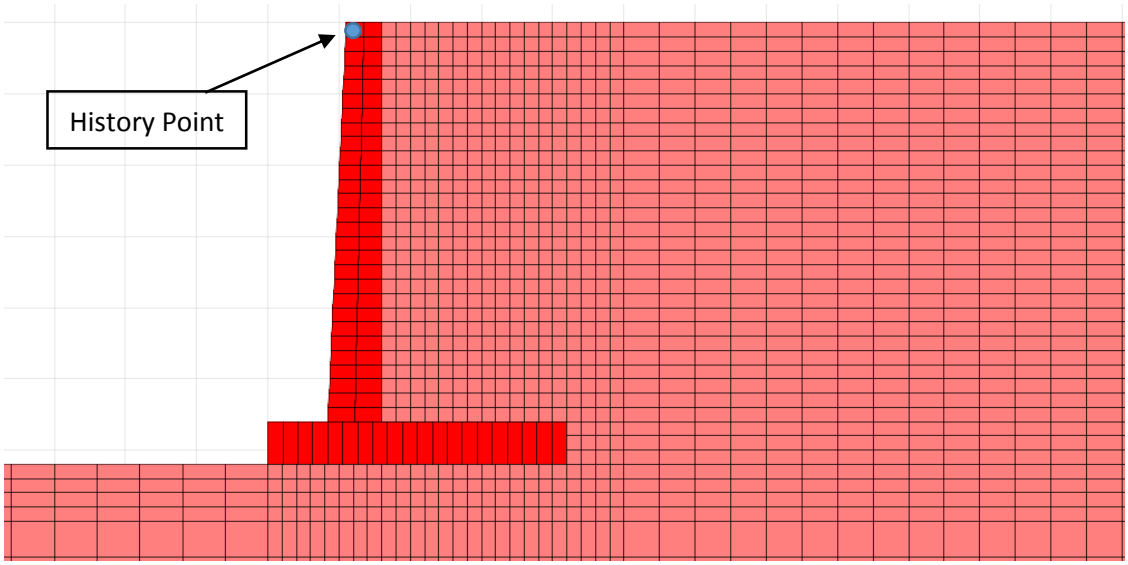

Figure 3.15. History point located in FLAC model

Figure 3.16 shows the model deformation after applying earthquake motion.

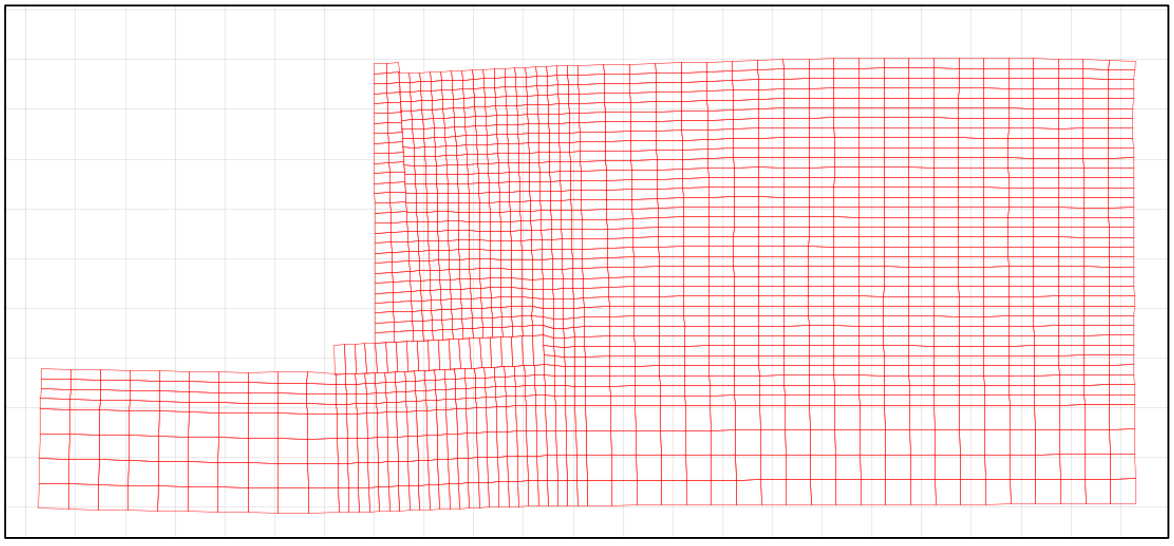

Figure 3.16. Model deformation in dynamic condition

Changes of displacements, stresses, acceleration and velocity of top of the wall was calculated in dynamic model. Figures 3.17 to 3.20 present the displacement and stress in both directions X and Y of top of the retaining wall, respectively.

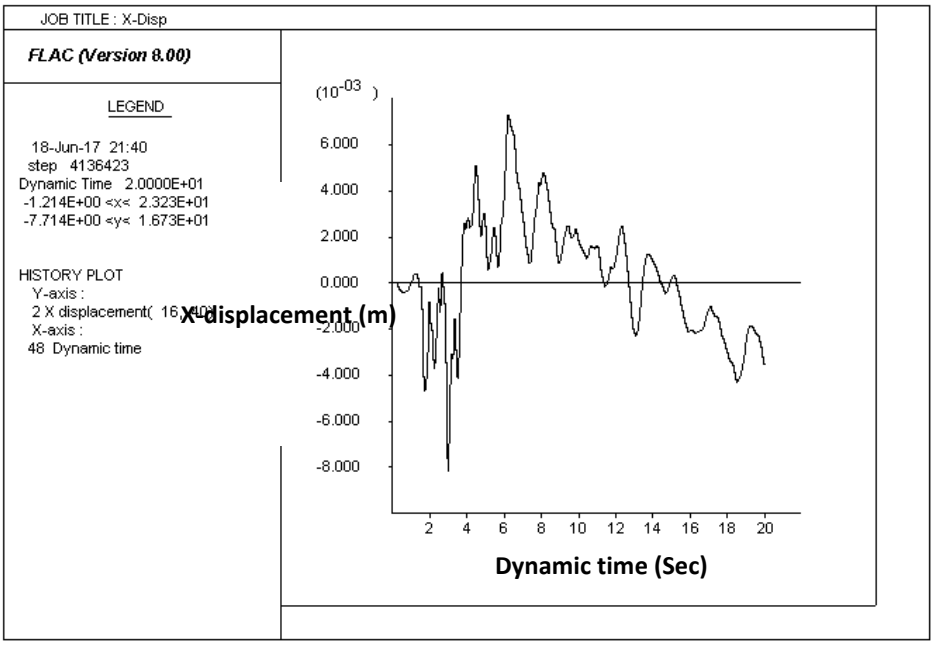

Figure 3.17. Displacement changes in X direction

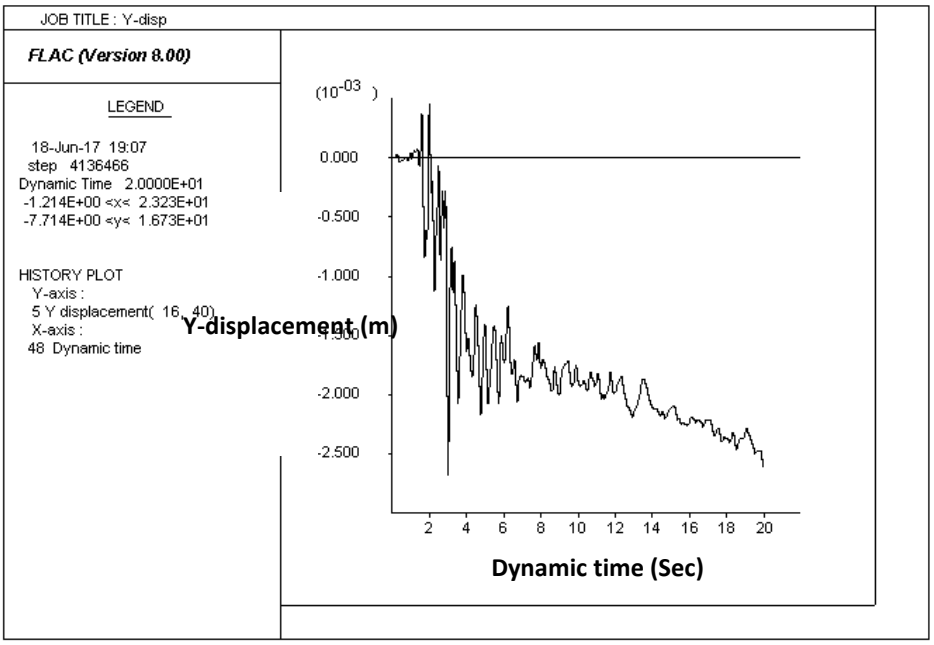

Figure 3.18. Displacement changes in Y direction

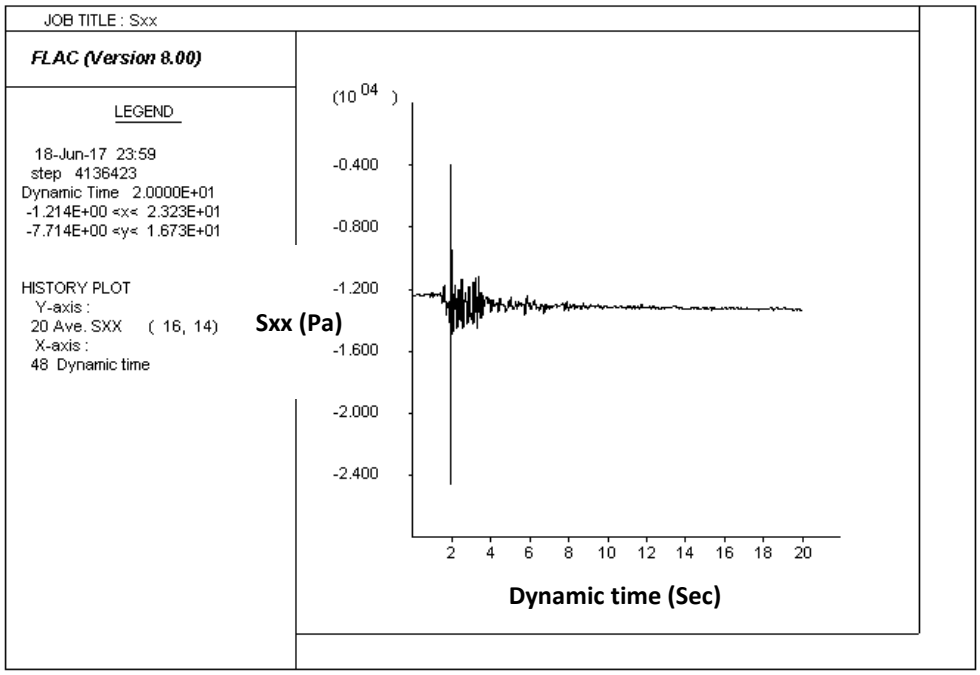

Figure 3.19. Stress changes in X direction

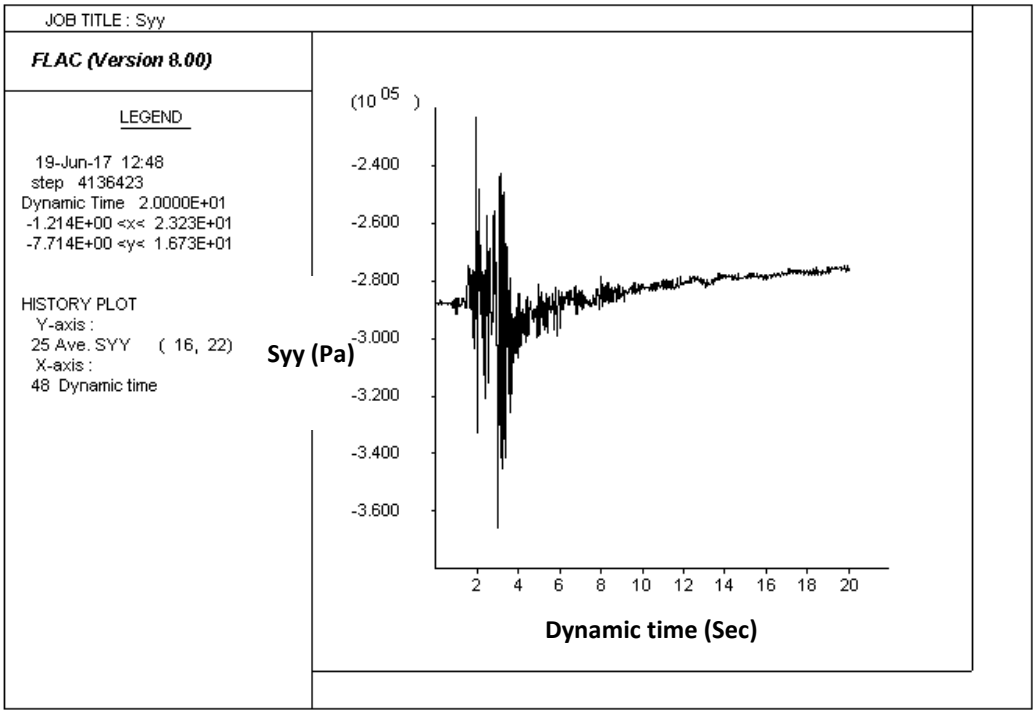

Figure 3.20. Stress changes in Y direction

The velocity and acceleration of the top of the retaining wall in X direction is shown in Figures 3.21 and 3.22.

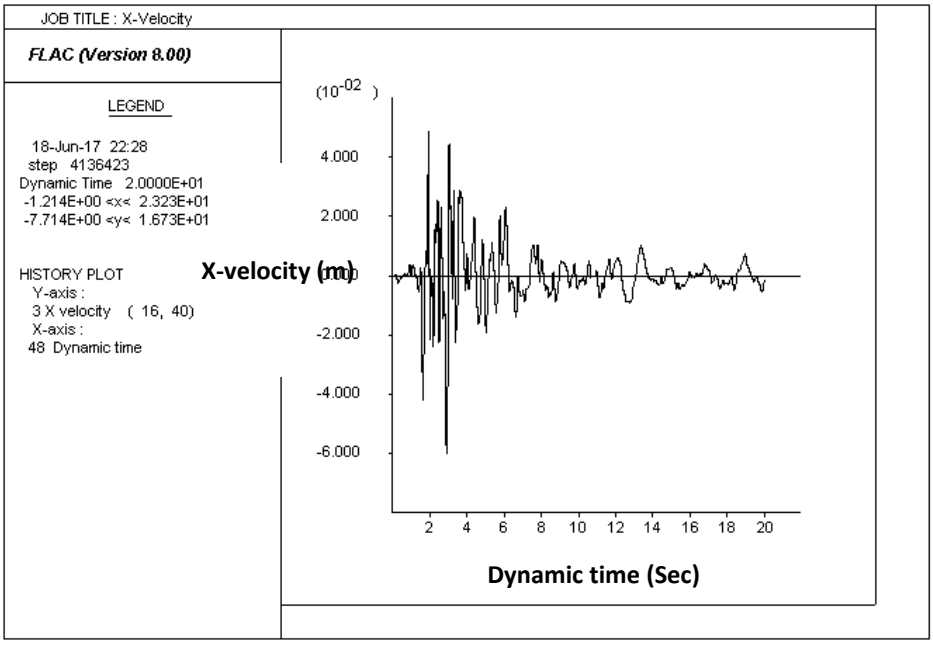

Figure 3.21. X-Velocity changes

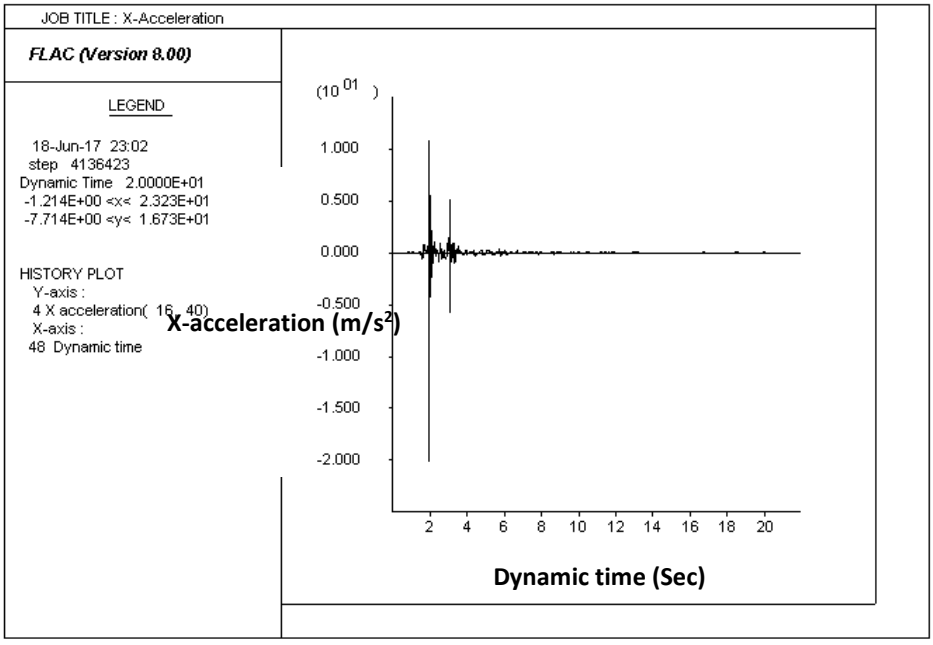

Figure 3.22. X-Acceleration changes

3.7. Model validation

For the purpose of validation, the numerical results are compared to available studies from the literature. The published numerical model in (Parihar and Saxena, 2010) is used for validation of the present numerical model. The geometry of cantilever retaining wall in (Parihar and Saxena, 2010) is shown in the Figure 2.28. Also, Parihar and Saxena (2010) used a Finite Element Method (FEM) using the commercially available software, ANSYS to look into wall-soil interaction behavior in retaining wall in both static and dynamic conditions. For validation of the baseline model is created in the present study, using the data for case study presented in (Parihar and Saxena, 2010). Furthermore, Parihar and Saxena (2010) investigated the behavior of wall-soil interface of retaining wall as well as the main subject of this research, which provides adequate data for validation.

Therefore, in the present study, a Finite Difference model of the retaining wall is set up according to the details given in Parihar et al. model (Parihar and Saxena, 2010). Then, the geometry, boundary condition and material properties in this study are considered according to that study. In the static condition, the lateral active pressure distribution is compared to the published numerical model in accordance with Figure 3.23.

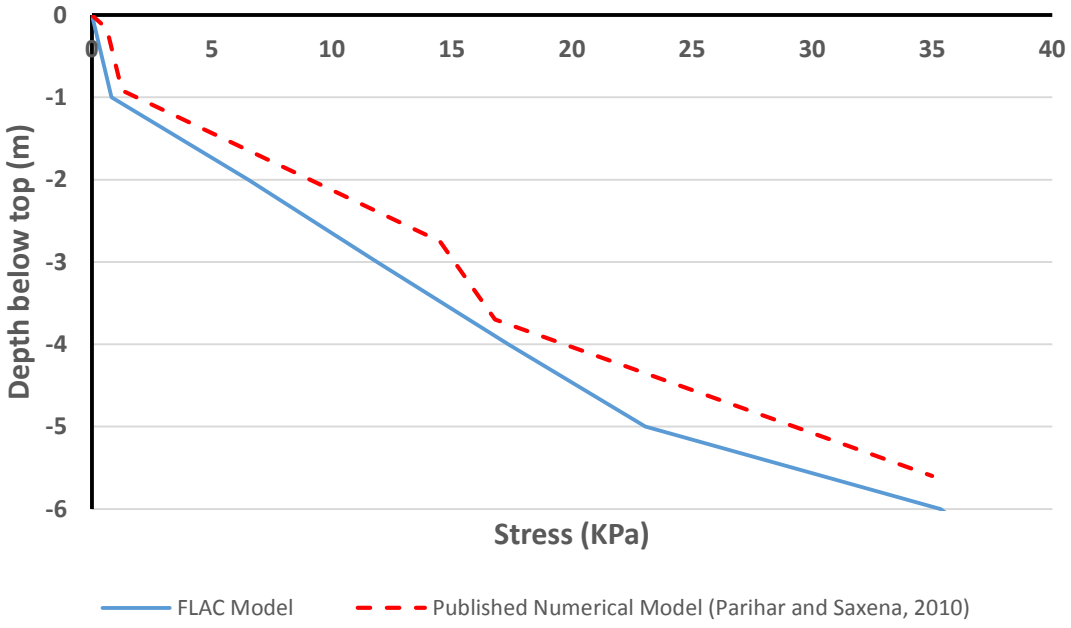

Figure 3.23. Lateral active pressure distribution in FLAC model and published numerical model

Also, the numerical model is compared in dynamic condition with published numerical model based on the maximum displacement on the top of the retaining wall in both X and Y direction according to the Table 3.3. Parihar and Saxena (2010) reported only the maximum displacements at the top of the wall based on the dynamic analysis. They compare quite well with results of the present analysis.

Table 3.3. Model validation in dynamic condition

Max Displacement in X direction		**Max Displacement in Y direction**	
FLAC Model	**Published numerical Model (Parihar and Saxena, 2010)**	**FLAC Model**	**Published numerical Model (Parihar and Saxena, 2010)**
8.2mm	8.51mm	2.7mm	2.39mm

Figure 3.21 and Table 3.3 show that, results obtained from the FLC model have good agreement with the published numerical model.

3.8. Summary

In this chapter, in the first part, the cantilever retaining wall modeled by Finite Difference Method (FDM) and FLAC software in static boundary condition with considering Mohr-Coulomb criteria as soil constitutive model. In the second part, according to boundary condition and also input earthquake motion, dynamic analysis of cantilever retaining wall conducted. Finally, for the purpose of validation, the numerical results in both static and dynamic condition compared with the available studies from the literature review (Parihar and Saxena, 2010).

Chapter 4. Effects of the Shear Strength and Stiffness Parameters of Wall-soil Interface under Earthquake Loading

4.1. Introduction

In this chapter, the wall interface shear behavior has been presented. The study includes a series of parametric studies, under static and earthquake loading. The wall interface system considered here is analyzed numerically by Finite Difference method as discussed Chapter 3. All of the interface parameters investigated in this section are based on shear strength and stiffness parameters and also dilation value.

Furthermore, based on acceleration time history of a typical earthquake which is recorded in India (20^{th} October, Uttarkashi, 1991), the dynamic deformation of the retaining wall under different loading conditions is investigated.

Finally, effect of interface roughness is investigated according to shear strength and stiffness parameters with dilation changes.

4.2. Wall-soil interface definition

Generally in geomechanics field, there are several instances when it is desirable to represent planes on which sliding or separation can occur as follow:

1. Joint, fault or bedding planes in a geologic medium

2. An interface between a retaining wall structure and the soil

3. A contact plane between a bin or chute and the material that it contains

4. A contact between two colliding objects

In this research used the second definition for investigation of the behavior of interface between structure and surrounding soil material of retaining walls.

Also, an interface is represented as a normal and shear stiffness between two planes that may contact each other. In fact, in FLAC program, the spring parameters (normal and shear stiffness) for the contact interfaces are defined from grid to grid. Figure 4.1 presents interface parameters in FLAC.

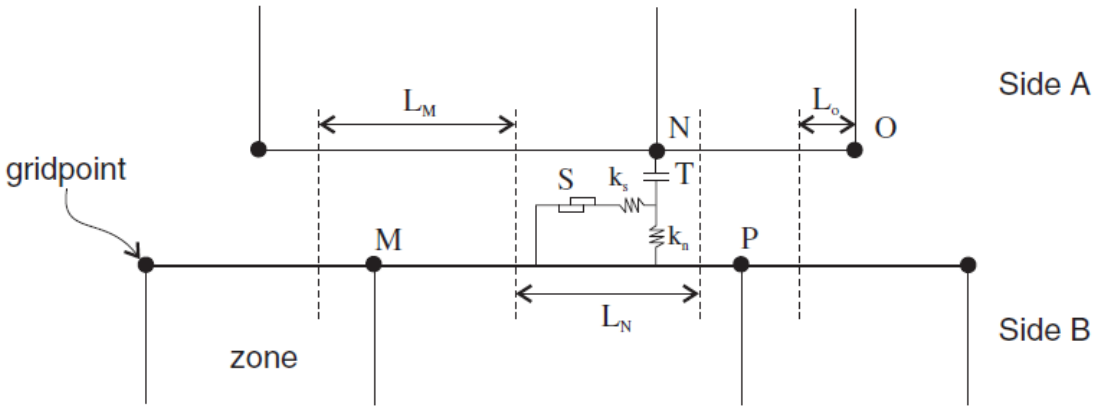

------ *Denotes limits for joint segments (placed halfway between adjacent grid points)*

Figure 4.1. Interface parameters in FLAC (Itasca, 2015)

Where;

S: Slider

T: Tensile Strength

K_n: Normal Stiffness

K_s: Shear Stiffness

L_n and L_m: Length associated with grid point N and M

4.3. Direct shear test

The purpose of doing direct shear test is to determine the shear strength parameters of soil. The shear strength is one of the most important engineering properties of a soil. The shear strength is needed for engineering situations such as determining the stability of slopes, calculating the bearing capacity for foundations, and also calculating the pressure exerted by a soil on a retaining wall. Furthermore, according to direct shear test, cohesion (C) and friction angle (ϕ) parameters will be obtained.

According to Figure 4.2, the soil sample is set in a cubic shear box composed of an upper and lower box. Distance between two parts of the box is approximately at the mid height of the sample. A normal stress applies at the top of loading plate and also shear stress applies from side of box. Horizontal and vertical displacements are controlled by a strain gage. These measurements are

then used to obtain the stress-strain curve of the sample during the loading for the given normal stress (Figure 4.3).

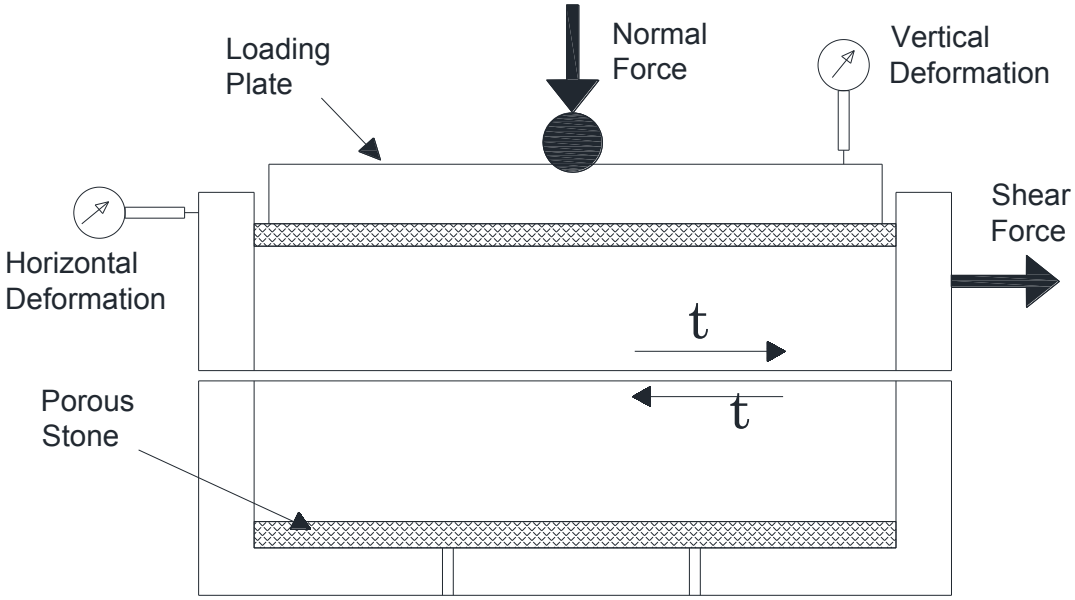

Figure 4.2. Direct shear test set up

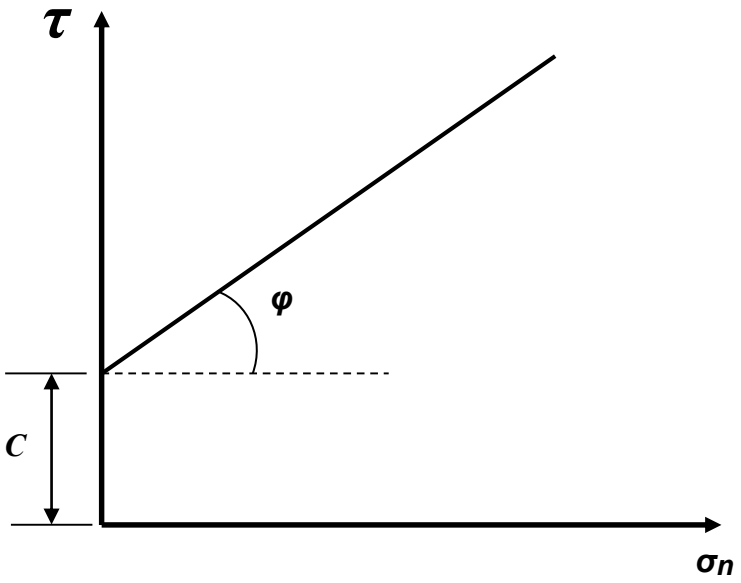

Figure 4.3. Shear strength curve

4.4. Mohr-Coulomb interface model

The coulomb shear-strength criterion is used in numerical models for simulation of wall-soil interface according to following equation (Itasca, 2015):

$$\tau = C + \sigma_n \tan \varphi \quad (4\text{-}1)$$

Where;

τ: Shear Stress

C: Cohesion

σ_n: Normal stress

φ: Friction Angle

4.5. Wall-soil interface parameters

Wall-soil interface parameters typically can be separated by shear strain parameters (cohesion and friction angle), stiffness parameters (normal and shear) and dilation value. The objective of this section is to investigate the behavior of retaining walls according to the change of interface parameters for both static and dynamic conditions. Deformation changes for different interface parameters are explained below in further detail. The ranges of values of each parameter are selected based on those reported in the literature (Green and Ebeling, 2003. Cheng et al, 2013. Krishna, 2010. El-Emam et al, 2004. Parihar et al, 2010. Hatami, and Bathurst, 2001).

4.5.1. Sensitivity analysis of shear strength parameters

In this section, a sensitivity analysis of the shear strength parameters associated is carried out by considering both static condition and also seismic excitation to retaining wall structures. Figures 4.4 to 4.11 show the displacement contours in the static state in X direction and Y direction for different values of cohesions (C=0, 1KPa, 10KPa and 100KPa). Displacement contours in Figures 4.4 to 4.11 show that in static condition with increasing cohesion, wall displacements in both horizontal and vertical direction will decreases.

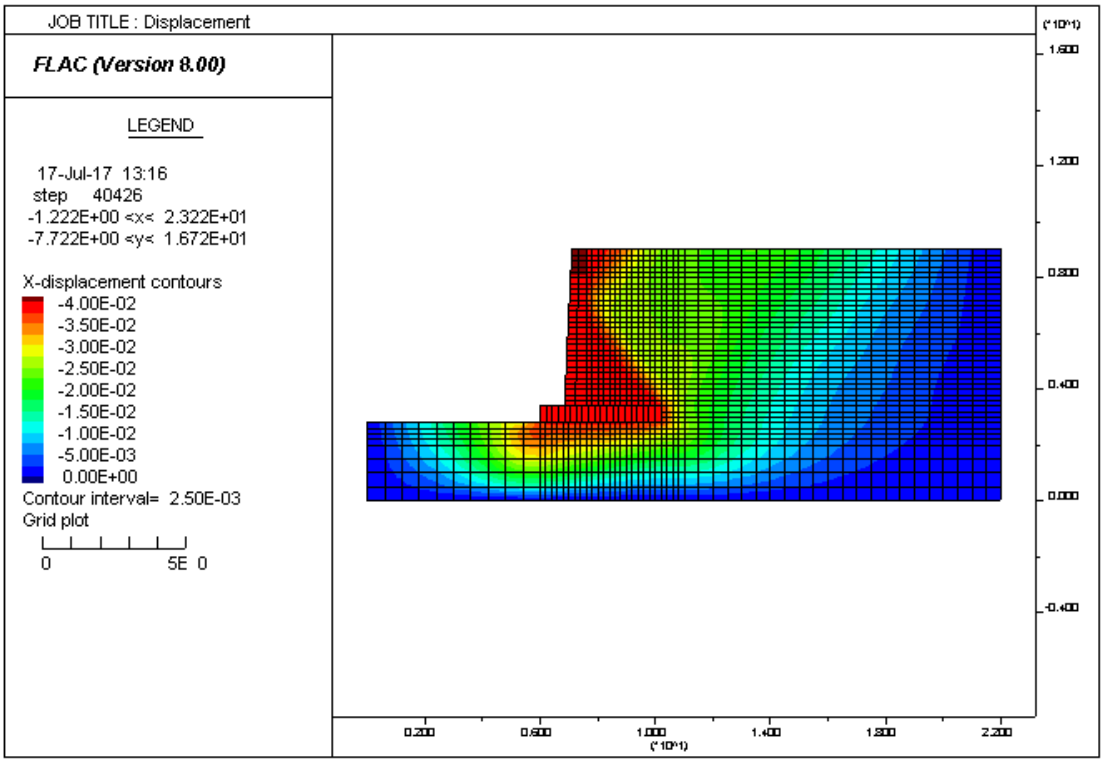

Figure 4.4. Displacement contours in X direction for C = 0 kPa

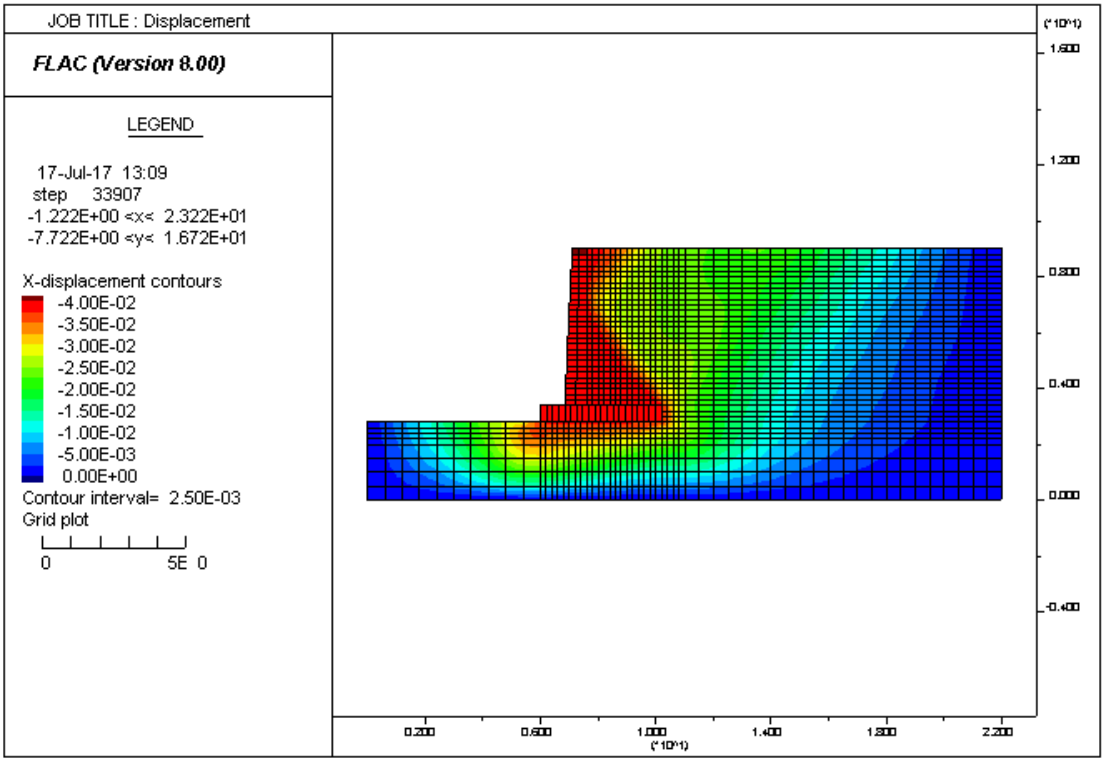

Figure 4.5. Displacement contours in X direction for C = 1 kPa

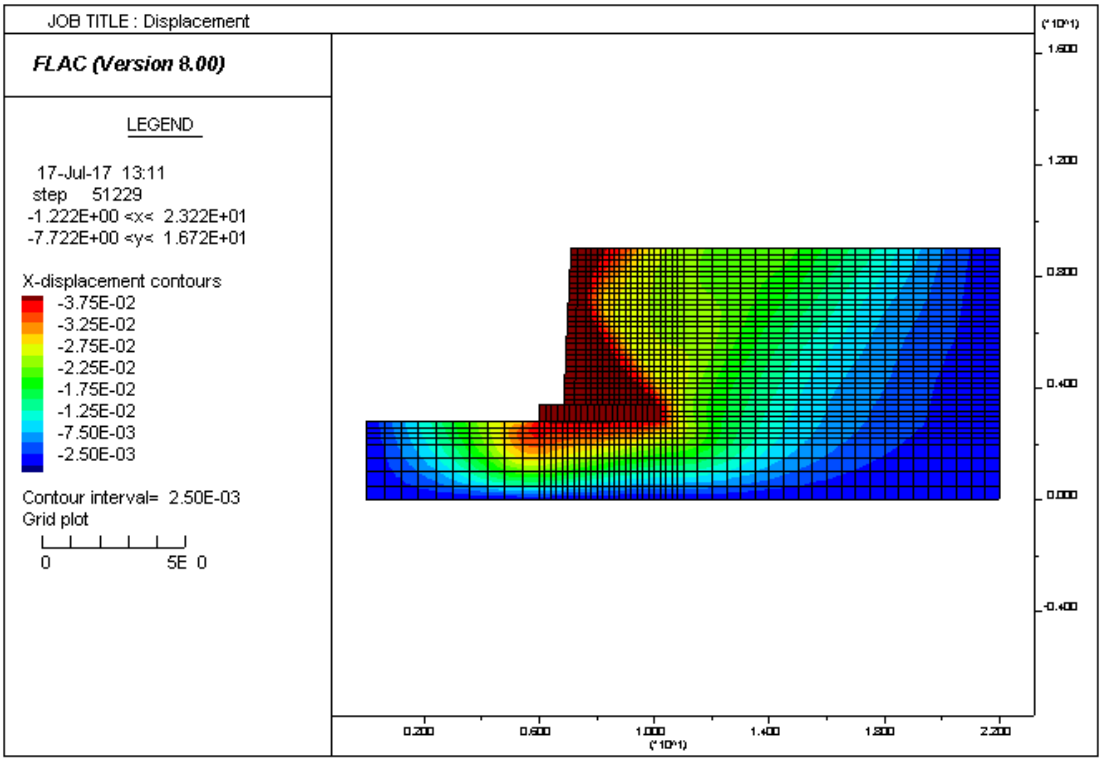

Figure 4.6. Displacement contours in X direction for C = 10 kPa

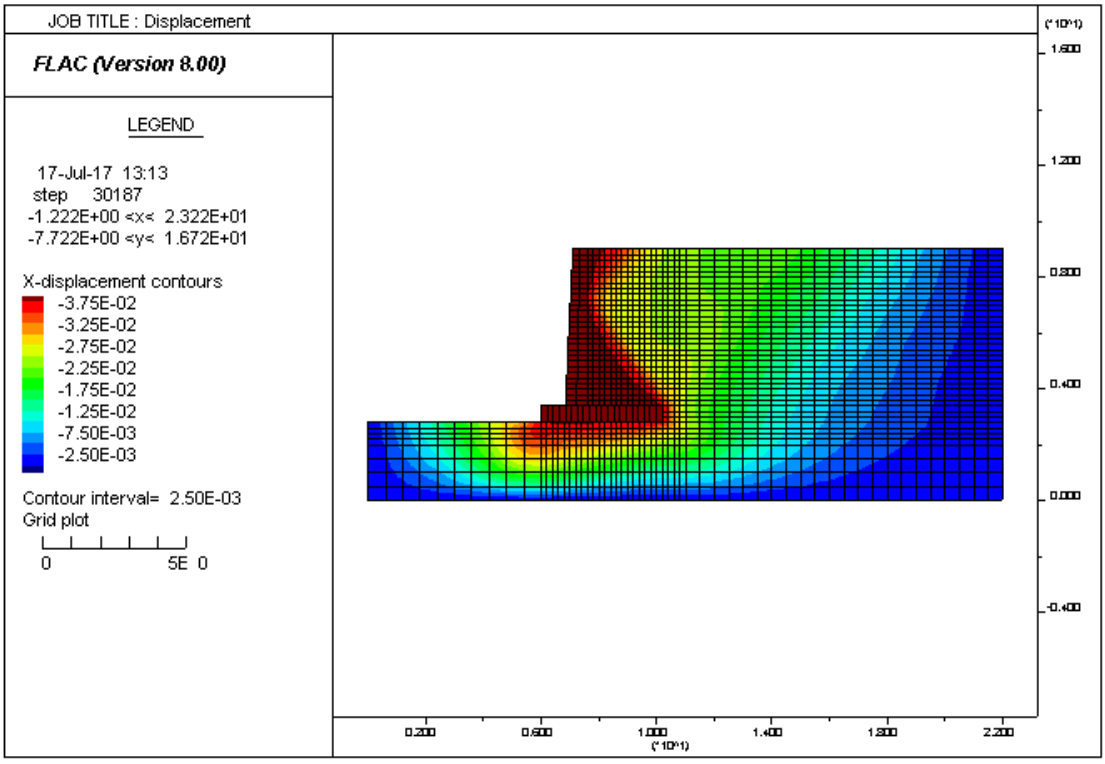

Figure 4.7. Displacement contours in X direction for C = 100 kPa

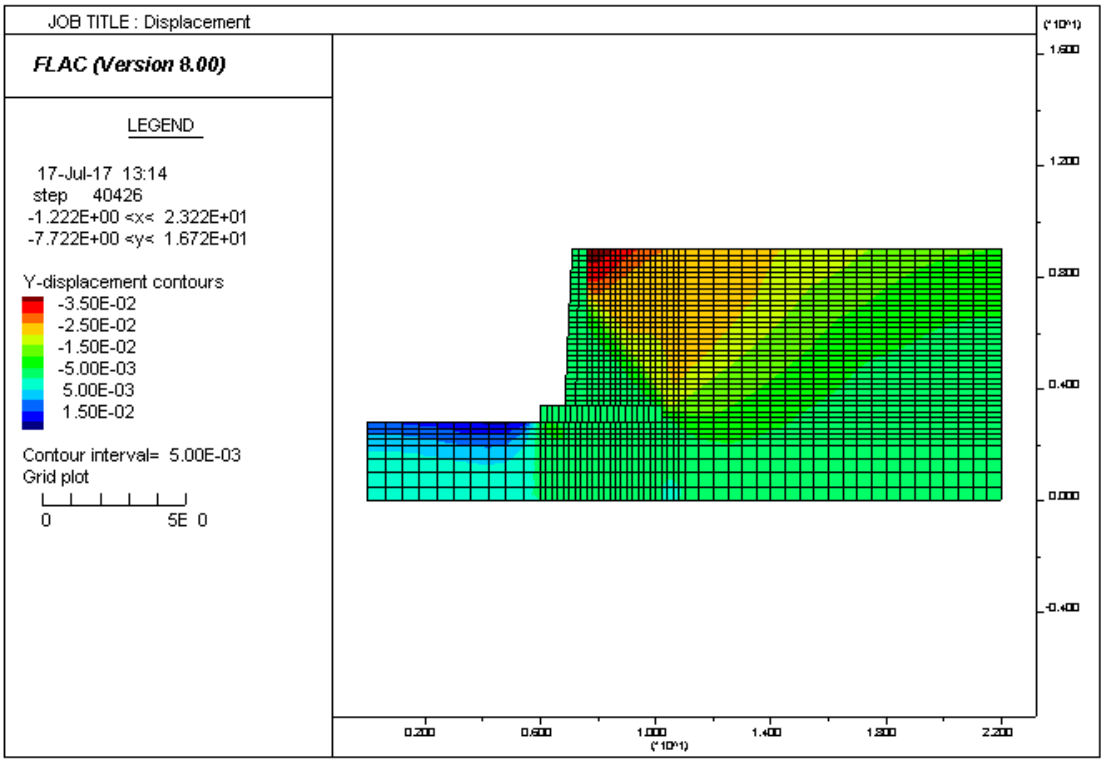

Figure 4.8. Displacement contours in Y direction for C = 0 kPa

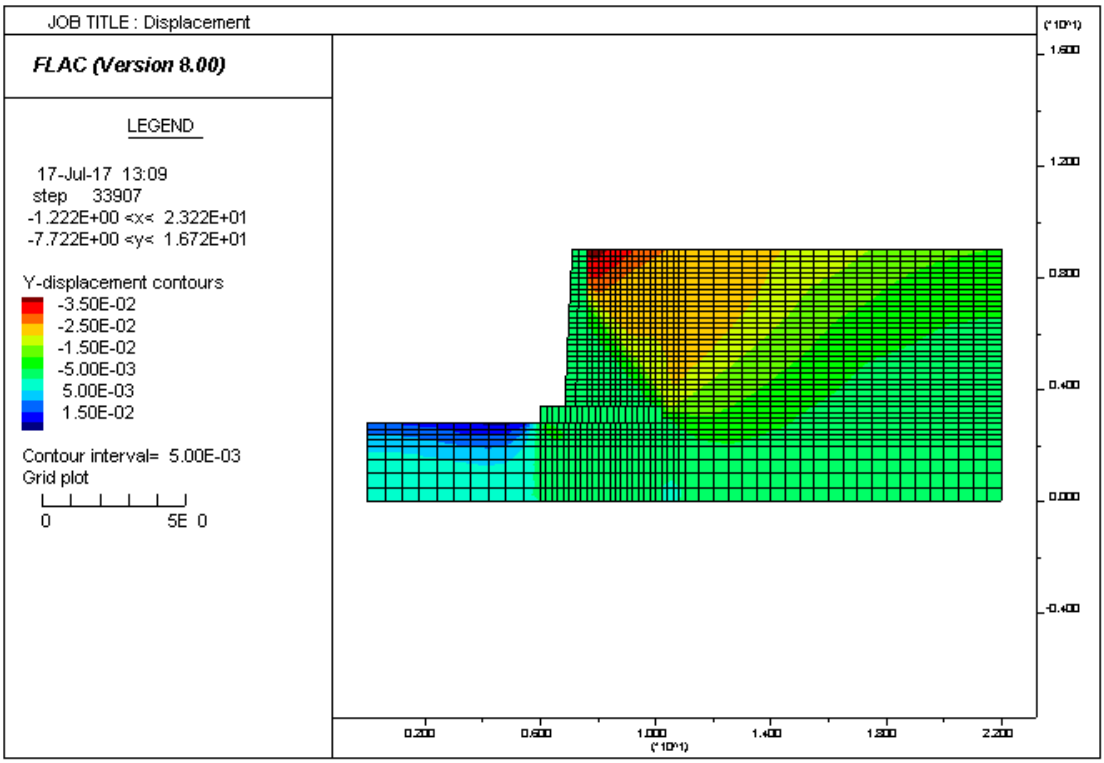

Figure 4.9. Displacement contours in Y direction for C = 1 kPa

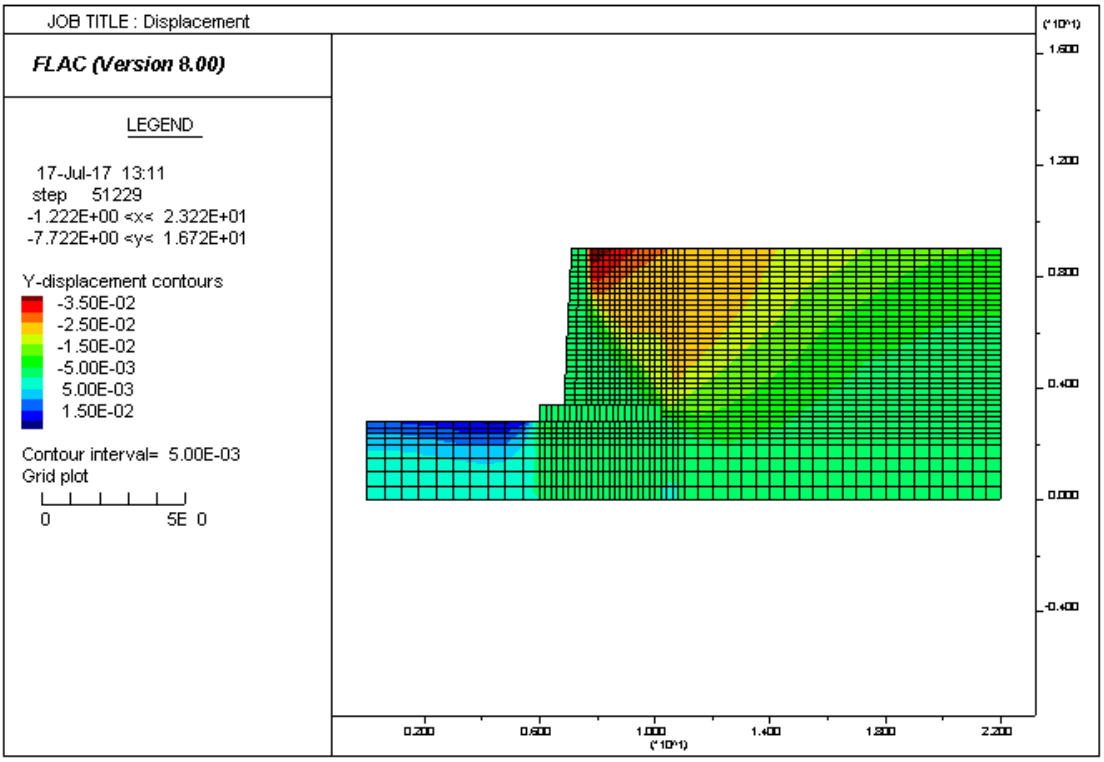

Figure 4.10. Displacement contours in Y direction for C = 10 kPa

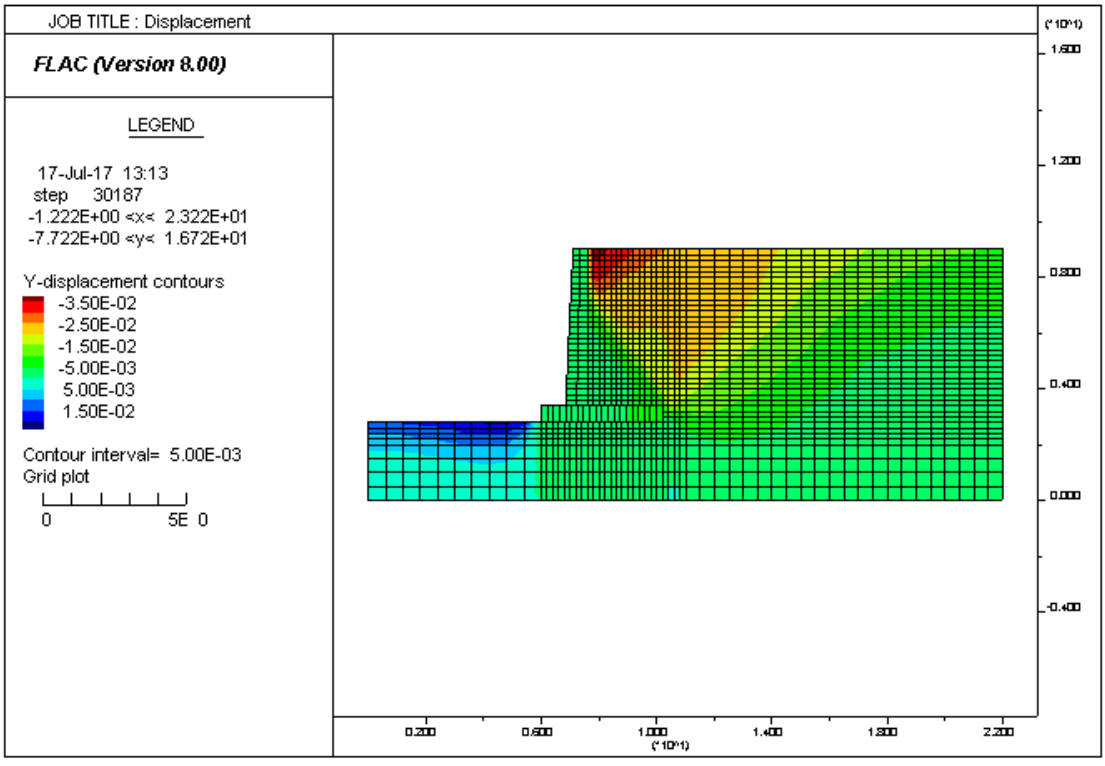

Figure 4.11. Displacement contours in Y direction for C = 100 kPa

Figures 4.12 and 4.13 show the variation of deformation at the top of retaining wall in both X and Y direction against different values of cohesion (C) between wall and soil in static and dynamic condition.

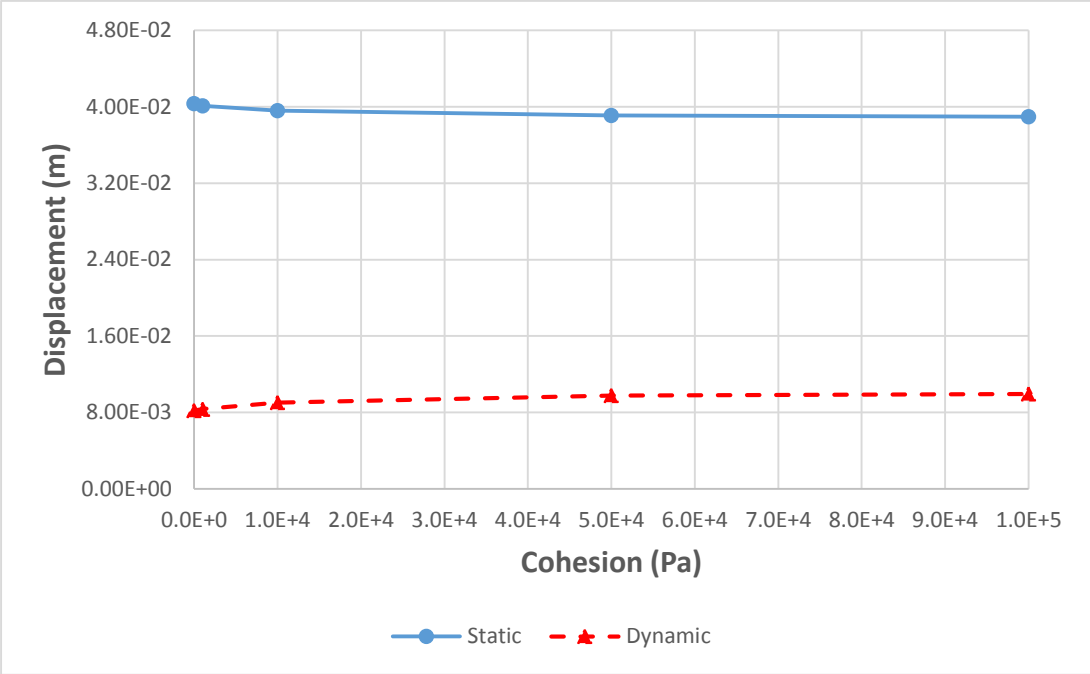

Figure 4.12. Displacement changes in X direction against different cohesion values

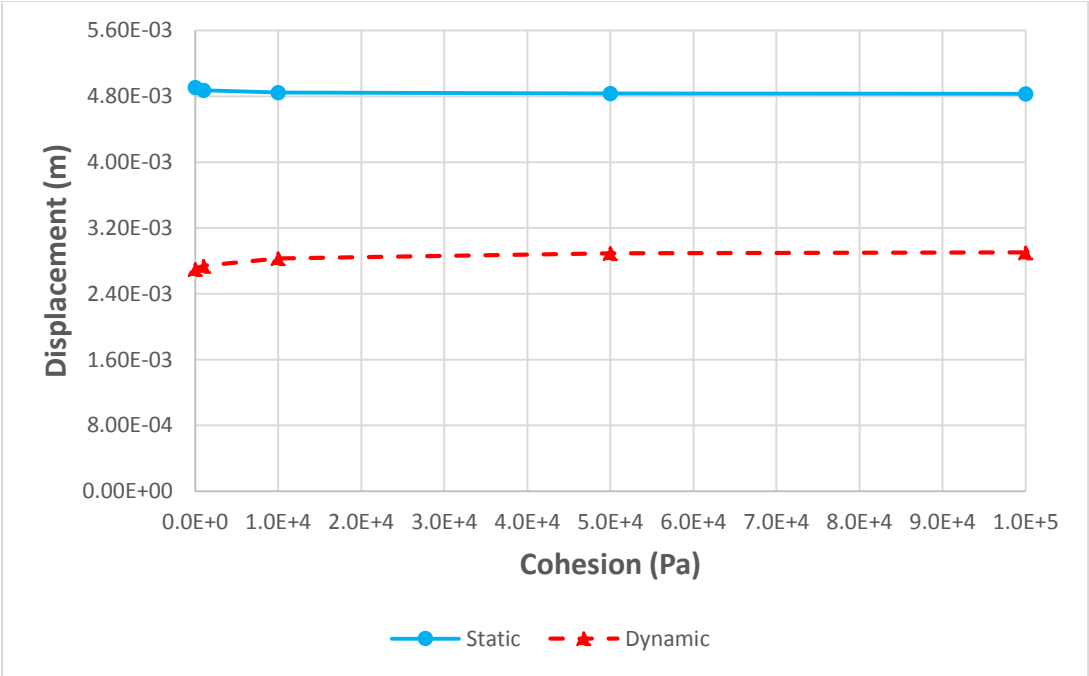

Figure 4.13. Displacement changes in Y direction against different cohesion values

Displacements contours in both X and Y direction are presented in Figures 4.14 to 4.21 for different values of friction angle (φ=29, 32, 35 and 38) in static condition. According to displacement contours, wall displacements in both X and Y direction will decrease with increasing friction angle values.

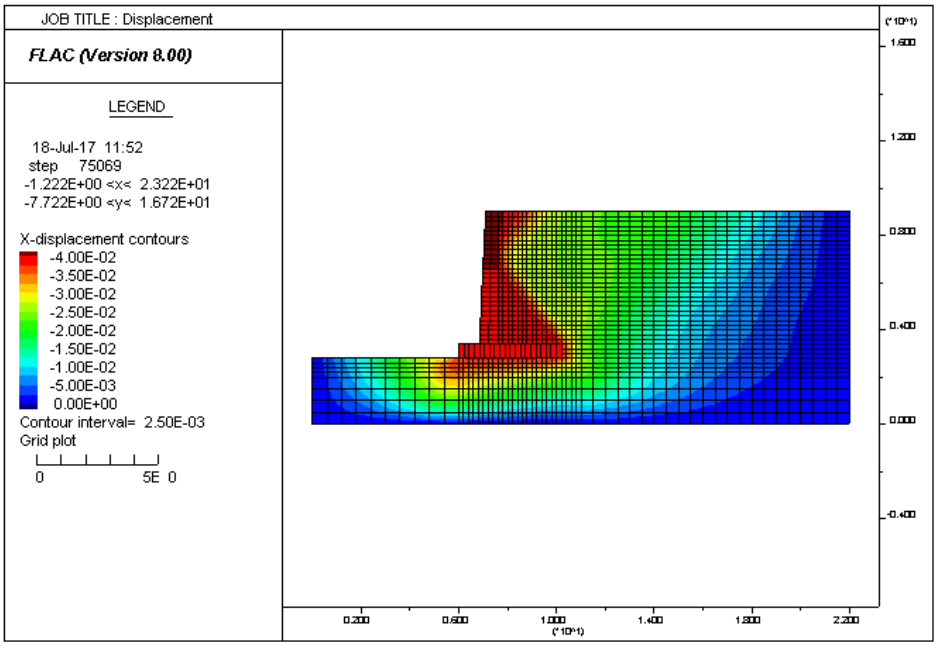

Figure 4.14. Displacement contours in X direction for φ=29 degree

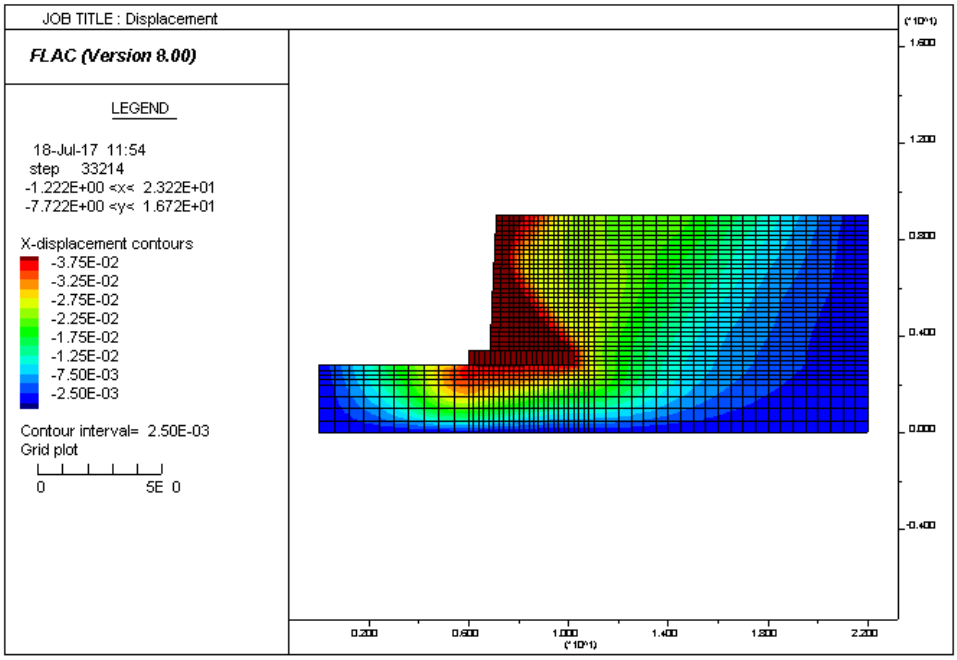

Figure 4.15. Displacement contours in X direction for φ=32 degree

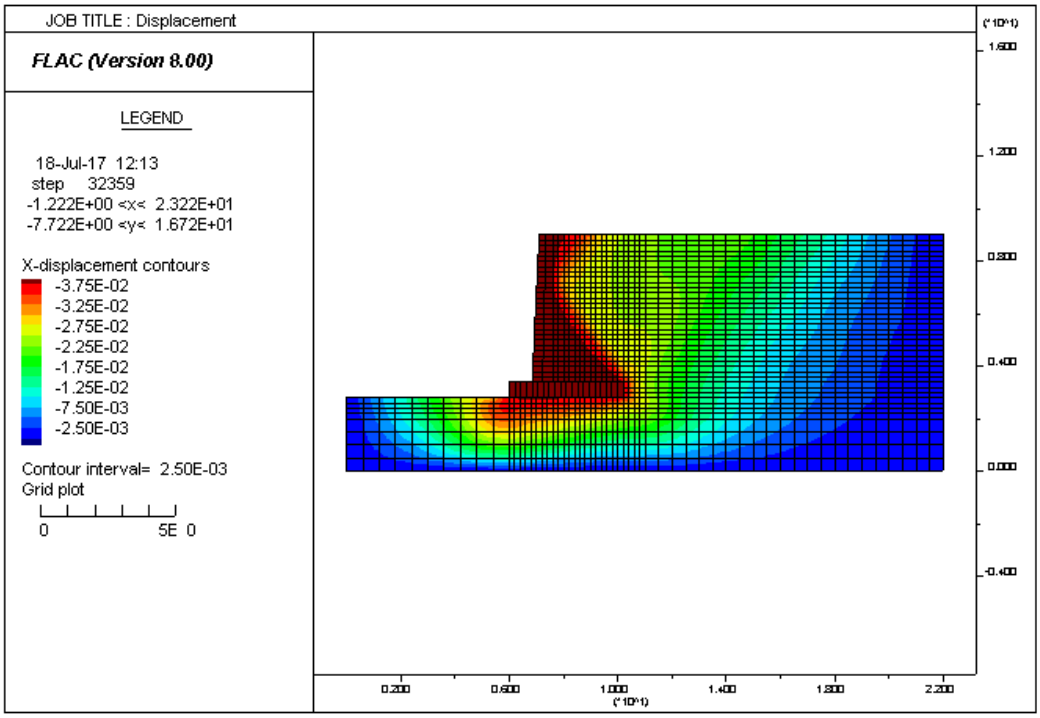

Figure 4.16. Displacement contours in X direction for φ=35 degree

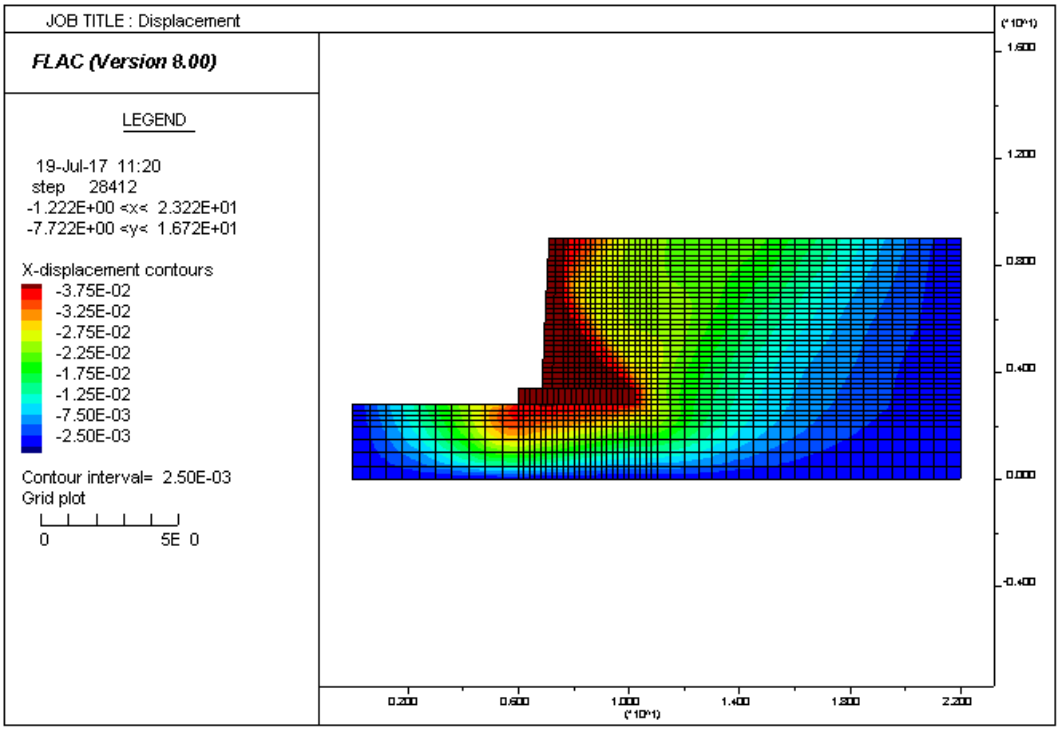

Figure 4.17. Displacement contours in X direction for φ=38 degree

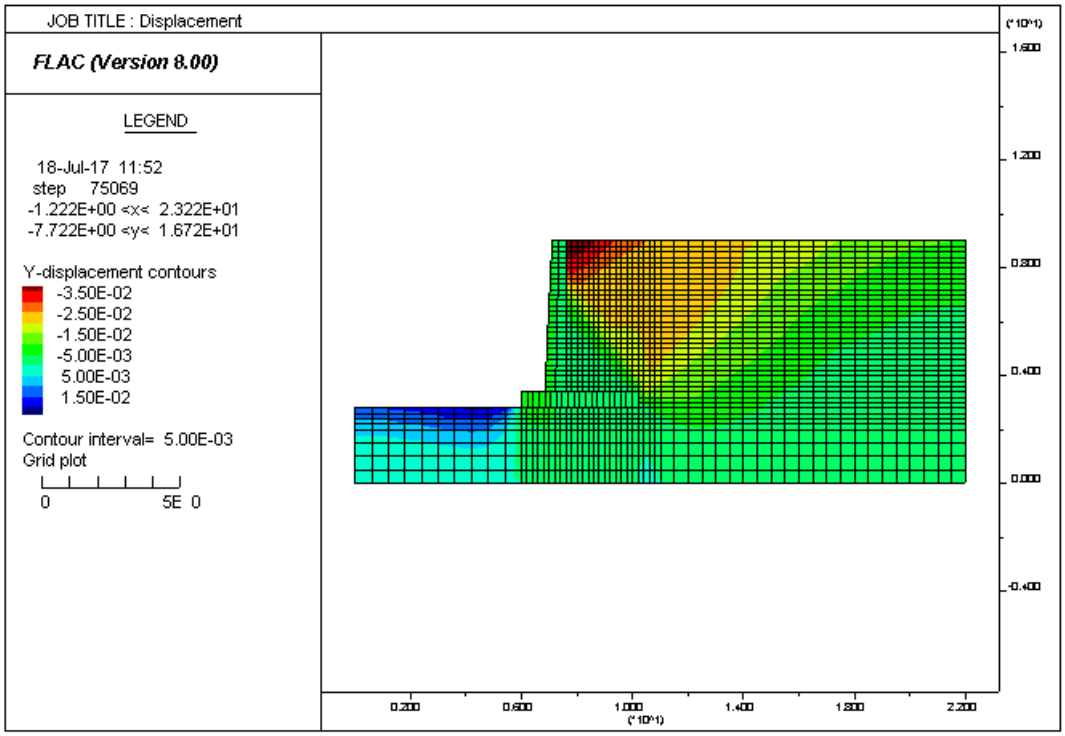

Figure 4.18. Displacement contours in Y direction for φ=29 degree

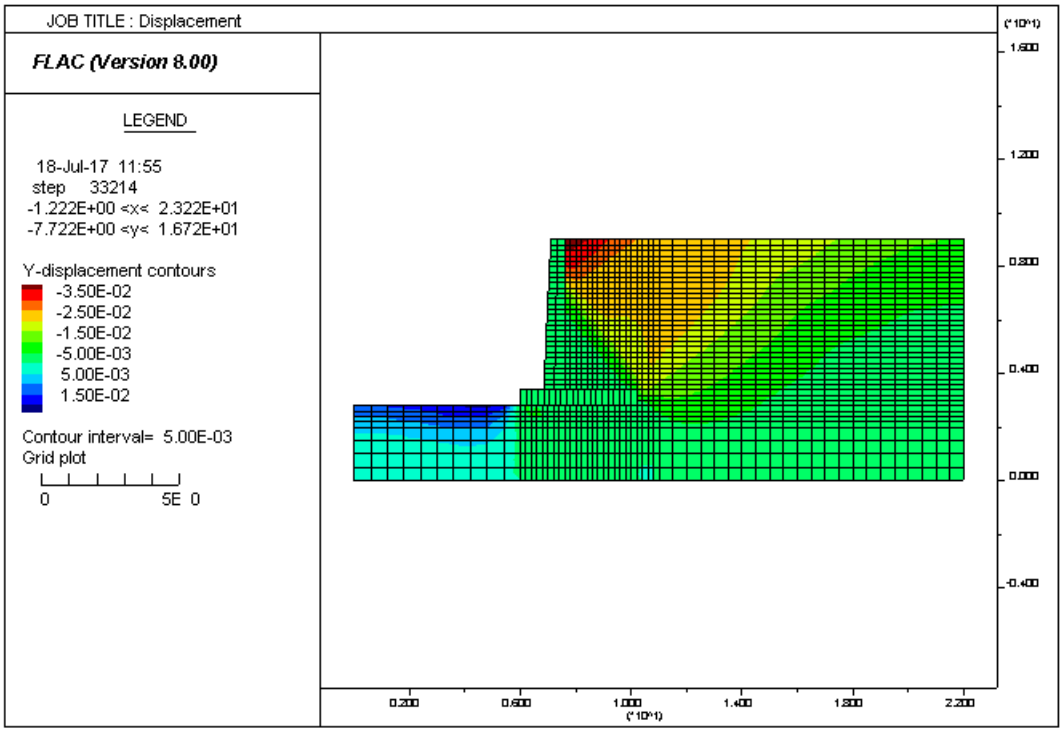

Figure 4.19. Displacement contours in Y direction for φ=32 degree

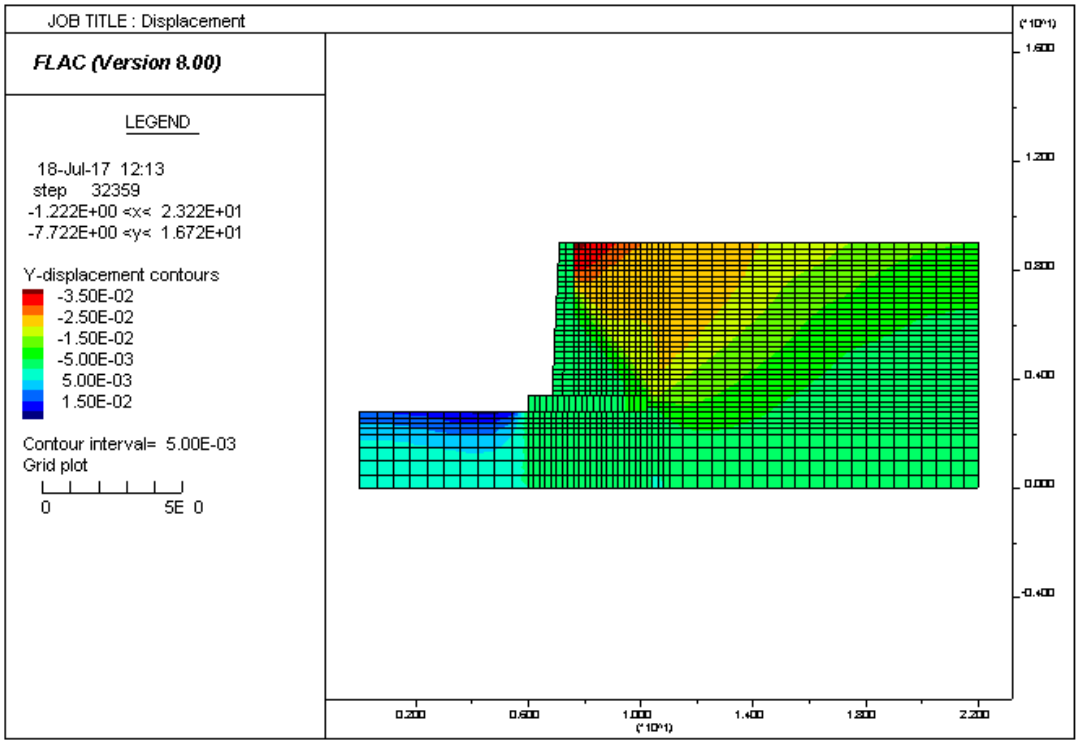

Figure 4.20. Displacement contours in Y direction for φ=35 degree

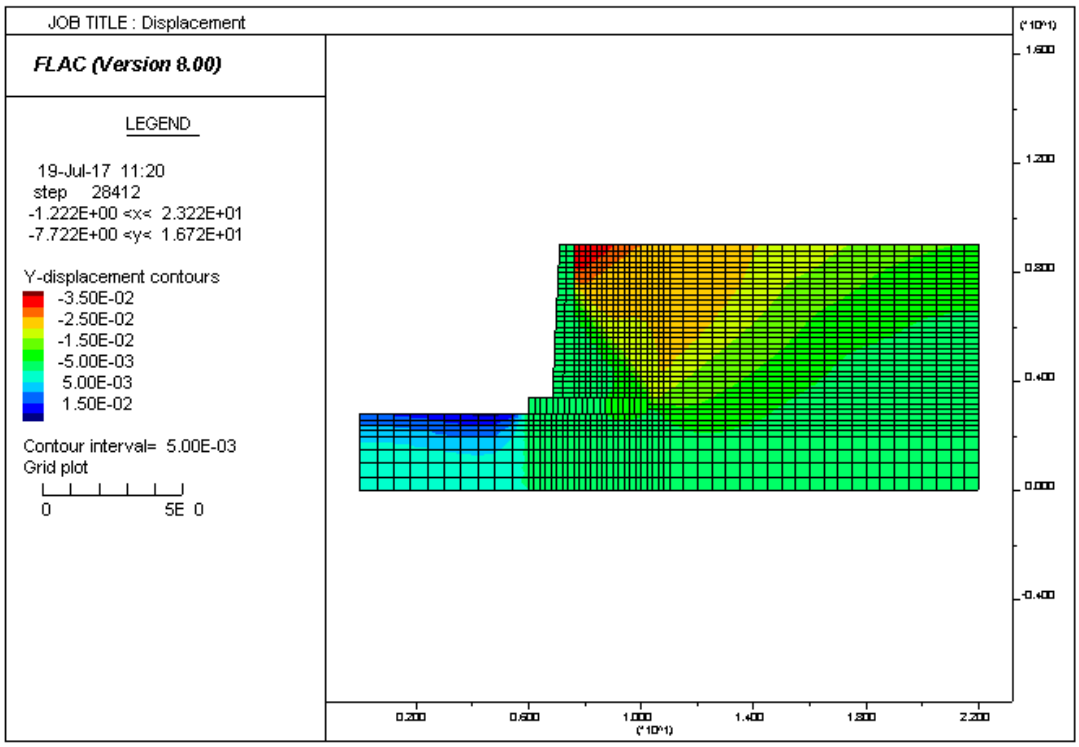

Figure 4.21. Displacement contours in Y direction for φ=38 degree

The behavior of retaining wall deformation against different values of friction angle for wall-soil interface are presented in Figures 4.22 and 4.23 in both static and seismic condition.

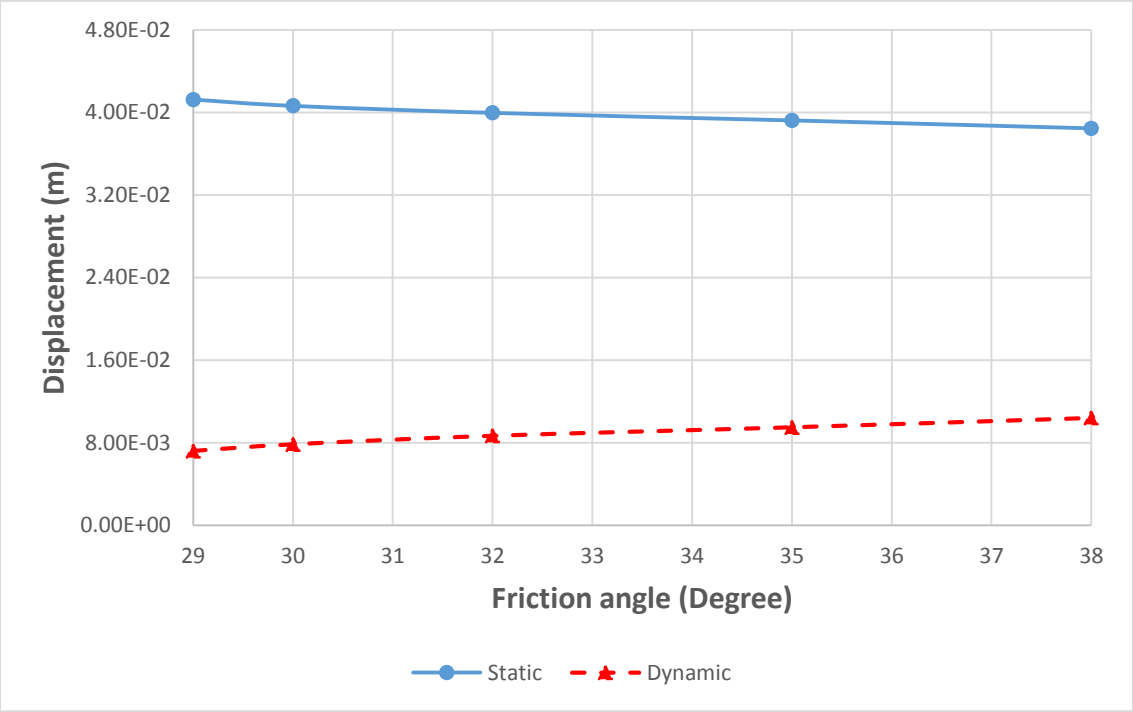

Figure 4.22. Displacement changes in X direction against different friction angle values

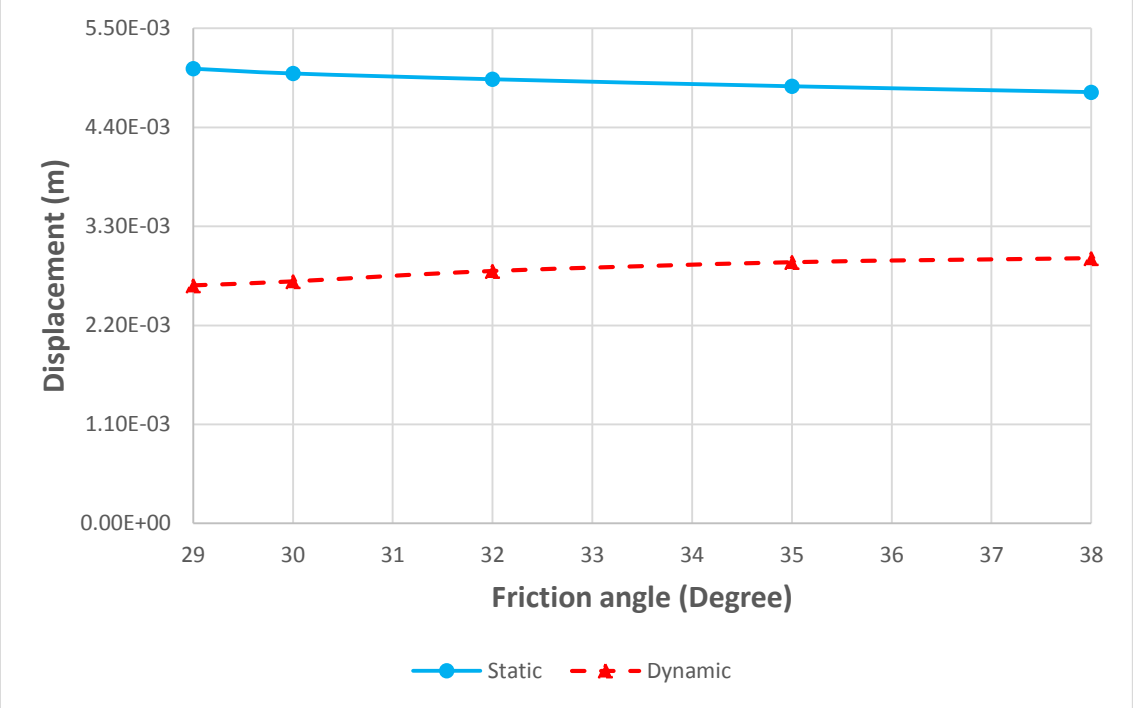

Figure 4.23. Displacement changes in Y direction against different friction angle values

The numerical results show that in the static condition, the wall displacements in both horizontal and vertical directions would decrease by increasing the cohesion (C) and friction angle (φ) values. But in dynamic analysis, the wall deformation is different and with increasing the values of shear strength parameters (Cohesion and friction angle) the wall displacements increase.

4.5.2. Sensitivity analysis of stiffness parameters

A schematic of the FLAC interface element is presented in Figure 4.24. According to interface mechanism, the element allows permanent separation and slip of the soil and the structure, as controlled by the parameters T and S, respectively. Furthermore, for the cohesionless soil is modeled with T = 0, while S is specified as a function of the interface friction angle (φ).

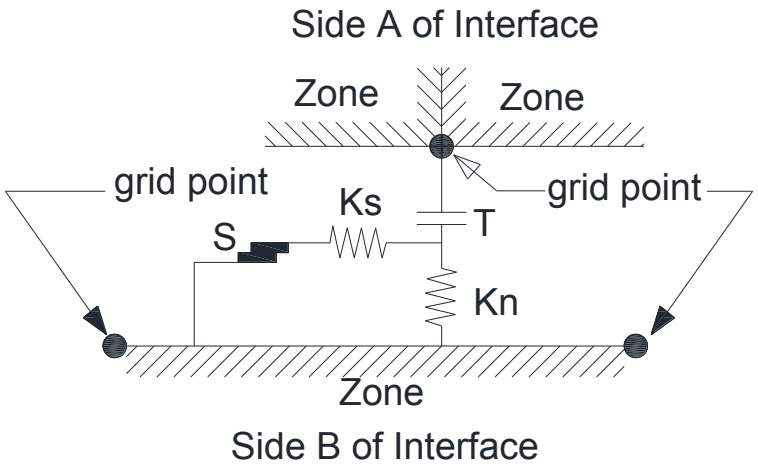

Figure 4.24. Schematic of FLAC interface element (Itasca, 2015)

Where;

S = Slider

T = Tensile Strength

K_n = Normal Stiffness

K_s = Shear Stiffness

According to the FLAC software (Itasca 2015, Theory and Background Manual), normal stiffness (Kn) and shear stiffness (Ks) be set to ten times the equivalent stiffness of the stiffest neighboring zone (Itasca, 2015). The apparent stiffness (expressed in stress-per-distance units) of a zone in the normal direction is obtained according to following equation:

$$K_n = 10 \times max\left[\frac{\left(K+\frac{4}{3}G\right)}{\Delta Z_{min}}\right] \quad (4\text{-}2)$$

Where;

K: Bulk moduli

G: Shear moduli

Δ_{zmin}: Smallest width of an adjoining zone in the normal direction

Moreover, the shear stiffness parameter (K_s) has the main role in the behavior of wall-soil interface. For this purpose, the determination of the shear stiffness (K_s) required considerably more effort than the determination of the other interface element parameters.

The interface element in FLAC, in shear behavior, essentially is an elasto-plastic model, with an elastic stiffness of K_s and yield strength S. Shear stiffness (K_s) value will obtained according to equation 4-3 (Itasca, 2015).

$$K_s = \frac{1}{\frac{1}{K_I \times \gamma_w \times \left(\frac{\sigma_n}{P_a}\right)^{n_j}} + \frac{R_{fj} \times \Delta r}{\sigma_n \times \tan(\delta)}} \quad (4\text{-}3)$$

K_I: Dimensionless interface stiffness number for initial loading

γ_W: Unit weight of water in consistent units as Δ_r

σ_n: Normal stress acting on the interface

P_a: Atmospheric pressure in the same units as σ_n

n_j: Dimensionless stiffness exponent

R_{fj}: Failure ratio

δ: Interface friction angle

Figures 4.25 to 4.32 illustrate displacement contours in X and Y direction for different values of shear stiffness (K_s = 3.3e6, 5.6e6, 2e7 and 5e7) in static state. Displacement contours in Figures 4.25 to 4.32 show that with increasing shear stiffness, wall deformation will decrease.

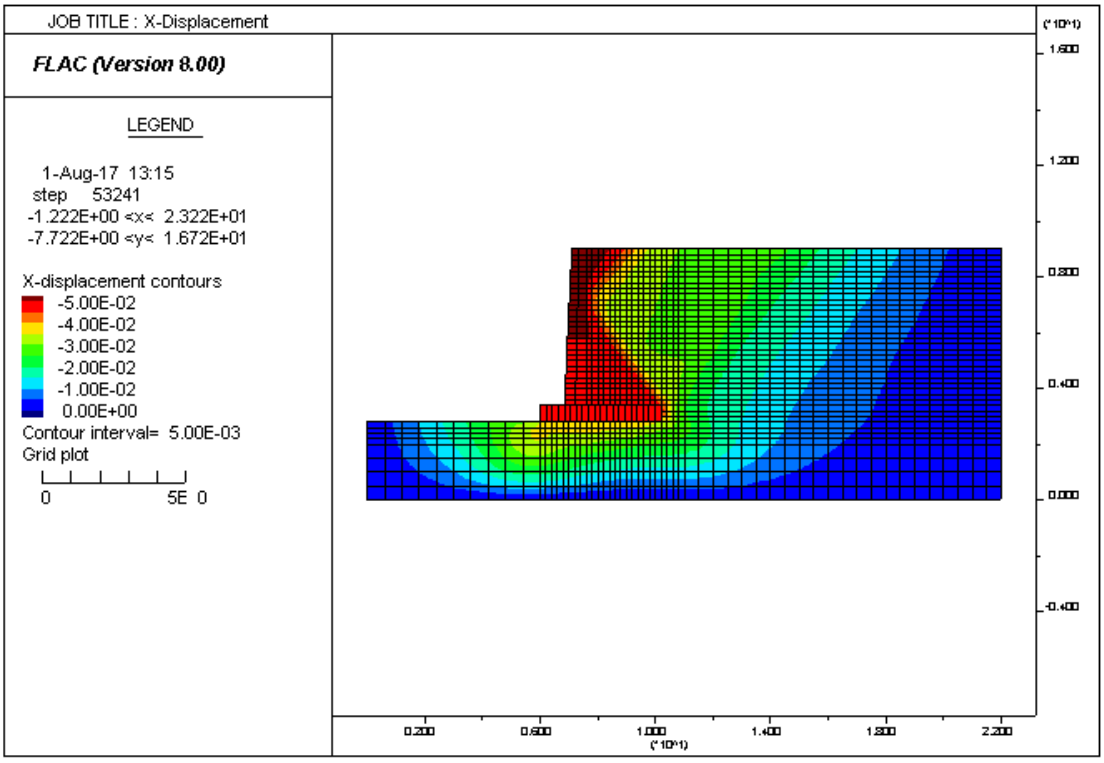

Figure 4.25. Displacement contours in X direction for K_s = 3.3e6 Pa

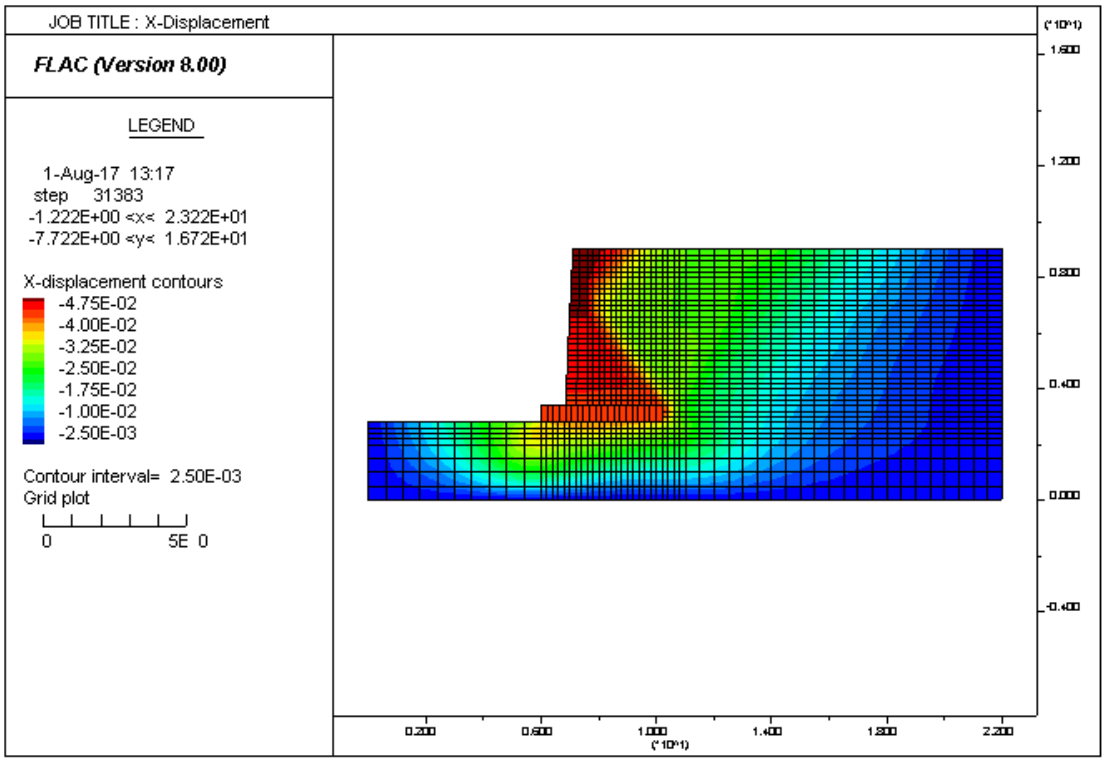

Figure 4.26. Displacement contours in X direction for K_s = 5e6 Pa

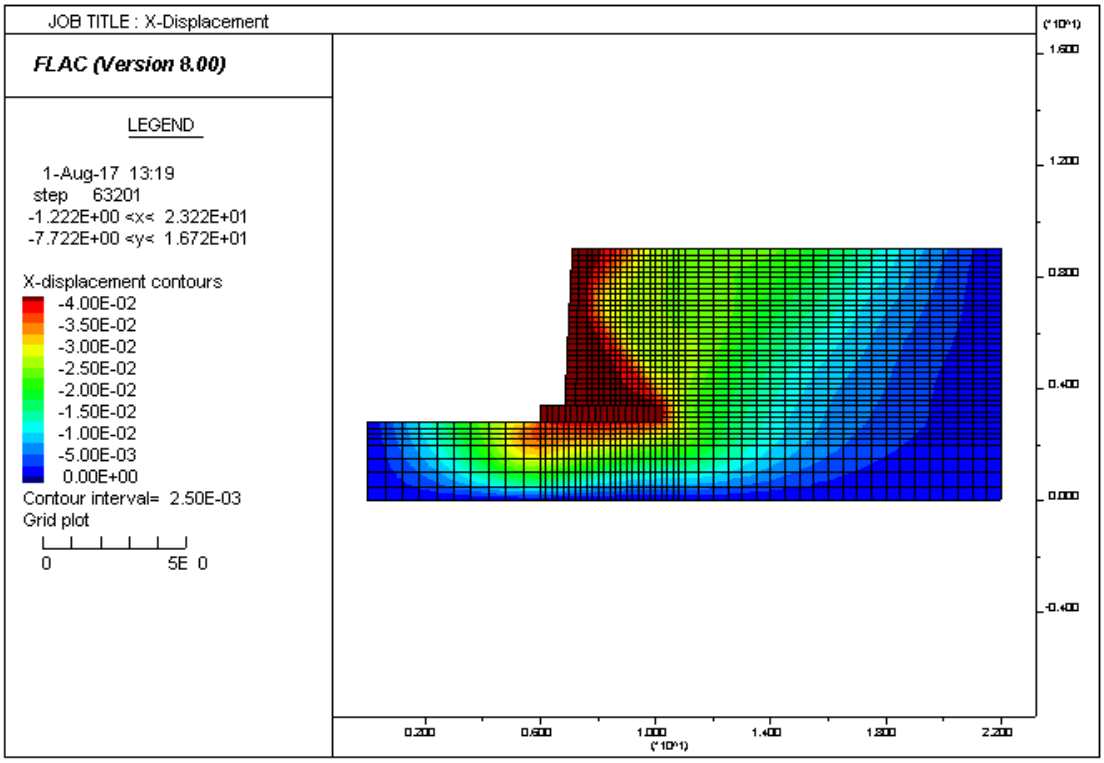

Figure 4.27. Displacement contours in X direction for K_s = 2e7 Pa

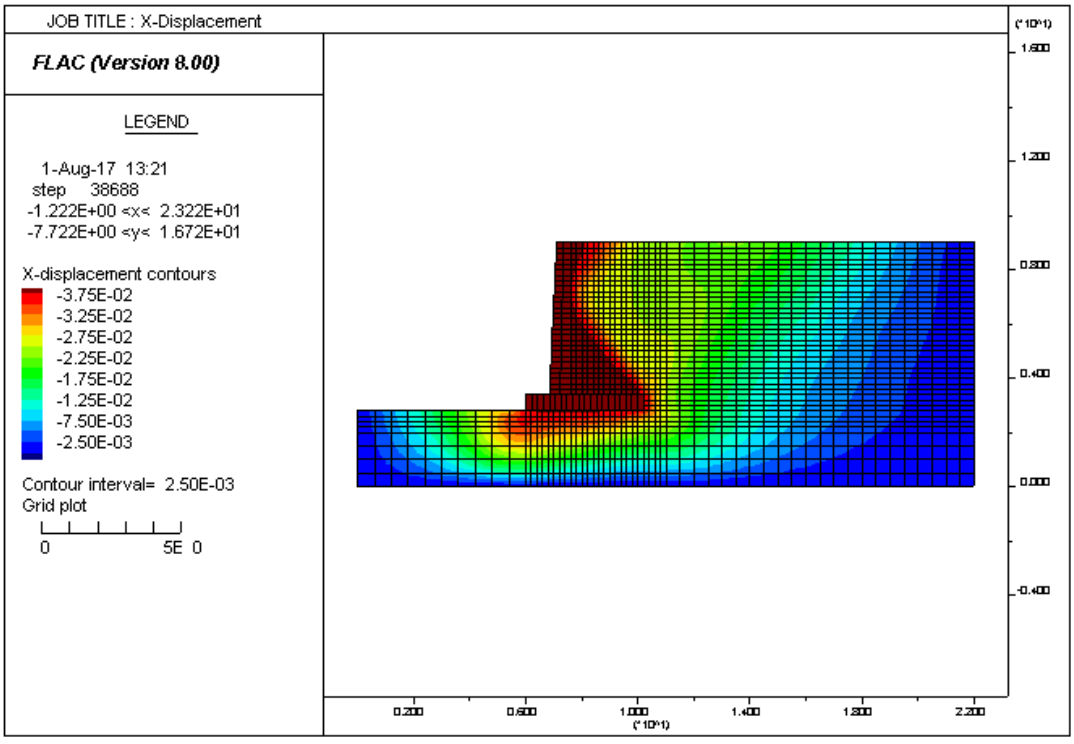

Figure 4.28. Displacement contours in X direction for K_s = 5e7 Pa

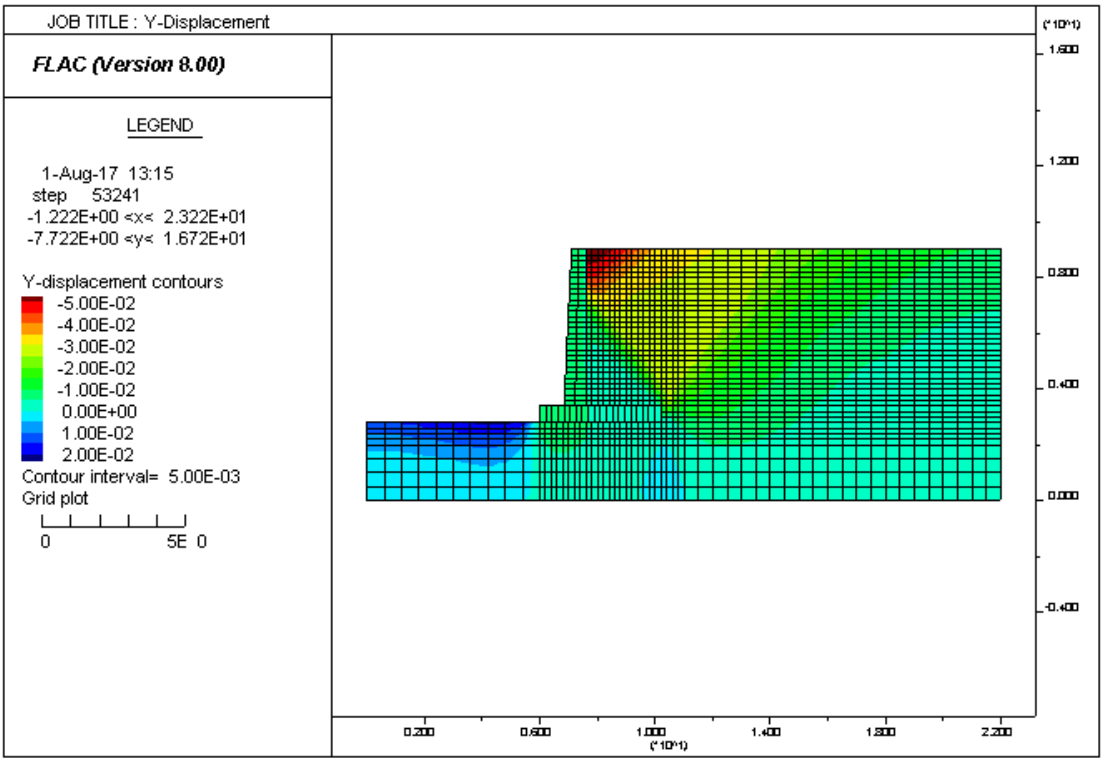

Figure 4.29. Displacement contours in Y direction for K_s = 3.3e6 Pa

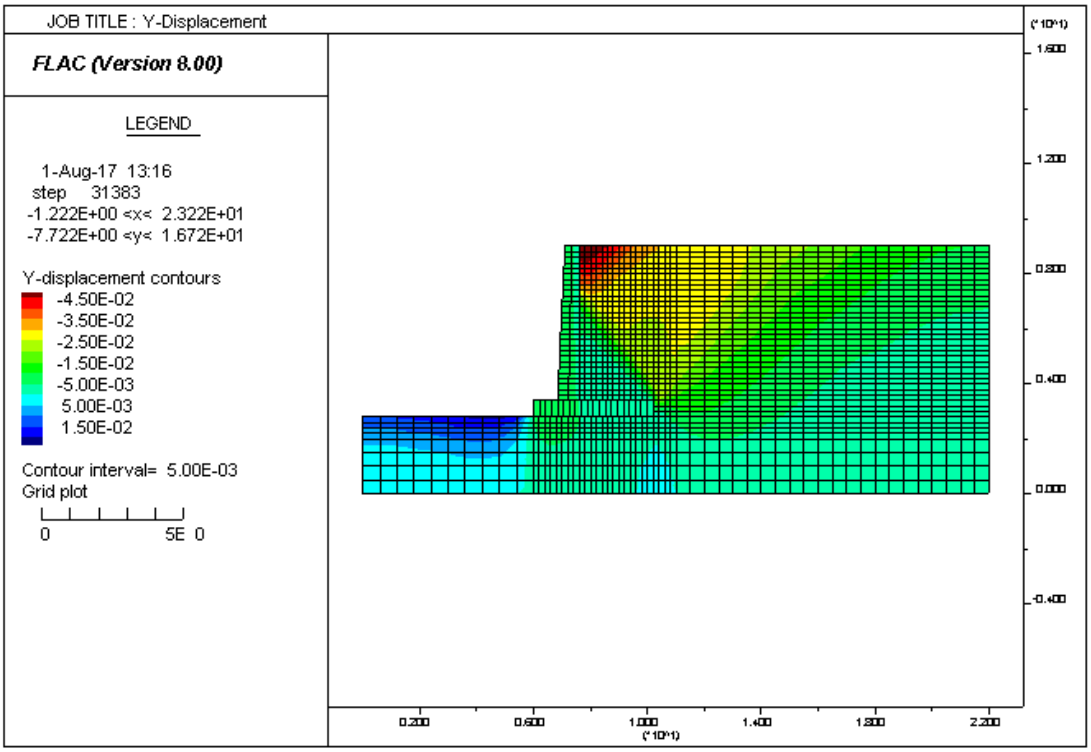

Figure 4.30. Displacement contours in Y direction for K_s = 5e6 Pa

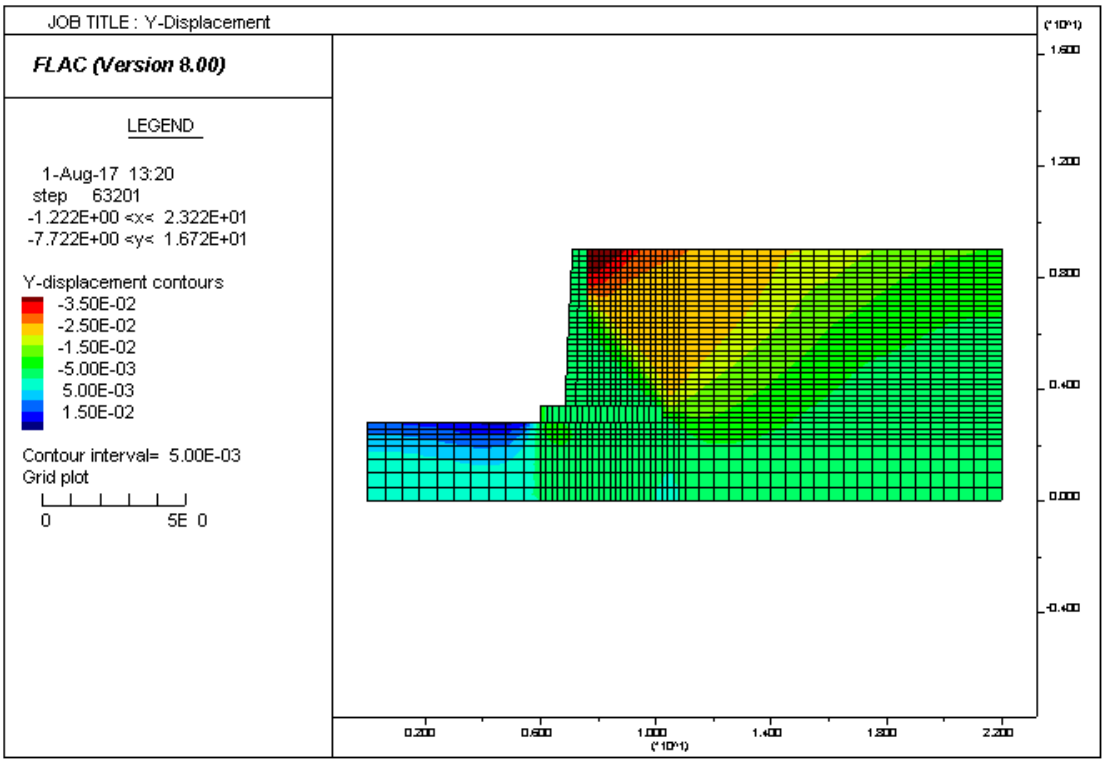

Figure 4.31. Displacement contours in Y direction for K_s = 2e7 Pa

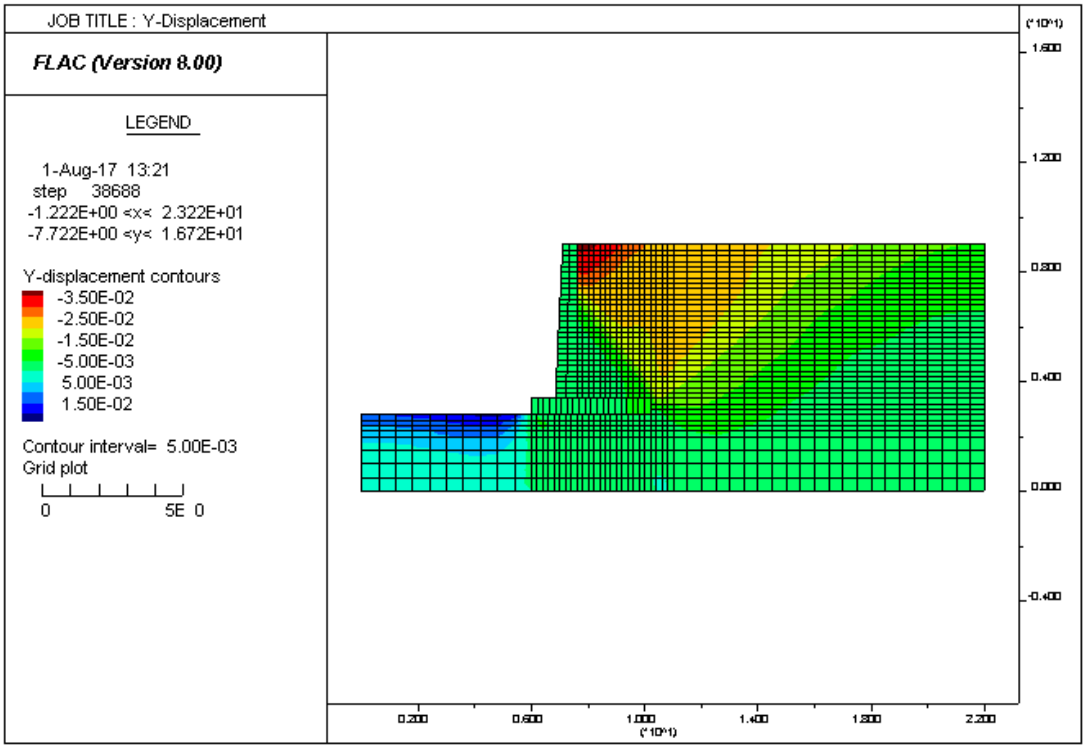

Figure 4.32. Displacement contours in Y direction for K_s = 5e7 Pa

Deformation changes against the shear strength value (K_s) are presented in Figures 4.33 and 4.34 for static and dynamic condition.

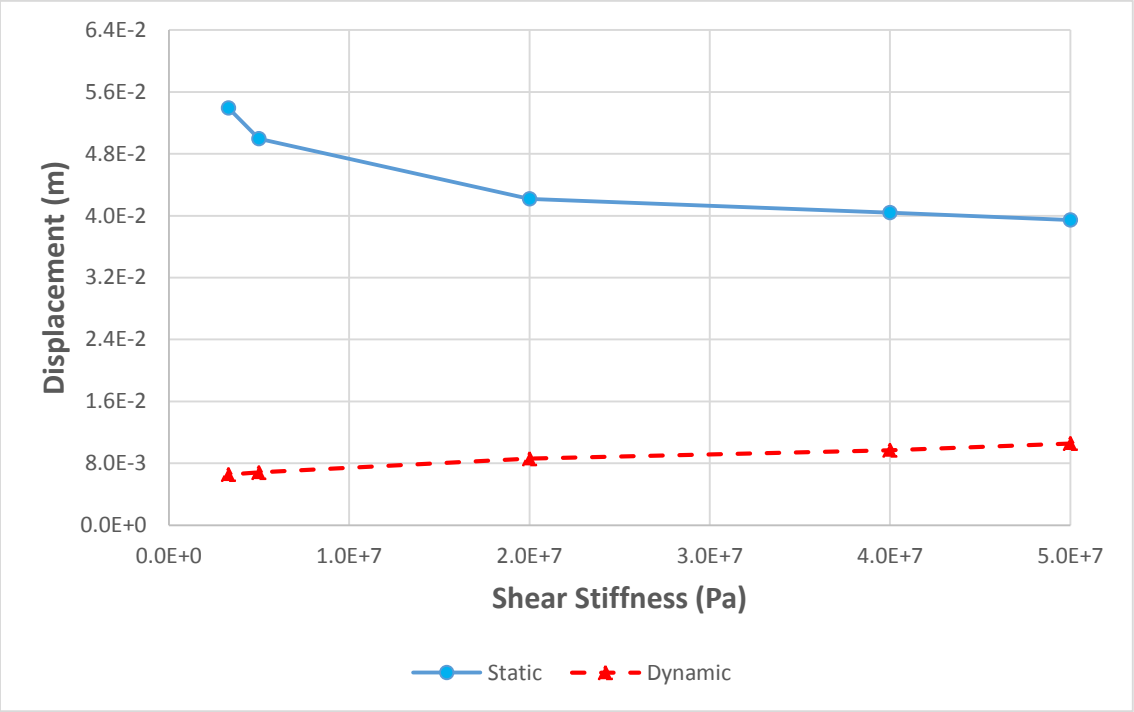

Figure 4.33. Displacement changes in X direction against different shear stiffness values in static condition

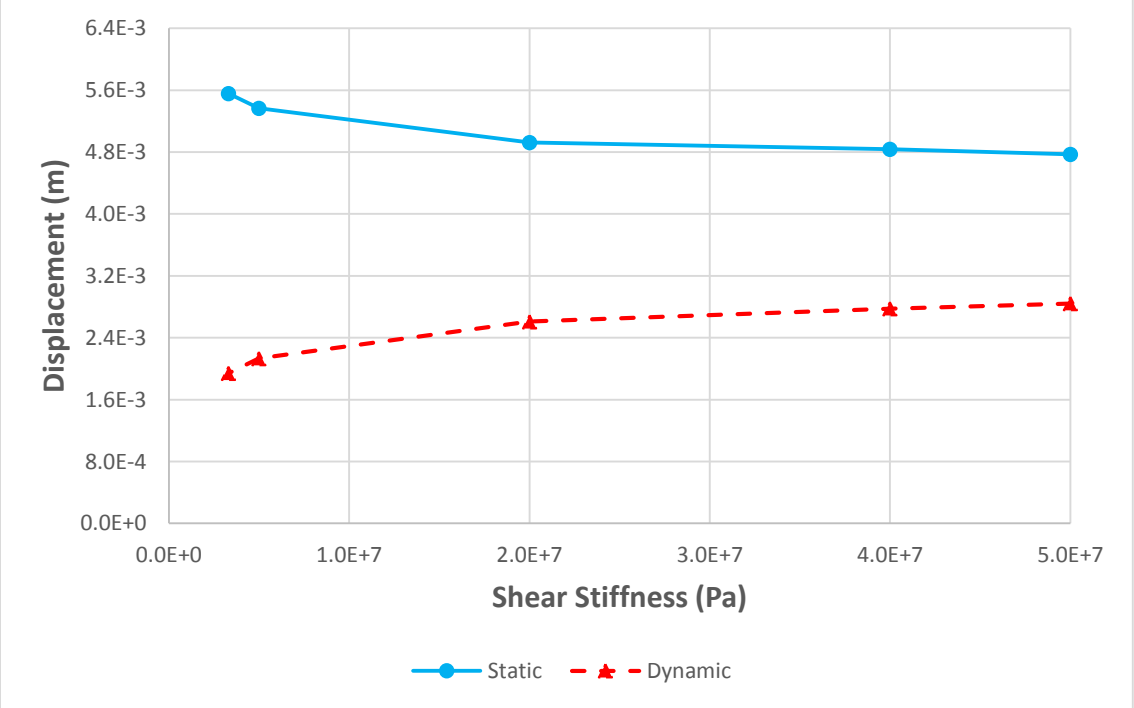

Figure 4.34. Displacement changes in Y direction against different shear stiffness values in static condition

Displacement contours for different values of normal stiffness (K_n=5e7Pa, 2e8Pa, 4e8Pa and 7e8Pa) in both X and Y direction are presented in Figures 4.35 to 4.42. These Figures show that with increasing normal stiffness parameter, wall displacement decreases.

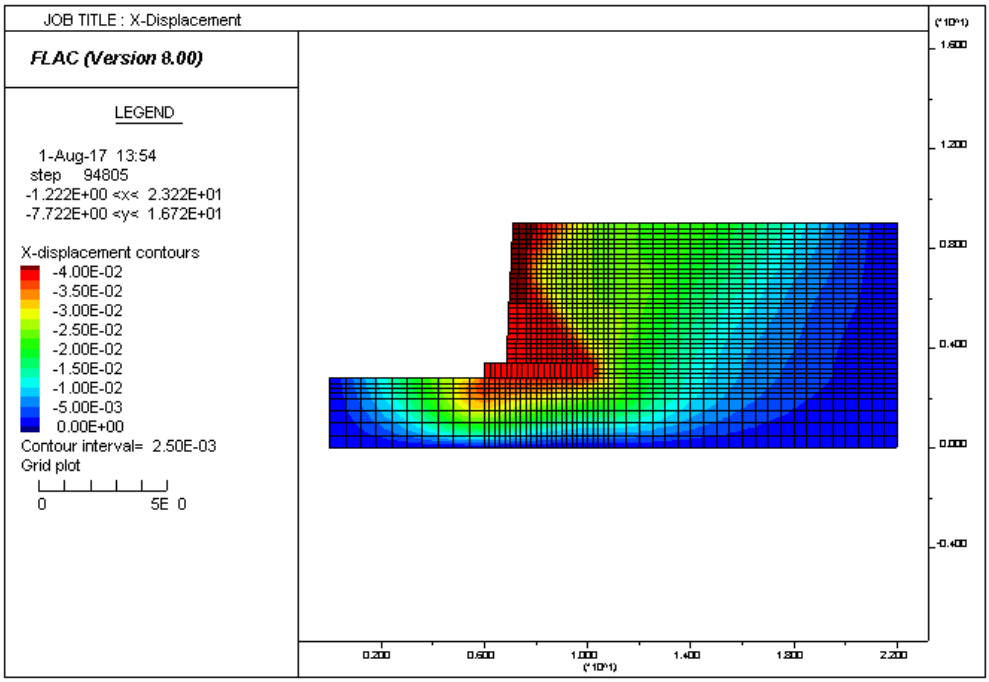

Figure 4.35. Displacement contours in X direction for K_n=5e7 Pa

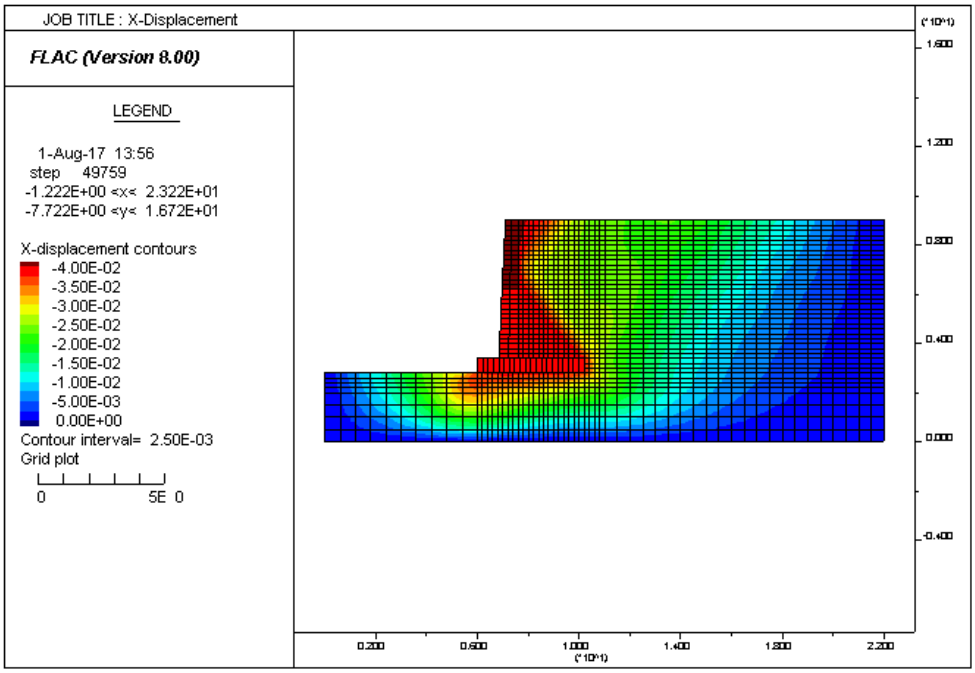

Figure 4.36. Displacement contours in X direction for K_n=2e8 Pa

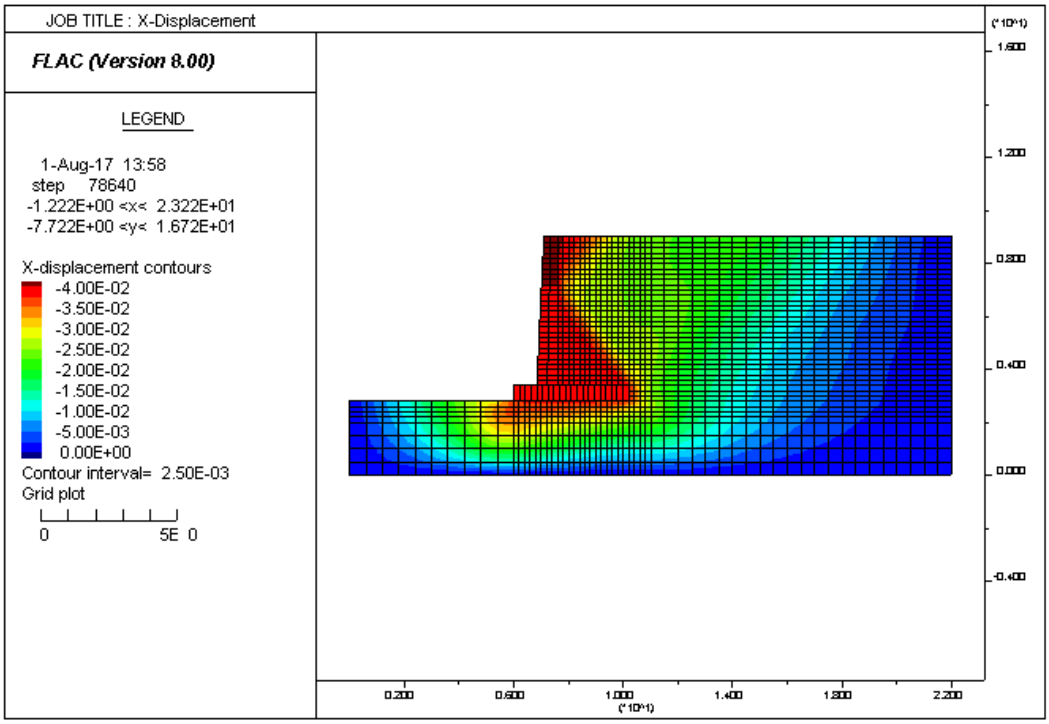

Figure 4.37. Displacement contours in X direction for K_n = 4e8 Pa

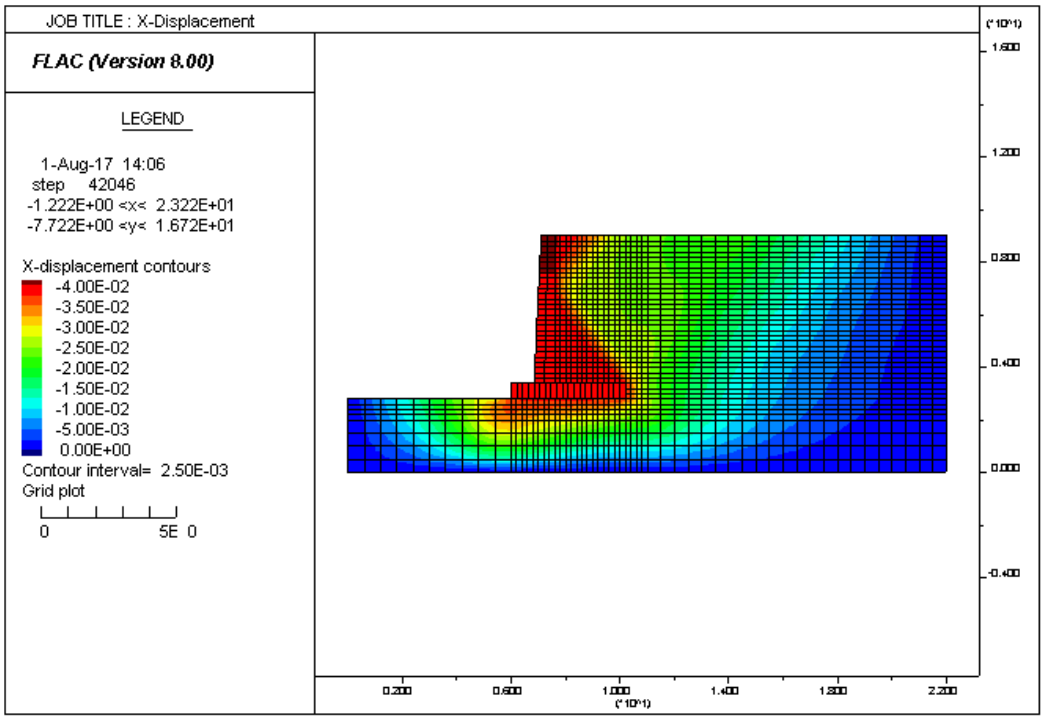

Figure 4.38. Displacement contours in X direction for K_n = 7e8 Pa

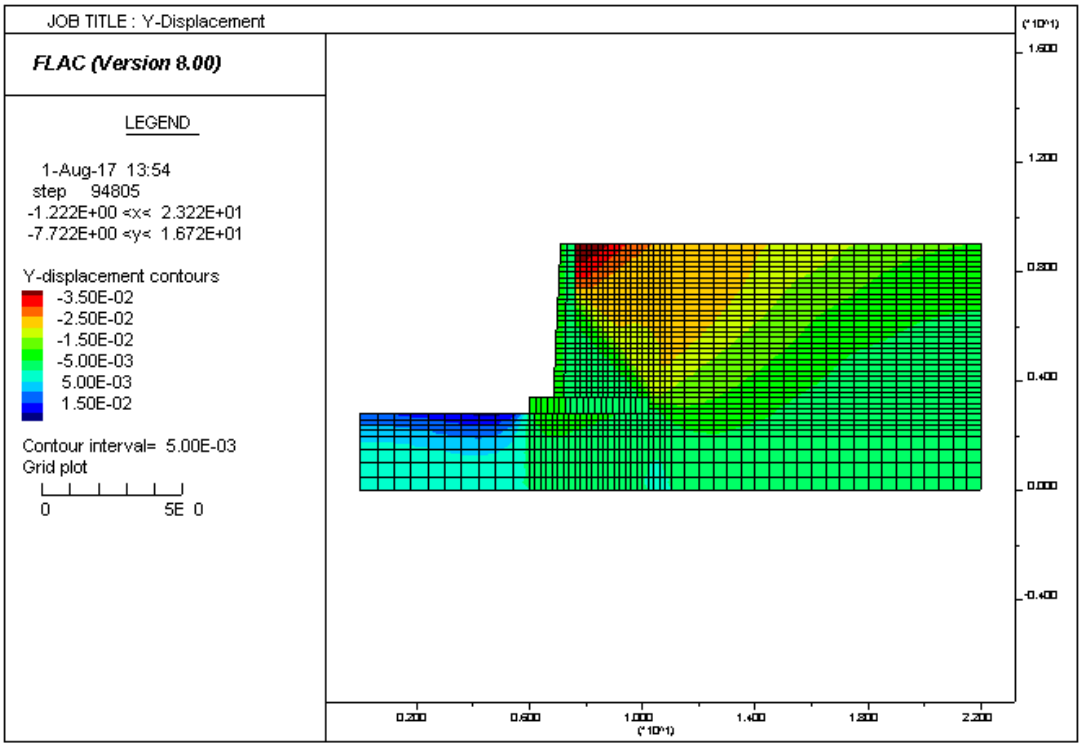

Figure 4.39. Displacement contours in Y direction for K_n = 5e7 Pa

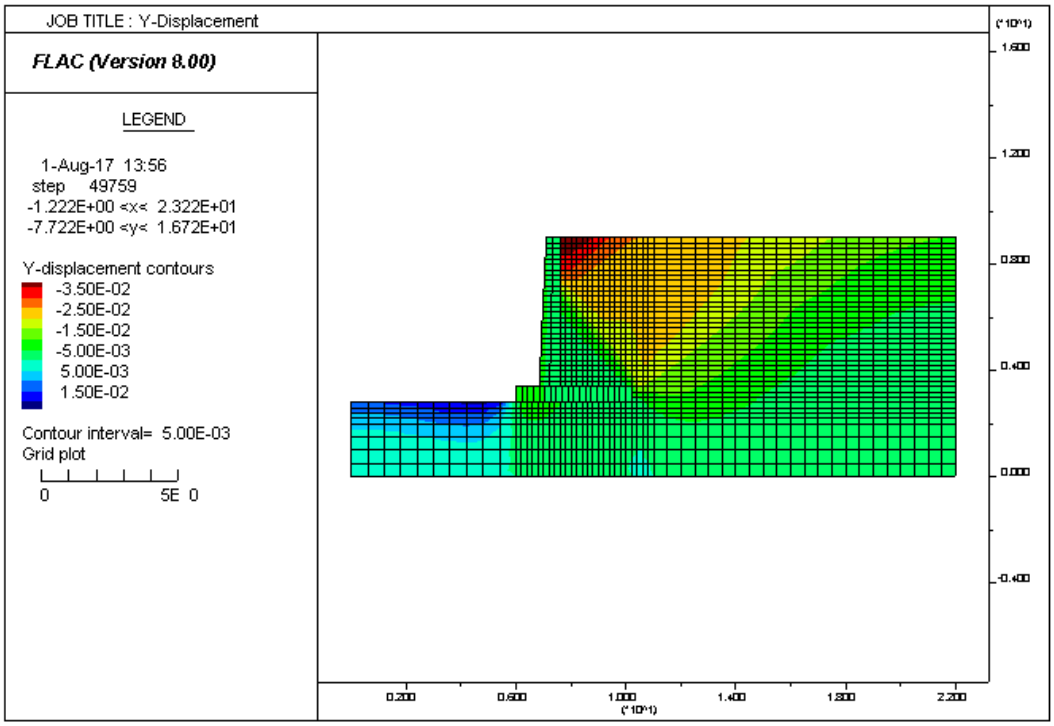

Figure 4.40. Displacement contours in Y direction for K_n = 2e8 Pa

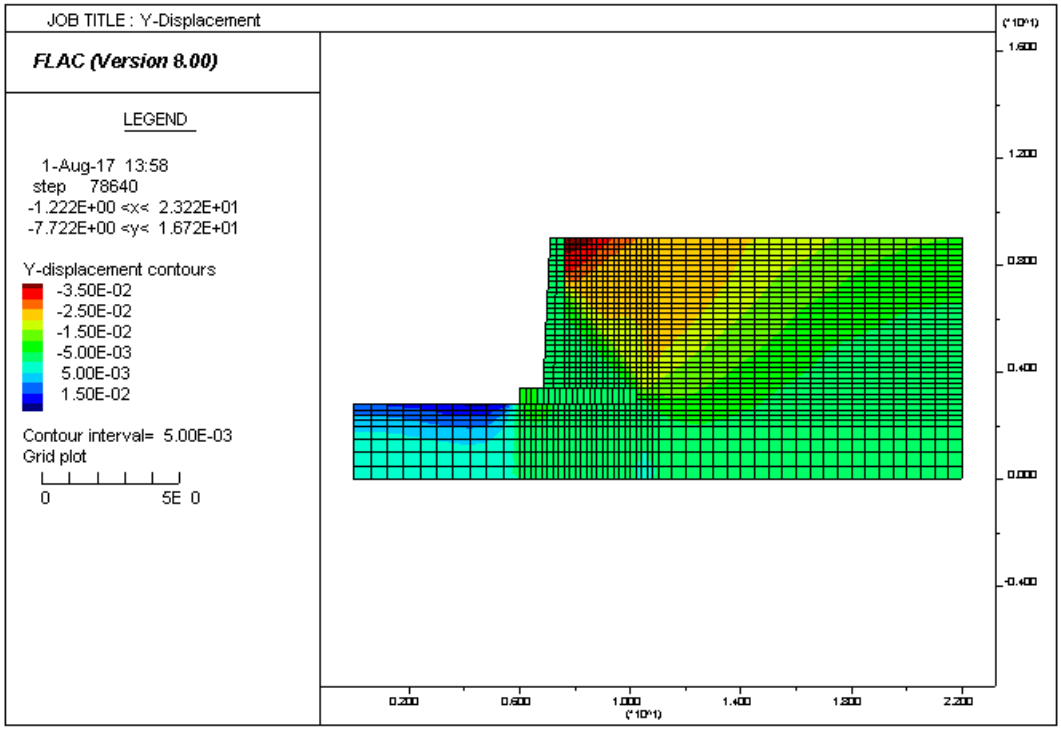

Figure 4.41. Displacement contours in Y direction for K_n = 4e8 Pa

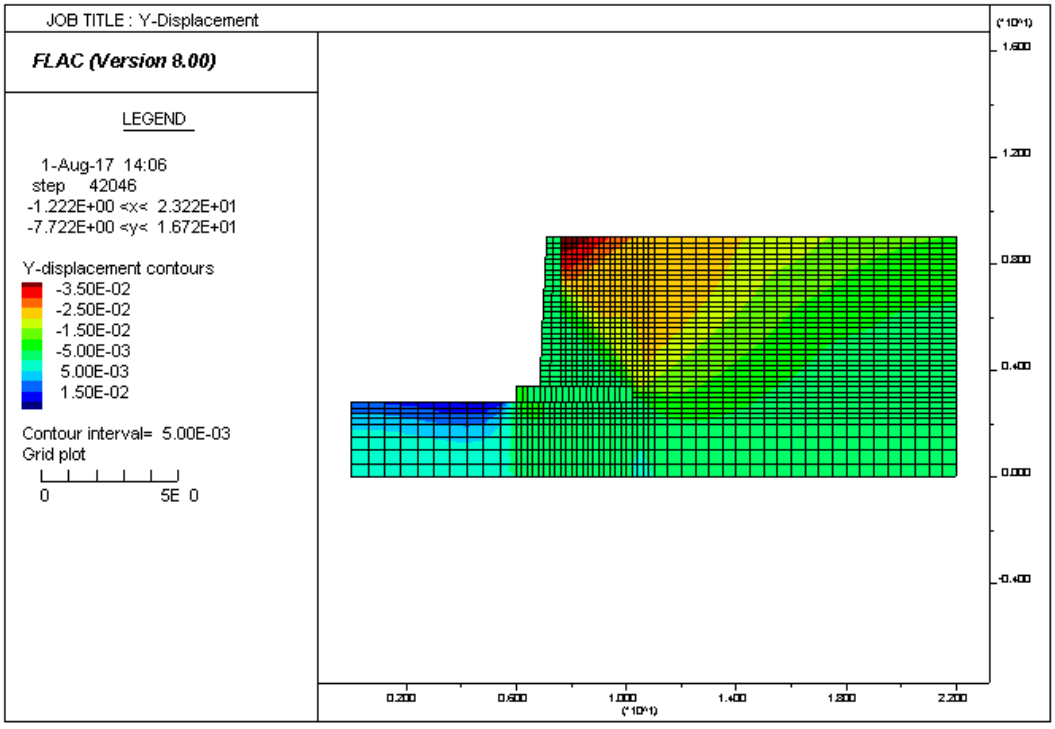

Figure 4.42. Displacement contours in Y direction for K_n = 7e8 Pa

Figures 4.43 and 4.44 illustrate the displacement changes of retaining wall with different value of shear stiffness parameter (K_n) for both static and seismic loading state.

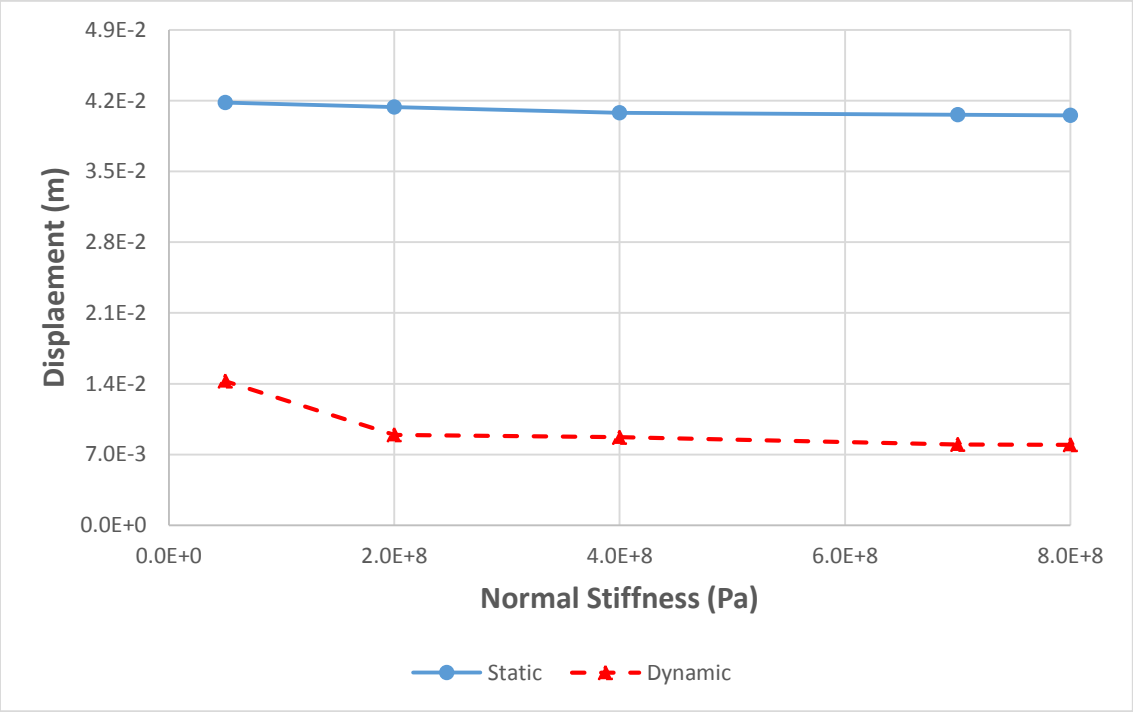

Figure 4.43. Displacement changes in X direction against different normal stiffness values in static condition

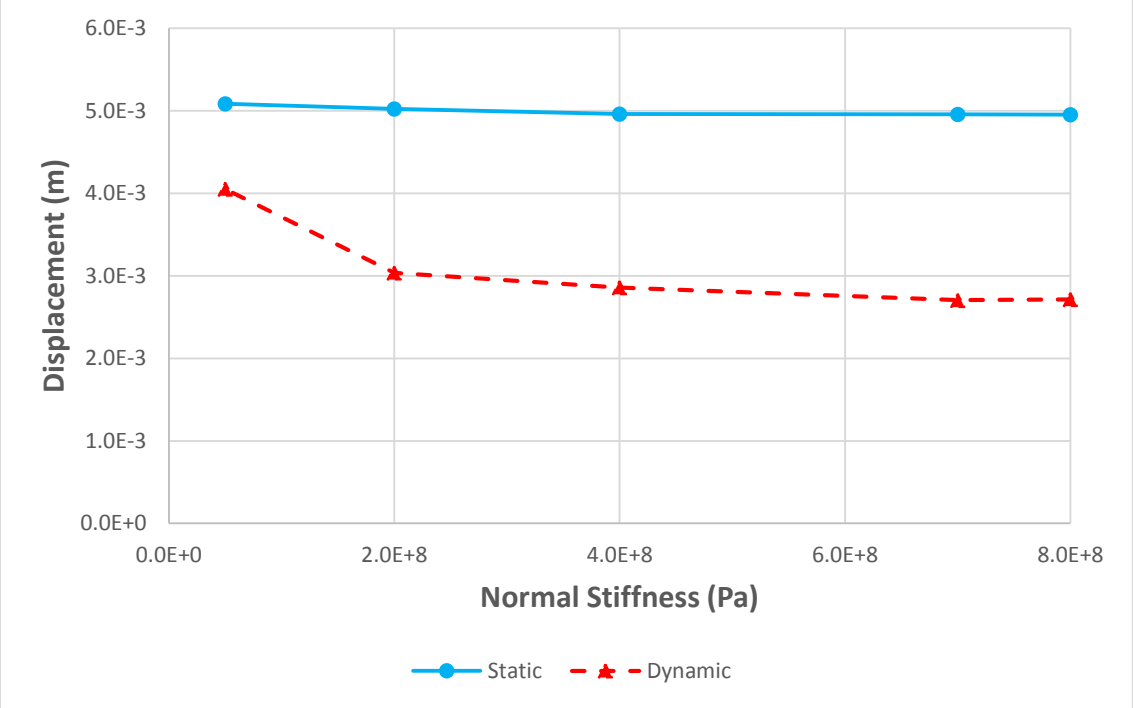

Figure 4.44. Displacement changes in Y direction against different normal stiffness values in static condition

Sensitivity analysis of the stiffness parameter of wall-soil interface shows that, in static condition with increasing normal and shear stiffness value, wall displacement would decreased in both X and Y direction. But in dynamic condition, wall displacement increase with increasing shear stiffness value whereas wall displacement would decrease by increasingly normal stiffness value.

4.5.3. Sensitivity analysis of dilation

Dilation is governed in the Mohr-Coulomb interface model by a specified dilation angle (ψ). Also, dilation is a function of the direction of shearing. When the shear displacement increment is in the same direction as the total shear displacement, dilation increases but the shear increment is in the opposite direction, dilation will decreases.

During sliding, shear displacement can cause an increase in the effective normal stress on the interface, according to the following equation (Itasca, 2015).

$$\sigma_n = \sigma_n + \frac{|F_s|_0 - \tau}{L \times K_s} \tan\psi \times K_n \quad (4\text{-}4)$$

Where;

τ: Shear Stress

ψ: Dilation Angle

σ_n: Normal stress

L: Effective Contact Length

K_n: Normal Stiffness

K_s: Shear Stiffness

$|F_s|_0$: Magnitude of Shear Force

In this section, a sensitivity analysis of the dilation parameter (ψ) has been conducted. According to different values of dilation angle (ψ=0°, 5°, 10° and 15°), displacement contours in X and Y direction are shown in Figure 4.45 to 4.52 for static condition. According to the displacements contours, with increasing dilation values, wall displacement decreases.

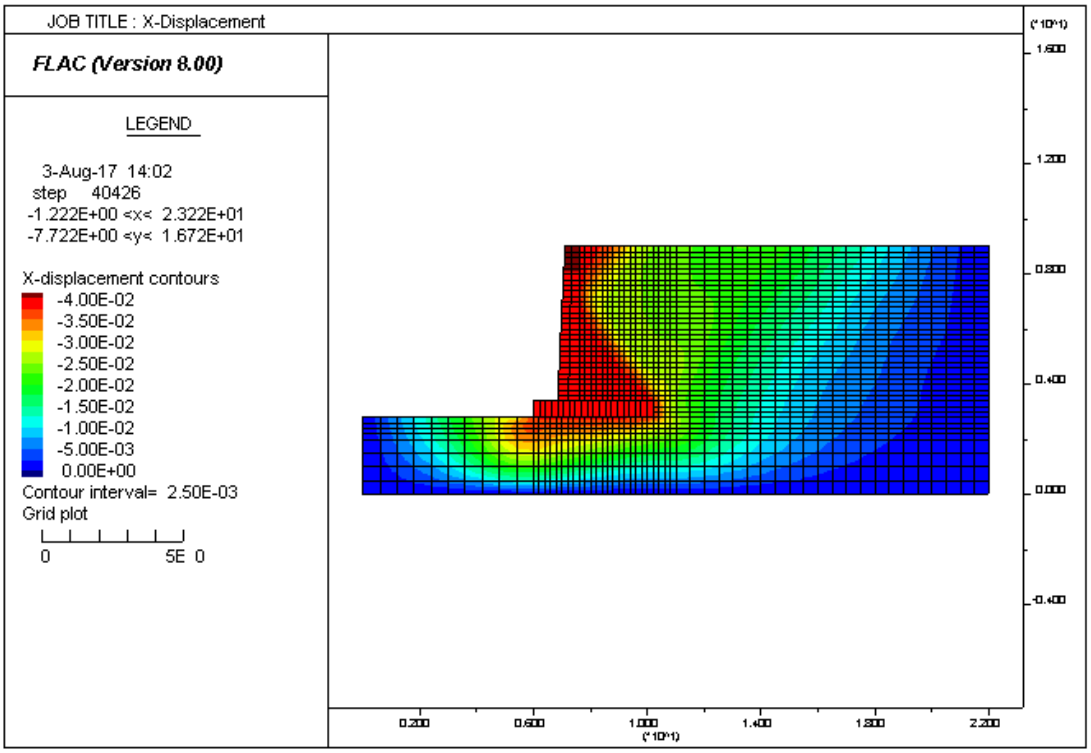

Figure 4.45. Displacement contours in X direction for ψ = 0 degree

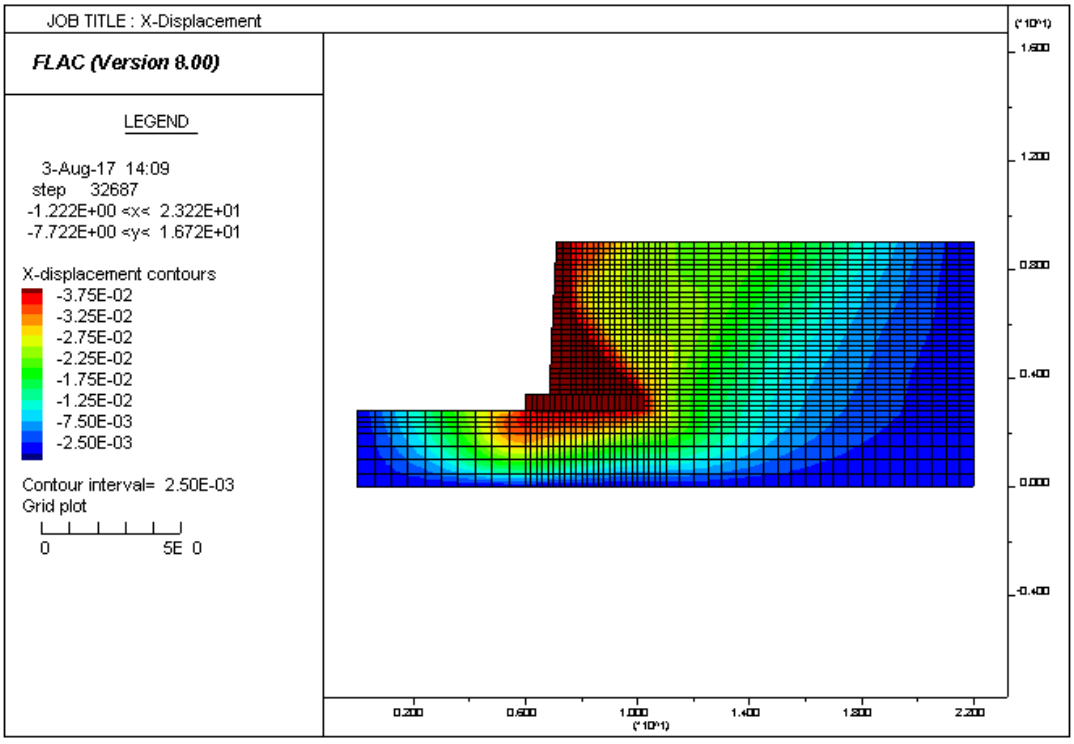

Figure 4.46. Displacement contours in X direction for ψ = 5 degree

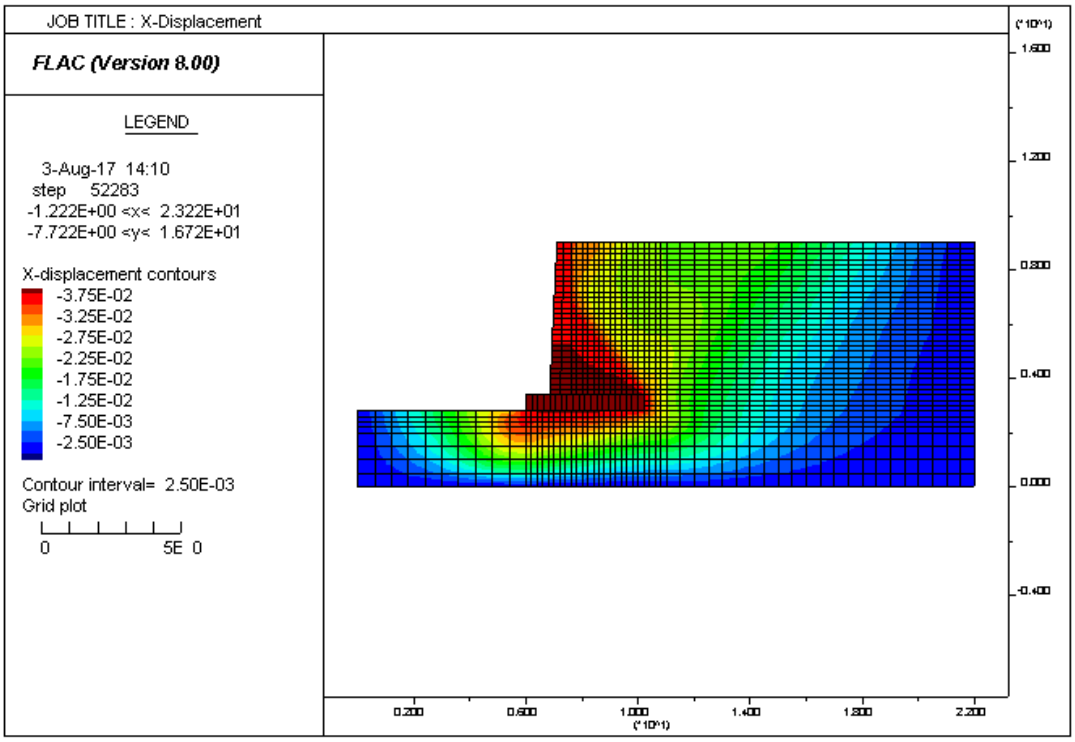

Figure 4.47. Displacement contours in X direction for ψ = 10 degree

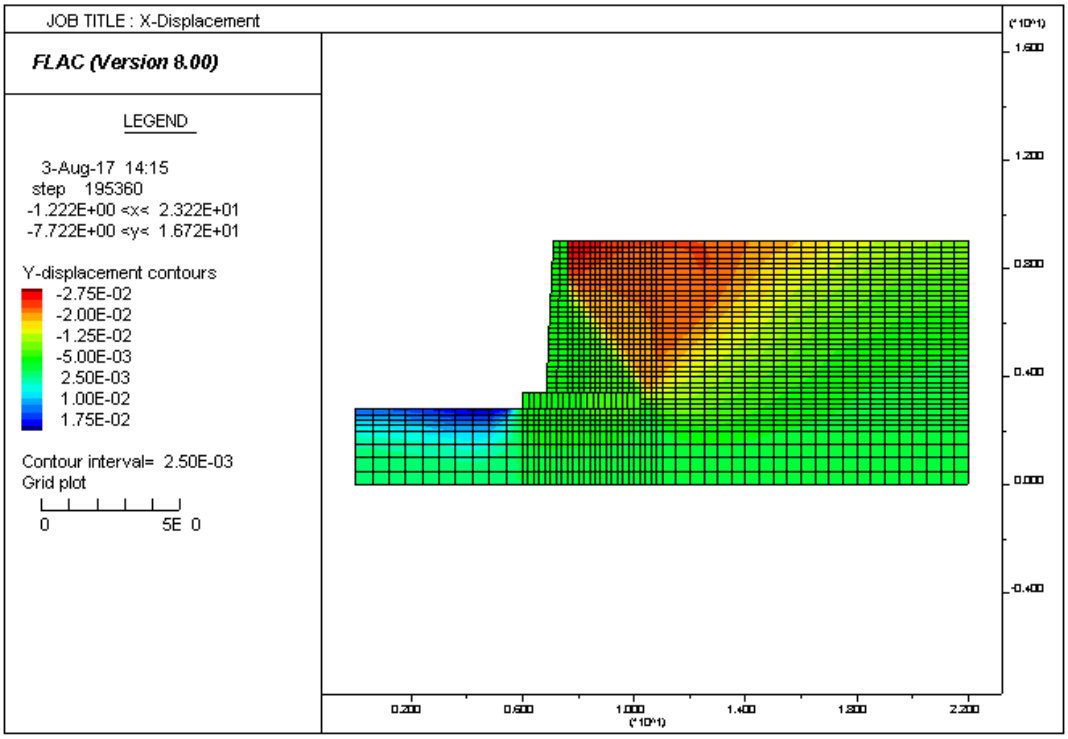

Figure 4.48. Displacement contours in X direction for ψ = 15 degree

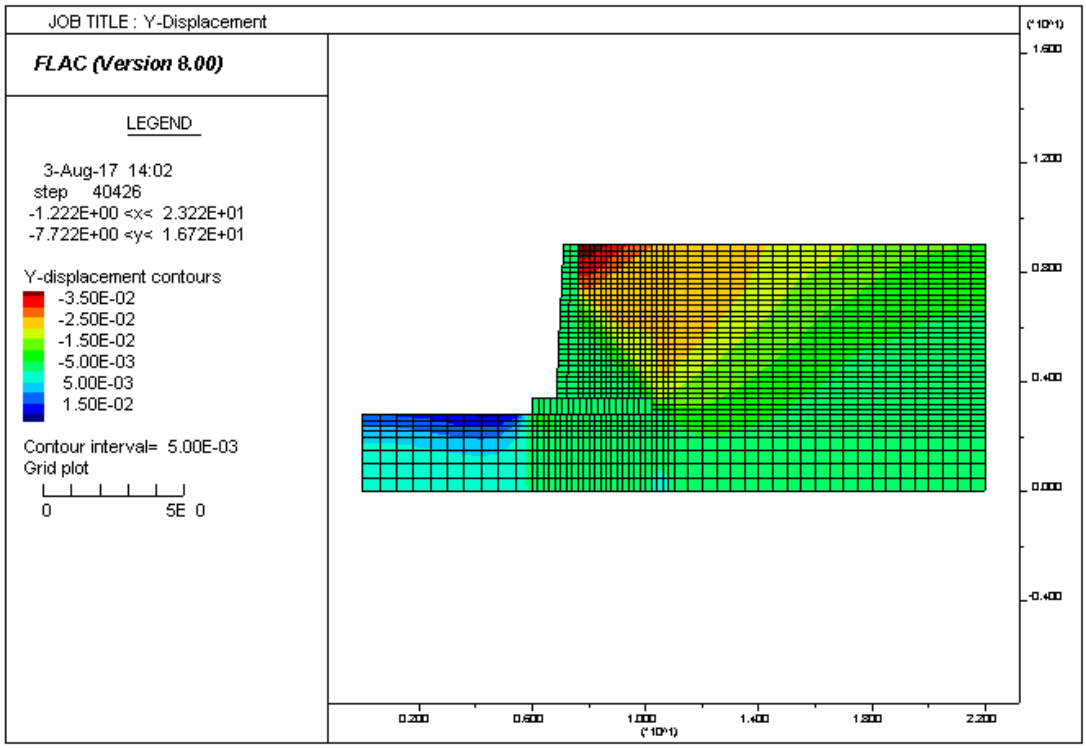

Figure 4.49. Displacement contours in Y direction for ψ = 0 degree

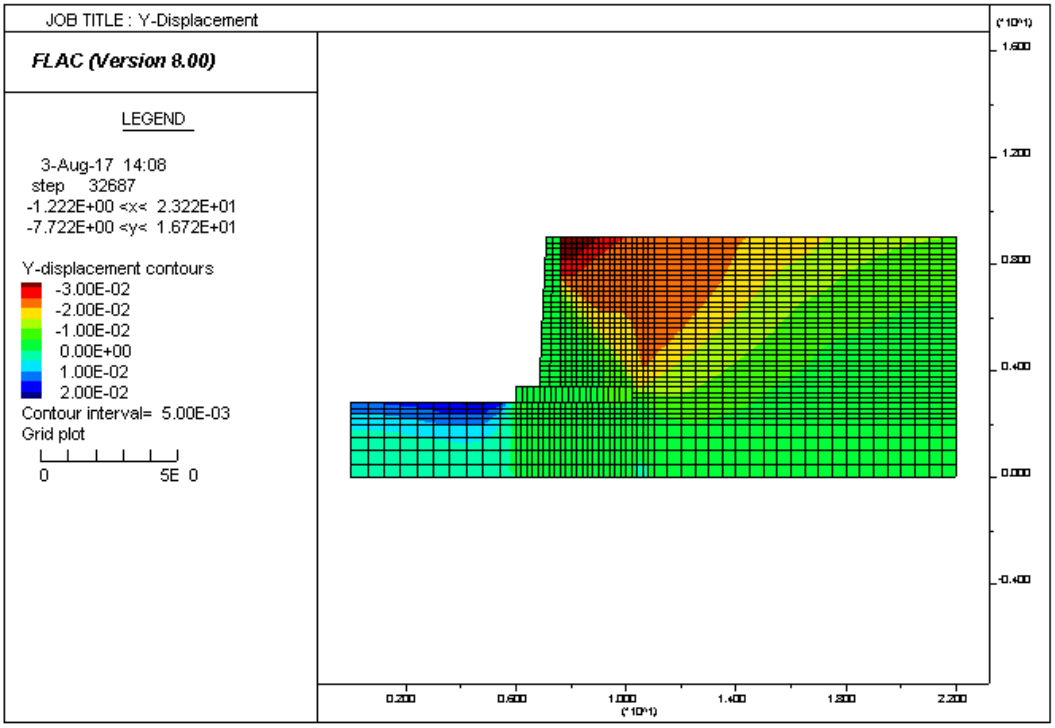

Figure 4.50. Displacement contours in Y direction for ψ = 5 degree

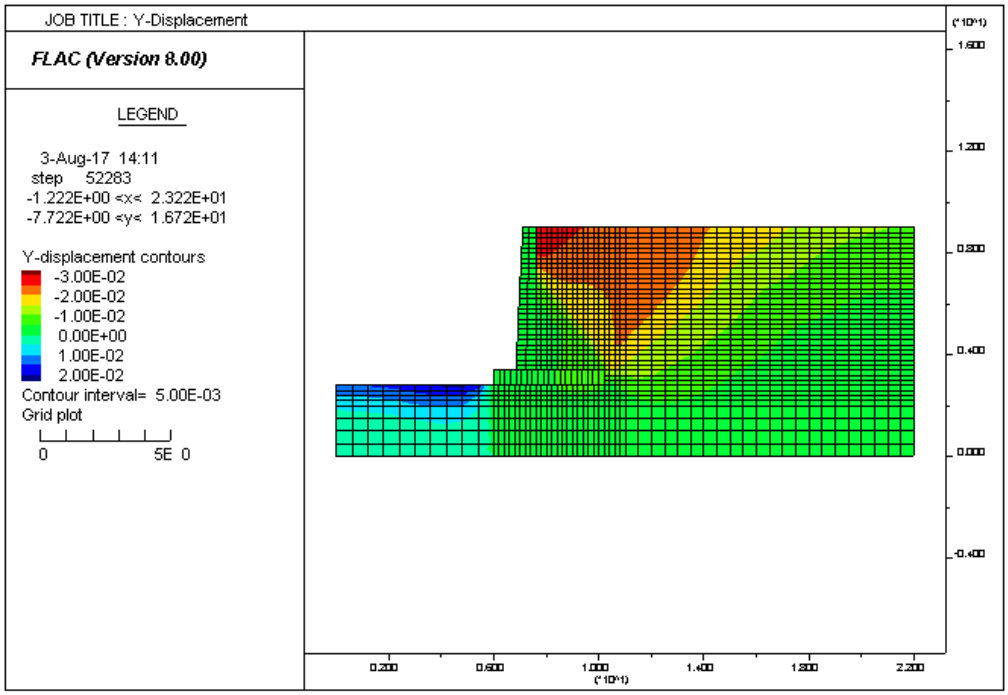

Figure 4.51. Displacement contours in Y direction for ψ = 10 degree

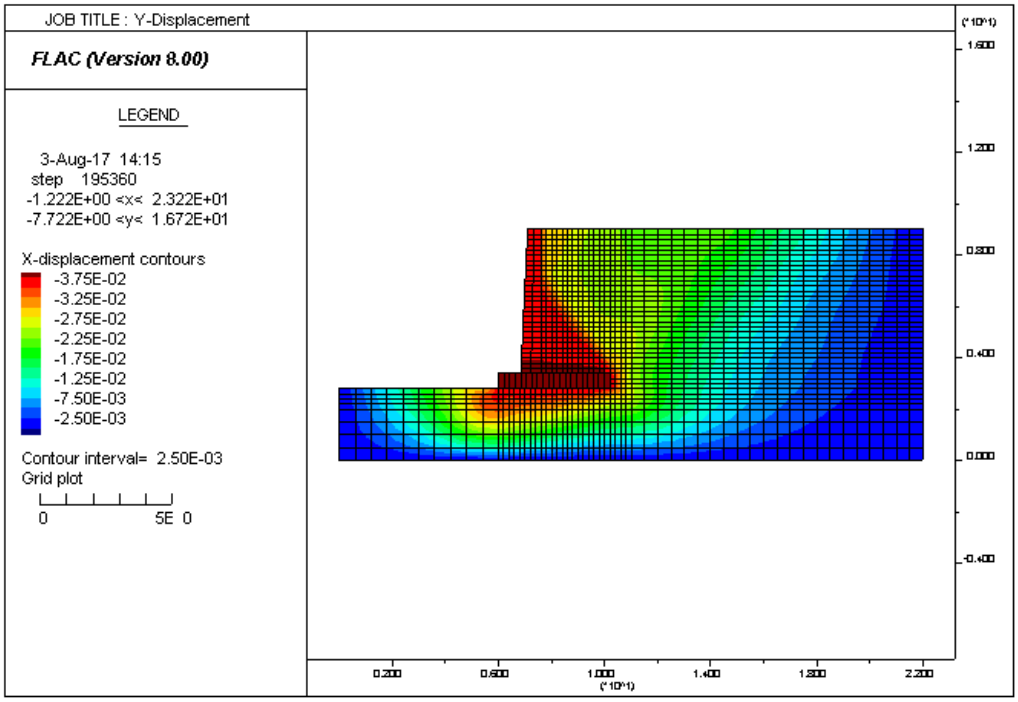

Figure 4.52. Displacement contours in Y direction for ψ = 15 degree

Displacements changes in lateral and vertical direction against the shear dilation wall-soil interface (ψ) are shown in Figures 4.53 and 4.54, respectively, for static and dynamic condition.

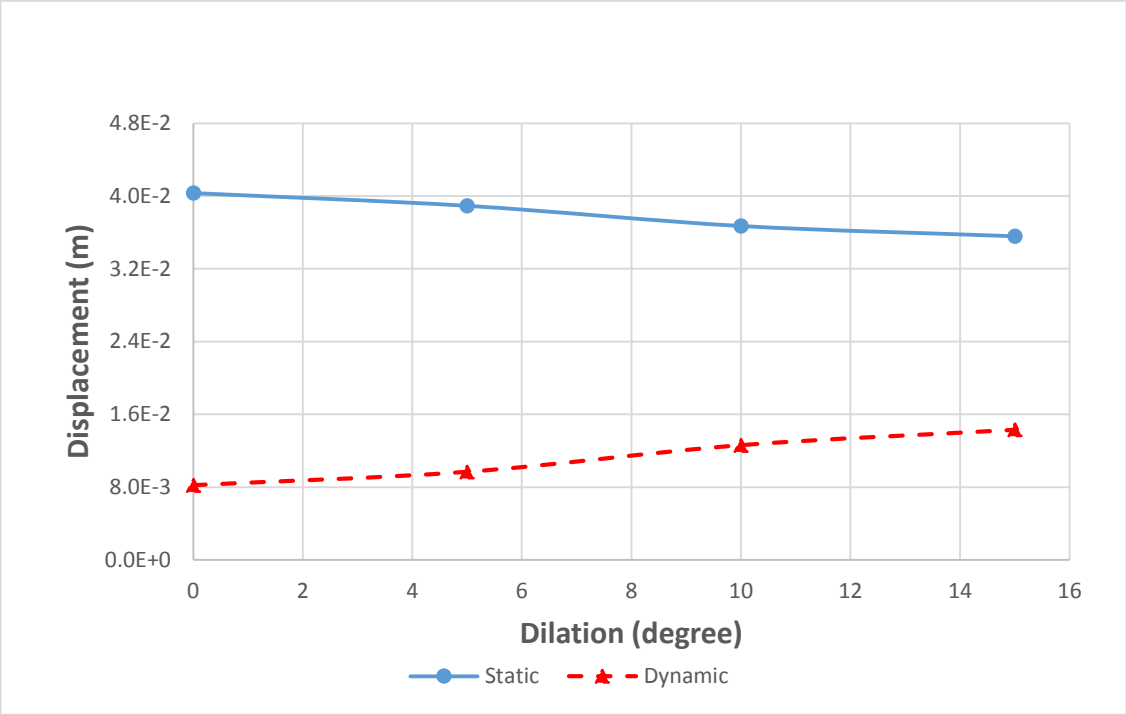

Figure 4.53. Displacement changes in X direction against different dilation values in static condition

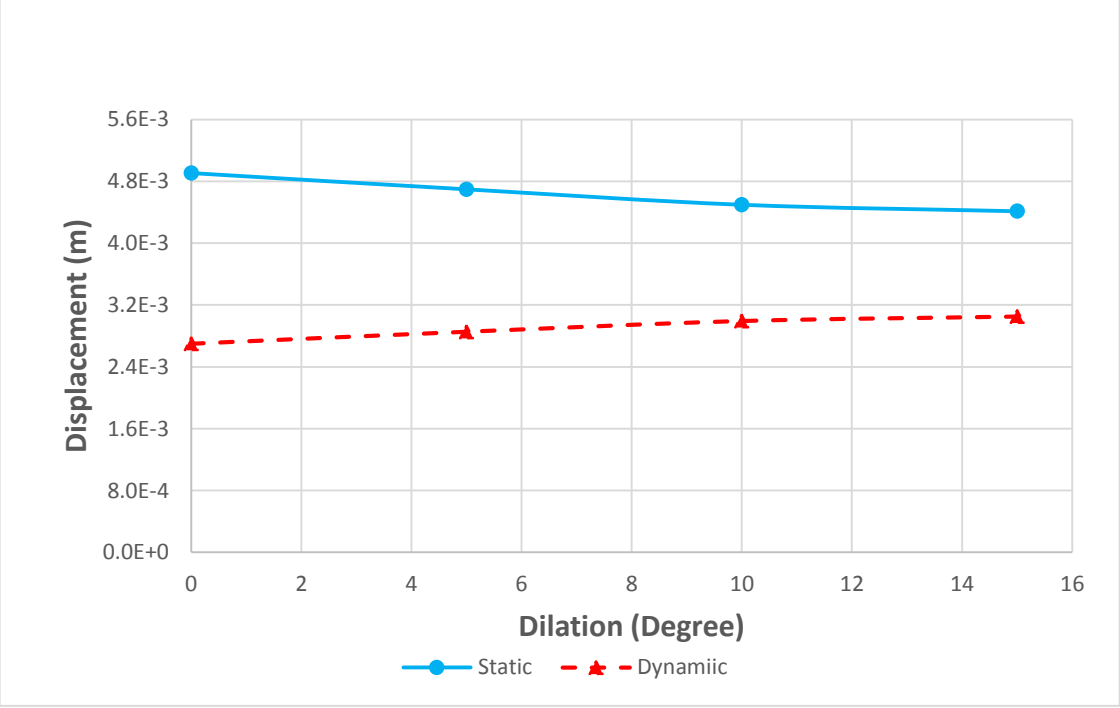

Figure 4.54. Displacement changes in Y direction against different dilation values in static condition

Figures 4.53 and 4.54 shows that, in static state with increasing dilation angle value, wall displacement in both lateral and vertical orientations would decreased sharply whereas in dynamic state wall deformation would increase with increasing dilation angle value.

4.6. Surface roughness

The effect of interface roughness is one of the most important issues in the interface behavior between wall and soil. For this purpose, much of the past research focused on interface type that does not experience normal unloading; and the conclusions from such studies were that a rougher interface exhibits higher shear strength and higher shear stiffness. In fact, interface roughness was found to have an effect on the shear zone thickness and shear failure model and even control the movement style of the soil particles along the interface (Cheng et al. 2013).

In the present research, the wall-soil interface is considered have a medium rough surface, where with increasing shear stiffness, friction angle and dilation parameters surface roughness increases. Furthermore, with decreasing shear stiffness and friction angle, a smooth surface is obtained. Figure 4.55 shows the interface roughness diagram.

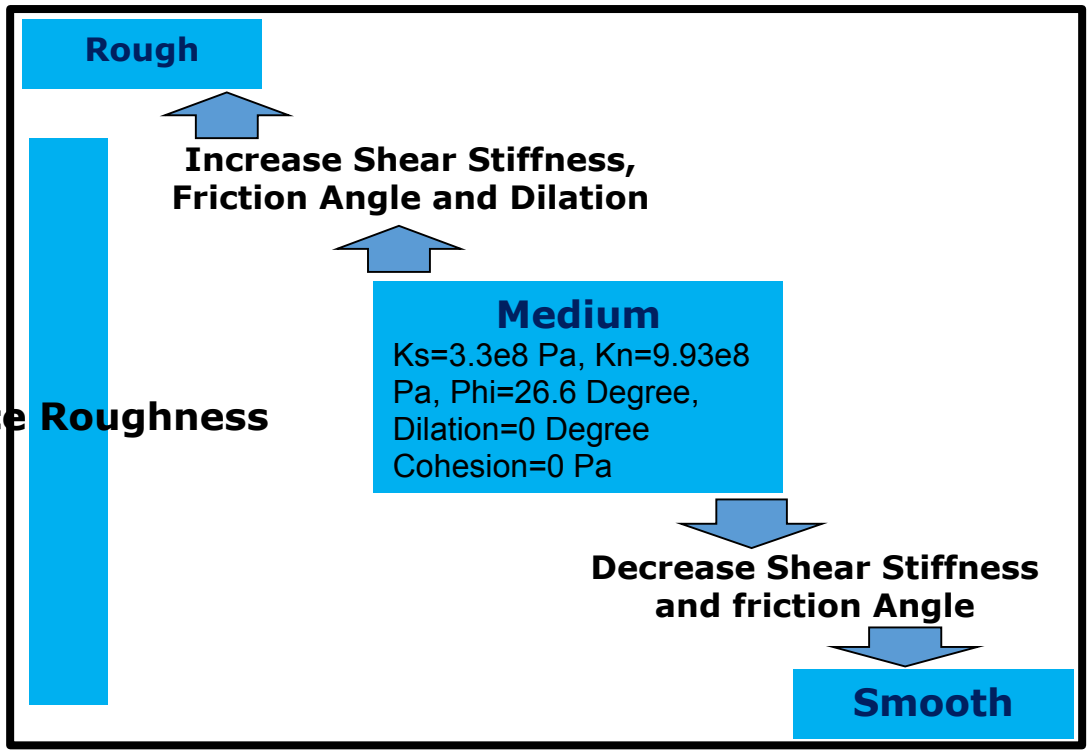

Figure 4.55. Interface roughness diagram

Figures 4.56 to 4.59 show the roughness surface for static and dynamic condition in both X and Y directions.

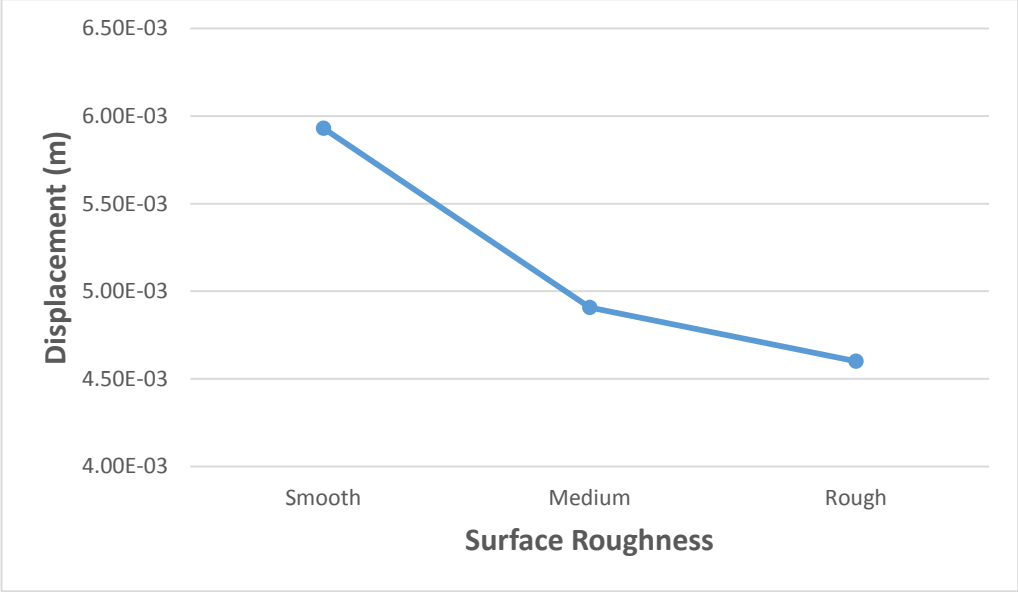

Figure 4.56. Surface roughness in static condition (X direction)

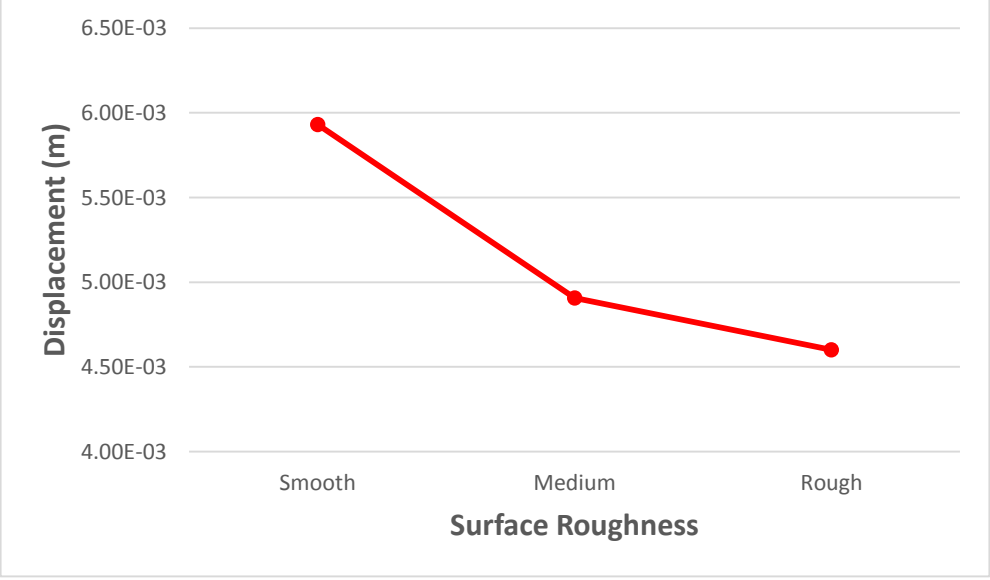

Figure 4.57. Surface roughness in static condition (Y direction)

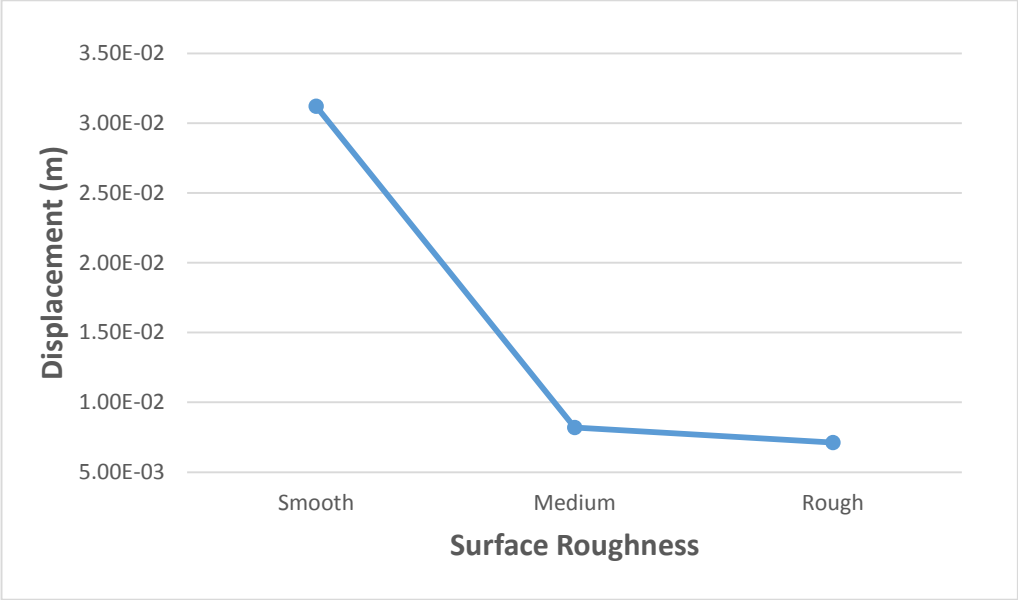

Figure 4.58. Surface roughness in dynamic condition (X direction)

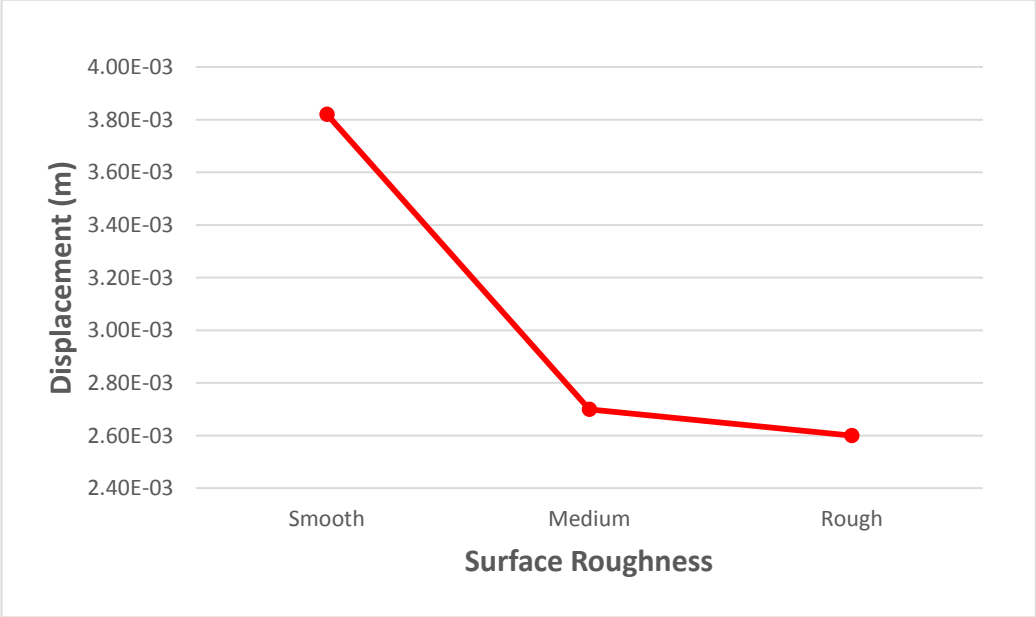

Figure 4.59. Surface roughness in dynamic condition (Y direction)

4.7. Summary

In chapter 4, the behavior of interface between structure and soil under various loading and boundary condition is investigated. In fact, the effect of shear strength parameters (cohesion and friction angle), stiffness parameters (normal and shear) and dilation of wall-soil interface on seismic response of retaining wall was investigated in both static and dynamic condition. Results showed that in the static condition, wall displacement was decreased by increasing the cohesion (C), friction angle (φ), shear stiffness (K_s), normal stiffness (K_n) and dilation (ψ) values. But in dynamic loading models, with increasing the values of shear strength parameters (Cohesion and friction angle) and shear stiffness (K_s), the wall displacements were increased whereas with increasing normal stiffness (K_n) value, wall deformation was decreased. In addition, the results at different surface roughness for static and dynamic conditions show that the rough interface results in higher stiffness and reduces the displacement in both X and Y directions.

Chapter 5. Sensitivity Analysis on the Behavior of Soil Retaining Walls under Seismic Response According to Canada Earthquake

5.1. Introduction

Dynamic analyses conducted in Chapters 3 and 4 were performed according to the model presented in (Parihar and Saxena, 2010) which used an Indian earthquake motion (20th October, Uttarkashi, 1991). The results in Chapter 3 was used primarily for validation purpose, while the results in Chapter 4 shows the sensitivity of different parameters to static and dynamic response of the wall-soil system.

In this chapter, the dynamic behavior of the reference wall-soil system is studied for a set of critical parameters found from the study in Chapter 4. Also, the retaining wall geometry considered here was proportioned according to the Indian seismic conditions as reported in Parihar et al. (2010). The study presented here uses an earthquake excitation corresponding to the Quebec region. For the purpose of comparison, the displacement response of the wall-soil system for the selected seismic events in India and Canada is computed for each case. Then a detailed parametric study is conducted for different soil properties.

In this chapter, a Canadian earthquake motion (6th March, Quebec, 2005) is applied to the wall-soil system and dynamic time history analysis has been conducted. For this purpose, a sensitivity analysis of the parameters associated with wall-soil interface is carried out looking into the seismic response of retaining wall structure and results are compared to results corresponding to the Indian earthquake.

5.2. Effects of the shear strength and stiffness parameters of wall-soil interface under Canada (Quebec) earthquake

In this section, a sensitivity analysis of the parameters associated with interface between soil and structure is carried out according to a selected Quebec earthquake. The assumption of dynamic model analyzed in this part is as same as the presented model in Chapter 3.

5.2.1. Quebec earthquake motion

According to Figure 5.1, the acceleration time-history used in the dynamic analysis is accordance with 6th March, 2005 Rivière-du-Loup earthquake in Quebec. The earthquake has a duration of

about 20 second and the peak ground acceleration (PGA) of about 3.2 m/s^2 or 0.32g which is slightly higher than the selected Indian earthquake.

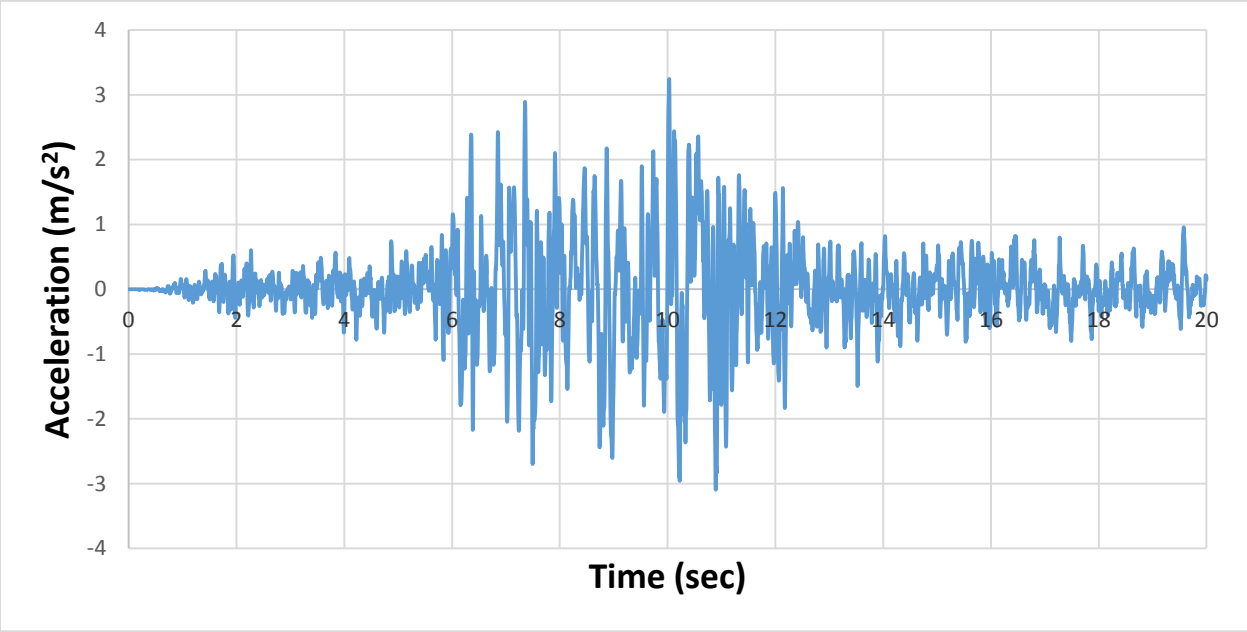

Figure 5.1. Quebec earthquake (Rivière-du-Loup) time history

5.2.2. Dynamic results according to Quebec earthquake motion

Dynamic model deformation according to Quebec ground motion is shown in Figure 5.2.

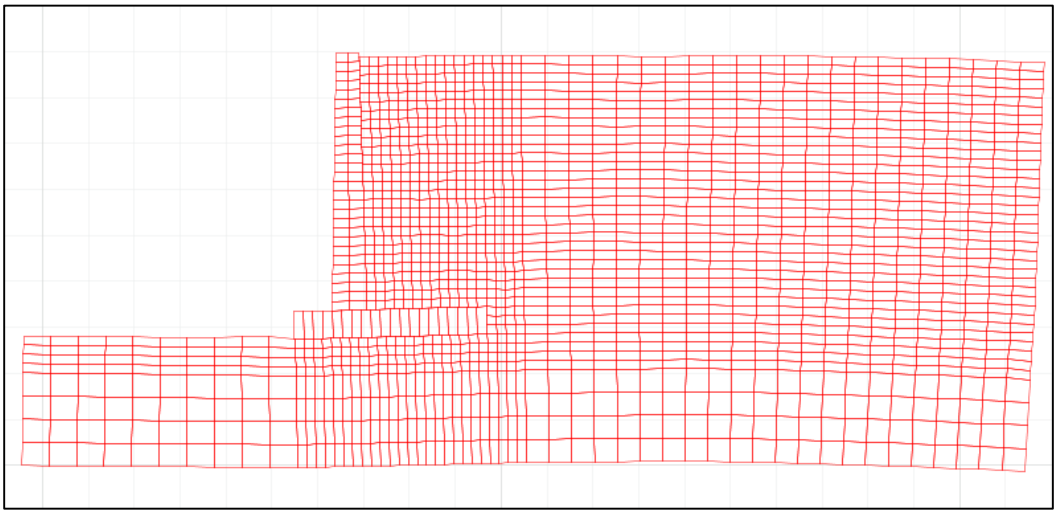

Figure 5.2. Model deformation according to Quebec earthquake

Displacement changes in X and Y direction of retaining wall according to Quebec earthquake are presented in Figures 5.3 and 5.4 respectively. Also, velocity and acceleration of the top of the retaining wall in X direction are illustrated in Figures 5.5 and 5.6.

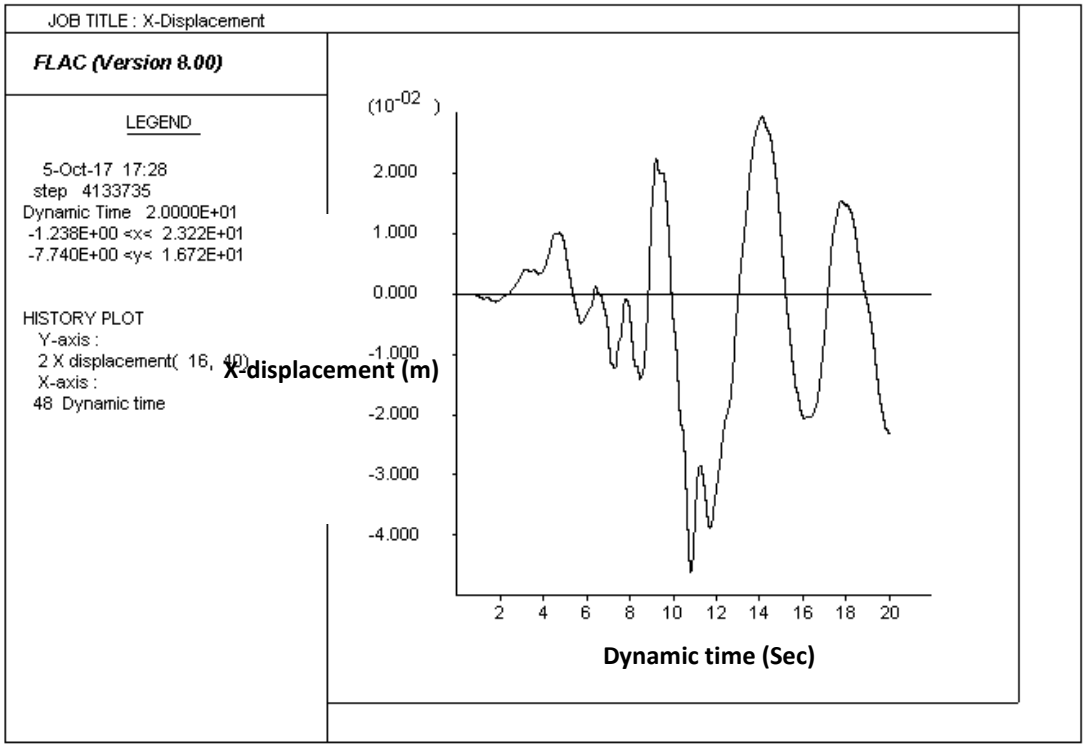

Figure 5.3. Displacement changes in X direction according to Quebec earthquake

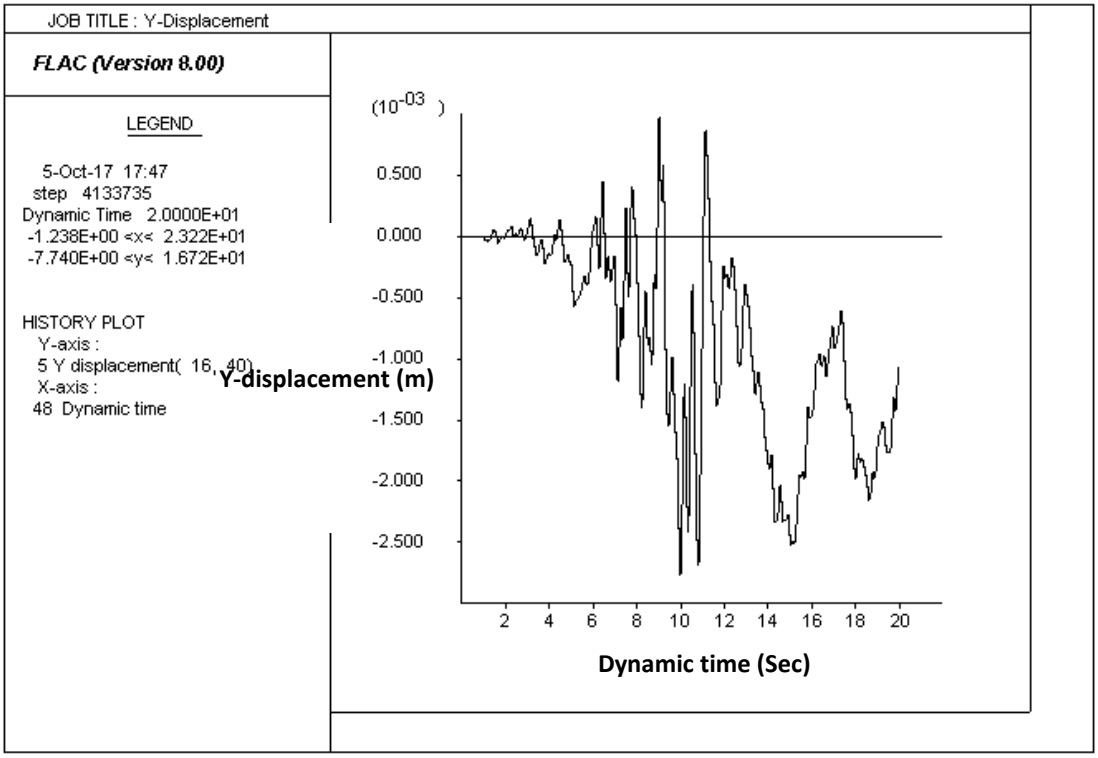

Figure 5.4. Displacement changes in Y direction according to Quebec earthquake

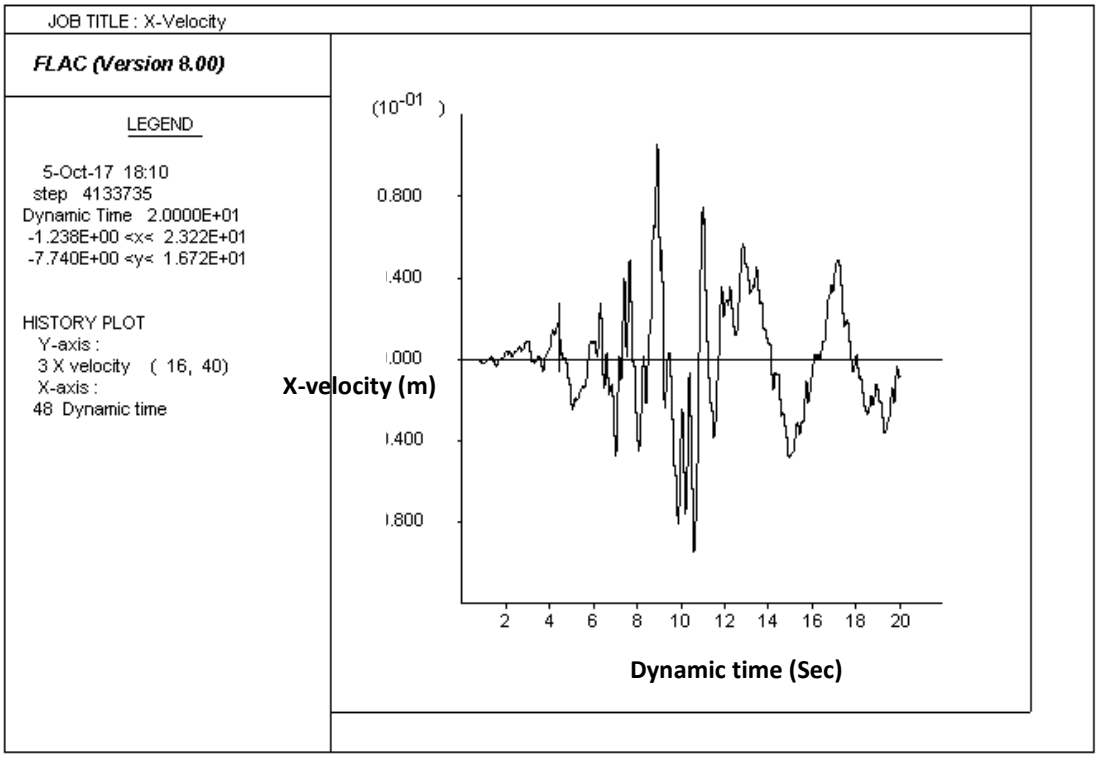

Figure 5.5. X-Velocity changes according to Quebec earthquake

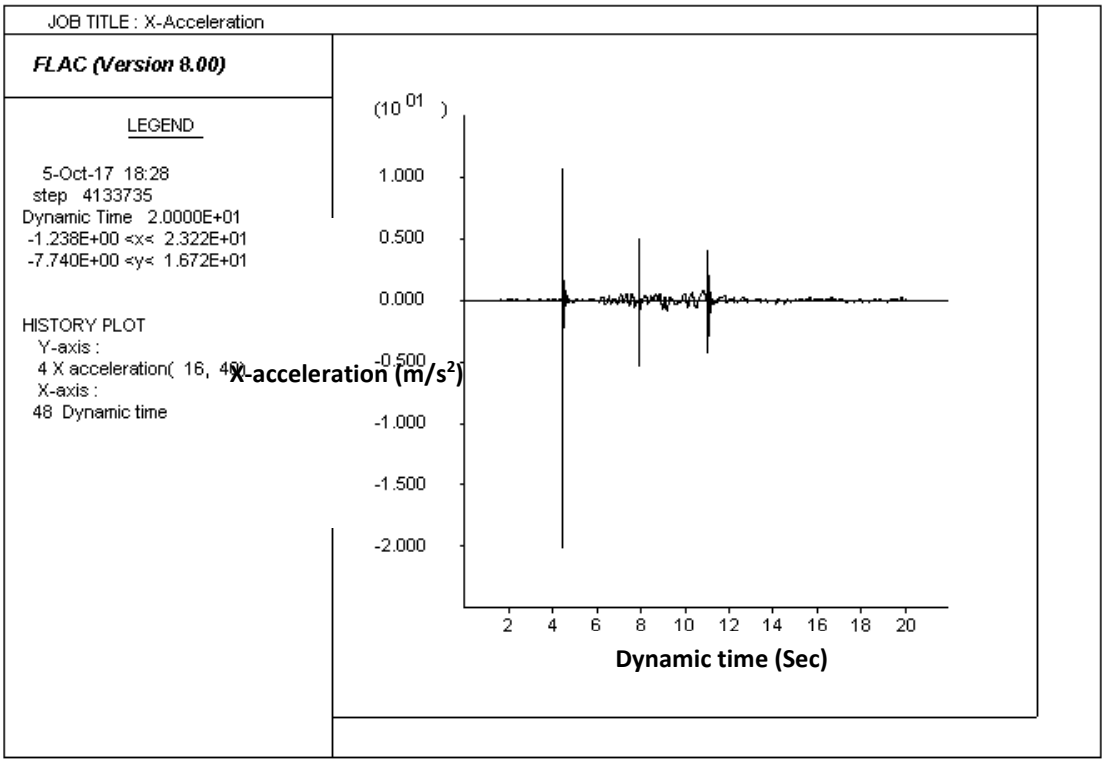

Figure 5.6. X-Acceleration changes according to Quebec earthquake

5.2.3. Sensitivity analysis

In this part, the soil-wall interface shear behavior is determined in a series of parametric studies under the selected 2005 Quebec earthquake as shown in Figure 5.1. The effect of shear strength parameters (cohesion and friction angle), stiffness parameters (normal and shear) and dilation of interface of retaining wall and soil under Quebec earthquake is investigated. In the sensitivity analysis with changing one parameter in turn, while other parameters are kept unchanged. And also, the dynamic analysis results are compared to the 1991 Indian earthquake.

5.2.3.1. Shear strength parameters

Figures 5.7 to 5.10 show the results of retaining wall deformation under an Indian and a Canadian (Quebec) earthquake of similar magnitudes. The displacements in X and Y directions at the top of the wall for different values of cohesion (C) and friction angle (φ) are shown in these figures.

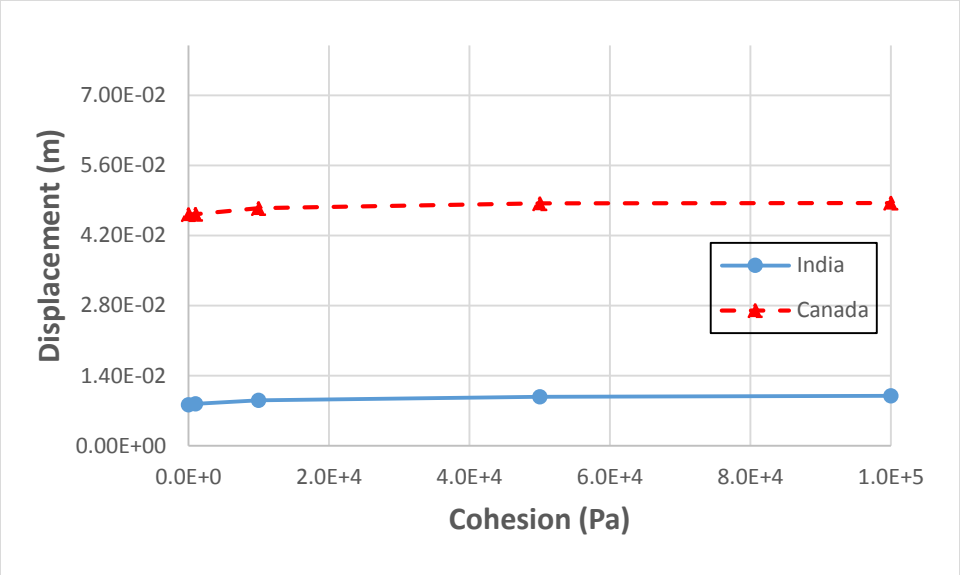

Figure 5.7. Displacement changes in X direction against different cohesion (C) values

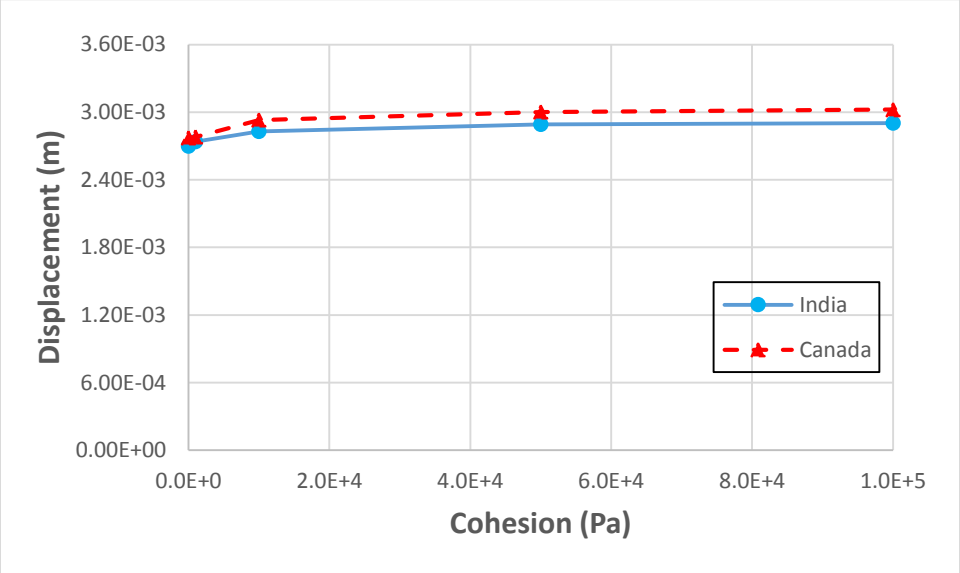

Figure 5.8. Displacement changes in Y direction against different cohesion (C) values

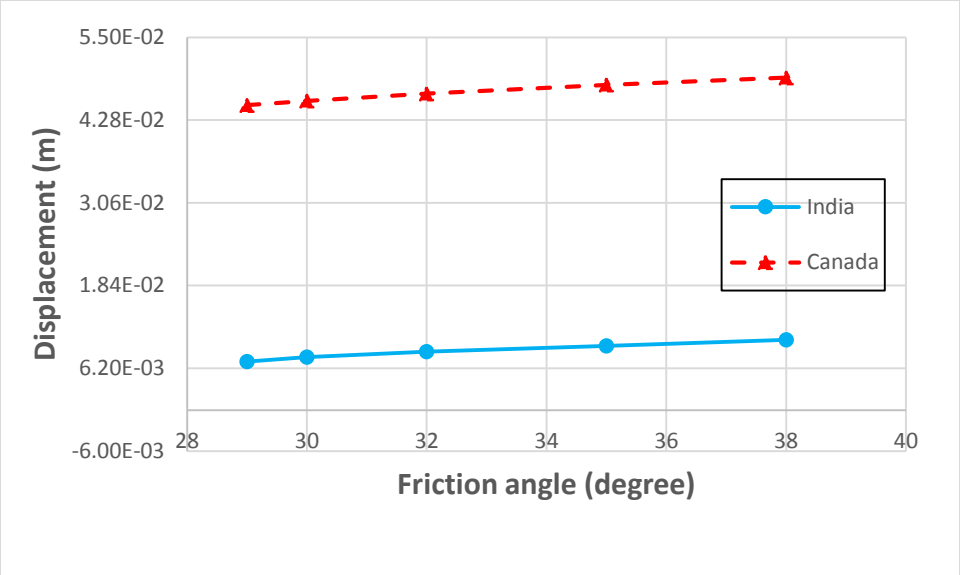

Figure 5.9. Displacement changes in X direction against different friction angle (ϕ) values

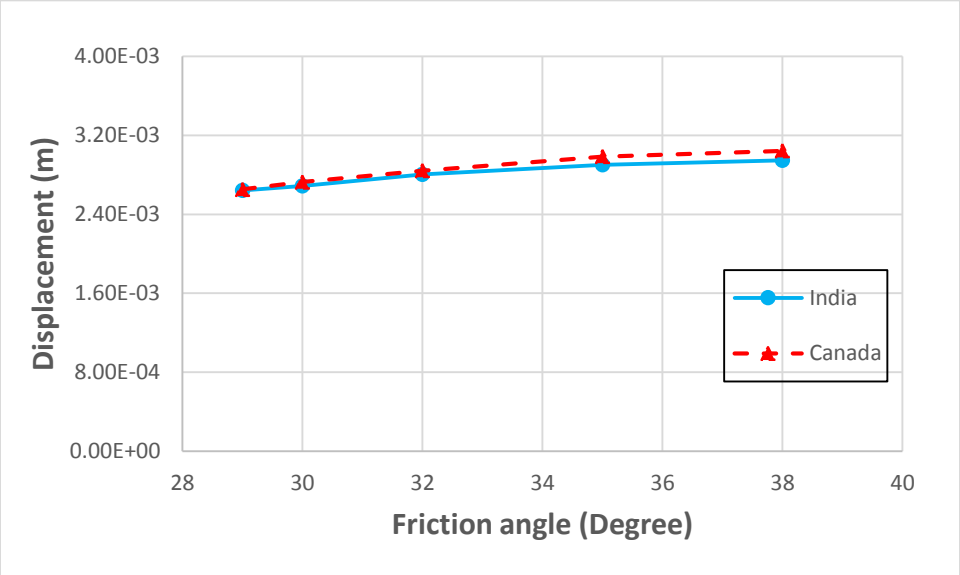

Figure 5.10. Displacement changes in Y direction against different friction angle (ϕ) values

Comparison results show that in dynamic condition with increasing shear strength parameter (cohesion and friction angle), the wall facing deformation in both X and Y directions increase for both India and Canada earthquake in a similar way.

5.2.3.2. Stiffness parameters

Displacement changes of retaining wall in horizontal and vertical directions with different values of stiffness parameters (shear and normal) according to India and Canada (Quebec) earthquake motion are shown in Figures 5.11 to 5.14.

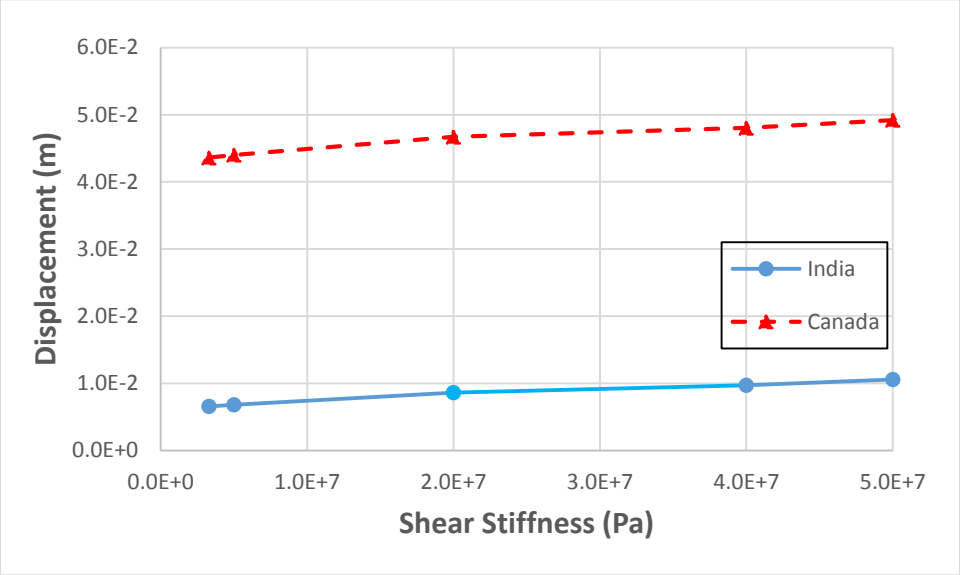

Figure 5.11. Displacement changes in X direction against different shear stiffness (k_s) values

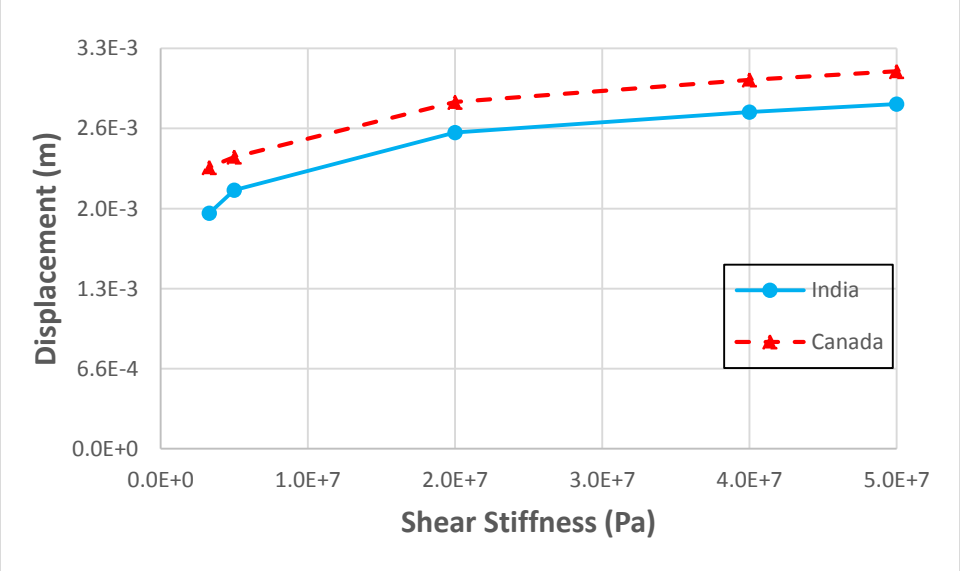

Figure 5.12. Displacement changes in Y direction against different shear stiffness (k_s) values

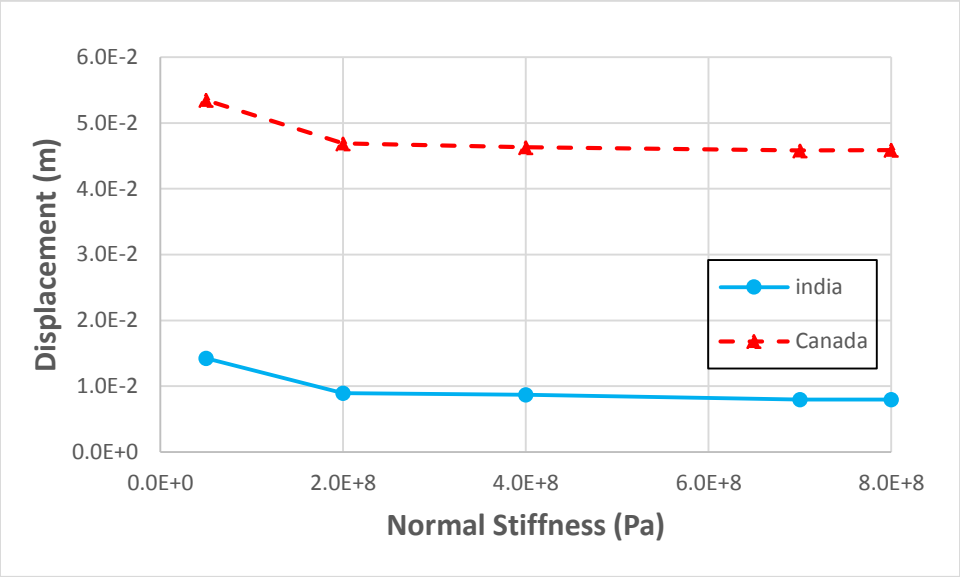

Figure 5.13. Displacement changes in X direction against different normal stiffness (k_n) values

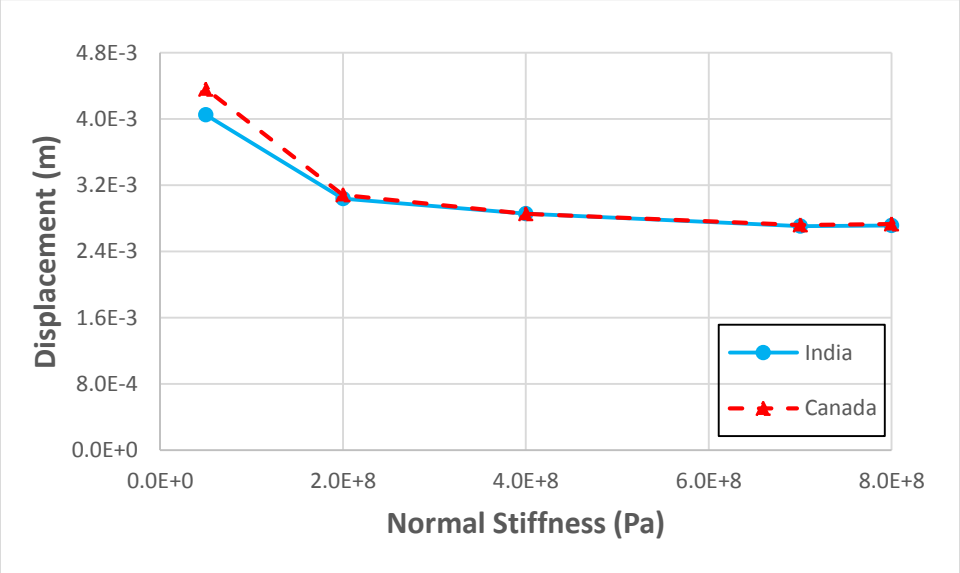

Figure 5.14. Displacement changes in Y direction against different normal stiffness (k_n) values

For both the Indian and Canadian earthquakes as input acceleration time-history in dynamic analysis, with increasing shear stiffness parameter (K_s), wall displacement in both X and Y direction increases. But with increasing normal stiffness value (K_n), wall deformation decreases.

5.2.3.3. Dilation

Figures 5.15 and 5.16 illustrate retaining wall deformation for different values of dilation according to India and Canada (Quebec) earthquake motion in both X and Y direction.

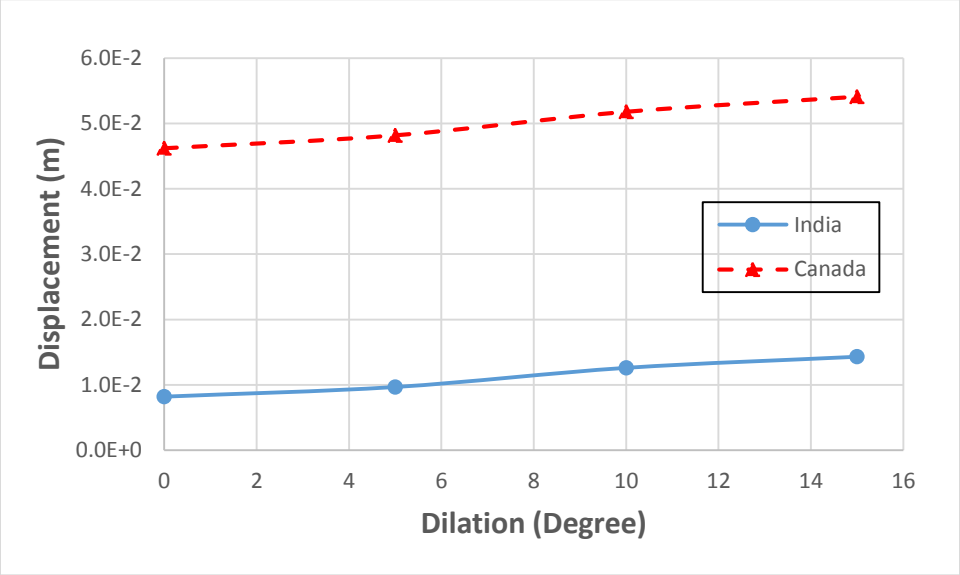

Figure 5.15. Displacement changes in X direction against different friction angle values

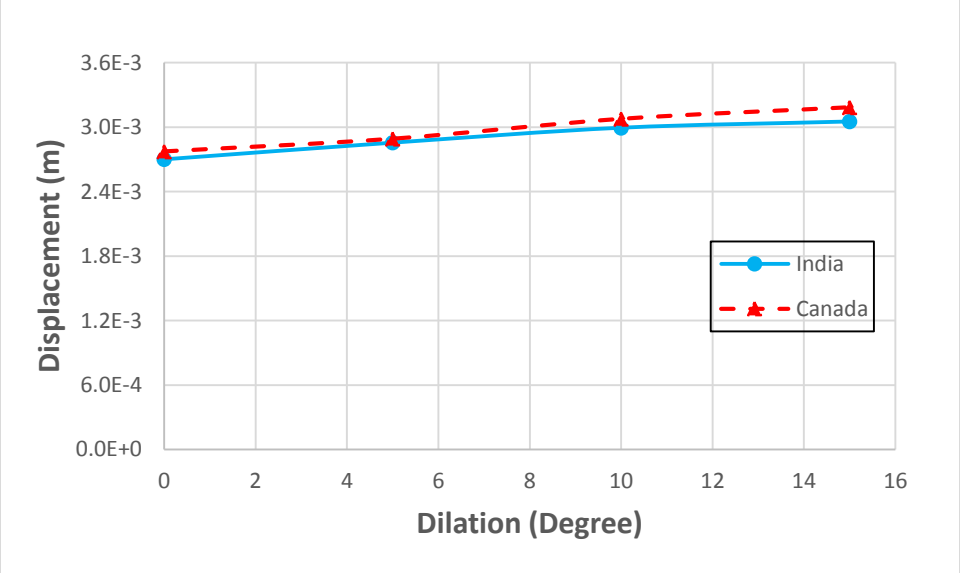

Figure 5.16. Displacement changes in Y direction against different friction angle values

Figures 5.15 and 5.16 show that, the wall deformation in both lateral and vertical orientation increases with increasing dilation value for both Canada and India earthquake.

5.2.3.4. Surface roughness

Effect of interface roughness on retaining wall deformation in horizontal and vertical direction are shown in Figures 5.17 and 5.18 for both the Indian and Canadian (Quebec) earthquake loading. The values of smooth, medium and rough parameters are presented in Table 5.1.

Table 5.1. Values of surface roughness parameters

Surface Roughness	Shear Stiffness(K_s) (Pa)	Normal Stiffness (K_n) (Pa)	Friction Angle (φ) (Degree)	Dilation (ϕ) (Degree)
Smooth	1.82e6	9.93e8	15	0
Medium	3.3e8	9.93e8	26.6	0
Rough	1.78e9	9.93e8	38	2

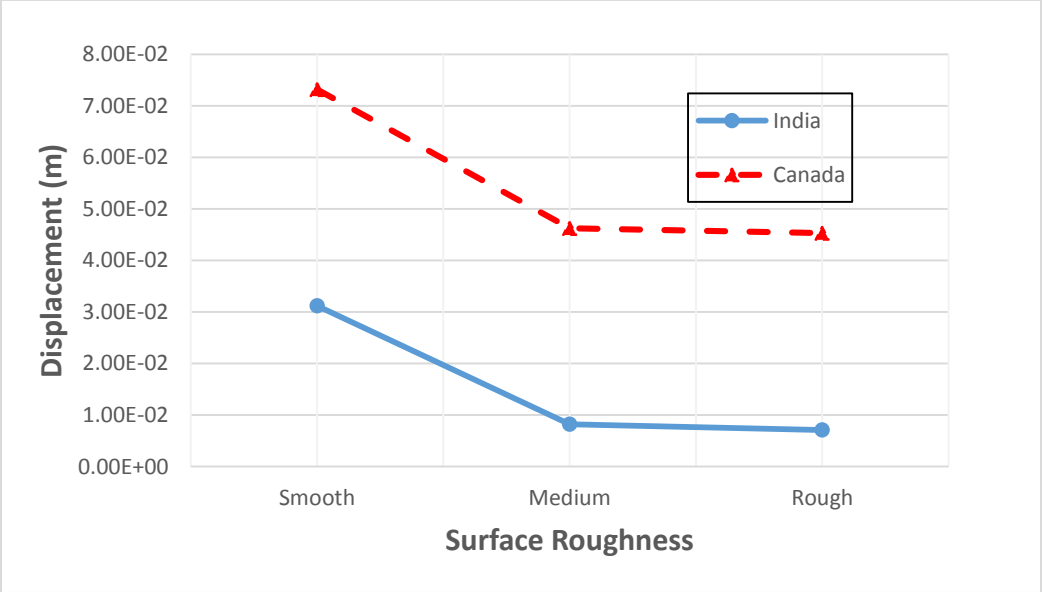

Figure 5.17. Surface roughness in static condition (X direction)

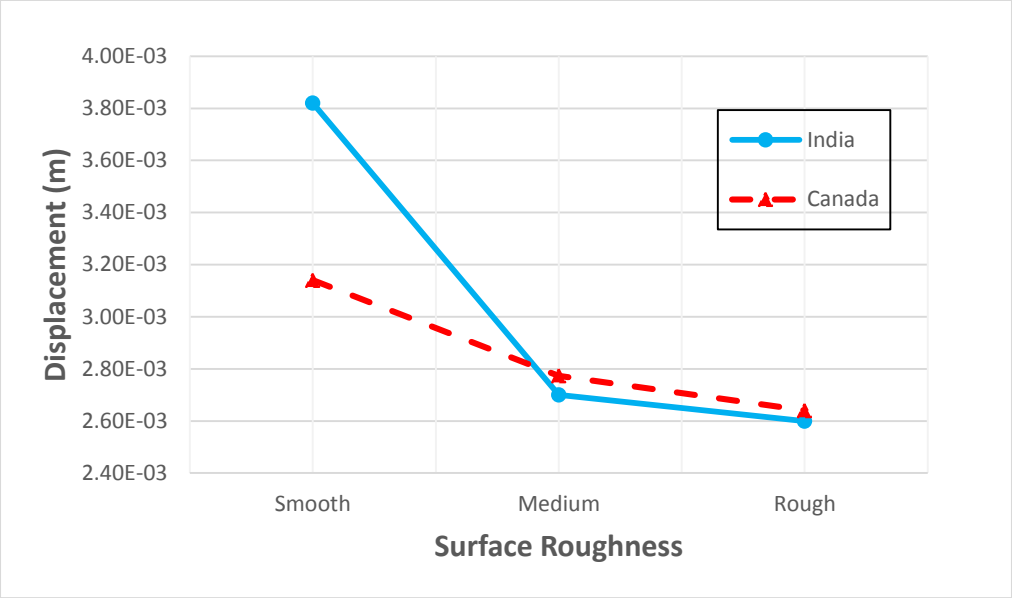

Figure 5.18. Surface roughness in static condition (Y direction)

Figures 5.17 and 5.18 show that, there is a good agreement between India and Canada earthquake in terms of surface roughness results. But the displacements of the wall corresponding to the Indian and Canadian earthquakes are different. The magnitude of the Indian earthquake is generally smaller than the selected Canadian earthquake. The figures show that as the surface roughness increases, the displacement in X and Y directions decreases.

5.3. Summary

According to the sensitivity analysis of the parameters associated with the interface between soil and retaining wall (Chapter 4), a summary of wall-soil interface behavior is presented here. Then, the conclusion of this research is presented.

A statistical assessment of wall-soil interface parameters in terms of retaining wall deformation is conducted to determine best-fit of parameters value. Appropriate estimate of the wall-soil interface parameters value, help to reduce the amount of more expensive field and laboratory procedures.

According to the sensitivity analysis conducted in this research, in order to obtain the lower and upper range of wall-soil interface parameter, cumulative percentage distribution of shear strength and stiffness parameters are calculated.

Figures 5.19, 5.20 and 5.21 illustrate the cumulative percentage of the value of the cohesion (C), shear stiffness (K_s) and normal stiffness (K_n) in terms of retaining wall deformation in both static and dynamic condition according to India (20th October, Uttarkashi, 1991) and Canada (6th March, Quebec, 2005) earthquake reprehensively.

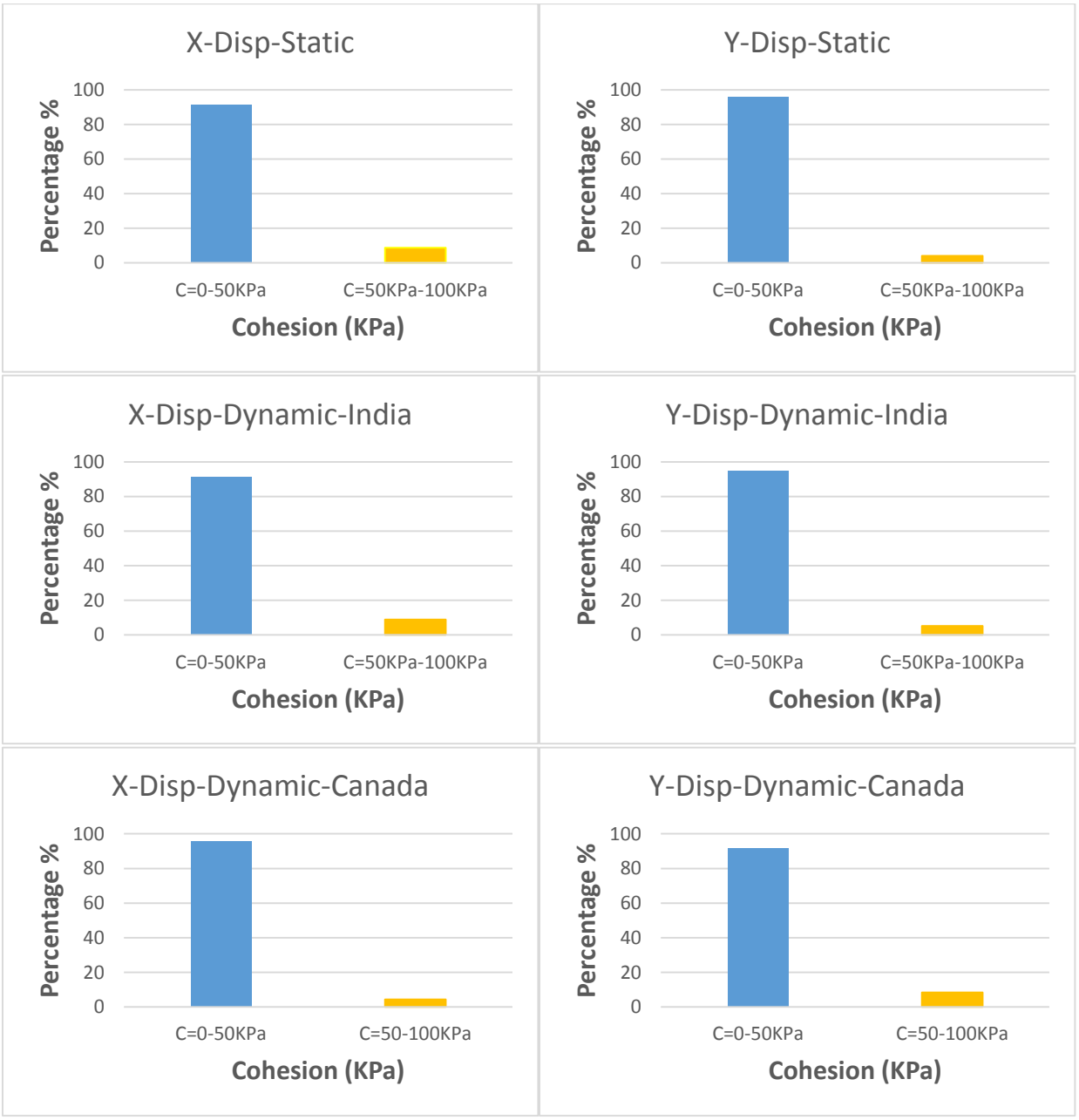

Figure 5.19. Cumulative percentage distribution of cohesion according to wall deformation (X & Y direction) in both static and dynamic condition for India and Canada earthquake

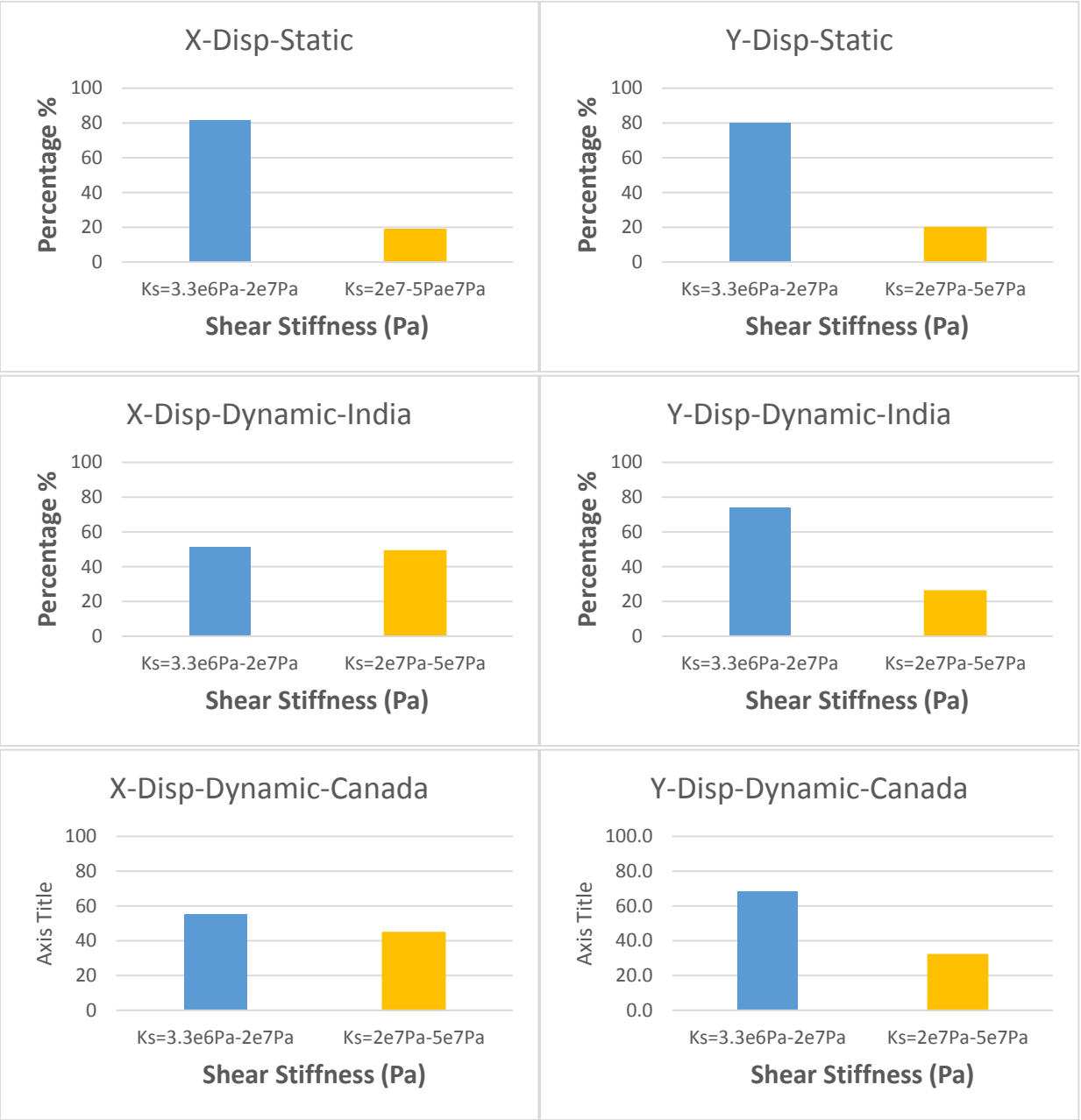

Figure 5.20. Cumulative percentage distribution of shear stiffness according to wall deformation (X & Y direction) in both static and dynamic condition for India and Canada earthquake

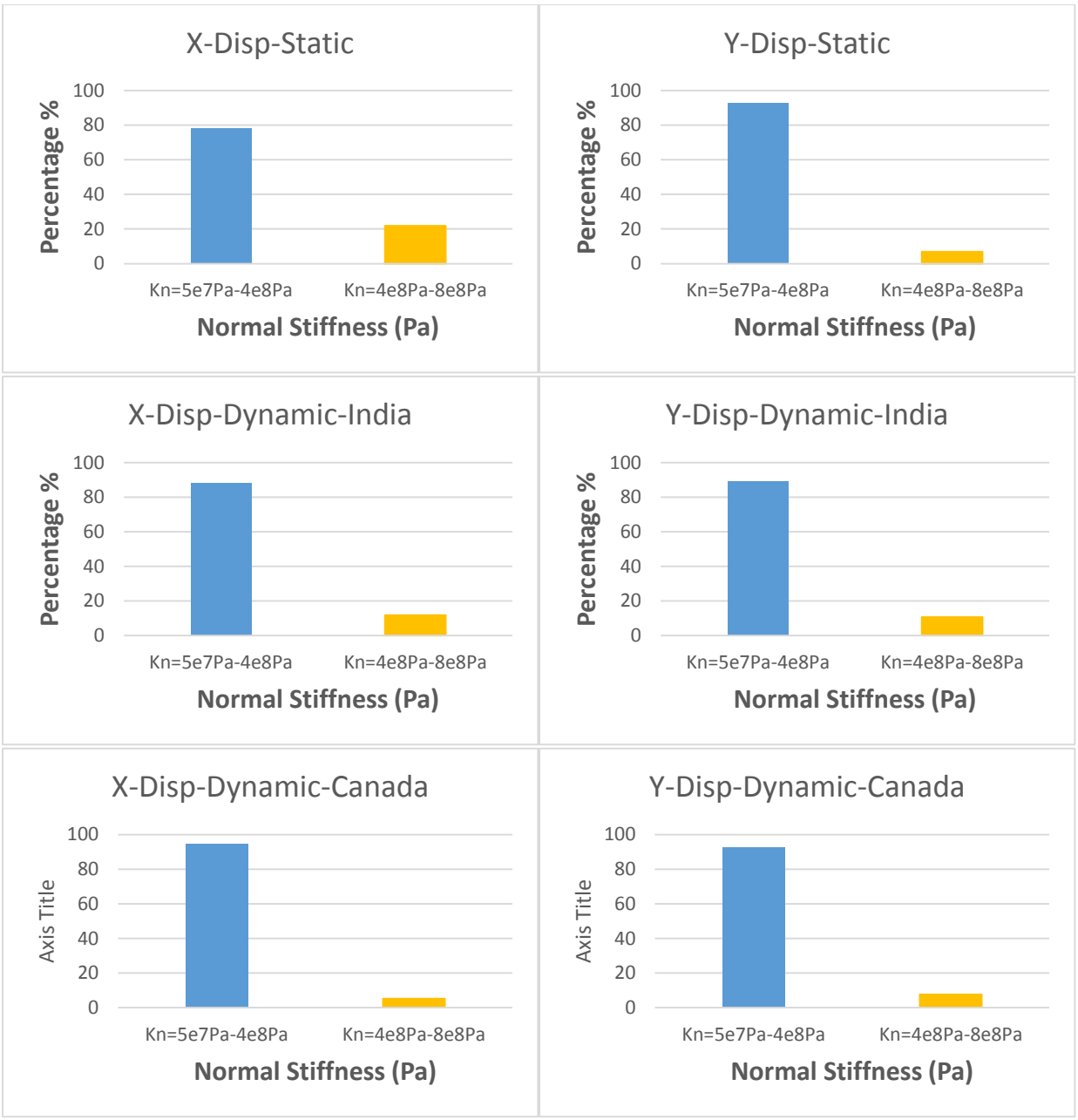

Figure 5.21. Cumulative percentage distribution of normal stiffness according to wall deformation (X & Y direction) in both static and dynamic condition for India and Canada earthquake

Table 5.2. Lower and upper bound values of wall-soil interface parameter

	Shear Strenght Parameters		Stiffness Parameters		Dilation (Ψ) Degree
	Cohesion (C) KPa	Friction Angle (ϕ) Degree	Shear Stiffness (K_s) Pa	Normal Stiffness (K_n) Pa	
Lower Bounda	0	29	3.3e6	5e7	0
Upper Bound	50	38	2e7	4e8	15

To determine the lower and upper range of friction angle (φ) and dilation (ψ), cumulative percentage distribution method does not work. Because the relationship between friction angle, dilation and wall displacement is linear. Thus, the minimum value as lower boundary and maximum value as upper boundary is considered in the linear function of changes friction angle and dilation against wall deformation. Table 5.2 present the lower and upper boundary of friction angle and dilation parameter.

Table 5.2 present the lower and upper boundary of each wall-soil interface parameter according to cumulative percentage distribution calculated.

Chapter 6. Parametric study on the soil-wall behavior for the reinforced soil retaining walls under seismic condition in Montreal

6.1. Introduction

The work presented in this chapter looks into the effects of soil properties, earthquake motions, and wall heights as major design parameters for soil retaining wall under earthquake loading. For this purpose, a parametric study on the behavior of the reinforced soil retaining walls under a set of eight earthquake motions corresponding to the seismic hazard of Montreal is conducted with different wall height and soil type. The retaining walls are analyzed with different height of 3 m, 6 m and 9 m and soil types of sand and clay under different earthquake records corresponding to Montreal. Based on acceleration time-history matched according to Montreal earthquakes, the dynamic displacement of the model under different loading conditions is investigated.

6.2. Input earthquake motions

In this part, the dynamic analyses are conducted with eight different records obtained from the Pacific Earthquake Engineering Research Institute (PEER) database, and the details are provided Table 6.1.

Table 6.1. North American earthquake recorded

Record Number	Location	Date	PGA (m/s^2)
1	IMPERIAL VALLEY	10/15/79	0.28
2	NORTHRIDGE	01/17/94	-0.04
3	KOBE	01/16/95	0.037
4	IMPERIAL VALLEY	10/15/79	-0.036
5	KOBE	01/16/95	0.13
6	KOBE	01/16/95	-0.44
7	NORTHRIDGE EQ	1/17/94	0.06
8	NORTHRIDGE	01/17/94	-0.55

Figures 6.1 to 6.8 show the original acceleration time-history of eight records.

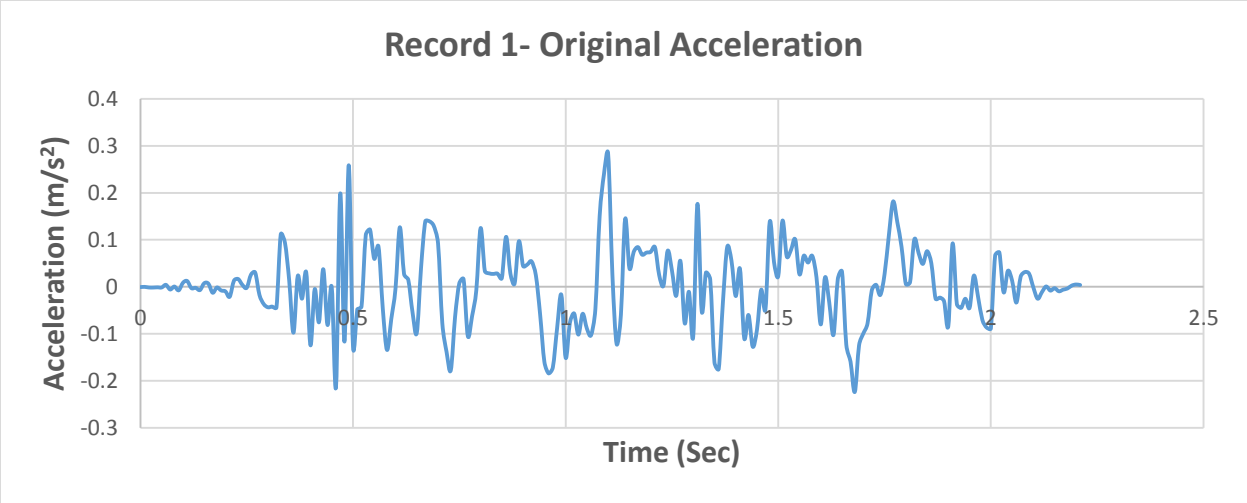

Figure 6.1. Original acceleration time-history of record 1

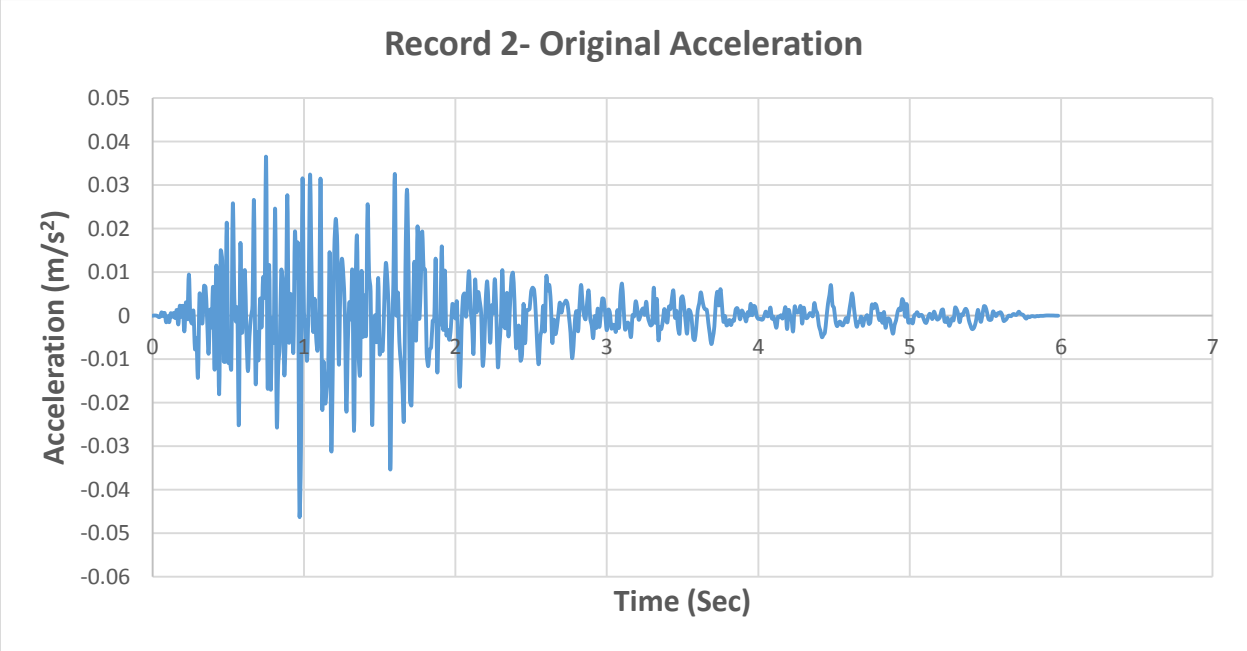

Figure 6.2. Original acceleration time-history of record 2

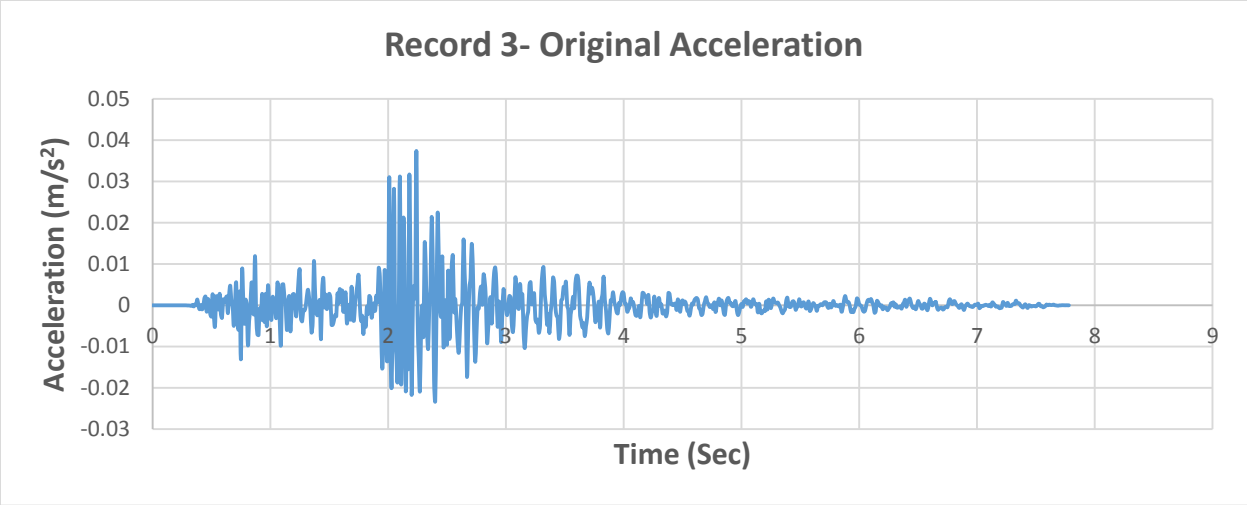

Figure 6.3. Original acceleration time-history of record 3

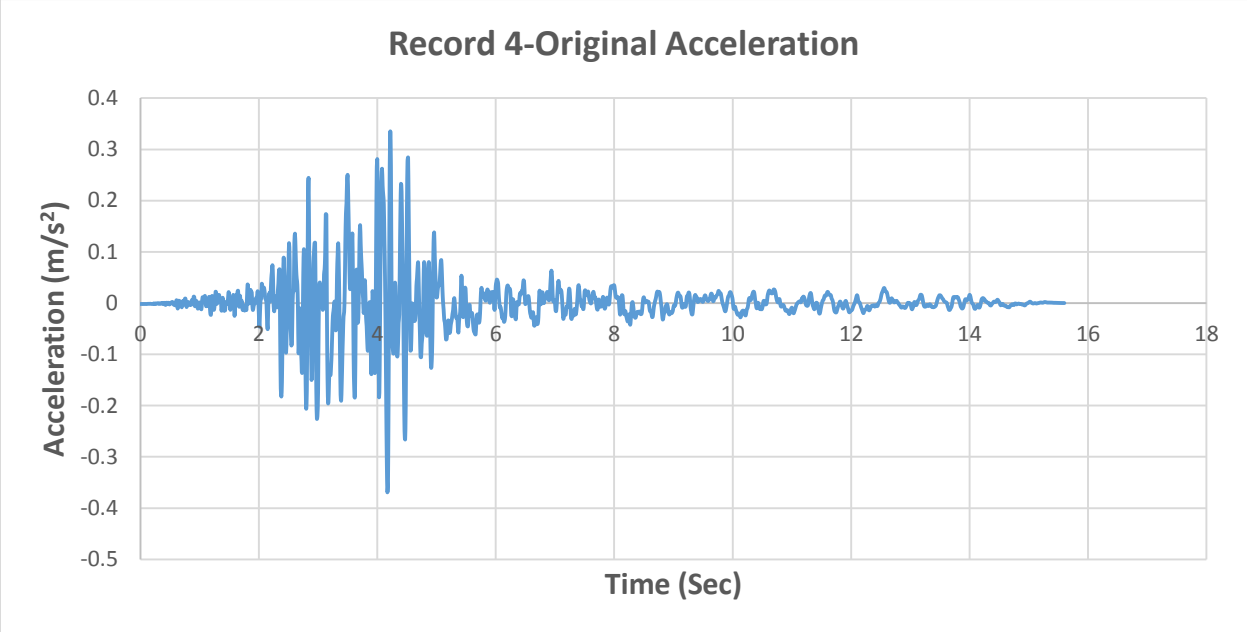

Figure 6.4. Original acceleration time-history of record 4

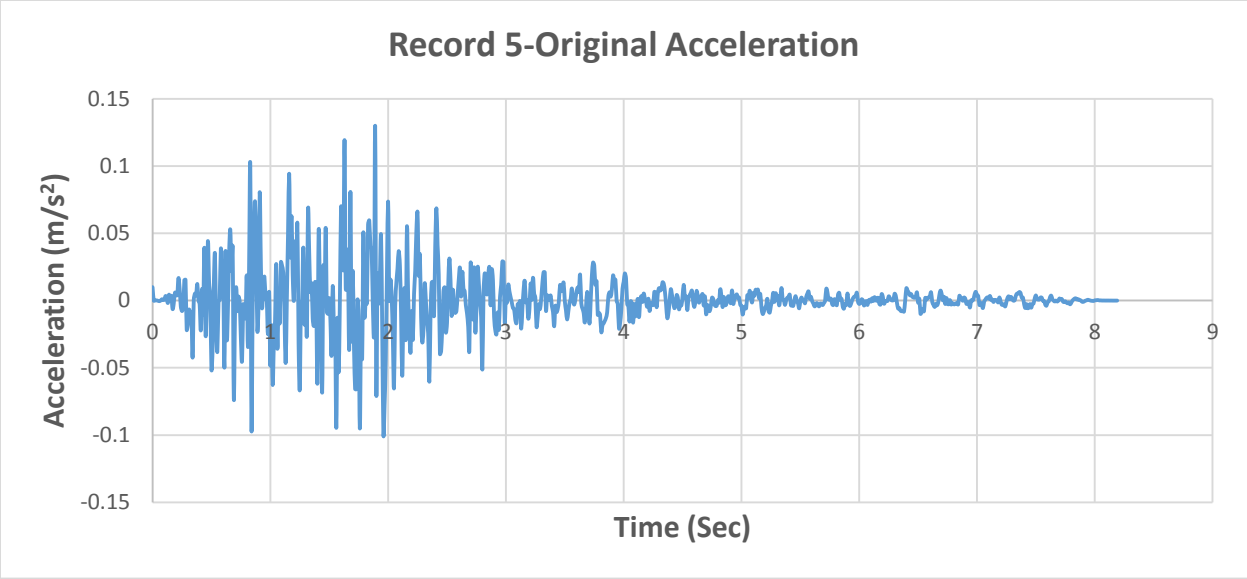

Figure 6.5. Original acceleration time-history of record 5

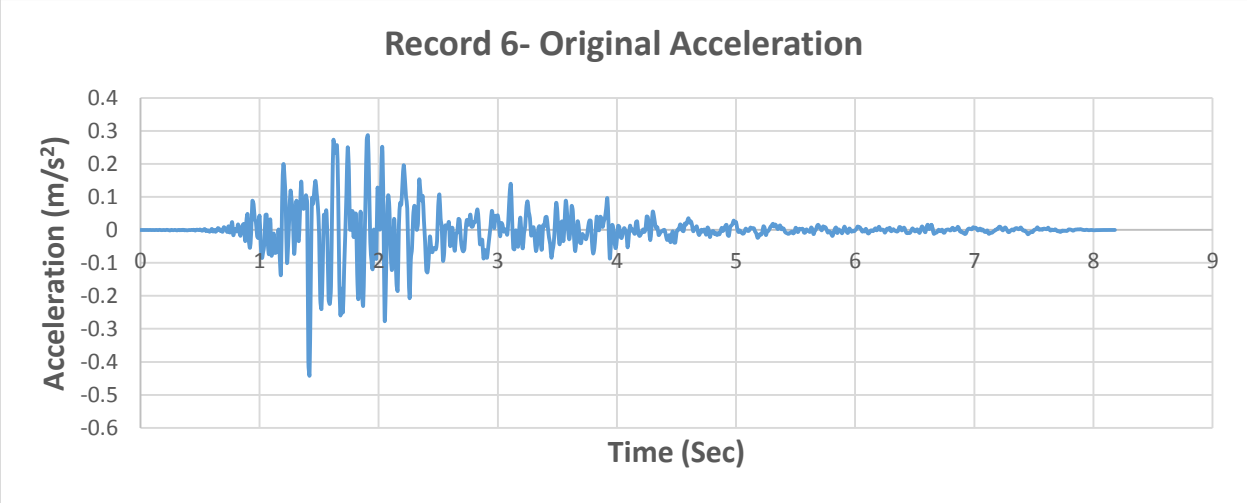

Figure 6.6. Original acceleration time-history of record 6

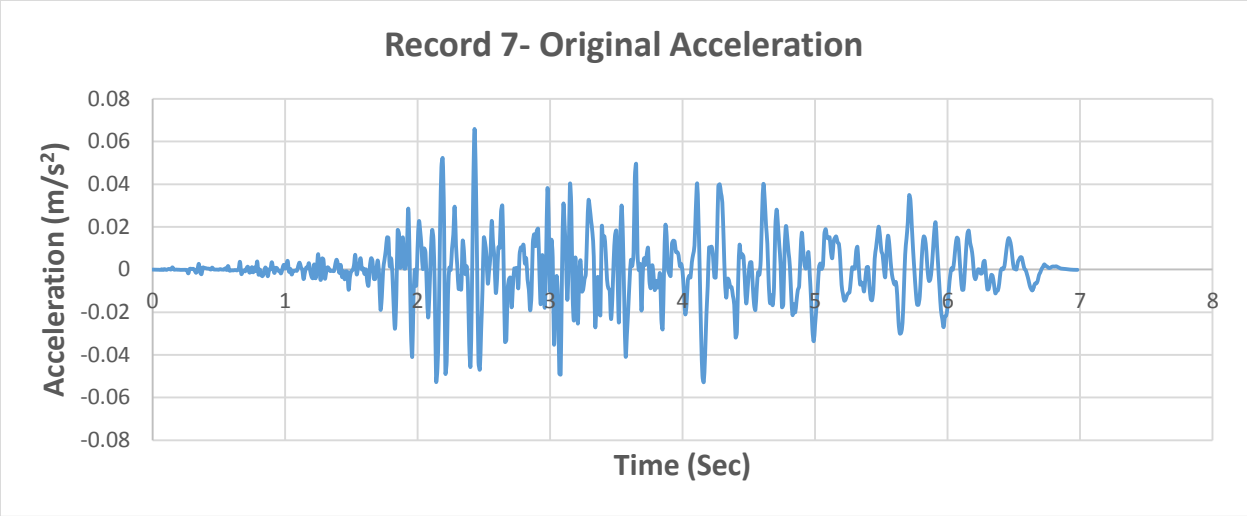

Figure 6.7. Original acceleration time-history of record 7

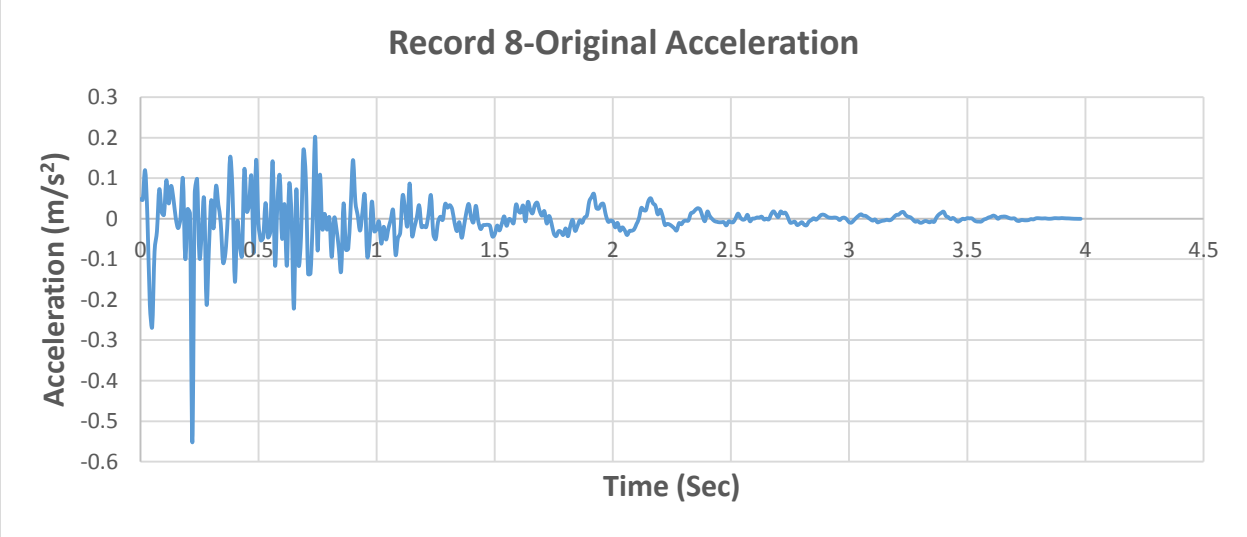

Figure 6.8. Original acceleration time-history of record 8

Eight earthquake records considered are matched according to the seismic response spectrum for Montreal (Figure 6.9) by SeismoMatch software (Version 2016). And also, Figures 6.10 to 6.17 present the matched acceleration time-history of those eight earthquake motions.

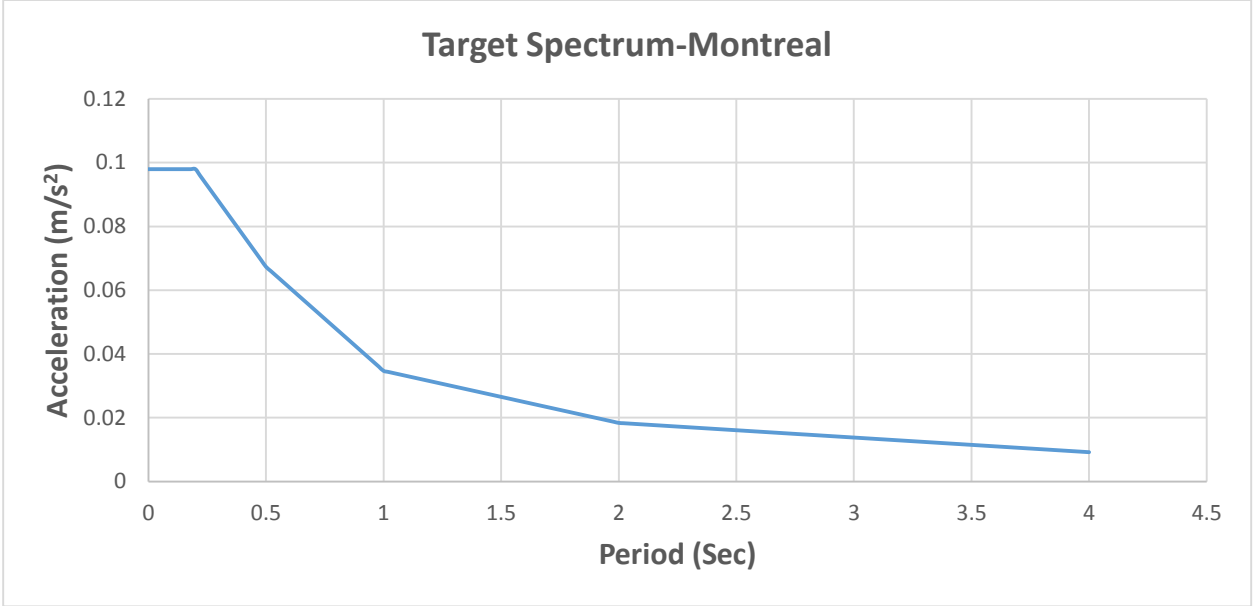

Figure 6.9. Target spectrum for Montreal

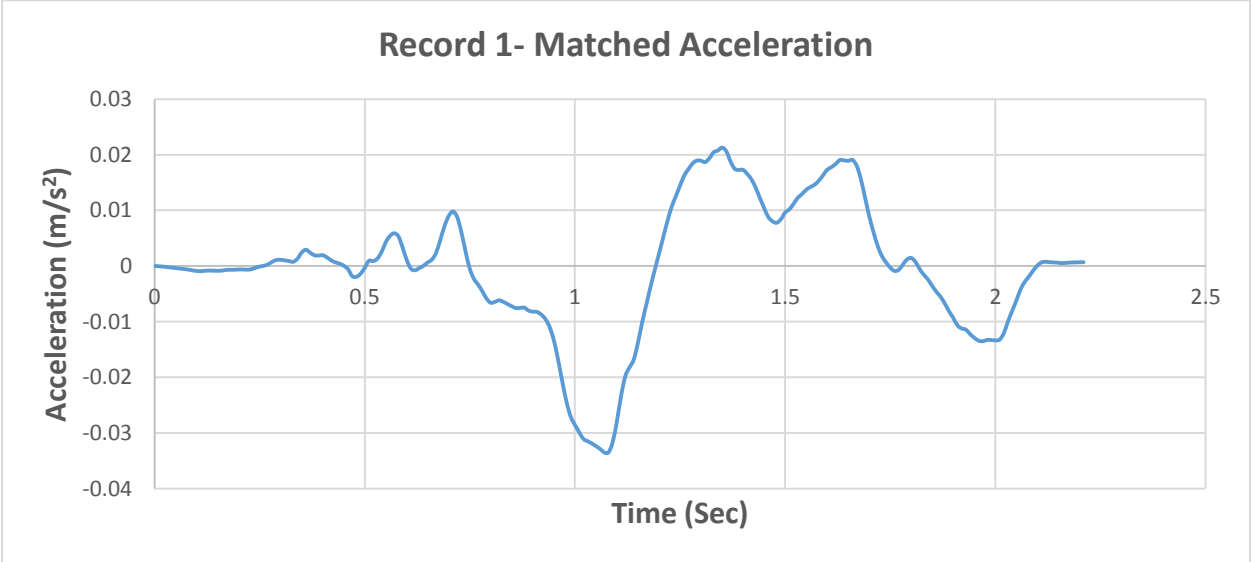

Figure 6.10. Matched acceleration time-history of record 1 according to Montreal spectrum

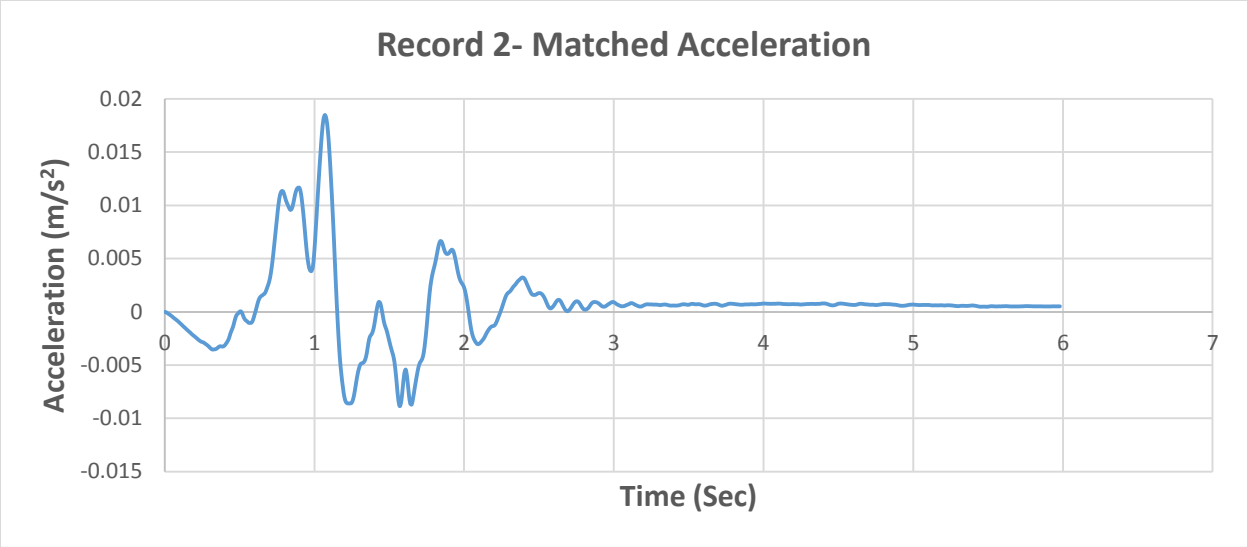

Figure 6.11. Matched acceleration time-history of record 2 according to Montreal spectrum

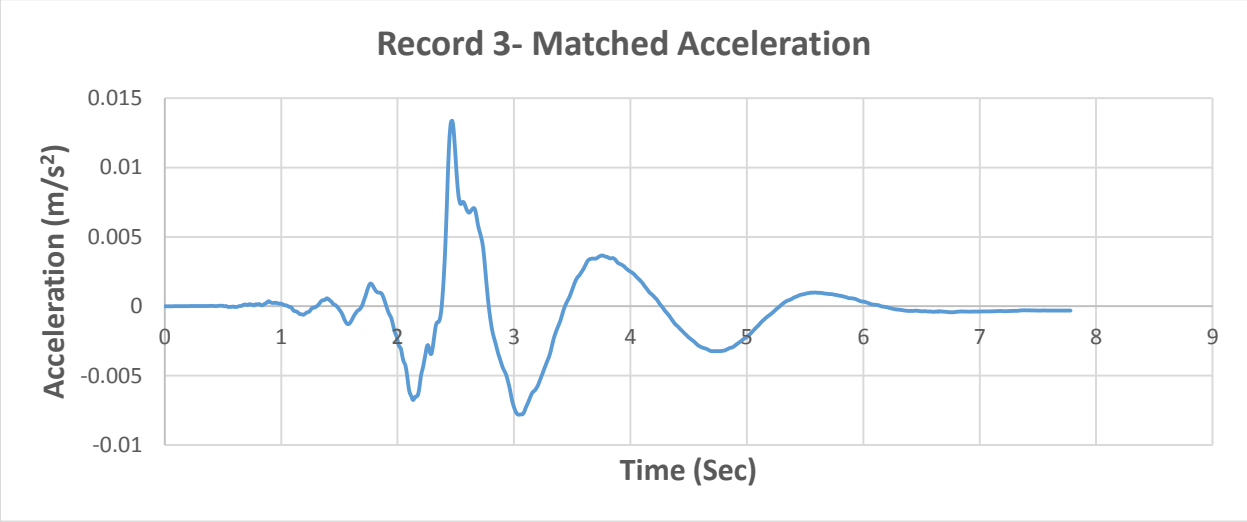

Figure 6.12. Matched acceleration time-history of record 3 according to Montreal spectrum

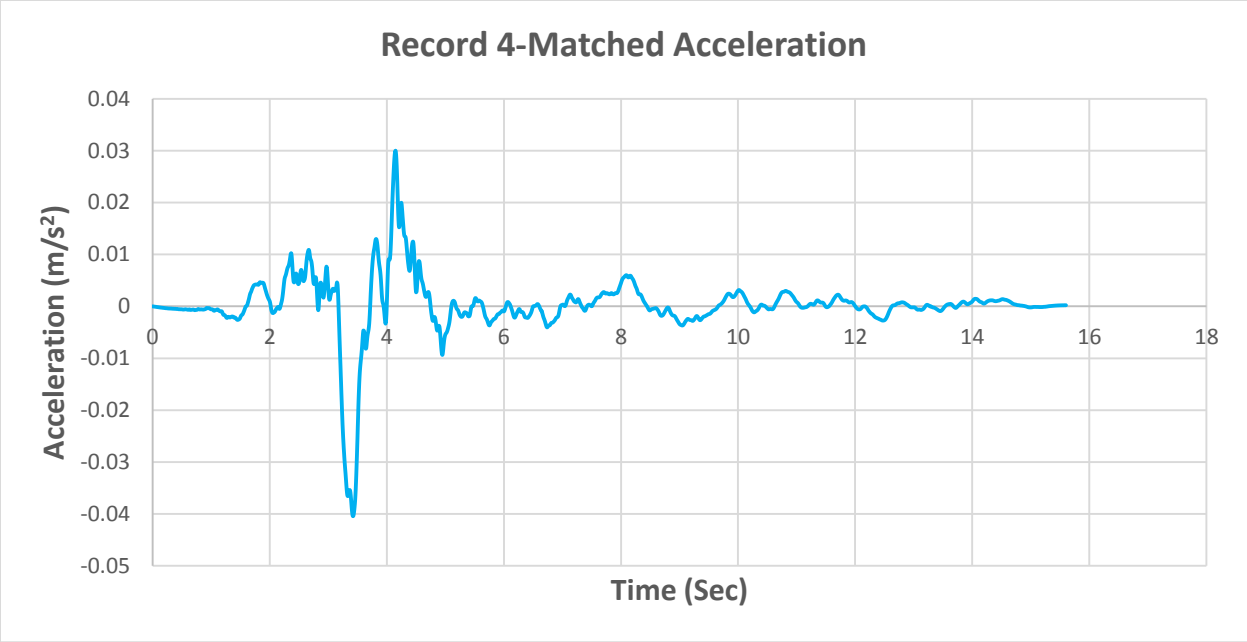

Figure 6.13. Matched acceleration time-history of record 4 according to Montreal spectrum

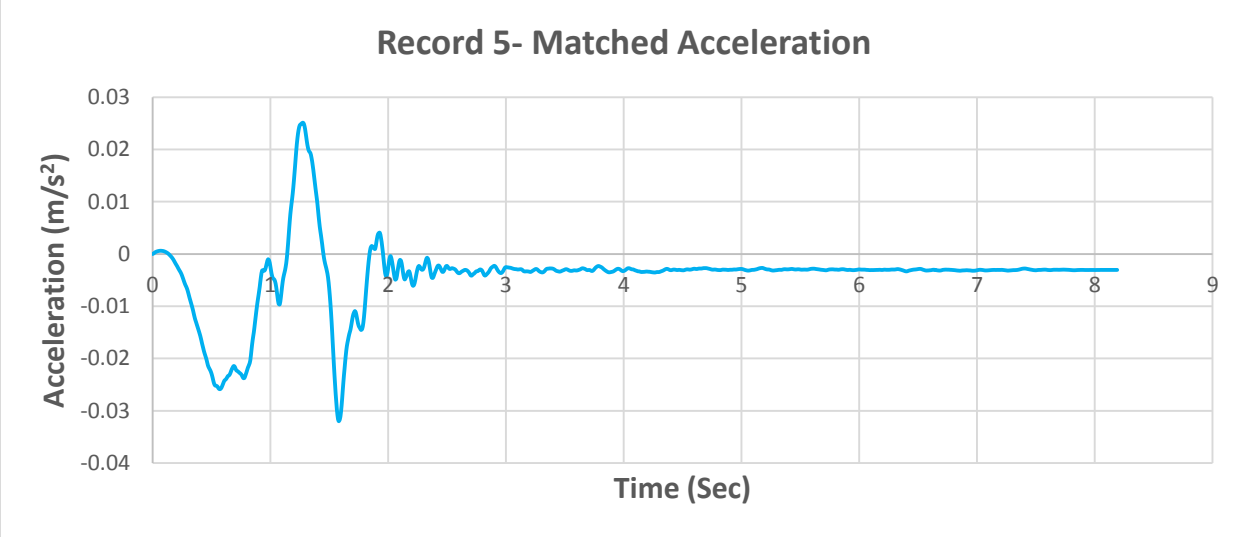

Figure 6.14. Matched acceleration time-history of record 5 according to Montreal spectrum

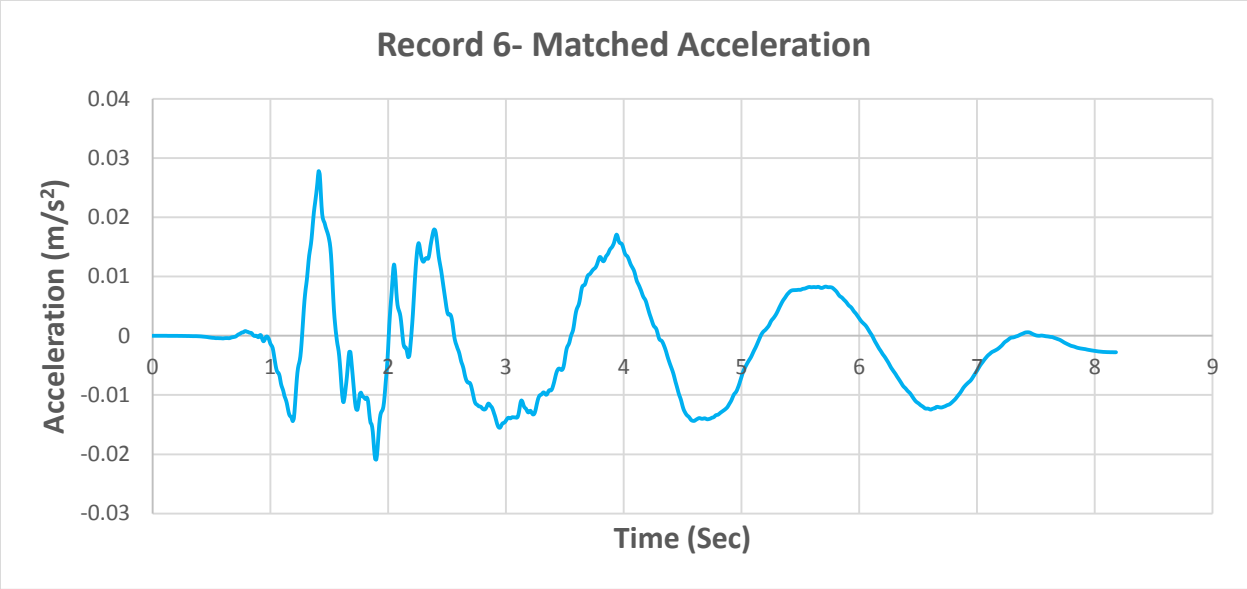

Figure 6.15. Matched acceleration time-history of record 6 according to Montreal spectrum

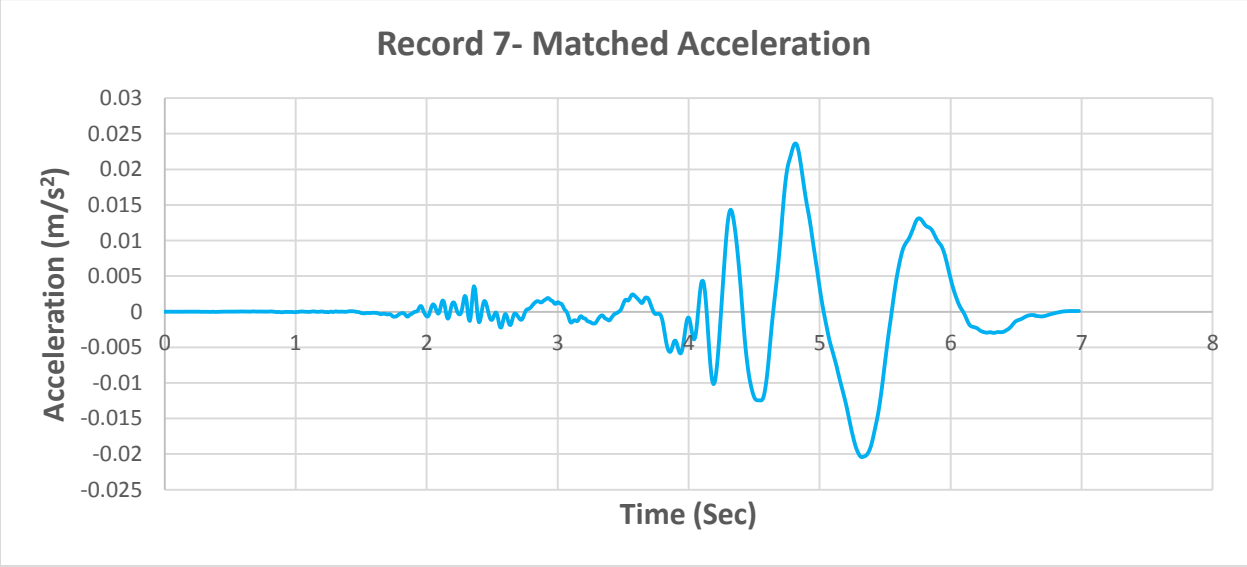

Figure 6.16. Matched acceleration time-history of record 7 according to Montreal spectrum

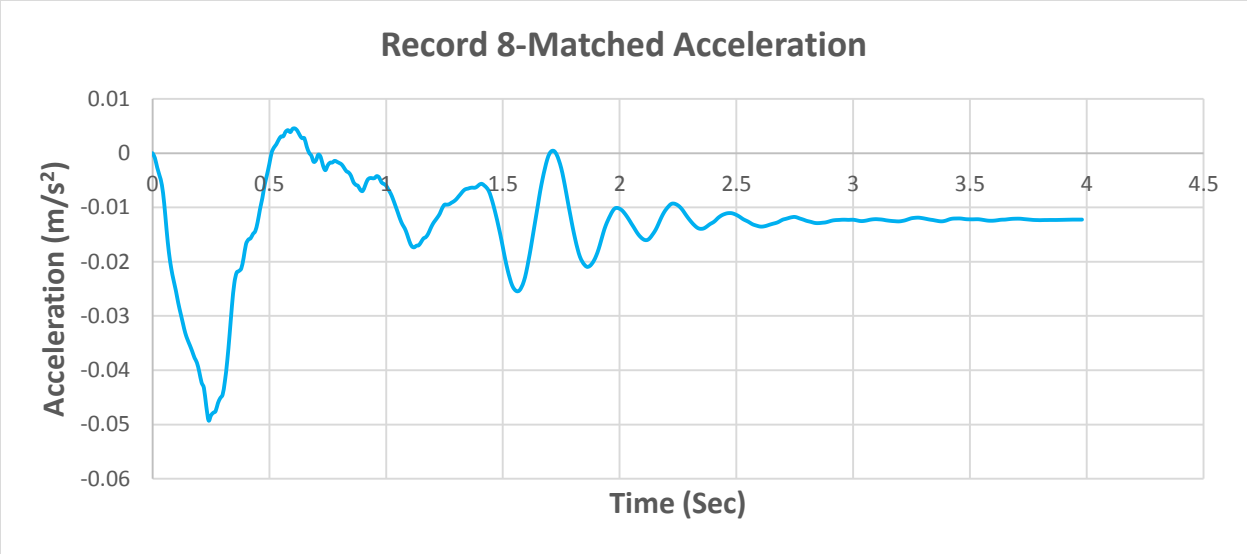

Figure 6.17. Matched acceleration time-history of record 8 according to Montreal spectrum

6.3. Soil properties

In order to consider different type of the soil in the parametric study of retaining wall, two different types of soil as backfill are modelled. Table 6.2 shows the material properties of sand and clay which are used in numerical models.

Table 6.2. Material Properties in parametric study (Itasca, 2015)

	Density (Kg/m3)	Bulk Modulus (Pa)	Shear Modulus (Pa)	Cohesion (Pa)	Friction Angle (Degree)	Dilation Angle (Degree)	Tension (Pa)
Sand	1600	1e7	6e6	0.0	32	0.0	0.0
Clay	1800	6.67e5	4e5	8e3	20	0.0	0.0

6.4. Retaining wall deformation according to Montreal earthquake motions

The dynamic displacements (at the top of the wall) in both lateral and vertical orientation for three different wall height in sand and clay are illustrated in Figures 6.18 to 6.21.

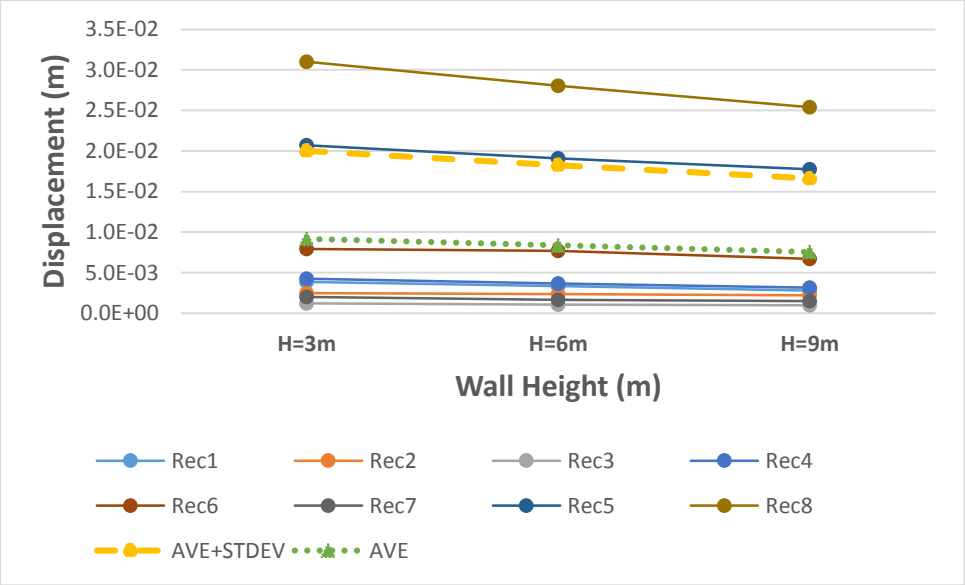

Figure 6.18. Wall displacement in X direction in Sand

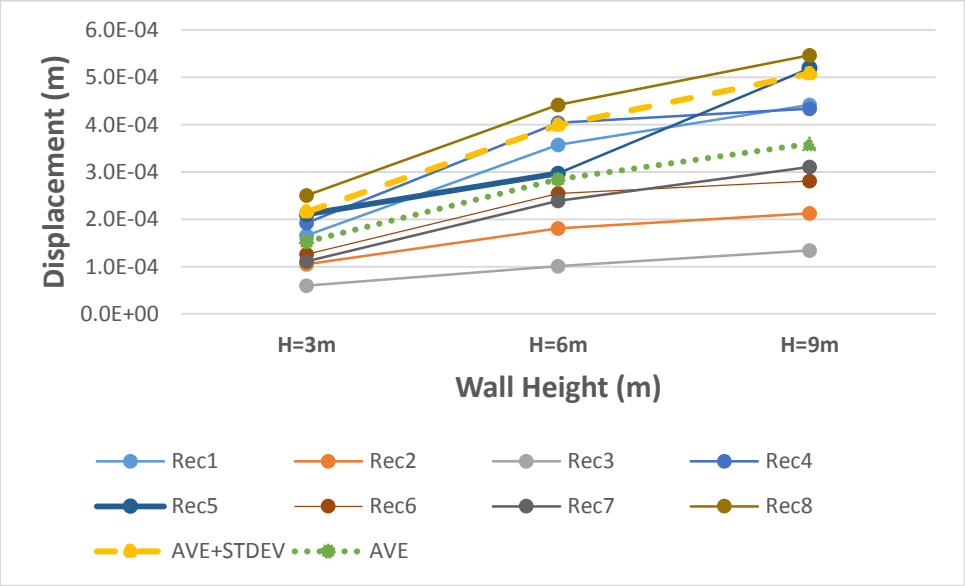

Figure 6.19. Wall displacement in Y direction in Sand

Figure 6.18 shows that for sandy soil, X-displacement at the top of the retaining wall decreases slightly with increasing height of the wall, while Figure 6.19 shows that the Y-displacement increases with the height of the wall.

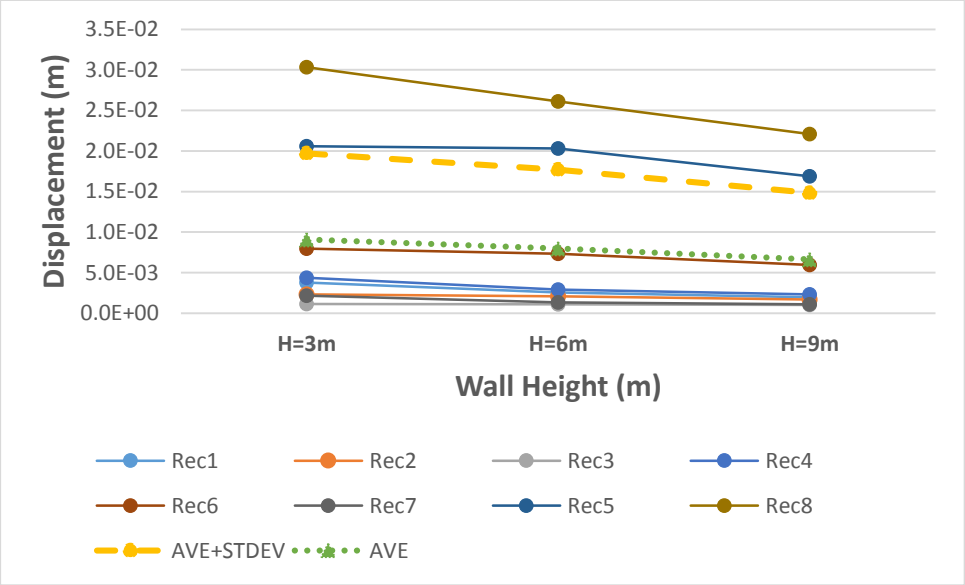

Figure 6.20. Wall displacement in X direction in Clay

Figure 6.21. Wall displacement in Y direction in Clay

The dynamic response of the soil-wall systems in clay is similar to that for sandy soil. Figure 6.20 shows that for clay, X-displacement at the top of the retaining wall decreases slightly with increasing height of the wall, while Figure 6.21 shows that the Y-displacement increases with the height of the wall.

The above results showed that the behavior of wall displacements in horizontal and vertical direction is different. And also, the kind of soil is a very effective parameter in the retaining wall deformation.

The normal stress on the retaining wall with different height (3m, 6m and 9m) for both static and dynamic condition in Sand and Clay are shown in Figures 6.22 to 6.27. From these figures it is observed that there is no significant difference in in the normal stress distribution on the soil-wall interface in the static and dynamic conditions.

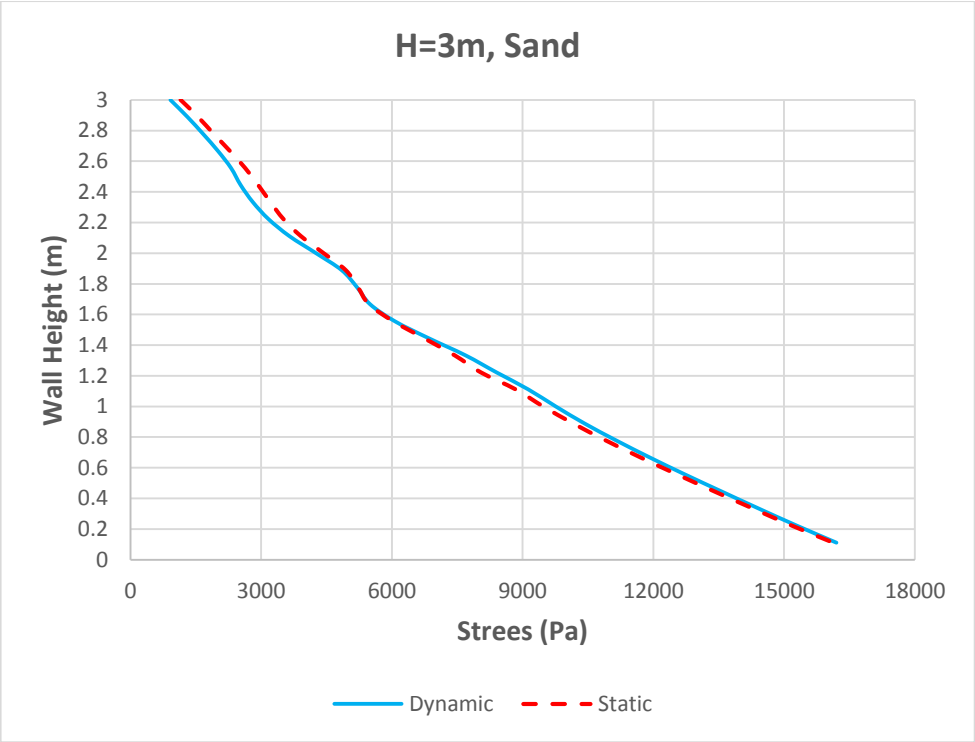

Figure 6.22. Stress on the retaining wall in both static and dynamic condition in Sand with height 3 m

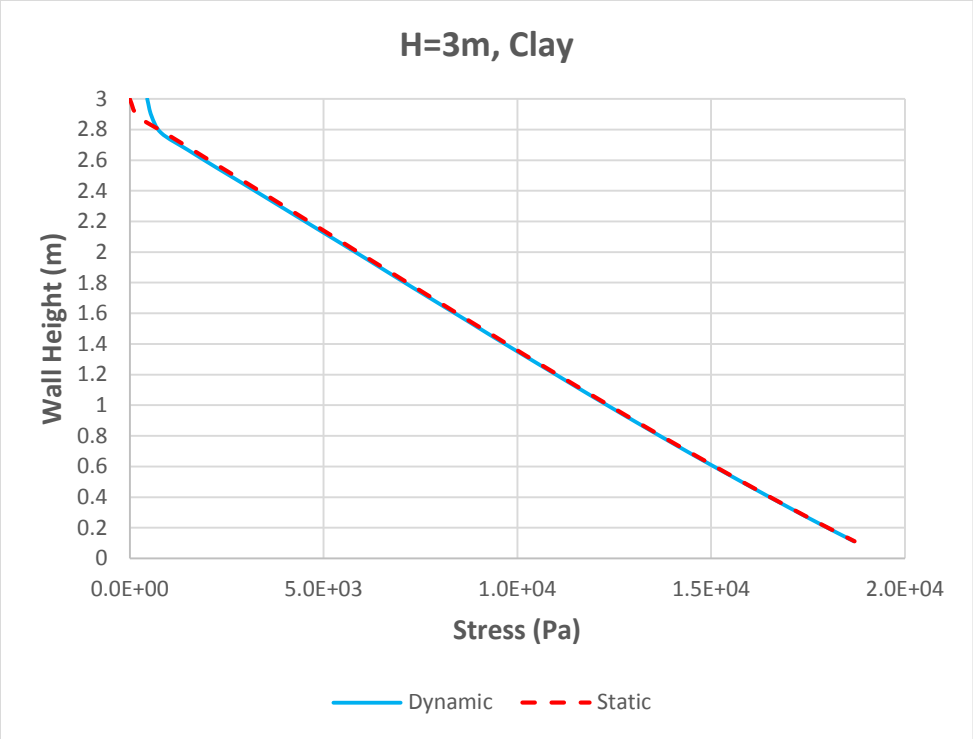

Figure 6.23. Stress on the retaining wall in both static and dynamic condition in Clay with height 3 m

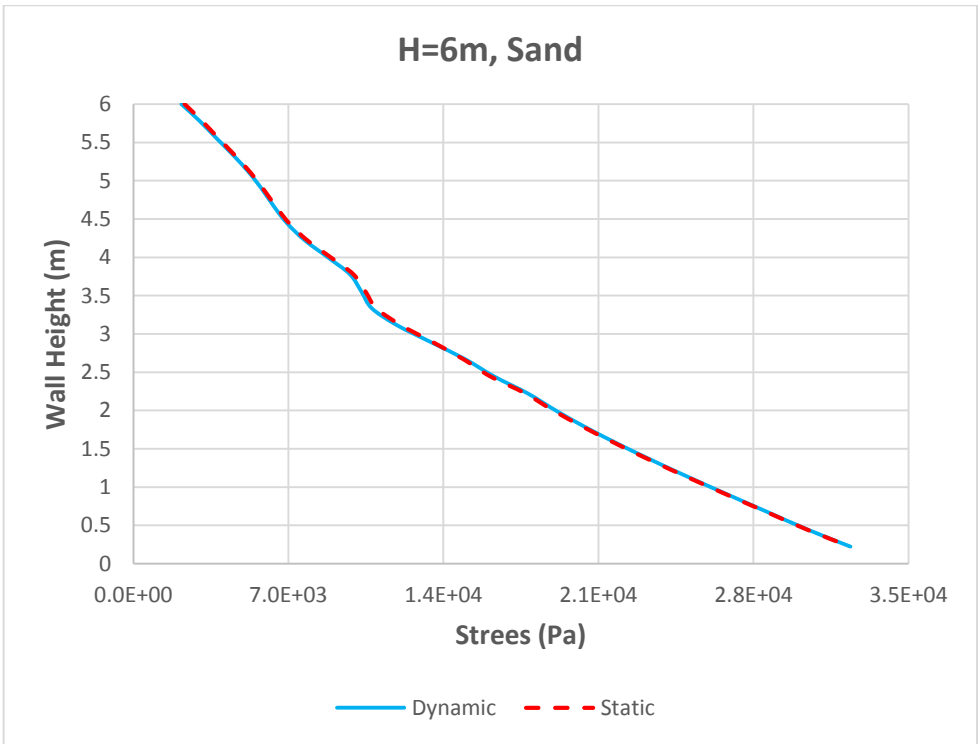

Figure 6.24. Stress on the retaining wall in both static and dynamic condition in Sand with height 6 m

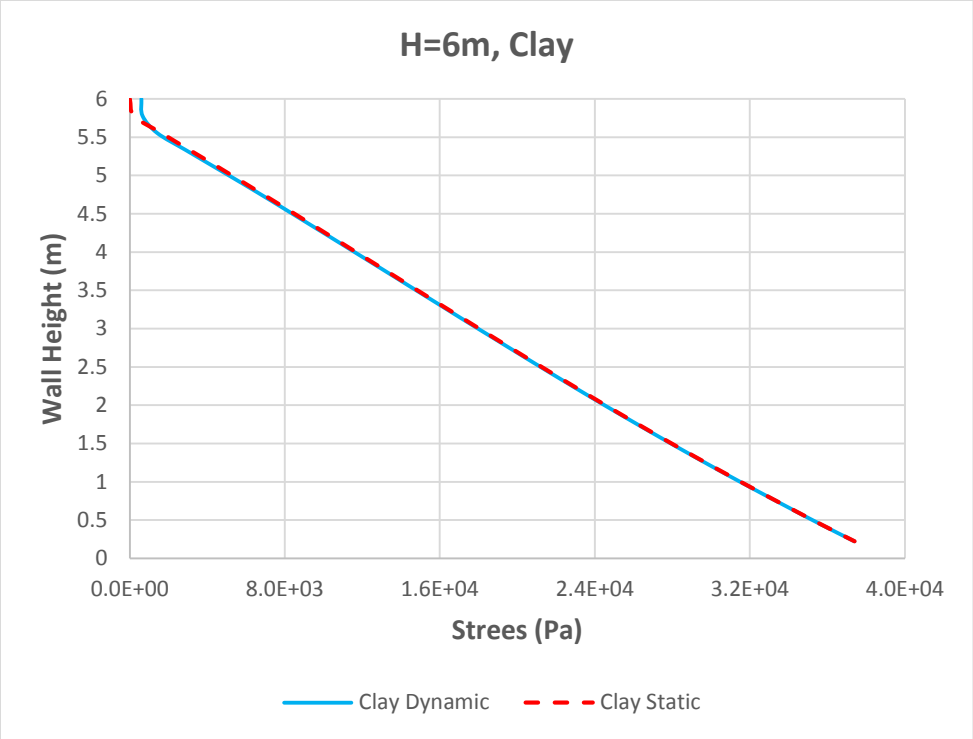

Figure 6.25. Stress on the retaining wall in both static and dynamic condition in Clay with height 6 m

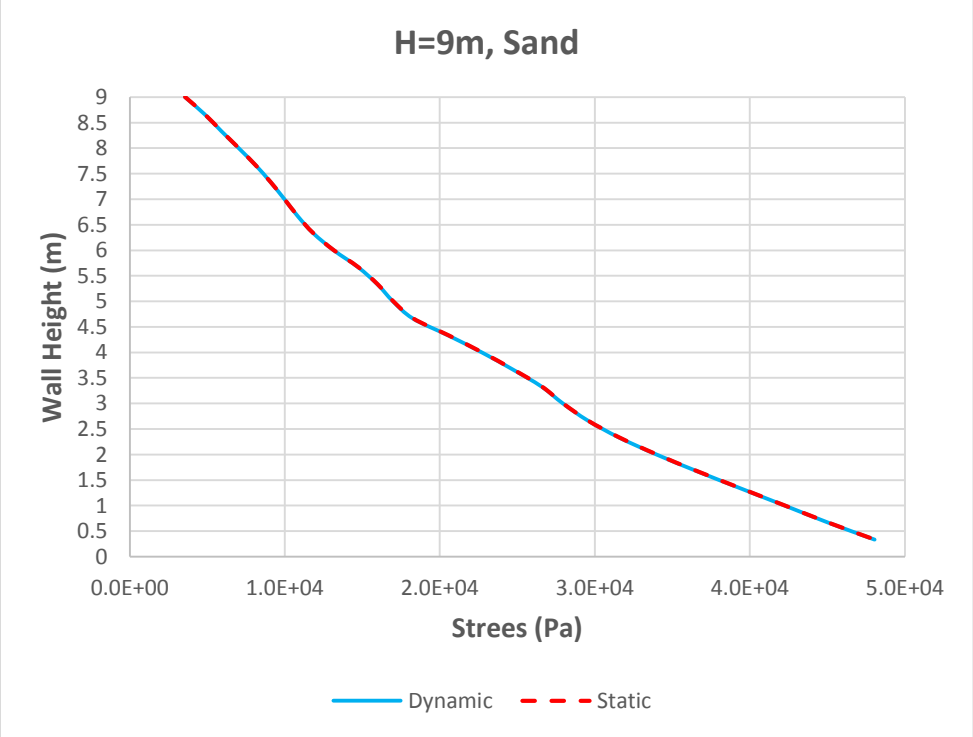

Figure 6.26. Stress on the retaining wall in both static and dynamic condition in Sand with height 9 m

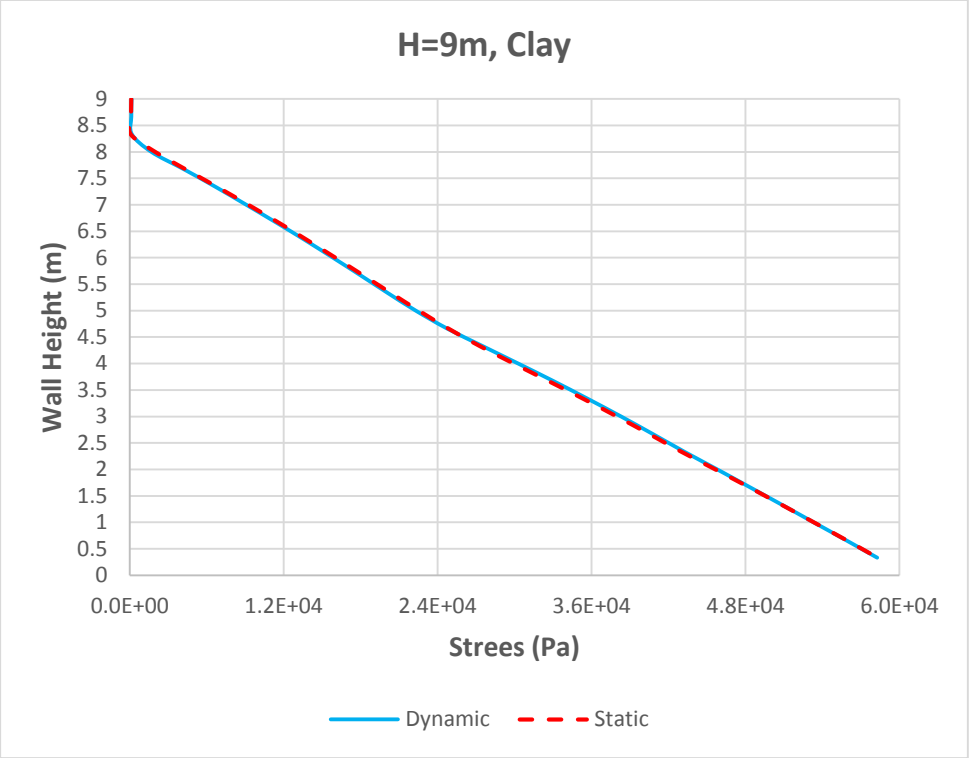

Figure 6.27. Stress on the retaining wall in both static and dynamic condition in Clay with height 9 m

6.5. Summary

In this chapter, a parametric study on the behavior of retaining wall in terms of wall deformation under earthquake loading is presented. For this purpose, numerical models was analyzed based on three different retaining wall height 3m, 6m and 9m, and soil types of sand and clay under eight different earthquake records of North America earthquake. Eight records applied in the numerical modes matched according to the seismic response spectrum for Montreal. The results showed that soil type is a very important factor in controlling the retaining wall deformation. Furthermore, with increase in the retaining wall height, wall deformation in the horizontal direction decreases and the displacement in the vertical direction increases, both for clay and sand. Finally, the normal stress distribution on the retaining wall for different height of walls for both static and dynamic condition show that the dynamic stress distribution is very similar to the static stress distribution.

Chapter 7. Summary and conclusions

7.1. Summary

Earth retaining walls are important public structures and they are vulnerable to seismic hazard causing public safety issues and economy. However, very limited studies are available on their seismic behaviour. In the current thesis, the seismic behaviour of reinforced concrete (RC) cantilever retaining was has been studied to address the following issues: (i) improve understanding of the behavior of the interface between structure and soil under various loading and boundary conditions for RC cantilever retaining walls; (ii) determine the sensitivity of the seismic response of such walls to key soil parameters such as the cohesion (C), friction angle (φ), shear stiffness (K_s), normal stiffness (K_n) and dilation (ψ); and (iii) determine size (height) effect of the relating walls on the seismic performance of such walls.

First, a baseline model of an RC cantilever retaining wall has been constructed and validated with a published work, followed by an extensive parametric study on the static and dynamic behavior of the system which is not available in the literature. A well-known Finite Difference Method (FDM)-based software, FLAC has been used to model and analyze the cantilever wall-soil systems considered in this study. The data for the baseline model were obtained from a published work (Parihar and Saxena, 2010), where the Finite Element Method (FEM) was used for modelling the wall-soil system. Both static and dynamic analysis were performed. For the dynamic analysis, an Indian earthquake record as used in (Parihar and Saxena, 2010) was used for comparison.

A sensitivity analysis of the key wall-soil interface parameters on seismic response of the retaining wall was performed for a Canadian similar to an Indian earthquake used in the published reference on which the baseline model was based on. Further parametric studies were conducted on the behavior of the earth retaining walls under a suite of eight earthquakes corresponding to seismic hazard of Montreal earthquake with three different height (3 m, 6 m and 9 m), and two different types of soil (clay and sand).

Finally, a statistical estimation of parameters was made for soil and retaining wall interface as considered here. Based on this study, the cumulative percentage distribution of cohesion (C) and stiffness parameters (shear and normal) against the wall deformation were calculated. Then, lower

and upper boundary ranges of wall-soil parameters were established for both static and dynamic condition.

7.2. Conclusions

The following observations and conclusions are made based on the numerical study presented in this thesis.

(1) The static and dynamic response of baseline model compare very well with the reference results presented in [17] in spite of the fact that the baseline model in the present thesis uses FDM, while the reference model used FEM.

(2) To investigate the effect of the shear strength and stiffness parameters of wall-soil interface on seismic response of retaining wall, the wall deformation was assessed in the both vertical and horizontal directions. The results show that

   a. In static state, with increasing shear strength parameters (cohesion and friction angle) and stiffness (shear and normal) parameters and also dilation value of wall-soil interface, wall deformation in both horizontal and vertical direction decrease.

   b. But in dynamic condition the wall response different. For this purpose, wall displacements increased with increasing shear strength parameters, shear stiffness and dilation value of wall-soil interface whereas with increasing normal stiffness value, wall deformation was decreased.

(3) Since the effect of interface roughness is one of the most significant issues in the wall-soil behavior, in this study the effect of rough surface on the retaining wall deformation was investigated. For this purpose, in the dynamic analysis, the wall-soil interface in numerical modeling was considered as a medium or moderately rough surface. Thus, rough surface was simulated by increasing shear stiffness, friction angle and dilation values. It is observed that with decreasing shear stiffness and friction angle, a smooth surface could be simulated.

(4) As the duration and the peak ground acceleration of the Indian earthquake considered in [17] are similar to the selected Canadian earthquake (6^{th} March, Quebec, 2005), the response of the soil-wall system subjected to these two earthquake records show a good agreement in terms of retaining wall deformation.

(5) According to statistical study conducted on the wall-soil interface parameter, a lower and upper range limit for each parameter was obtained. In fact, this estimation can be used to design the retaining wall and establish a data range for laboratory and field tests.

(6) The parametric study based on wall height variation and different kind of soil subjected to a suite of eight earthquake records for Montreal earthquake are presented ins statistical format. The results of this parametric study show that the deformation of the wall facing in horizontal and vertical directions was changed according to kind of soil and earthquake motion. In fact, the following two parameters: soil type and acceleration time-history, play the main role in the wall deformation.

(7) There is no significant difference observed in in the normal stress distribution on the soil-wall interface in the static and dynamic conditions.

(8) According to conducted parametric study with different ground motion records, in both sand and clay soil, wall displacements in X direction decreased with increasing wall height but in Y direction, the wall deformation was increased with the increasing wall height.

7.3. Contribution

The main contribution of the present research is explained as below:

- Identification of the critical soil parameters for earth retaining structures, especially, cantilever walls.
- Wall-soil deformation characteristic in different dynamic motions
- Identification of the range of values for the critical parameters

7.4. Scope for future study

The scope for the future study can be proposed as below:

- Calculation of bending's moment and shear forces in a retaining wall based on the dynamic soil pressure
- Effect of wall-soil interface parameters on retaining wall deformation by different overburden under earthquake ground motion

References

Bathurst R.J. and Hatami, K., (1988), "Seismic response analysis of a geosynthetic-reinforced soil retaining Wall", Geosynthetics International, 5 (1-2): 127-166.

Brooks, H., (2010), "Basics of retaining wall design," HBA Publication.

Cai, Z. & Bathurst, R. J., (1995), "Seismic response analysis of geosynthetic reinforced soil segmental retaining walls by finite element method", Computers and Geotechnics, 17(4), 523-546.

Callisto, L., and Soccodato, F. M., (2007), "Seismic analysis of an embedded retaining structure in coarse-grained soils", Proc., 4th Int. Conf. on Earthquake Gotechnical Engineering. Aristotele Univ. of Thessaloniki, Thessaloniki, Greece.

Clough, R. W., and Penzien, J. (1993), "Dynamics of Structures", McGraw Hill, 2nd ed.

Collin, J. G. (1986), "Earth Wall design", PhD thesis, Univ. of California, Berkeley, Calif.

Cheng, Z., Chunfeng, Z., and Hui, G., (2013), "Elastoplastical analysis of the interface between clay and concrete incorporating the effect of the normal stress history," Journal of Applied Mathematics, vol. 2013, Article ID 673057, 12 pages.

El-Emam, M., Bathurst, R.J. and Hatami, K., (2004), "Numerical modeling of reinforced soil retaining walls subjected to base acceleration", 13th World Conference on Earthquake Engineering, Vancouver BC, 15.

Finn, W.D.L., Yogendrakimar, M., and Yoshida, N., TARA -3 (1986), "a program to compute the response of 2-D embankment and soil-sttucture interaction systems to seismic loading," Department of Civil Engineering, University of British Columbia, Vancouver, Canada.

Ghanbari, S. S., (2008), "A Pseudo-Dynamic Method to Analyze Retaining Wall with Reinforced Backfill", JSEE, pp.41-48.

Green, R.A., and Ebeling, R.M., (2003), "Modeling the dynamic response of cantilever earth-retaining walls using FLAC", Proceedings of the 3rd International Symposium on FLAC and FLAC3D: Numerical modeling in geomechanics, Sudbury, ON, Canada.

Government of India M O., (2005), "Concept and Design of Reinforced Earth Structures", Geo-technical Engineering Directorate Research Designs and Standards Organisation, Lucknow, India.

Hatami, K., and Bathurst, R. J., (2001), "Investigation of seismic response of reinforced soil retaining walls", Proc., Int. Conf. on Recent Advances in Geotechnical Earthquake Engineering and Soil Dynamics, Paper No. 7.18.

Helwany, S. M. B., Budhu, M., and McCallen, D., (2001), "Seismic analysis of segmental retaining walls. I: Model verification", J. Geotech. Geoenviron. Eng., 127(9), 741–749.

Itasca, (2015), FLAC (Fast Largrangian Analysis of Continua) User's Manuals. Minneapolis: Itasca Consulting Group, Inc.

Itasca (2008), Fast Lagrangian Analysis of Continua Version 6.0, Itasca Consulting Group Inc., Minneapolis.

Je, L., (1973), "Dynamic Structure Soil Structure Interaction", Bulletein of Seismological Society AMerica, pp.1289-1303.

Kishan, D. N., (2010), "Analysis and Design of 44 meter M.S.E using Plaxis", *IJAET*, 41-49.

Krishna, A. M., (2010), "Seismic Lateral Earth Pressures on Retaining Structures", Proc., 5th Int. Conf. on Recent Advances in Geotechnical Earthquake Engineering and Soil Dynamics. Missouri University of Science and Technology.

Karpurapu, R. G., and Bathurst, R. J., (1995), "Behaviour of geosynthetic reinforced soil retaining walls using the finite element method", Comput. Geotech, 17(3), 279–299.

Kaliakin, V. N., and Xi, F., (1992), "Modeling of interfaces in finite element analyses of geosynthetically reinforced walls", Earth reinforcement practice, H. Ochiai et al., eds., Balkema, Rotterdam, The Netherlands, 351–356.

Kapurapu, R., and Bathurst, R. J., (1995), "Behavior of geosynthetic reinforced soil retaining walls using the finite element methods", Comput. Geotech, 17, 279–299.

Lysmer, J., and Kuhlemeyer R.L., (1969) "Finite dynamic model for infinite media", Journal of Engineering Mechanics, Vol. 95(EM4), 859-877.
Ling, H. I., Liu, H., Kaliakin, V., and Leshchinsky, D., (2004), "Analyzing dynamic behavior of geosynthetic-reinforced soil retaining walls", J. Eng. Mech., 130(8), 911–920.

Ling, H. I., Liu, H., and Mohri, Y., (2005), "Parametric studies on the behavior of reinforced soil retaining walls under earthquake loading", J. Eng. Mech., 131(10), 1056–1065.

Ling, H. I., Tatsuoka, F., and Tateyama, M., (1995), "Simulating performance of GRS-RW by finite-element procedure", J. Geotech. Eng., 121(4), 330–340.

Ling, H. I., and Liu, H., (2003), ''Pressure-level dependency and densification behavior of sand through generalized plasticity model,'' J. Eng. Mech., 129-8, 851–860.

Muthucumarasamy, Yogendrakumar, R. J., (1992), "Dynamic Response Soil Analysis of Reinforced Soil Wall", Journal of Geotechnical Engineering, pp. 1158-1167.

Mononobe, N. M., (1929), “Determination of Earth Pressure during Earthquake”, World Engineering Conference, pp.172-195, Japan.

Nouri, S. M., (2008), “Seismic Stability of Reinforced Retaining Wall”, WCEE, Beijing.

Naumoski, N., Heidebrecht, A.C., and Rutenberg, A.V., (1993), “Representative Ensembles of Strong Motion Earthquake Records,“ EERG Report 93-01, McMaster University, Hamilton, Ontario, Canada.

Okabe, S., (1926), “General Theory of Earth Pressure”, J. of the Japanese soc. of civ. Engrs., Tokyo, Japan 12(1).

Pastor, M., Zienkiewicz, O. C., and Chan, A. H. C., (1990), ‘‘Generalized plasticity and the modeling of soil behavior,’’ Int. J. Numer. Analyt. Meth. Geomech., 14, 151–190.

Parihar, Aditya, Navjeev Saxena, and D. K. Paul, (2010), “Effects of Wall-Soil-Structure Interaction on Seismic Response of Retaining Wall”, Proc., 5th Int. Conf. on Recent Advances in Geotechnical Earthquake Engineering and Soil Dynamics. Missouri University of Science and Technology.

Portland Cement Association, PCA Soil Primer, 1992.

Richardson, G.N., Lee, K.L., (1975), “Seismic design of reinforced earth walls”, ASCE Journal of Geotechnical Engineering Division 101 (2), 167–188.

Rowe, R. K., and Ho, S. K., (1997), “Continuous panel reinforced soil walls on rigid foundations”, Liq. Cryst. Ordered Fluids, 123(10), 912–920.

Segrestin, P. and Bastick, M.J., (1988), “Seismic design of reinforced earth retaining walls - the contribution of finite element analysis”, Proc. International Symposium on Theory and Practice of Earth Reinforcement, IS-Kyushu '88, Fukuoka, Japan, 577-582.

Siddharth M., and Siddharth S., (2015), “Seismic Analysis of Reinforced Earth Wall: A Review”, International Journal of Structural and Civil Engineering Research, Vol. 4, No. 1, pp.132-140.

Segrestin, P., and Bastick, M. J., (1988), “Seismic design of reinforced earth retaining walls-The contribution of finite element analysis”, Theory and practice of earth reinforcement, H. Ochiai et al., eds., Balkema, Rotterdam, The Netherlands, 577–582.

Seismosoft, (2018), Earthquake Engineering Software Solution, Seismomatch, http://www.seismosoft.com/SeismoMatch-2016-Release-1 (last accessed, January, 2018).

Yogendrakumar, M., Bathurst, R. J., and Finn, W. D. L., (1992), “Dynamic response analysis of reinforced-soil retaining wall”, J. Geotech. Eng., 118(8), 1158–1167.

Yogendrakumar, M., Bathurst, R. J., and Finn, W. D. L., (1992), “Dynamic response analysis of reinforced-soil retaining wall”, J. Geotech. Eng., 118(8), 1158–1167.

Zienkiewicz, O. C., Chan, A. H. C., Pastor, M., Schrefler, B. A., and Shiomi, T. (1998), “Computational geomechanics with special reference to earthquake engineering,” Wiley, Chichester, England.